



BIBLIOTHÈQUE

CÉGEP DE L'ABITIBI-TÉMISCAMINGUE
UNIVERSITÉ DU QUÉBEC EN ABITIBI-TÉMISCAMINGUE

Mise en garde

La bibliothèque du Cégep de l'Abitibi-Témiscamingue et de l'Université du Québec en Abitibi-Témiscamingue (UQAT) a obtenu l'autorisation de l'auteur de ce document afin de diffuser, dans un but non lucratif, une copie de son œuvre dans [Depositum](#), site d'archives numériques, gratuit et accessible à tous. L'auteur conserve néanmoins ses droits de propriété intellectuelle, dont son droit d'auteur, sur cette œuvre.

Warning

The library of the Cégep de l'Abitibi-Témiscamingue and the Université du Québec en Abitibi-Témiscamingue (UQAT) obtained the permission of the author to use a copy of this document for nonprofit purposes in order to put it in the open archives [Depositum](#), which is free and accessible to all. The author retains ownership of the copyright on this document.

UNIVERSITÉ DU QUÉBEC EN ABITIBI-TÉMISCAMINGUE

COMPRENDRE LES PATRONS DE BIODIVERSITÉ DES CRYPTOGRAMES
(BRYOPHYTES ET LICHENS) DANS LES FORÊTS BORÉALES GRÂCE À LA
TÉLÉDÉTECTION

THÈSE

PRÉSENTÉE

COMME EXIGENCE PARTIELLE

DU DOCTORAT EN SCIENCES DE L'ENVIRONNEMENT

PAR

CARLOS CERREJÓN LOZANO

AOÛT 2022

UNIVERSITÉ DU QUÉBEC EN ABITIBI-TÉMISCAMINGUE

UNDERSTANDING THE BIODIVERSITY PATTERNS OF CRYPTOGRAMS
(BRYOPHYTES AND LICHENS) IN BOREAL FORESTS THROUGH REMOTE
SENSING

THESIS

PRESENTED

AS PARTIAL REQUIREMENT

OF THE PH.D. IN ENVIRONMENTAL SCIENCES

BY

CARLOS CERREJÓN LOZANO

AUGUST 2022

ACKNOWLEDGEMENTS

This adventure linked to the completion of the PhD thesis is finishing, but before putting an end to it, I would like to take this opportunity to thank the contribution, both direct and indirect, of many people (and other living beings!) who have made it possible.

Many thanks to my two directors, Nicole Fenton and Osvaldo Valeria, for instructing and guiding me at all times, as well as for their attention and availability. But above all, a huge thank you for your closeness, empathy, and support that have helped me overcome all the challenges encountered during this long journey.

Also a big thank you to Danièle Laporte and Marie-Hélène Longpré, for their great professionalism, and for making me smile even on the worst days. You give life to the IRF and each of its members. *Danièle, merci surtout pour tout l'amour que tu m'as témoigné ces années et pour tes sincères câlins pleins de vitalité. Je n'arrêterai jamais de m'arrêter à ta porte.*

Many thanks to Julie Arseneault for having welcomed me from the beginning with that good energy that characterizes you and for really making me feel like a member of the lab. I will not forget all your support and the good times lived during these years.

I also thank Goldcorp Eleonore Mine and Environment and Climate Change Canada for funding this project. I want to particularly thank the Eleonore Mine's environmental team for their warm welcome and hospitality during my fieldwork. Without a doubt, my stay there has been one of the best adventures of my life. Thanks likewise to Mireille Martel for her excellent company, instruction and good advices during this stay. You made me feel safe and continue firm even in the most adverse conditions.

I am also super grateful to the members of my new "Canadian" family, Tati, Juanita, Mat, Jeffrey, Enrique, Mariano, Sameera, Xiangbo, Myriam, José, Marta, Lili and Stephan for offering me such good times. Without you, I definitely would not have

been able to continue my Ph.D. on several occasions, so this achievement is as much yours as it is mine. As my good friend Jeffrey told me with certainty over and over again "we are not going to die because of this". And no, I have not forgotten to include you in this paragraph, Osvaldo. I can't remember a single time when you didn't put my well-being above all else. Really, thank you for being a second father to me and a great friend.

Many thanks to Marianne, Maxence and Marine for welcoming me so warmly and sweetening the last stage of my doctorate with such good times. *Et merci de m'apprendre qu'il est possible de cuisiner avec moins d'huile, et de manger un peu plus de légumes!*

Thanks also to Jesús Muñoz for his excellent contribution to one of the scientific chapters of this thesis, but especially for giving me the opportunity to carry out the research internship that led to its development in my country of origin and for welcoming me with open arms. Those months mark a before and after in my path both academically and personally. Thank you for promoting me professionally and also for your great friendship, which is very, very far from being "un mojón!".

I want to make a special mention to Sandra and my "archienemigo" Milka (my unconditional doggy friend), for having followed me, not only to a new country across the ocean, but to a remote village with abundant snow and mosquitoes, to support me every day during the early years of this thesis. *Muchísimas gracias!*

Many thanks to the members of the "Banda del pimiento" Samsi, Nachet and Cresti, for supporting me unconditionally from the beginning of my research career and for offering me so many moments of happiness. *Vuestra capacidad de ver la belleza incluso en los defectos me hizo aprender a mostrarme tal como soy y ese sentimiento de libertad es insuperable.*

Marion, *merci beaucoup de m'avoir soutenu et de m'avoir offert tant de bons moments. (je n'aurais jamais pensé voir un goéland déguisé en aigle!). Tu as fait de la dernière étape de mon doctorat une aventure, j'en ai joui comme un enfant. Ahora es tu turno y ahí estaré para ti.*

Finally, infinite thanks to my *mama* and my *papacha*, my sister Anita and my little niece Lucia, and my grandparents Manolita, Ana, Antonio and Antonio, for always supporting me and motivating me to keep growing, even if it meant putting an ocean between us. It seems that this has paid off and that the student stage is coming to an end (I was close to being named student emeritus!) and all thanks to you. *Como muestra de mi profundo agradecimiento, os dedico esta tesis con todo mi amor.*

DEDICATION

To my parents, sister, niece and grandparents,

which will always be in my heart

FOREWORD

This thesis is presented in the form of three scientific articles corresponding to Chapters II, III and IV, being completed by a general introduction and conclusion (Chapters I and V, respectively). Chapters II and III have been published while Chapter IV is being prepared for submission. One additional review article is included in Annex A, which was carried out and published during the development of the present thesis.

The three main scientific articles (Chapters II, III and IV) were developed with the collaboration and from the essential contribution of each of their authors. As the main responsible for the development of these articles, including data preparation, exploration and analysis, as well as their writing, I am the first author of all of them. My supervisors, Dr. Osvaldo Valeria and Dr. Nicole J. Fenton occupy the first and last co-author positions, respectively, in all these articles. Both actively contributed to their development, from the conception of the studies and data acquisition (either field and remote sensing data) to the interpretation of results and revision of the manuscripts. Dr. Marion Barbé and Dr. Nicolas Mansuy provided field and remote sensing data, respectively, for Chapter II, as well as critical and constructive reviews of the manuscript. Dr. Jesús Muñoz was significantly involved in the development of Chapter 3, including the conceptualization of the study, data curation, statistical analyses and manuscript review and editing. The first two articles (Chapters II and III) focus on bryophytes and were conducted in the same region using a database built from field data from three previous studies carried out by Marion Barbé, Chafi Chaieb and Joëlle Castonguay. A certain degree of repetition is therefore inevitable. However, since the extension of the study area was different for both articles, the field data used for their development was not the same. The third article (Chapter IV) focuses on lichens in a study area located further north. The field data used for this third chapter were collected by lichenologist Mireille Martel within the framework of this thesis project.

The additional review article included as Annex A was performed in parallel to the scientific chapters. The decision to include this review as annexe was based on its proximate topic but not closely linked to those of the main scientific chapters of this thesis. Specifically, it provides a synthesis on the use of remote sensing to detect and predict the occurrence of rare plants. I am the first author of this article as the main responsible for carrying out the systematic search, information extraction, production and interpretation of results, and the preliminary version of the manuscript. All co-authors, including my supervisors, Dr. Richard T. Caners, and Dr. Philippe Marchand contributed to its conceptualization and provided critical and constructive reviews of the manuscript

Chapter I. General introduction

Chapter II. Cerrejón, C., Valeria, O., Mansuy, N., Barbé, M., Fenton, N. J. (2020). Predictive mapping of bryophyte richness patterns in boreal forests using species distribution models and remote sensing data. *Ecological Indicators*, 119, 106826.

Chapter III. Cerrejón, C., Valeria, O., Muñoz, J., Fenton, N. J. (2021). Small but visible: Predicting rare bryophyte distribution and richness patterns using remote sensing-based ensembles of small models. *Plos one*, 17(1), e0260543.

Chapter IV. Cerrejón, C., Valeria, O., Fenton, N. J. (2022). Assessing alpha and beta diversity in inconspicuous species using satellite data at different spatial resolutions. In preparation for *Biological Conservation*.

Chapter V. General conclusion

Annex A. Cerrejón, C., Valeria, O., Marchand, P., Caners, R. T., Fenton, N. J. (2021). No place to hide: Rare plant detection through remote sensing. *Diversity and Distributions*, 27(6), 948-961.

TABLE OF CONTENTS

LIST OF FIGURES	xiv
LIST OF TABLES	xvii
LIST OF ABBREVIATIONS	xix
ABSTRACT	xxi
RÉSUMÉ	xxiv
CHAPTER I	1
1.1 Study organisms.....	1
1.2 Small but essential species: cryptogams and their ecological role	1
1.3 Underrepresentation of cryptogams in conservation planning	5
1.4 Conservation effectiveness resides in complementarity of biodiversity components	6
1.5 Use of remote sensing in cryptogam biodiversity assessments and its potential for conservation purposes.....	7
1.6 Boreal forests	10
1.7 Objectives	11
CHAPTER II.....	14
2.1 Abstract.....	15
2.2 Résumé	16
2.3 Introduction.....	17
2.4 Materials and methods	21
2.4.1 Study area	21
2.4.2 Species field data set.....	22
2.4.3 Environmental predictors.....	23
2.4.4 Statistical analyses	27
2.5 Results	33
2.5.1 Model performance.....	33
2.5.2 Predictors and their importance	35
2.5.3 Predictive mapping	36
2.6 Discussion.....	39
2.6.1 Predicting bryophyte richness patterns	39

2.6.2	Remote sensing predictors	40
2.6.3	Implications for conservation strategies	44
2.7	Conclusion	45
2.8	Acknowledgements.....	46
CHAPTER III		47
3.1	Abstract.....	48
3.2	Résumé	49
3.3	Introduction.....	50
3.4	Materials and methods.....	53
3.4.1	Bryophyte field data set	53
3.4.2	Remote sensing environmental predictors	55
3.4.3	Modeling approach: Ensembles of Small Models	59
3.4.4	Species traits characterization.....	61
3.5	Results	62
3.5.1	ESMs' predictive performance versus number of occurrences and bryophyte guilds	62
3.5.2	Richness patterns of rare bryophyte species	63
3.6	Discussion.....	65
3.7	Conclusions.....	68
3.8	Acknowledgements.....	69
CHAPTER IV		70
4.1	Abstract.....	71
4.2	Résumé	72
4.3	Introduction.....	74
4.4	Materials and methods.....	77
4.4.1	Study area	77
4.4.2	Lichen field data set.....	79
4.4.3	Environmental characterization of plots through remote sensing variables	82
4.4.4	Statistical analyses	84
4.5	Results	88
4.5.1	Describing lichen alpha diversity.....	88
4.5.2	Describing lichen beta diversity.....	91
4.6	Discussion.....	95

4.6.1	Lichen biodiversity and the influence of environmental variability at different scales.....	95
4.6.2	Assessing habitat types as lichen's biodiversity hotspots.....	96
4.6.3	Assessing lichen alpha and beta diversity and habitat types through remote sensing.....	98
4.7	Conclusions.....	102
4.8	Acknowledgements.....	103
CHAPTER V.....		104
5.1	Remote sensing as a tool to inform conservation actions in cryptogams: Possibilities for improvement are at hand.....	106
ANNEX A.....		111
A.1	Abstract.....	112
A.2	Résumé	114
A.3	Introduction.....	116
A.4	Methods	119
A.5	Remote sensing direct approach— Detection of rare plants.....	131
A.6	Remote sensing indirect approach— Prediction of rare plant distributions	133
A.6.1	Considerations of predictive performance measures for rare plants	136
A.7	Remote sensing based on the characteristics of rare plants	137
A.7.1	Morphology.....	137
A.7.2	Phenology.....	137
A.7.3	Physiology.....	139
A.7.4	Ecological niche.....	139
A.8	Relating rarity forms with model predictive performance.....	140
A.9	Conclusion	142
A.10	Acknowledgements.....	144
A.11	References.....	144
APPENDIX A Out-of-bag mean square error OOB MSE versus ntree, mtry and nodesize parameter values of the Random Forest regression models for bryophytes, mosses, liverworts and sphagna		156

APPENDIX B Modeled rare bryophyte species including their number of occurrences, ESMS' predictive performance, and species traits.....	157
APPENDIX C Species occurrence coordinates used for modeling	162
APPENDIX D Standardized predictor values used for modeling	179
APPENDIX E Re-scaled Lee's L bivariate spatial association between rare and overall bryophyte, moss, liverwort, and sphagna species richness	190
APPENDIX F Lichen species identified and used for modeling.....	191
APPENDIX G Pearson correlation coefficients among variable pairs at both targeted spatial resolutions	193
APPENDIX H List of microhabitats included	194
APPENDIX I Mantel test results between lichen species composition (Sørensen's dissimilarity) and microhabitat-based dissimilarity	195
APPENDIX J Species rarefaction curve	196
APPENDIX K Diagnostic graphs of the WV3 band model including outliers	197
APPENDIX L Diagnostic graphs of the WV3 EVI2 model including outliers	198
APPENDIX M Diagnostic graphs of the S2 band model including outliers	199
APPENDIX N Diagnostic graphs of the S2 EVI2 model including outliers	200
APPENDIX O Diagnostic graphs of the WV3 band model excluding outliers.....	201
APPENDIX P Diagnostic graphs of the WV3 EVI2 model excluding outliers	202
APPENDIX Q Diagnostic graphs of the S2 band model excluding outliers	203
APPENDIX R Diagnostic graphs of the S2 EVI2 model excluding outliers	204
APPENDIX S PCoA on lichen community composition (including outliers)	205
APPENDIX T Boxplots of microhabitat richness per habitat type.....	206

APPENDIX U Number of lichen species versus the number of habitat types in which they occur	207
APPENDIX V Boxplots of variables included in the models at both targeted spatial resolutions per habitat type	208
REFERENCES.....	209

LIST OF FIGURES

Figure	Page
1.1 Study areas of the three scientific articles included in this thesis corresponding to Chapters II, III and IV.	13
2.1 Study area and sampling plots (n = 326) in the boreal black spruce forest of eastern Canada	22
2.2 Observed versus predicted richness values (black points) of (A) total bryophytes, (B) mosses, (C) liverworts, and (D) sphagna. The dashed line represents a 1:1 relationship. Note that x-axes and y-axes are variable.	35
2.3 Predictor importance measures (%IncMSE) for regression models of (A) total bryophyte, (B) moss, (C) liverwort, and (D) sphagna richness.	36
2.4 Predictive cartography of (A) total bryophyte, (B) moss, (C) liverwort, and (D) sphagna richness for the study area at 30m resolution. Red colors correspond to areas predicted to be species rich, while yellow and blue colours correspond to areas predicted to harbour intermediate and low levels of richness. White areas on maps correspond to non-forest areas for which soil information was not available (Ministère des Forêts, de la Faune et des Parcs du Québec, 2018).	37
2.5 Maps of coefficient of variation associated to the predictive mapping of (A) total bryophyte, (B) moss, (C) liverwort, and (D) sphagna richness. Measures were derived from predictions of individual Random Forest trees at each pixel.	39
2.6 Relationship between the observed richness of total bryophytes, mosses, liverworts, and sphagna and their five best predictors (in decreasing order of importance from left to right; see Table 2.1 for predictor description).	44
3.1 A: Study area and sampling plots (n=389) in the boreal black spruce forest of western Quebec. B: Location of the study area within Quebec. C: Location of Quebec (eastern Canada).	54

3.2	Example of (A) continuous and (B) binary predictive mapping of the moss <i>Trematodon ambiguus</i> (Hedw.) Hornsch. for the study area at 30m spatial resolution.....	61
3.3	AUC values versus number of occurrences (Overall Pearson $r = -0.34$). Bryophyte guilds are indicated.	63
3.4	Mapping of (A) total rare bryophyte, (B) rare moss, (C) rare liverwort, and (D) rare sphagna richness (species number) for the study area at 30m resolution. Computed from stacked predicted rare species distributions.....	64
3.5	Correlation between rare and overall (A) bryophyte, (B) moss, (C) liverwort, and (D) sphagna species richness as measured by re-scaled Lee's L statistic for the study area of Cerrejón <i>et al.</i> (2020) at 300 m spatial resolution. "Positive" (blue) and "Negative"(red) indicate significant positive (quantile > 0.975) and negative (quantile < 0.025) Lee's L values derived from Monte Carlo test. Continuous values of the re-scaled Lee's L statistic are shown in Appendix E.	65
3.6	Boxplots of standardized uncorrelated predictors used for modeling. See Table 3.1 for predictor descriptions. Measurement units are indicated in parentheses. Unit abbrev.: DN, digital number; TOA, top-of-atmosphere reflectance.	66
4.1	Study area and sampling plots (n = 45) within the Eeyou Istchee James Bay region in Northern Quebec. Two plots were located outside the Eleonore Mine property.....	79
4.2	A: Boxplots of lichen richness per habitat type; different letters indicate significant differences in lichen richness among habitat types based on the Tukey test. B: Linear regression between lichen richness and microhabitat richness. Outliers were not included. Habitat type abbrev.: B, bog; B_B, bog burned; CF, coniferous forest; CF_B, coniferous forest burned; DF, deciduous forest; Fen, Fen; R, Rock.	89
4.3	Linear relationship between the observed lichen richness and the explanatory variables included in the models at both targeted spatial	

resolutions (WV3, WorldView-3 at 1.2m resolution; S2, Sentinel-2 at 10m resolution). Units of explanatory variables are expressed in digital numbers. See section 4.4.3 for explanatory variable description. Habitat type abbrev.: B, bog; B_B, bog burned; CF, coniferous forest; CF_B, coniferous forest burned; DF, deciduous forest; Fen, Fen; R, Rock.....	91
4.4 Principal coordinates analysis (PCoA) on lichen community composition based on the Sørensen's dissimilarity index. Habitat type abbrev.: B, bog; B_B, bog burned; CF, coniferous forest; CF_B, coniferous forest burned; DF, deciduous forest; Fen, Fen; R, Rock.....	92
4.5 Relationship between lichen species composition (Sørensen's dissimilarity) and microhabitat-based dissimilarity. Mantel coefficients (r and p-value) resulting from 999 permutations are indicated. See Appendix I for Mantel upper confidence limits.....	93
4.6 Generalized dissimilarity models of lichen beta diversity (Sørensen's dissimilarity) using spectral dissimilarity from the two different set of variables (Red + NIR; EVI2) at both targeted spatial resolutions (WV3, WorldView-3 at 1.2m resolution; S2, Sentinel-2 at 10m resolution). See section 4.4.3 for variable description.....	95
A.1 Distribution map of reviewed studies. Numbers correspond to those appearing in the column "location on map" in Table A.1.....	132
A.2 Classification of rarity forms showing the potential changes in model predictive performance (solid arrows), based on the three criteria used for such classification: geographic distribution range, habitat specificity, and local population size. The arrowhead indicates the direction of improvement (+) in predictive performance. Adapted from Rabinowitz (1981).....	142

LIST OF TABLES

Table	Page
2.1 Description of selected predictors by category and source used to model and predict total bryophyte (Bry), moss (Mos), liverwort (Liv), and sphagna (Sph) richness.....	29
2.2 Parameters and coefficients of regression models for total bryophyte richness and richness at the guild level (mosses, liverworts and sphagna) along with prediction coefficients resulting from their validation. See Table 2.1 for a description of predictors.	34
2.3 Coefficient of variation statistics associated to the predictive mapping of total bryophyte, moss, liverwort and sphagna richness shown in Figure 2.4 (see Figure 2.5 for coefficient of variation maps).....	38
3.1 Description of predictors by category and source. Uncorrelated predictors finally selected to model bryophyte distribution are shown in bold.	58
4.1 Habitat types sampled, abbreviation codes used in this study, number of plots, total number of species and description. Numbers in parentheses indicate the number of plots used for alpha and beta diversity analyses after removing outliers (see methods section).....	81
4.2 Remote sensing-based Poisson models of lichen richness (alpha diversity) tested in the present study. Significant variables are shown in bold. Models were computed from 42 plots after removing outliers.....	85
4.3 Results of PERMANOVA for lichen species composition (Sørensen's dissimilarity), microhabitat-based and spectral dissimilarities (based on both set of variables – Red + NIR; EVI2 – from both sensors – WV3, WorldView-3; S2, Sentinel-2) according to the habitat type based on 999 permutations. Groups of sampling units were defined by habitat type.....	93

A.1 Reviewed literature using remote sensing at very high, high, or medium resolutions to detect or predict the occurrence of rare plants. See Glossary Box for sensor and RS data/predictor abbreviations..... 121

LIST OF ABBREVIATIONS

AIC	Akaike Information Criterion
AICc	Second-order AIC
ALOS	Advanced Land Observing Satellite
AUC	Area Under the receiver operating characteristic Curve
BSI	Bare Soil Index
dNBR	Difference normalized burn ratio
ESMs	Ensemble of Small Models
EVI2	2-band Enhanced Vegetation Index
GDM	Generalized Dissimilarity Modeling
LiDAR	Light Detection and Ranging
NDVI	Normalized Difference Vegetation Index
NDWI	Normalized Difference Water Index
NIR	Near Infrared
PALSAR	Phased Array L-band SAR
PCoA	Principal Coordinates Analysis
RF	Random Forest
RS	Remote Sensing

S2	Sentinel-2
SDMs	Species Distribution Models
SRTM	Shuttle Radar Topography Mission
SWIR	Shortwave Infrared
TPI	Topographic Position Index
TSS	True Skills Statistic
VCF	Vegetation Continuous Fields
WV3	WorldView-3

ABSTRACT

Cryptogams (bryophytes and lichens) are ubiquitous non-vascular species that contribute significantly to total biodiversity and play an essential ecological role in ecosystem functioning worldwide. Specifically, cryptogams influence water, carbon and nutrient cycles, as well as physical and chemical weathering, and increase stability of soils, preventing their erosion and regulating their temperature and humidity. Cryptogams facilitate ecosystem recovery following disturbances, and provide microhabitats for micro- and macroorganisms, and a food source for invertebrates and herbivores. These species are also reliable and highly sensitive indicators to environmental disturbances and currently face numerous human-induced threats mainly derived from land use and climate change. Despite this, cryptogams are generally neglected in conservation planning mostly due to current knowledge gaps in their diversity, ecology and distribution, which jeopardizes the maintenance of their species and ecological role. New technologies and data sources such as remote sensing (RS) can significantly help to fill these gaps and ultimately improve the representation of cryptogams in systematic conservation planning. The contribution of RS to cryptogam biodiversity assessments can be particularly valuable in vast and largely unknown regions such as boreal forests, where these species and their habitats face increasing human-induced threats. The general objective of this thesis is to elucidate the role that RS can play in the evaluation and generation of information on cryptogam biodiversity in a boreal context. The study region is located in the Canadian boreal forest, within the Eeyou-Istchee James Bay region in Northern Quebec. As specific objectives, Chapter II aims to predict and map diversity (species richness) patterns of i) total bryophytes, and ii) bryophyte guilds (mosses, liverworts and sphagna) using RS data; Chapter III focusses on producing predictive models of rare bryophyte species using RS-derived predictors in an Ensembles of Small Models (ESMs) framework; and Chapter IV is intended to describe and model the lichen alpha diversity (species richness) and beta diversity (species turnover) components parallelly using two set of RS-derived variables (Red and NIR; EVI2) from two sensors (Worldview-3, WV3; Sentinel-2, S2) at different high spatial resolutions (1.2m; 10m), and ii) to identify which habitat types represent lichen biodiversity hotspots.

The Random Forest algorithm used in Chapter II allowed us to develop spatially explicit models and to generate predictive cartography at 30m resolution of total bryophyte, moss, liverwort and sphagna richness. These models explained a significant fraction of the variation in total bryophyte and guild level richness, both in the calibration (42 to 52%) and validation sets (38 to 48%), and consistently identified vegetation (mainly NDVI) and climatic variables (temperature, precipitation, and freeze-thaw events) as the most important predictors for all bryophyte groups modeled. Guild-level models identified differences in important factors determining the richness

of each of the guilds and thus in their predicted richness patterns, which provide valuable information for management and conservation strategies for bryophytes. The RS-based ESMs developed in Chapter III built from Random Forest and Maxent techniques using predictors related to topography (TPI) and vegetation (EVI2, NDWI1, Vegetation Continuous fields, and PALSAR HVHH) yielded poor to excellent prediction accuracy ($AUC > 0.5$) for 38 of the 52 modeled species despite their low number of occurrences (< 30), with AUC values > 0.8 for 19 species. The actual presences of the 38 species modeled better than random ($AUC \leq 0.5$) were accurately predicted, as supported by the high sensitivity values obtained that ranged from 0.8 to 1 with an average of 0.959 ± 0.063 . The distribution of these 38 species and the richness patterns both for total rare bryophytes and rare species at the guild level were mapped at 30m resolution. Chapter III also revealed a spatial concordance between rare (present chapter) and overall bryophyte richness patterns (Chapter II) in different regions of the study area, which has important implications for conservation planning. In Chapter IV, a total of 116 lichen species were identified. While high lichen richness was generally found across our plots (36.5 ± 9 species), those richer in microhabitats often harbored more species ($R^2 = 0.22$) regardless of the habitat type. Differences in species composition were identified among plots (25.6% explained by PCoA) and habitat types (PERMANOVA $R^2 = 0.35$), both being supported by differences in microhabitat composition (Mantel $r = 0.22$ and PERMANOVA $R^2 = 0.29$, respectively). Rocky outcrops and undisturbed coniferous forests represented the main lichen biodiversity hotspots, while other habitat types were also important for maintaining overall biodiversity. Red and NIR variables were effective for modeling alpha and beta diversity at both resolutions, while EVI2, either from WV3 or S2, was only informative for assessing beta diversity. Poisson models explained up to 32% of the variation in lichen richness. Generalized dissimilarity models described well the relationship between beta diversity and spectral dissimilarity (R^2 from 0.25 to 0.30), except for the S2 EVI2 model ($R^2 = 0.07$), confirming that more spectrally and thus environmentally different areas tend to harbor different lichen communities. While WV3 often outperformed the S2 sensor, the latter still provides a powerful tool for the study of lichens and their conservation.

This thesis demonstrated the ability for RS at medium and high spatial resolutions to characterize the habitat of inconspicuous cryptogam species, to capture diverse meaningful ecological features shaping their distribution, and thus to better understand and/or predict their biodiversity patterns. RS-based modeling frameworks proved to be informative even when the available baseline information on cryptogam biodiversity was limited. By identifying environmental drivers of cryptogam biodiversity that can guide specific management actions, and by providing predictive mapping of their spatial patterns at high level of detail across the landscape, this work unequivocally highlighted the high potential of RS technology for conservation purposes of

cryptogams. This thesis thus represents a very important step to achieve the inclusion of these inconspicuous and generally overlooked species into systematic conservation planning.

Keywords: Alpha diversity; Beta diversity; Biodiversity components; Black spruce forests; Boreal forests; Conservation; Digital mapping; Machine learning; Predictive modeling; Rarity; Remote sensing predictors; Satellite sensors; SDMs; Unseen biodiversity.

RÉSUMÉ

Les cryptogames (bryophytes et lichens) sont des espèces non vasculaires omniprésentes qui contribuent de manière significative à la biodiversité et jouent un rôle écologique essentiel dans le fonctionnement des écosystèmes à l'échelle mondiale. Plus précisément, les cryptogames influencent les cycles de l'eau, du carbone et des nutriments, ainsi que l'altération physique et chimique des roches, et augmentent la stabilité des sols, empêchant leur érosion et régulant leur température et humidité. Les cryptogames facilitent le rétablissement des écosystèmes après des perturbations et fournissent des microhabitats pour des micro- et macro-organismes, ainsi qu'une source de nourriture pour des invertébrés et herbivores. Ces espèces sont également des indicateurs fiables mais très sensibles aux perturbations environnementales et sont actuellement confrontées à de nombreuses menaces d'origine humaine principalement dérivées de l'utilisation des terres et du changement climatique. Malgré cela, les cryptogames sont généralement négligés dans la planification de la conservation, principalement en raison des lacunes actuelles dans les connaissances sur leur diversité, écologie et distribution, ce qui met en péril le maintien de leur espèces et rôle écologique. Les nouvelles technologies et sources de données telles que la télédétection peuvent contribuer de manière significative à combler ces lacunes et, en fin de compte, à améliorer la représentation des cryptogames dans la planification systématique de la conservation. La contribution de la télédétection aux évaluations de la biodiversité des cryptogames peut être particulièrement précieuse dans des régions vastes et largement inconnues telles que les forêts boréales, où ces espèces et leurs habitats sont confrontés à des menaces croissantes d'origine humaine. L'objectif général de cette thèse est d'élucider le rôle que peut jouer la télédétection dans l'évaluation et la génération d'informations sur la biodiversité des cryptogames en contexte boréal. La région d'étude est située dans la forêt boréale canadienne, dans la région d'Eeyou-Istchee Baie-James dans le Nord du Québec. En tant qu'objectifs spécifiques, le chapitre II vise à prédire et à cartographier les patrons de diversité (richesse en espèces) i) des bryophytes totaux et ii) des guildes de bryophytes (mousses, hépatiques et sphaignes) à l'aide de données de télédétection; le chapitre III se concentre sur la production de modèles prédictifs d'espèces de bryophytes rares à l'aide de prédicteurs dérivés de la télédétection dans un cadre d'ensembles de petits modèles; et le chapitre IV est destiné à décrire et modéliser les composantes alpha (richesse des espèces) et beta (changements de composition de la communauté) de la biodiversité des lichens en utilisant en parallèle deux ensembles de variables dérivées de la télédétection (Red et NIR; EVI2) à partir de deux capteurs (Worldview-3 , WV3 ; Sentinel-2, S2) à différentes résolutions spatiales élevées (1,2 m ; 10m), et ii) à identifier les types d'habitats qui représentent les points chauds de la biodiversité des lichens.

L'algorithme Random Forest utilisé dans le chapitre II nous a permis de développer des modèles spatialement explicites et de générer une cartographie prédictive à 30m de résolution de la richesse totale en bryophytes, mousses, hépatiques et sphaignes. Ces modèles expliquent une fraction importante de la variation de la richesse totale en bryophytes et au niveau de la guildes, à la fois dans les ensembles de calibration (42 à 52 %) et de validation (38 à 48 %), et identifient systématiquement la végétation (principalement NDVI) et les variables climatiques (température, précipitations et événements de gel-dégel) comme les prédicteurs les plus importants pour tous les groupes de bryophytes modélisés. Les modèles au niveau de la guildes ont identifié des différences dans des facteurs importants déterminant la richesse de chacune des guildes et donc dans leurs modèles de richesse prédits, qui fournissent des informations précieuses pour les stratégies de gestion et de conservation des bryophytes. Les ensembles de petits modèles basés sur la télédétection développés au chapitre III construits à partir des techniques Random Forest et Maxent en utilisant des prédicteurs liés à la topographie (TPI) et à la végétation (EVI2, NDWI1, Vegetation Continuous fields et PALSAR HVHH) ont donné une précision de prédiction de faible à excellente ($AUC > 0.5$) pour 38 des 52 espèces modélisées malgré leur faible nombre d'occurrences (< 30), avec des valeurs $AUC > 0.8$ pour 19 espèces. Les présences réelles des 38 espèces modélisées mieux que aléatoires ($AUC \leq 0.5$) ont été prédites avec précision, comme en témoignent les valeurs de sensibilité élevées obtenues allant de 0.8 à 1 avec une moyenne de 0.959 ± 0.063 . La distribution de ces 38 espèces et les patrons de richesse à la fois pour les bryophytes rares totales et les espèces rares au niveau de la guildes ont été cartographiés à une résolution de 30m. Le chapitre III a également révélé une concordance spatiale entre les patrons de richesse en bryophytes rares (chapitre présent) et totaux (chapitre II) dans différentes régions de la zone d'étude, ce qui a des implications importantes pour la planification de la conservation. Au chapitre IV, un total de 116 espèces de lichens ont été identifiées. Alors qu'une grande richesse en lichens était généralement observée dans nos parcelles (36.5 ± 9 espèces), celles plus riches en microhabitats abritaient souvent plus d'espèces ($R^2 = 0.22$) quel que soit le type d'habitat. Des différences dans la composition des espèces ont été identifiées entre les parcelles (25.6 % expliquées par la PCoA) et les types d'habitats (PERMANOVA $R^2 = 0.35$), tous deux étayés par des différences dans la composition des microhabitats (Mantel $r = 0.22$ et PERMANOVA $R^2 = 0.29$, respectivement). Les affleurements rocheux et les forêts de conifères non perturbées représentaient les principaux points chauds de la biodiversité des lichens, tandis que d'autres types d'habitats étaient également importants pour le maintien de la biodiversité totale. Les variables Red et NIR étaient efficaces pour modéliser la diversité alpha et bêta aux deux résolutions, tandis que EVI2, soit de WV3 ou S2, n'était informatif que pour évaluer la diversité bêta. Les modèles de Poisson expliquaient jusqu'à 32% de la variation de la richesse en lichens. Les modèles de dissimilarité généralisée décrivaient bien la relation entre la diversité bêta et la dissimilarité spectrale (R^2 de 0.25 à 0.30),

sauf pour le modèle S2 EVI2 ($R^2 = 0.07$), confirmant que des zones plus spectralement et donc environnementales différentes ont tendance à abriter différentes communautés de lichens. Alors que WV3 a souvent surpassé le capteur S2, ce dernier fournit toujours un outil puissant pour l'étude des lichens et leur conservation.

Cette thèse a démontré la capacité de la télédétection à moyenne et haute résolution spatiale à caractériser l'habitat d'espèces cryptogames discrètes, à capturer diverses caractéristiques écologiques significatives façonnant leur distribution, et ainsi à mieux comprendre et/ou prédire leurs patrons de biodiversité. Les cadres de modélisation basés sur la télédétection se sont avérés informatifs même lorsque les informations de base disponibles sur la biodiversité des cryptogames étaient limitées. En identifiant les facteurs environnementaux de la biodiversité des cryptogames qui peuvent guider des actions de gestion spécifiques et en fournissant une cartographie prédictive de leurs patrons spatiaux à un niveau de détail élevé à travers le paysage, ce travail a mis en évidence sans équivoque le potentiel élevé de la technologie de télédétection à des fins de conservation des cryptogames. Cette thèse représente donc une étape très importante pour parvenir à l'inclusion de ces espèces discrètes et généralement négligées dans la planification systématique de la conservation.

Mots clés: Apprentissage automatique; Biodiversité inaperçue; Capteurs satellitaires; Cartographie numérique; Composantes de la biodiversité; Conservation; Diversité alpha; Diversité bêta; Forêts boréales; Forêts d'épinettes noires; Modélisation prédictive; Prédicteurs de télédétection; Rareté; SDMs.

CHAPTER I

INTRODUCTION

1.1 Study organisms

The present thesis targets bryophytes and lichens as study organisms. Both taxonomic groups are part of the group of cryptogams, which has traditionally encompassed those plants (in the wide sense of the word) that reproduce through spores instead of seeds and which therefore also includes algae, ferns and fungi. In fact, the Latin term "Cryptogamae", which derives from the Greek roots κρυπτός (kryptos) and γάμος (gamos), means "hidden sexual reproduction". This concept, however, lacks taxonomic value due to the polyphyletic origin of the above-mentioned groups. Taking this into account and for brevity reasons, the term "cryptogam" will be used throughout this thesis to refer jointly but exclusively to bryophytes and lichens, which are known to share important physiological similarities as well as ecological attributes and roles.

1.2 Small but essential species: cryptogams and their ecological role

Cryptogams (bryophytes and lichens) are ubiquitous small-size non-vascular species that contribute significantly to total biodiversity worldwide (approximately 25,000 and 20,000 species, respectively; Hawksworth and Lücking, 2017; Li and Chang, 2021; Lücking *et al.*, 2017). Cryptogams are descendants of green algae and belong to the first photoautotrophic multi-cellular eukaryotes colonising terrestrial habitats (Lakatos, 2011; Simpson, 2010). They share a poikilohydric physiology allowing them to survive in a wide range of environmental conditions, including biomes with extreme environments such as hot and cold deserts (Lakatos, 2011; Robinson *et al.*, 2003). Cryptogams occur on highly diverse microhabitats ranging from soils to leaves, bark, rocks, or even substrates of anthropogenic origin. Bryophytes and lichens are however phylogenetically distinct. Bryophytes form a monophyletic group of non-vascular

plants *sensu stricto*, as they present plant tissues (leaves-like and stem-like structures) and enclosed reproductive systems (archegonium, antheridium) but with water- and food-conducting tissues lacking lignin (Lakatos, 2011; Su *et al.*, 2021). Unlike all other land plants, bryophytes have a dominant haploid gametophyte whereas the sporophyte, nutritionally dependent on the gametophyte, is small and ephemeral (Simpson, 2010). Bryophytes are composed of three monophyletic lineages, namely mosses, liverworts, and hornworts, which display diverse morphologies ranging from thalloid to leaf possessing structures (Goffinet and Shaw, 2000; Simpson, 2010). Beyond their phylogenetic differentiation, these lineages are made up of species that generally share ecological preferences and tolerances which are commonly known as guilds. Sphagna species, which are included in the clade of mosses, are frequently considered as another independent guild based on their distinctive taxonomical and functional traits (e.g. Fenton and Bergeron, 2006, 2008). Lichens, meanwhile, form a polyphyletic group composed by mutualistic symbiotic organisms that have traditionally comprised a fungal mycobiont and one or more photobiont partners (photosynthetic algae and/or cyanobacteria; Lakatos, 2011).

Lichens do not present plant tissues and the chloroplasts are exclusively contained in their photobiont partners, which are found extracellularly within the lichen thallus. The fungal mycobiont provides the photobiont with structure, protection, nutrients, and water, while the photobiont provides the fungal mycobiont with carbohydrates from photosynthesis. Approximately 85% of the symbiosis in lichens is made with a green algae partner, 10% with cyanobacteria, and 3-4% with both photobiont types (Honegger, 1998). A recent research showed that a second fungus, namely a basidiomycete yeast, can also be involved in the symbiosis, being found in the peripheral cortex of lichens (Spribille *et al.*, 2016), although the circumstances associated with its appearance are not yet clear (Lendemmer *et al.*, 2019). The whole organism of the lichen is often referred as the holobiont, which is mainly differentiated

into three growth forms ranging from foliose (leaf-like with discernable lower or upper surfaces) to fruticose (shrub-like without discernable upper and lower surfaces), and crustose (crust directly attached to a substrate and thus with only the upper cortical surface; Asplund and Wardle, 2017). Foliose and fruticose lichens are commonly referred as macrolichens, while crustose lichens, whose discriminating characteristics are not normally visible to the human eye, are known as microlichens.

Cryptogams play an essential ecological role in water, carbon and nutrient cycles, as well as in physical and chemical weathering (Adamo and Violante, 2000; Porada *et al.*, 2014, 2018). Specifically, these species significantly influence global rainfall interception and evaporation, being also able to uptake water from fog, dew or snow melt, and thus influencing hydrologic cycling and climate at different scales (Belnap and Lange, 2001; Porada *et al.*, 2018). They represent important carbon reservoirs, particularly in northern latitude ecosystems, thus mitigating the adverse effects of climate change (Bond-Lamberty and Gower, 2007; Bond-Lamberty *et al.*, 2004; O'Neill, 2000; Turetsky *et al.*, 2010). They also strongly influence nutrient flows through nitrogen fixation and phosphorus uptake, incorporating them into the biosphere and thus making them accessible to other organisms (Porada *et al.*, 2014; Turetsky, 2003). Cryptogams also increase the stability of soils by creating a protective and insulating layer that prevents soil erosion and regulates their temperature and humidity (Belnap and Lange, 2001). At the same time, this favors the preservation of permafrost in arctic and subarctic areas, promoting the ecosystem resistance to climate change (Bokhorst *et al.*, 2012; Porada *et al.*, 2016; Turetsky *et al.*, 2010). Moreover, pioneer cryptogam species allow the colonization of newly exposed surfaces resulting from both natural and anthropogenic disturbances, which is essential to reach more advanced succession stages and thus for ecological functional recovery (Cutler, 2010; Hugron *et al.*, 2011; Ryömä and Laaka-Lindberg, 2005). This is due to their capability to survive in extreme environments (very cold, dry or nutrient-poor) thanks to their ability to

withstand desiccation events as poikilohydric organisms, as well as their generally low dependence from the substrate for nutrient uptake (Belnap and Lange, 2001; Proctor *et al.*, 2007; Song *et al.*, 2016; Takezawa, 2018). Furthermore, they provide microhabitats for a broad diversity of micro- and macroorganisms, and a food source for invertebrates and herbivores, including emblematic and threatened species such as the caribou (*Rangifer tarandus*; Boertje, 1984; Longton, 1992; Nash, 2008). Cryptogams are also recognized as reliable bioindicators of environmental contamination, forest naturalness, and ecological continuity (Brunialti *et al.*, 2010; Czerepko *et al.*, 2021; Frego, 2007; Seaward, 2004).

Since cryptogams are highly sensitive to environmental disturbances, cryptogam species and the functions they support are currently facing numerous threats mainly derived from the increase in intensity and extent of human development activities worldwide, but also from global climate change (Bokhorst *et al.*, 2012; Chuquimarca *et al.*, 2019; Vellak and Ingerpuu, 2005). More precisely, land use changes and forest resource extraction are leading to the degradation and loss of cryptogam habitats, thereby reducing habitat continuity and/or connectivity (Hallingbäck and Hodgetts, 2000; Pykälä, 2019), and inducing significant changes in their diversity and community composition (Chuquimarca *et al.*, 2019; Newmaster and Bell, 2002; Ross-Davis and Frego, 2002). While the impacts of climate change have been less documented, growing evidence shows that cryptogams are undergoing changes in their distributions, abundances and community composition as a result of global warming (e.g. Aptroot, 2009; Bergamini *et al.*, 2009; Cornelissen *et al.*, 2001; Frahm and Klaus, 2001; Walker *et al.*, 2006). In consequence, efforts directed at the study and preservation of these ecologically important but vulnerable species should be a current priority.

1.3 Underrepresentation of cryptogams in conservation planning

While some valuable efforts have been made in the last decades to increase the representativeness of cryptogams in conservation planning (e.g. Faubert *et al.*, 2010; Goward *et al.*, 1998; Vanderpoorten *et al.*, 2005), they are still often neglected, jeopardizing not only these species but also their ecological role (McMullin, 2015; Scheidegger and Goward, 2002; Vanderpoorten and Hallingbäck, 2009). This is mainly due to their small size and inconspicuousness, which has historically fostered low recognition by conservation authorities and managers, politicians and the broader public (Scheidegger and Goward, 2002).

The main challenge to achieve the systematic integration of cryptogams in conservation planning lies in filling the current knowledge gaps existing on their diversity, ecology and distribution, which is an essential requirement to develop and implement effective management and conservation measures (McMullin, 2015). The increasing anthropogenic pressure on species worldwide and the continuing advance of climate change have increased the need to develop and apply new technologies and data sources in the field of ecology in order to efficiently and quickly meet conservation and monitoring targets. In this sense, relatively new research areas such as remote sensing (see section 1.5) or citizen science are called upon to play a central role as informative tools for conservation, especially in the case of inconspicuous and neglected species such as cryptogams (Cerrejón *et al.*, 2020, unpublished; Feldman *et al.*, unpublished). Specifically, cryptogams can benefit from citizen science for two main reasons. First, citizen science can raise public awareness of these species through the participation and contribution of volunteers in scientific studies. Secondly, this approach allows the acquisition and generation of information related to cryptogams of a very diverse nature, encompassing scopes as varied as biodiversity monitoring, effects of land-use changes, environmental contamination, conservation of species at risk, and so on (Feldman *et al.*, unpublished). Therefore, the possibility of approaching the broad non-scientific

public to the hidden biodiversity through the citizen science may be key for the future preservation of cryptogam species.

1.4 Conservation effectiveness resides in complementarity of biodiversity components

Biodiversity can be split in multiple components, while the most traditionally used in the literature are those defined by Whittaker (1960): i) alpha diversity, which refers to species richness within homogeneous sampling units in the landscape; ii) beta diversity, which describes community composition changes or species turnover between those units; and iii) gamma diversity, which corresponds to the overall species diversity in the landscape, resulting from the combination of alpha and beta diversities from all sampling units. Rare species represent another fundamental component of biodiversity, not only for their significant contribution to total species richness and functional diversity (Bracken and Low, 2012; Kearsley *et al.*, 2019; Leitao *et al.*, 2016; Mouillot *et al.*, 2013; Patykowski *et al.*, 2018; Rejžek *et al.*, 2016; Umaña *et al.*, 2017), but also for their ecological importance (Dee *et al.*, 2019; Hooper *et al.*, 2012; Jolls *et al.*, 2019; Soliveres *et al.*, 2016; Xu *et al.*, 2020; Zavaleta and Hulvey, 2004) and vulnerability to extinction (Sykes *et al.*, 2019; Weisser *et al.*, 2017; Zhang, 2019). More specifically, rare species refer to those species restricted either in geographic distribution range, prevalence, environmental conditions and/or abundance (Faubert *et al.*, 2010; Flather and Sieg, 2007; Porley, 2013; Rabinowitz, 1981). The study of the above-mentioned biodiversity components can provide very valuable information for the preservation of inconspicuous and less studied taxa such as cryptogams. However, as these biodiversity components are complementary, their joint assessment allows to increase the robustness of biodiversity estimates and thus the development of more effective management and conservation measures.

1.5 Use of remote sensing in cryptogam biodiversity assessments and its potential for conservation purposes

Remote sensing (hereafter RS) is a detection method of electromagnetic radiation coming from the earth surface through satellites or aircraft sensors which produces overhead-perspective images from which it is possible to derive information about Earth's land and water surfaces (Campbell and Wynne, 2011; Turner *et al.*, 2003;). This information can be used to assess biodiversity over large areas at regular intervals of time. Biodiversity can be studied using two different RS approaches, namely direct and indirect. The direct approach consists in detecting species by directly capturing their spectral information. The indirect approach, in contrast, is not focused on the species but on its habitat. More precisely, the indirect approach makes it possible to characterize the habitats where the species occur and to analyse this information through statistical and modeling tools to assess species-environment relationships and to spatialize biodiversity estimates across the landscape.

Both RS approaches can provide interesting and powerful tools for the study of cryptogams. However, since cryptogams are very small species located in the understory and normally covered by other vegetation layers (Yang *et al.*, 2006), the applicability of the direct approach is often limited. Specifically, the direct approach is restricted to non-forest areas, and even in those areas, cushions of cryptogams large enough and very high spatial resolution RS imagery are required to achieve their direct detection. Therefore, studies using the RS direct approach on cryptogams have been located mainly in Arctic and Antarctic regions and have focused almost exclusively on mapping their cover or health status (Cerrejón *et al.*, unpublished). Fortunately, the indirect approach provides a powerful alternative for the study of cryptogams under environmental conditions where their direct detection is not possible. In terms of potential and applicability in conservation, this approach is very attractive for several reasons: i) it allows the evaluation of a wide variety of cryptogam-related aspects,

including their main biodiversity components, i.e., alpha and beta diversity, and the presence of rare species; ii) the development and test of a large array of RS-based indicators as potential drivers of biodiversity related to different environmental features (topography, vegetation, moisture, geology, etc.; Annex A; Cerrejón *et al.*, 2021a), iii) the spatialization of biodiversity estimates at a fine level of detail (spatial resolution) and at scales relevant to ecological planning, iv) it can be applied to all types of environments, including forest landscapes, which normally harbor high cryptogam diversity (e.g. Benítez *et al.*, 2015; Jonsson and Esseen, 1990) but also suffer the impacts of increasing anthropogenic pressure worldwide (Benítez *et al.*, 2012, 2015; Mansuy *et al.*, 2020; Riffo-Donoso *et al.*, 2021); and v) it provides a cost-effective approach, since it does not require the purchase of very high resolution RS imagery. All this makes RS, and in particular its indirect approach, a tool designed to improve our understanding on cryptogam biodiversity and thus to facilitate their integration in systematic conservation planning.

Despite its potential benefits, only a few relatively recent studies have so far used the RS indirect approach for the study of cryptogam alpha and beta biodiversity components, and none for the presence of rare species (Cerrejón *et al.*, unpublished). Most of these articles have assessed the performance of a single or a few RS variables for answering specific questions. More precisely, RS has been used to assess the performance of the Light Detection and Ranging (LiDAR)-derived depth-to-water index to detect the moisture gradient and, ultimately, its influence on bryophyte cover, richness, diversity and composition across boreal forest types (Bartels *et al.*, 2018) and different levels of harvest retention (Bartels *et al.*, 2019); the importance of snow persistence, as captured by the Normalized Difference Snow Index (NDSI), as predictor of cryptogams species distributions and community composition in Finnmark (Norway; Niittynen and Luoto, 2018); and the recovery dynamics of cryptogams (cover, richness and composition) after fires characterized through either Difference

Normalized Burn Ratio (dNBR), relativized dNBR (RdNRB) or traditional colour images (Hammond *et al.*, 2019; Root *et al.*, 2017; Whitehead and Baines, 2018). Studies testing a larger set of RS variables were almost exclusively aimed at evaluating and predicting cryptogam richness in Switzerland. Two of these articles were carried out combining RS and non-remotely sensed variables as models' inputs. Specifically, modest to relatively good predictions were achieved for specific cryptogam subgroups, namely edaphic bryophytes and epiphytic lichens (R^2 of 0.40 and 0.23, respectively; Camathias *et al.*, 2013), and for overall bryophyte and forest species richness (R^2 of 0.24 and 0.20, respectively; Zellweger *et al.*, 2015). On the other hand, RS data alone from high resolution satellite and airborne sensors provided accurate predictions of total ($R^2 = 0.58$), tree ($R^2 = 0.79-0.80$), rock ($R^2 = 0.54-0.56$) and soil lichen richness ($R^2 = 0.48-0.50$; Waser *et al.*, 2004, 2007). A recent study performed in New Brunswick (Canada), however, demonstrated the usefulness of LiDAR alone to derive a wide set of environmental variables and identify the main drivers of bryophyte richness and composition across a variety of mature, managed or unmanaged, forest habitat types (Bourgouin *et al.*, 2022). This allowed the authors to provide accurate predictions of bryophyte richness ($R^2 = 0.30$) and composition ($R^2 = 0.71$). Beyond alpha and beta diversity assessments, additional works have also followed a RS indirect approach to jointly estimate the probability of occurrence of certain bryophyte guilds/groups, namely epiphyllous liverworts (Jiang *et al.*, 2013, 2014) or *Sphagnum* spp. (Harris and Baird, 2019), and to map the distribution of the invasive moss *Campylopus introflexus* (Hedw.) Brid. (Skowronek *et al.*, 2017, 2018).

While the aforementioned works have provide valuable insights on the use of RS technology for the study of cryptogams, their applicability for conservation issues can often be limited by the costs associated to the high resolution RS data acquisition, either from satellite or airborne sensors (e.g. LiDAR), as well as by their limited spatial coverage, which can lead to a low representativeness of the results with respect to the

scale at which conservation planning is carried out. Likewise, the low prevalence of studies focusing on the main biodiversity components (alpha and beta diversity), either in bryophytes or lichens, and the total absence of studies regarding rare species, highlights that more effort should be made to assess the role that RS can play in the assessment and conservation of cryptogam communities.

1.6 Boreal forests

Circumboreal forests are the largest terrestrial biome in the world, constituting 14 million km² (32%) of the global forest cover (Burton *et al.*, 2003). These forests are found in the northernmost regions of North America, Europe and Asia, which are mainly characterised by a cold continental climate with harsh snowy winters and a short growing season. The terrain presents a generally gently relief, with wet and cold soils often poorly drained, leading to a mosaic of forests intersperse with wetlands across the boreal landscape (Burton *et al.*, 2003). The presence of permafrost, i.e. permanently frozen soils, is more notable towards high latitudes of the boreal biome. Boreal forest dynamics are mainly driven by natural disturbances (wildfires, insect outbreaks) and succession (Burton *et al.*, 2003; Lecomte *et al.*, 2006), although anthropogenic activities such as logging are also a notable influential factor (Cyr *et al.*, 2009).

In terms of vegetation, the boreal biome is mainly dominated by coniferous forests, while mixed and deciduous forests are also present. The diversity of tree species is however relatively low and limited to a few coniferous (*Pinus*, *Larix*, *Picea*, *Abies*) and broadleaf genera (*Betula*, *Populus*, *Salix*, *Alnus*, *Sorbus*; Burton *et al.*, 2003). In contrast, inconspicuous species such as cryptogams constitute a highly diverse and abundant group (Androsova *et al.*, 2018; Jonsson and Esseen, 1990; Turetsky *et al.*, 2010, 2012). The ecological role played by cryptogams worldwide (see section 1.2) extends to the boreal biome, where their influence on ecosystem functioning and service provision has been widely documented (e.g. Bond-Lamberty and Gower, 2007;

Bond-Lamberty *et al.*, 2004; Kivinen *et al.*, 2010; Nilsson and Wardle, 2005; Turetsky, 2003; Turetsky *et al.*, 2012). Cryptogams are however part of the extensive unseen biodiversity found in boreal forests for which ecology and distribution information is deficient. Documentation on these aspects is therefore crucial to ensure the preservation of these species and the ecosystem functions they support.

Due to the human-induced threats currently faced by cryptogams and their habitats in boreal forests (mostly related to forest management; Boudreault *et al.*, 2018; Dettki and Esseen, 2003; Johansson, 2008; Venier *et al.*, 2014), obtaining and generating new information on these species has become a top priority. Unfortunately, the acquisition of information on cryptogams in boreal forest regions is greatly limited by the paucity of specialized bryologists and lichenologists as well as the vastness and/or inaccessibility of many forest areas. At the same time, however, these vast and largely unknown regions provide a valuable opportunity for the development and application of new approaches and techniques aimed at acquiring new and/or updated biodiversity-related information quickly and efficiently such as RS. Until now, RS studies encompassing cryptogams in boreal forests have been very rare (Bartels *et al.*, 2018, 2019; Hammond *et al.*, 2019; Niittynen and Luoto, 2018) and have focused on relatively specific ecological questions (see section 1.5 for more details). While these works can inform management actions for cryptogams, they can be of limited use for achieving the systematic conservation of these species.

1.7 Objectives

The general objective of this thesis is to elucidate the role that RS can play in the evaluation and generation of information on cryptogam biodiversity in a boreal context. This objective is determined by the need to achieve a systematic integration of inconspicuous species such as cryptogams in conservation planning as well as to develop tools that allow obtaining and generating valuable information for these

purposes. All the studies included in this thesis (Chapters II, III and IV) are located in the Canadian boreal forest, more specifically within the Eeyou-Istchee James Bay region in Northern Quebec (Figure 1.1). This region includes extensive areas of boreal forest in which there are still important knowledge gaps on cryptogams, although important efforts for their study have been made in recent years (Barbé *et al.*, 2017; Castonguay, 2016; Route, 2020).

Bryophytes and lichens are studied in separate chapters in this thesis, while satellite RS data is used for the development of all of them. More specifically, and in terms of biodiversity components, bryophyte alpha diversity and rare species are respectively targeted in Chapters II and III, while lichen alpha and beta diversity are assessed in Chapter IV. The specific objectives of these three chapters are the following:

- Chapter II: To predict and map diversity patterns (in terms of species richness) of i) total bryophytes, and ii) bryophyte guilds (mosses, liverworts and sphagna) using RS data.
- Chapter III: To produce predictive models of rare bryophyte species using RS-derived predictors in an Ensembles of Small Models (ESMs) framework. Additionally, we assess i) if there is a relationship between the number of occurrences and the predictive performance of ESMs, ii) if the predictive performance of models varies by the modeled bryophyte guild (mosses, liverworts and sphagna), and iii) if there is a spatial relationship between the richness patterns of rare bryophyte species (from the present chapter) and overall bryophyte species (from Chapter II) both for bryophytes as a whole and at the guild level.
- Chapter IV: i) to describe and model the lichen alpha diversity (in terms of species richness) and beta diversity (species turnover) biodiversity components

using high resolution RS-derived variables, and ii) to identify which habitat types represent lichen biodiversity hotspots.

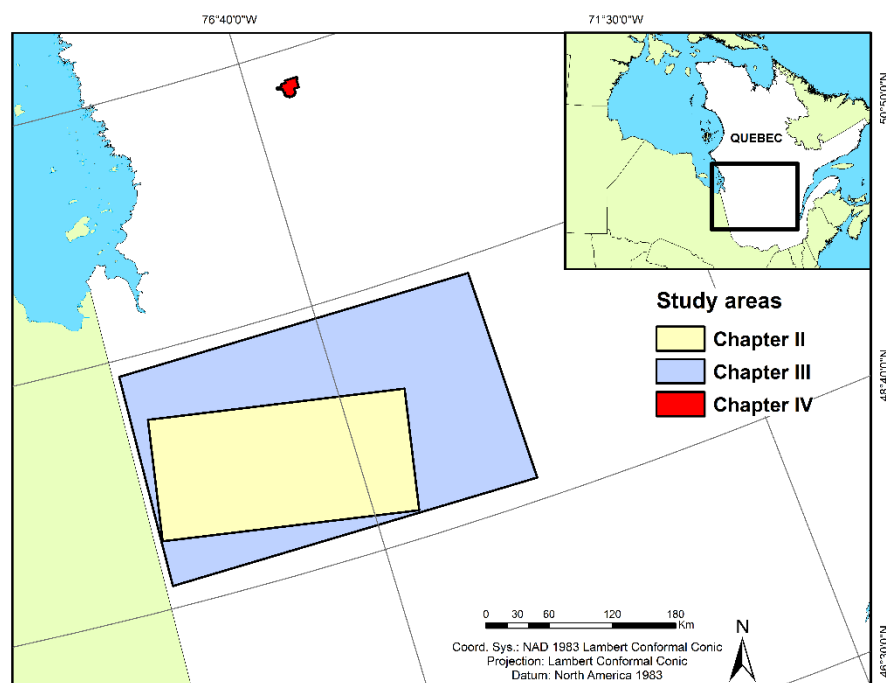


Figure 1.1 Study areas of the three scientific articles included in this thesis corresponding to Chapters II, III and IV.

CHAPTER II

PREDICTIVE MAPPING OF BRYOPHYTE RICHNESS PATTERNS IN BOREAL FORESTS USING SPECIES DISTRIBUTION MODELS AND REMOTE SENSING DATA

Carlos Cerrejón^{1,*}, Osvaldo Valeria¹, Nicolas Mansuy², Marion Barbé³ and
Nicole J. Fenton¹

¹ Institut de recherche sur les forêts, Université du Québec en Abitibi-Témiscamingue,
445 boul. de l'Université, Rouyn-Noranda, Québec, J9X 5E4, Canada

² Natural Resources Canada, Canadian Forest Service, Northern Forestry Centre, 5320
122 st. Edmonton, Alberta, T6H 3S5, Canada

³ Exploramex, 1 rue du Quai, Sainte-Anne-des-Monts, Québec, G4V 2B6, Canada

* Corresponding author: carlos.cerrejonlozano@uqat.ca

Ecological Indicators, 119, 106826

2.1 Abstract

Bryophytes represent an essential component of global biodiversity and play a significant role in many ecosystems, including boreal forests. In Canadian boreal forests, industrial exploitation of natural resources threatens bryophyte species and the ecological processes and services they support. However, the consideration of bryophytes in conservation issues is limited by current knowledge gaps on their distribution and diversity patterns. This is mainly due to the ineffectiveness of traditional field surveys to acquire information over large areas. Using remote sensing data in combination with species distribution models (SDMs), we aim to predict and map diversity patterns (in terms of richness) of i) total bryophytes, and ii) bryophyte guilds (mosses, liverworts and sphagna) in 28,436 km² of boreal forests of Quebec (Canada). A bryophyte presence/absence database was used to develop four response variables: total bryophyte richness, moss richness, liverwort richness and sphagna richness. We pre-selected a group of 38 environmental predictors including climate, topography, soil moisture and drainage as well as vegetation. Then a final set of predictors was selected individually for each response variable through a two-step selection procedure. The Random Forest (RF) algorithm was used to develop spatially explicit regression models and to generate predictive cartography at 30m resolution for the study area. Predictive mapping-associated uncertainty statistics were provided. Our models explained a significant fraction of the variation in total bryophyte and guild level richness, both in the calibration (42 to 52%) and validation sets (38 to 48%), outperforming models from previous studies. Vegetation (mainly NDVI) and climatic variables (temperature, precipitation, and freeze-thaw events) consistently appeared among the most important predictors for all bryophyte groups modeled. However, guild-level models identified differences in important factors determining the richness of each of the guilds and, therefore, in their predicted richness patterns. For example, the predictor number of days > 30°C was especially relevant for liverworts, while

drainage class, topographic position index and PALSAR HH-polarized L-band were identified among the most important predictors for sphagna. These differences have important implications for management and conservation strategies for bryophytes. This study provides evidence of the potential of remote sensing for assessing and making predictions on bryophyte diversity across the landscape.

2.2 Résumé

Les bryophytes représentent une composante essentielle de la biodiversité mondiale et jouent un rôle important dans de nombreux écosystèmes, y compris les forêts boréales. Dans les forêts boréales canadiennes, l'exploitation industrielle des ressources naturelles menace les espèces de bryophytes et les processus et services écologiques qu'elles soutiennent. Cependant, la prise en compte des bryophytes dans les problèmes de conservation est limitée par les lacunes actuelles dans les connaissances de leur distribution et patrons de diversité. Cela est principalement dû à l'inefficacité des enquêtes de terrain traditionnelles pour acquérir des informations sur de grandes superficies. En utilisant des données de télédétection en combinaison avec des modèles de distribution d'espèces, nous visons à prédire et à cartographier les patrons de diversité (en termes de richesse) de i) les bryophytes dans leur ensemble, et ii) les guildes de bryophytes (mousses, hépatiques et sphaignes) dans 28,436 km² de forêts boréales du Québec (Canada). Une base de données de présence/absence de bryophytes a été utilisée pour développer quatre variables de réponse: la richesse totale en bryophytes, la richesse en mousses, la richesse en hépatiques et la richesse en sphaignes. Nous avons présélectionné un groupe de 38 prédicteurs environnementaux, notamment le climat, la topographie, l'humidité et le drainage du sol ainsi que la végétation. Ensuite, un ensemble final de prédicteurs a été sélectionné individuellement pour chaque variable de réponse au moyen d'une procédure de sélection en deux étapes. L'algorithme Random Forest a été utilisé pour développer des modèles de régression spatialement explicites. et générer des cartographies prédictives à une résolution de

30m pour la zone d'étude. Des statistiques d'incertitude associées aux cartographies prédictives ont été fournies. Nos modèles expliquaient une fraction significative de la variation de la richesse totale des bryophytes et des guildes, à la fois dans les ensembles d'étalonnage (42 à 52%) et de validation (38 à 48%), surpassant les modèles des études précédentes. La végétation (principalement NDVI) et les variables climatiques (température, précipitation et événements de gel-dégel) figuraient systématiquement parmi les prédicteurs les plus importants pour tous les groupes de bryophytes modélisés. Cependant, les modèles au niveau de la guildes ont identifié des différences dans des facteurs importants déterminant la richesse de chacune des guildes et, par conséquent, dans leurs patrons de richesse prédits. Par exemple, le prédicteur nombre de jours > 30°C était particulièrement pertinent pour les hépatiques, tandis que la classe de drainage, l'indice de position topographique et la bande L polarisée PALSAR HH ont été identifiés parmi les prédicteurs les plus importants pour les sphaignes. Ces différences ont des implications importantes pour les stratégies de gestion et de conservation des bryophytes. Cette étude démontre le potentiel de la télédétection pour évaluer et faire des prédictions sur la diversité des bryophytes à travers le paysage.

2.3 Introduction

Climate and land use changes as a result of the increase in human development activities, both in intensity and extent (Butchart *et al.*, 2010; Kerr and Ostrovsky, 2003), are currently cited as the primary threats to global biodiversity (Chapin Iii *et al.*, 2000; Millennium Ecosystem Assessment, 2005; Newbold *et al.*, 2015; Pereira *et al.*, 2010). According to the Global Assessment Report on Biodiversity and Ecosystem Services of IPBES (Brondizio *et al.*, 2019), 1 million of animal and plant species face extinction at present, jeopardizing ecosystem functions and services and thus affecting human well-being. Therefore, conservation of biodiversity is a top priority to promote and maintain global ecosystem functioning and services (Cardinale *et al.*, 2012; Isbell *et al.*, 2011).

Biodiversity conservation planning should ideally integrate as many taxonomic groups as possible. However, inconspicuous and poorly known species such as bryophytes (i.e. mosses, sphagna, liverworts and hornworts; Hespanhol *et al.*, 2015; Larraín *et al.*, 2019) tend to be overlooked when developing conservation plans and programs (Cornwell *et al.*, 2019; Rowntree *et al.*, 2011; Vanderpoorten and Hallingbäck, 2009). Bryophytes represent an essential part of global biodiversity and play a significant role in many diverse ecosystems on earth (Hallingbäck and Hodgetts, 2000). Bryophytes are reliable but extremely vulnerable indicators to environmental disturbances and currently face numerous human-induced threats (Frego, 2007). These threats derive mainly from land use changes (e.g. forestry, mining, infrastructure construction), which leads to the loss and degradation of bryophyte habitats (Hallingbäck and Hodgetts, 2000; Pykälä, 2019; Söderström *et al.*, 1992), inducing changes in bryophyte community composition (Caners *et al.*, 2013; Fenton and Frego, 2005; Lehosmaa *et al.*, 2017; Tolkkinen *et al.*, 2016). Therefore, much more attention should be given to the preservation of these species groups on a global scale.

Specifically, in Canadian boreal forests, which account for 24% of the world's boreal forest (Natural Resources Canada, 2017), bryophytes represent an abundant and diverse plant group. They are the main ground vegetation layer (Bond-Lamberty and Gower, 2007; Fenton and Bergeron, 2011; Gower *et al.*, 2001) and account for an important fraction of total diversity (Cole *et al.*, 2008; Möls *et al.*, 2013; Turetsky *et al.*, 2012). The essential contributions of this taxonomic group in ecosystem functioning and service provision of boreal forests have been largely documented. Concretely they account for a significant portion of the net primary production, representing up to 20% and 48% of wetland and upland productivity, respectively (Bond-Lamberty *et al.*, 2004; Gower *et al.*, 1997; Turetsky *et al.*, 2010), and exceeding in some cases overstory production (Peckham *et al.*, 2009). Bryophytes also have a strong influence on water, carbon and nutrient cycles (Bond-Lamberty and Gower,

2007; Skre and Oechel, 1981; Turetsky, 2003; Turetsky *et al.*, 2010). They regulate the moisture and temperature of soils, prevent erosion (Turetsky *et al.*, 2010, 2012), and exert an insulating effect protecting permafrost (Porada *et al.*, 2016). Likewise, these species promote key processes determining the stability and resilience of boreal ecosystems (Turetsky *et al.*, 2012). In Canada, the degradation of mature and old-growth boreal forests driven by the cumulative effects of natural resources extraction (mainly related to mining and forestry; Mansuy *et al.*, 2020) seriously threatens bryophytes (Boudreault *et al.*, 2018; Paquette *et al.*, 2016; Venier *et al.*, 2014). This issue is accentuated in the case of more vulnerable bryophyte species such as liverworts, which often depend on microhabitat conditions provided by mature forests (Barbé *et al.*, 2017). Despite the ecological benefits provided by bryophytes in boreal forest ecosystems, their distribution and diversity patterns have been poorly documented (Belland, 1998; Faubert, 2012; Faubert and Gagnon, 2013; Faubert *et al.*, 2010; Locky, 2010), endangering the maintenance of their ecological roles in the current context of anthropogenic pressure. Therefore, the acquisition and integration of knowledge on bryophyte diversity into industrial sustainable development strategies and plans become essential (Hallingbäck and Hodgetts, 2000; Vanderpoorten *et al.*, 2001). This may greatly facilitate the conservation of biodiversity and consequently ecosystem service provision in boreal forest regions.

The remoteness and inaccessibility of many Canadian boreal forests can make field surveys challenging, limiting the acquisition of critical information on biodiversity (Gillis *et al.*, 2005). In parallel, species distribution models (SDMs) combined with remote sensing data provide a powerful alternative tool to overcome these limitations offering a non-expensive method to remotely assess biodiversity over large areas at regular intervals over time (Corbane *et al.*, 2015; Turner *et al.*, 2003; Tweddale and Melton, 2005). SDMs offer tools to quantify species-environment relationships from known locations in order to evaluate species' ecological preferences or predict their

distributions using the relevant environmental conditions as proxies of species occurrence (Guillera-Arroita *et al.*, 2015; Mateo *et al.*, 2011). Therefore, SDMs provide supplementary information making them a suitable tool for conservation planning (Hespanhol *et al.*, 2015). SDMs have been widely used to assess distribution and diversity patterns of different organisms (Mateo *et al.*, 2011) including bryophytes (e.g. Bakkestuen *et al.*, 2009; Hespanhol *et al.*, 2015). Increasing numbers of studies integrate remote sensing methods with SDMs to assess, model, predict or map species' distributions and therefore different aspects of biodiversity (e.g. Buermann *et al.*, 2008; Jiang *et al.*, 2013; Saatchi *et al.*, 2008; Zimmermann *et al.*, 2007).

The use of the direct remote sensing approach on bryophytes was initially proposed based on the spectral differences found through laboratory tests, both among bryophytes (Bubier *et al.*, 1997) and between bryophytes and vascular plants (Vogelmann and Moss, 1993). However, the direct approach is in most cases unable to directly capture reflectance-based information from bryophytes as they are understory species that are normally covered by forest canopy (Yang *et al.*, 2006). The indirect approach, conversely, examines different aspects of bryophyte biodiversity based on the existing relationships between these species groups and their environment. Few remote sensing studies have been done for bryophyte cover detection (Bartels *et al.*, 2019, 2018; Ewalda *et al.*, 2019; Peckham *et al.*, 2009; Rapalee *et al.*, 2001), distribution (Goguen and Arp, 2017; Jiang *et al.*, 2014, 2013; Skowronek *et al.*, 2017, 2018) and diversity (Bartels *et al.*, 2018, 2019; Moeslund *et al.*, 2019).

Here, we use the Random Forest machine learning method (hereafter “RF”; Breiman, 2001) to predict and map diversity patterns, in terms of species number (hereafter “richness”), of i) total bryophytes, and ii) bryophyte guilds (i.e. mosses, liverworts and sphagna) in boreal forests of Quebec (Canada) using remote sensing data. With this study, we contribute to the acquisition and integration of knowledge on bryophyte diversity to promote industrial sustainable development strategies and ecological

planning framework that improve decision making for governments and industries. The consideration of bryophyte diversity will help the conservation of biodiversity along with the maintenance of ecosystem service supply in the boreal forest regions, where the footprint of the mining and forestry industries is large.

2.4 Materials and methods

2.4.1 Study area

The study area is located in western Quebec within the James Bay region, and covers 28,436 km² (between 48° 53' and 49° 57'N latitude and 75° 50' and 79° 22'W longitude; Figure 2.1). This region is dominated by black spruce (*Picea mariana* [Mill.] BSP)–feathermoss (*Pleurozium schreberi* [Brid.] Mitt.) forests whose dynamic is subject to natural disturbances (Lecomte *et al.*, 2006) and logging activities (Cyr *et al.*, 2009). Fire is the main natural disturbance (Fenton and Bergeron, 2013) with a cycle of 398 years since 1920 (Bergeron *et al.*, 2004). In the absence of fire, the forests in this region are prone to paludification, especially in areas located in the Clay Belt physiographic region (Bergeron *et al.*, 2007; Boudreault *et al.*, 2002) which is characterized by the deposits left by the proglacial lakes Barlow and Ojibway (Vincent and Hardy, 1977). This process consists in the accumulation of organic matter over time (Fenton and Bergeron, 2008, 2013) due to a flat topography with a dominance of clay soils, low drainage capacity and a moderately humid and cold climate (927.8 mm of precipitation annually; annual mean temperature 1.0°C; Environment Canada, 2010).

Mature forests in the study area are characterized by a high frequency of perennial mosses and liverworts (Barbé *et al.*, 2017) with feathermosses (*P. schreberi*, *Ptilium crista-castrensis* (Hedw.) De Not., and *Hylocomium splendens* (Hedw.) Schimp.) dominating the soil (Boudreault *et al.*, 2002). They tend to be naturally replaced by *Sphagnum* species under more humid conditions (Barbé *et al.*, 2017). In contrast, disturbed forests are characterized by pioneer and colonist bryophyte species such as

Ceratodon purpureus (Hedw.) Brid., *Pohlia nutans* (Hedw.) Lindb. and *Polytrichum juniperinum* Hedw. (Baldwin and Bradfield, 2005; Barbé *et al.*, 2017; Fenton and Frego, 2005).

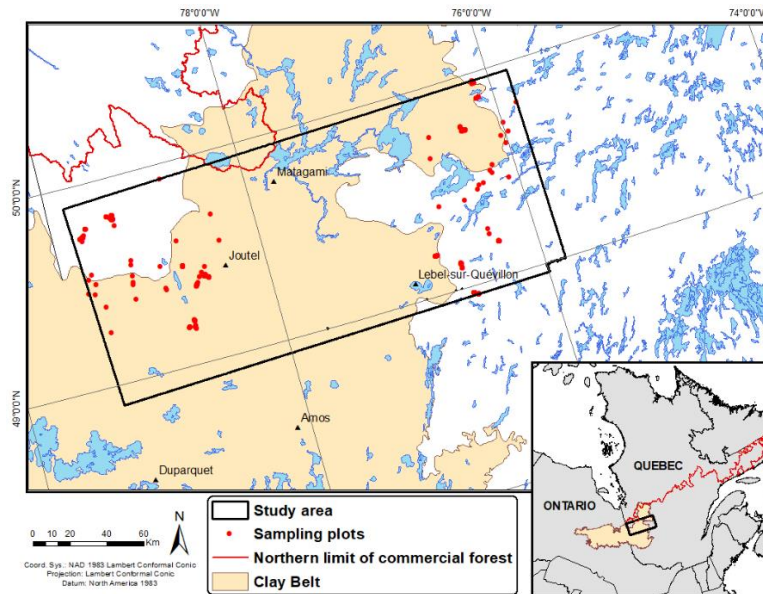


Figure 2.1 Study area and sampling plots (n = 326) in the boreal black spruce forest of eastern Canada.

2.4.2 Species field data set

The bryophyte presence/absence database used in this study was developed using the field sampling data recorded in three previous studies carried out in the same study area (Barbé *et al.*, 2017; Castonguay, 2016; Chaieb *et al.*, 2015; Figure 2.1). These studies sampled young, mature and old-growth forests and both recent fires and cut-blocks, using a modified “floristic habitat sampling” method (Newmaster *et al.*, 2005), consisting in collecting all bryophytes present in all microhabitats within 5 x 10m plots. Due to the computational capacity and processing time necessary for the development of remote sensing predictors (see section 2.4.3 for descriptions), Landsat-derived predictors already developed by the laboratory of geographic information systems of

the UQAT (Université du Québec en Abitibi Témiscamingue) were used in this study. The spatial extent of these predictors limited the number of selected study plots to a total of 326 plots, ensuring an equal number of predictors per observation. Bryophyte species richness at the microhabitat level were grouped by plot to obtain plot-level total bryophyte richness. Species richness by guild (mosses, liverworts and sphagna) was also calculated at the plot level in order to develop individual predictive models for each of them. The 326 plots accounted for a total of 207 different bryophyte species (mean: 22; max: 54; min: 2), including 119 mosses (mean: 11; max: 32; min: 0), 67 liverworts (mean: 7; max: 26; min: 0) and 21 sphagna (mean: 3; max: 10; min: 0). Total bryophyte richness and the richness at the guild level were used as response variables in our models (4 models in total). Methods to geolocate the plots differed among the studies, consequently the *Fishnet* tool implemented in ArcGIS v.10.5 (ESRI, 2016) was employed to standardize the GPS coordinates of all plots. The *Fishnet* tool allows the building a georeferenced vector grid from which it is possible to correct the location of plots. As *Fishnet* input parameters, we set *template extent* to the extent of our study area and both *cell size height* and *cell size width* to 10m. The location of the plots was thus corrected according to their position on a 10m grain-size georeferenced grid.

2.4.3 Environmental predictors

The preselection of variables as potential predictors of total bryophyte richness and richness at the guild level was carried out according to their known influence on the bryophyte distribution and diversity. These factors are related with climatic conditions (Chen *et al.*, 2015a, 2015b; Jiang *et al.*, 2014; Medina *et al.*, 2014); topographic features (Ah-Peng *et al.*, 2007; Bruun *et al.*, 2006; Rey Benayas, 1995); soil attributes such as composition (Tyler *et al.*, 2018) and moisture content (Bartels *et al.*, 2018, 2019; Raabe *et al.*, 2010); and forest properties such as canopy cover (Couvreur *et al.*, 2016; Raabe *et al.*, 2010) and structure (Grandpré *et al.*, 2011; Hespanhol *et al.*, 2011; Jiang *et al.*, 2014). The variables are described in detail below.

2.4.3.1 Climate data

Climate variables for the 1981-2010 period at a 10km spatial resolution were obtained from the Canadian Consortium on Regional Climatology and Adaptation to Climate Change database (known as Ouranos, <https://www.ouranos.ca/en/ouranos/>; Charron, 2016). These variables are adequate for our study area where climatic fluctuations are quite moderate. Climatic data were derived from a subset of downscaled climate model simulations selected using cluster analysis following Casajus *et al.* (2016) from the regional climate models developed by Ouranos. A total of six annual climatic variables were selected: average temperature (°C), total precipitation (mm), freeze-thaw events (days), growing degree days (GDD), number of days > 30°C (days), and maximum 5-Day precipitation (mm). Seasonal variables (autumn, spring, summer and winter) of average temperature, total precipitation and freeze-thaw events were also chosen (12 in total). These variables were resampled at a 30m resolution. We anticipated a high correlation between annual variables and their corresponding seasonal variables, so annual variables were finally selected for further analyzes.

2.4.3.2 Topographic data

The digital elevation model was obtained from the Shuttle Radar Topography Mission (SRTM) at 30m resolution and was used to derive different topographic variables using ArcGIS v.10.5. Eight topographic variables that are important in describing landscape geomorphology and hydrology (Doetterl *et al.*, 2013; Walsh *et al.*, 1998) were included in our analyses: elevation, slope, aspect, profile curvature, topographic position index, topographic convergence index, flow direction and flow accumulation. All of these topographic features govern water flow both above and within soil. Therefore, they influence hydrologic processes that determine the water table level (Mansuy *et al.*, 2018), which ultimately affects bryophyte diversity (Bartels *et al.*, 2018, 2019). Aspect is a measure of incident solar radiation (Vanderpuyé *et al.*, 2002), which has

been shown to influence bryophyte richness (Austrheim, 2002; Kuzemko *et al.*, 2016; Turtureanu *et al.*, 2014). Profile curvature describes the concavity/convexity of the land surface in the direction of the aspect of the slope and thus influences erosion and deposition (Bourg *et al.*, 2005; Mansuy *et al.*, 2018). The topographic position index measures the relative elevation at one point compared to its surrounding environment (Jenness, 2006) and can be used as a proxy of microclimate conditions (Bennie *et al.*, 2008). The topographic convergence index is related to surface water availability due to the contribution of runoff water from upslope areas (Keitt and Urban, 2005). Flow direction describes the downslope direction of runoff water and thus also affects soil erosion and deposition. Flow accumulation is an indicator of drainage water collection.

2.4.3.3 Soil data

As indicators of soil texture and hydrologic processes, we used the surface deposits and their drainage classes obtained from the MFFP (Ministère des Forêts, de la Faune et des Parcs du Québec, 2018). The surface deposits and their drainage affect the water flow content in the soil and also the moisture content of the litter as well as the vegetation (Mansuy *et al.*, 2011, 2012). Vector layers were transformed to raster and resampled to 30m resolution.

2.4.3.4 Vegetation data

Spectral bands 2, 3 (visible spectrum; green and red respectively), 4 (near infrared; NIR), 5 and 7 (shortwave infrared; SWIR) from 30m resolution Landsat 7 Enhanced Thematic Mapper Plus (ETM+) imagery for the summer season 2010 already radiometric corrected were used in this study. We selected these spectral variables based on their different ecological applications related with the assessment of forest and soil attributes such as moisture content, vegetation vigour and biomass, and forest development stage and composition (Hall *et al.*, 2006; Kerr and Ostrovsky, 2003; Valeria *et al.*, 2012).

The Normalized Difference Vegetation Index (NDVI; $(\text{NIR} - \text{Red}) / (\text{NIR} + \text{Red})$) was also included in our analyses. NDVI has been used to assess diversity in different studies (e.g. Gould, 2000; Levin *et al.*, 2007; Seto *et al.*, 2010). This index was derived from Landsat 8 ETM+ single date images of bands 4 (Red) and 5 (NIR) for the summer season of 2016.

We also selected the Difference Normalized Burn Ratio (dNBR) as potential predictor of bryophyte richness. dNBR is derived from the difference between pre-fire and post-fire Normalized Burn Ratio (NBR; $(\text{NIR} - \text{SWIR}) / (\text{NIR} + \text{SWIR})$) products and is related to the change experienced by the vegetation between two different dates. This index which has been largely used to assess fire severity (e.g. Bobbe *et al.*, 2001; Hudak *et al.*, 2004; for further details see the review of French *et al.*, 2008) was used here as a proxy for the vegetation change rate over time, which should indirectly take into account disturbance events like fires. dNBR was calculated from Landsat 7 ETM+ and Landsat 8 ETM+ single date images of NIR and SWIR bands for the period between 1990 and 2016. This period was selected as we thought it was a large enough time window to perceive changes in the vegetation in a study area where both natural and anthropogenic disturbances are frequent.

Japanese Advanced Land Observing Satellite (ALOS) Phased Array L-band SAR (PALSAR) sensor data were also used in our analyses. We selected both HH-polarized (PALSAR_HH) and HV-polarized (PALSAR_HV) L-bands, which are related with aboveground biomass and forest structure (Lucas *et al.*, 2010; Mansuy *et al.*, 2018; Proisy *et al.*, 2003). PALSAR_HH is also informative of surface moisture in humid sites (Lucas *et al.*, 2010; Mitchard *et al.*, 2011), thus it was used as an indicator for soil moisture. However, PALSAR_HV is related to biomass since it is not affected by soil moisture content (Kuenzer *et al.*, 2011; Mitchard *et al.*, 2011). Annual PALSAR images between 2007 and 2010 were filtered through speckle filtering for reducing backscatter noise, averaged and subsequently resampled to 30m resolution. The

polarization index HV/HH which also relates to forest biomass and structure according to Mansuy *et al.* (2018) was likewise included in our analyses.

2.4.4 Statistical analyses

The analyses were carried out individually for each category of the response variables: total bryophyte richness and richness at the guild level, i.e. mosses, liverworts and sphagna. All analyzes were performed in R v.1.1.456 (R Development Core Team, 2018).

2.4.4.1 Predictor selection

A total of 38 potential predictors were preselected. A large set of variables can decrease the accuracy of machine-learning methods (Nguyen *et al.*, 2015) and require a greater computational capacity and processing time, especially when generating predictive mapping. We used a method similar to Rudiyanto *et al.* (2018) and Mansuy *et al.* (2018) to select the most important environmental predictors for each response variable using the *Boruta* package v.6.0.0 (Kursa and Rudnicki, 2010). The algorithm implemented in *Boruta* uses a wrapper method developed around RF (Kursa and Rudnicki, 2010) to determine the relevance of each predictor. This algorithm works by generating copies of the input predictors by shuffling their original values and subsequently comparing the importance of the real predictors with that of the randomly generated copies. As output, it provides a list of both predictors confirmed as important and those rejected for the target response variable. The model must be specified using a formula or a data frame containing the response variable and predictors. We set the arguments *ntree* (number of trees to grow) and *maxRuns* (maximal number of importance source runs) to 5000 and 1000, respectively. This package allowed us to identify and keep only relevant predictors in our models. The selection of predictors was then further refined by using the Pearson correlation coefficient to identify highly correlated variables ($|r| > 0.7$) and avoid the inclusion of redundant variables in our models. Among correlated

variables, those that had more ecological meaning were retained for further analyses. The final sets of predictors, which varied from 11 to 13 predictors depending on the response variable, are shown in Table 2.1

Table 2.1 Description of selected predictors by category and source used to model and predict total bryophyte (Bry), moss (Mos), liverwort (Liv), and sphagna (Sph) richness.

Bry	Mos	Liv	Sph	Predictors	Description	Category	Data source
x	x	x	x	Temperature	Average annual temperature (°C)	Climate	Ouranos
x	x	x	x	Precipitation	Total annual precipitation (mm)		
x	x	x	x	Freeze_thaw	Annual number of days with freeze-thaw events (days)		
x	x	x	x	Days_30degrees	Annual number of days with temperatures greater than 30°C (days)		
x			x	Slope	Maximum rate of change in value from one cell to its immediate neighbors (degrees)	Topographic	SRTM
			x	Beers_asp	Beers aspect (heat index) = $1 + \cos((45^\circ - \text{aspect}) / \text{slope})$		

Table 2.1 continued

x	x	x	x	TPI	Topographic position index; relative topographic position of each cell in terms of elevation compared to the surrounding neighborhood (m)		
	x			Flow_acc	Flow accumulation in each cell determined by the accumulation of the weight of all cells flowing into each downslope cell (unitless)		
x	x	x		Surf_depo ¹	Surface deposit; types defined according to the shape of the land, the position on the slope and soil texture, inter alia (44 categories)	Soil	MFFP forest map
x	x	x	x	Drai_class ²	Drainage class; soil drainage capacity based on topographic position, soil and bedrock permeability, surface deposit thickness, abundance and regularity of water supplies and water table levels (8 categories)		
x	x	x	x	B4	Band 4 (near infrared (NIR), 0.76–0.9µm); relates to vegetation biomass	Vegetation	Landsat 7 ETM+

Table 2.1 continued

x	x	x	x	B5	Band 5 (shortwave infrared (SWIR), 2.08–2.35µm); relates to moisture content in vegetation and soil and thus to newly burned areas	
x	x	x	x	NDVI	Normalized Difference Vegetation Index ((NIR – Red) / (NIR + Red)); relates to photosynthetically active radiation of plants and thus to vegetation biomass and health	Landsat 8 ETM+
	x		x	PALSAR_HH	HH-polarized L-band; relates to soil moisture content, especially in open forest stands	ALOS PALSAR
x	x	x	x	PALSAR_HVHH	Polarization index, as the ratio of HV-polarized to HH-polarized L-bands; relates to forest biomass and structure	

Data source abbrev.: SRTM, Shuttle Radar Topography Mission; MFFP, Ministère des Forêts, de la Faune et des Parcs du Québec; ETM+, Enhanced Thematic Mapper Plus; ALOS PALSAR, Japanese Advanced Land Observing Satellite Phased Array L-band SAR.

¹ Surf_depo categories range from organic to rock.

² Drai_class categories range from xeric to subhydric.

2.4.4.2 Random forest approach

Spatially explicit predictive models of both total bryophyte richness and richness at the guild level were developed using the RF algorithm (Breiman, 2001) implemented in the *randomForest* package v4.6.14 (Liaw and Wiener, 2002). As richness is a continuous response variable, we performed RF regression models. RF is an effective and flexible approach to make predictions, which is not subject to overfitting (Breiman, 2001; He *et al.*, 2010). It does not require distribution assumptions or transformations (Drew *et al.*, 2010), deals efficiently with outliers, and provides variable importance measures and unbiased error estimates (Breiman, 2001). The RF algorithm uses a modified bagging (bootstrap aggregation) technique to generate a multitude of independent decision trees from randomly selected subsamples (or bootstrap samples) from the training dataset outputting the mean prediction (Breiman, 2001). For each node of each individual tree, a random subset of candidate predictors is assessed, selecting from them the predictor providing the most information to split that node (Liaw and Wiener, 2002). The observations from the original dataset that are not included in a bootstrap sample are known as out of bag (OOB) observations, which are used to estimate both the mean square error (MSE) and the importance of the predictors. The importance of each predictor (%IncMSE) is estimated by calculating, tree by tree, the difference between the OOB MSE derived from predictions on the OOB observations by using its real values and the OOB MSE obtained from the same procedure but using randomly permuted values of that predictor. The OOB MSE differences are subsequently averaged across all trees and normalized by their standard deviation (Liaw and Wiener, 2002).

Data were randomly split into a calibration (70%) and a validation dataset (30%) using the *sample.split()* function from the *caTools* package v.1.17.1.1 (Tuszynski, 2018). In order to improve model performance, the values of the parameters *ntree* (number of trees to grow), *mtry* (number of variables randomly sampled as candidates at each

split), and *nodesize* (minimum size of terminal nodes) of the RF algorithm were optimized independently for each model, selecting those that minimized the OOB MSE. After training models, they were tested on the validation datasets to check their behavior beyond the data from which they were built. This step has been considered as a requirement for predictive modeling with conservation purposes since it provides an estimate of model reliability (Maes *et al.*, 2005). The predictive performance of the regression models was assessed using the root mean square error (RMSE) and R^2 estimates obtained with the *postResample()* function implemented in the *caret* package v.6.0.80 (Kuhn, 2018), which only requires two input numeric vectors containing observed and predicted values. Subsequently, predictive cartography at 30m resolution of both total bryophyte richness and richness at the guild level was generated for the whole study area. To provide an uncertainty measure of RF predictions, coefficient of variation maps were also produced for each richness from predictions of individual RF trees at each pixel. The coefficient of variation mapping was performed using the *model.mapmake()* function implemented in the *ModelMap* package v.3.4.0.1 (Freeman *et al.*, 2018) by using the previously built RF models as the model objects (*model.obj* argument) for predictions and by setting the *map.sd* argument to “TRUE”. Additionally, coefficient of variation statistics (min., 1st quantile, median, 3rd quantile and max.) were calculated.

2.5 Results

2.5.1 Model performance

The RF algorithm parameters used to develop the models, as well as R^2 and error estimates associated with both their training and validation are listed in Table 2.2. Among the four, the total bryophyte richness model was the best adjusted explaining 52% of the variation in the training dataset, although it also showed the highest OOB MSE (78.23). The amount of variation explained by the guild level models was lower,

ranging from 42 to 48%, while their OOB MSE was considerably lower (< 25) compared to that of the total bryophyte richness model.

Testing the models with the validation datasets, models at the guild level yielded better results than the model encompassing total bryophyte species (Table 2.2). Guild models explained 39 to 48% of the variation in the validation datasets and had lower MSE estimates, ranging from 3.25 to 25.9. In contrast, the total bryophyte richness model explained 38% of the variation in the validation dataset with an MSE of 102.91. Plots of observed versus predicted richness values by group are shown in Figure 2.2. Our four models showed a better predictive performance for low levels of observed richness, decreasing their accuracy as the number of observed species increased; no overestimation or underestimation trends were observed.

Table 2.2 Parameters and coefficients of regression models for total bryophyte richness and richness at the guild level (mosses, liverworts and sphagna) along with prediction coefficients resulting from their validation. See Table 2.1 for a description of predictors.

	Regression models					
	# of predictors	ntree	mtry	nodesize	OOB MSE	R ²
Bryophytes	12	5000	2	10	78.23	0.52
Mosses	13	3000	2	2	24.84	0.48
Liverworts	11	3000	1	7	19.70	0.45
Sphagna	13	3000	1	6	3.43	0.42
	Prediction coefficients					
	MSE	R ²				
Bryophytes	102.91	0.38				
Mosses	25.90	0.39				
Liverworts	18.29	0.44				
Sphagna	3.25	0.48				

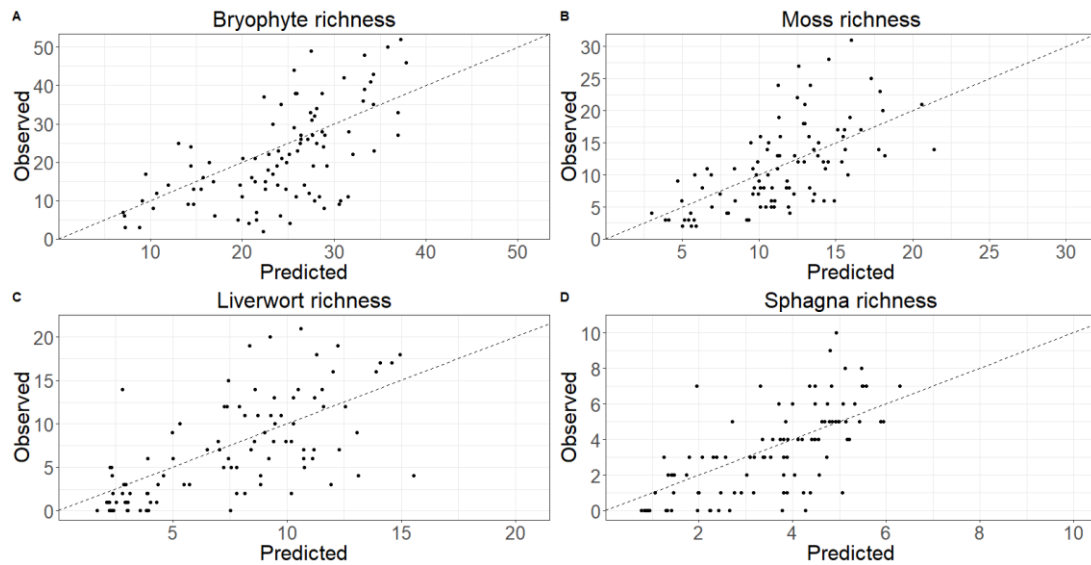


Figure 2.2 Observed versus predicted richness values (black points) of (A) total bryophytes, (B) mosses, (C) liverworts, and (D) sphagna. The dashed line represents a 1:1 relationship. Note that x-axes and y-axes are variable.

2.5.2 Predictors and their importance

Our models showed differences in terms of both the selected predictors (Table 2.1) and the importance of the predictors shared by two or more models (%IncMSE; Figure 2.3). However, vegetation and climatic variables consistently appeared among the most important predictors for the richness of the four bryophyte groups modeled. Overall bryophytes and mosses shared the same set of most important predictors, which were NDVI, B4, Precipitation, Temperature and Freeze_thaw (Figure 2.3A and B). For liverwort richness, NDVI, Temperature, Precipitation, Days_30degrees and Freeze_thaw were the best predictors (Figure 2.3C). For the sphagna guild, soil and topographic variables also ranked among the most relevant predictors along with climatic and vegetation variables. The best predictors of the sphagna richness were Drai_class, Temperature, TPI, Precipitation and PALSAR_HH (Figure 2.3D).

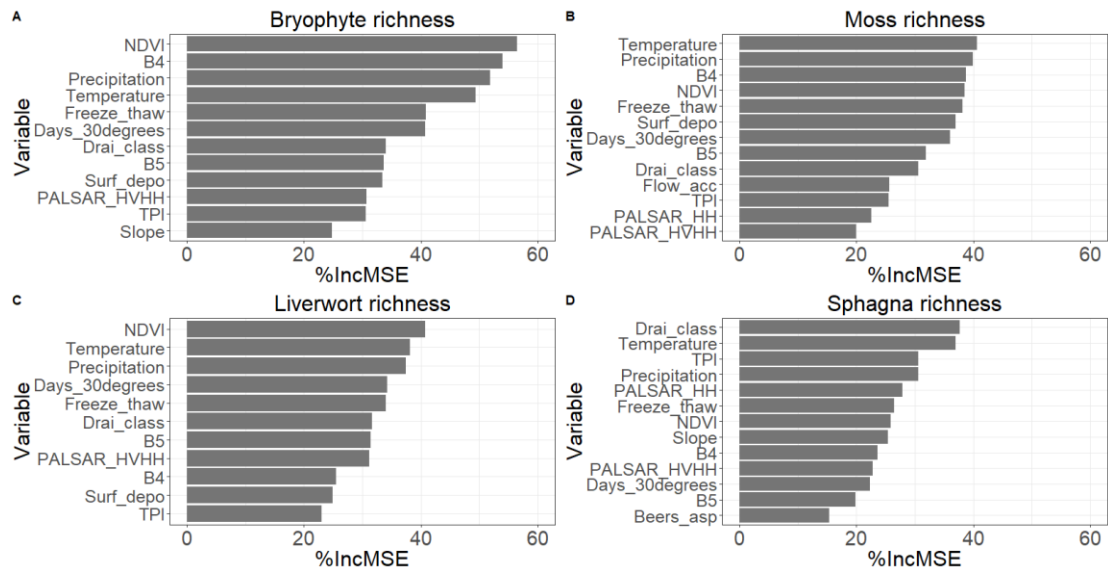


Figure 2.3 Predictor importance measures (%IncMSE) for regression models of (A) total bryophyte, (B) moss, (C) liverwort, and (D) sphagna richness.

2.5.3 Predictive mapping

The results from the predictive mapping of the total bryophyte richness and the richness at the guild level are shown in Figure 2.4. Predicted richness values ranged from 6 to 41 for total bryophytes, 3 to 27 for mosses, 1 to 17 for liverworts and 0 to 7 for sphagna. Different richness patterns were obtained for each mapped group. Regarding the results for total bryophytes, two diversity hotspots are located in the north-northeast and southwest of the study area, while we find a zone especially poor in species in the southeast (Figure 2.4A). At the guild level, moss species display a similar pattern but with a second zone of low richness in the west-northwest (Figure 2.4B). Likewise, high richness levels can be found in the north-northeast for liverworts and in the northwest for sphagna, although both guilds present a particularly low richness in the southeast (Figure 2.4C and D).

The statistics of the coefficient of variation showed that, overall, predictions from individual RF trees of both total bryophyte richness and richness at the guild level were

stable (Table 2.3; Figure 2.5). In 75% of the cases the coefficient of variation did not reach the value of 1 species for any of the modeled groups (third quartiles ranging from 0.45 to 0.75), with total bryophyte richness predictions showing the least uncertainty. For all groups, higher predictive uncertainty was found in areas showing lower predicted species richness (Figure 2.4; Figure 2.5).

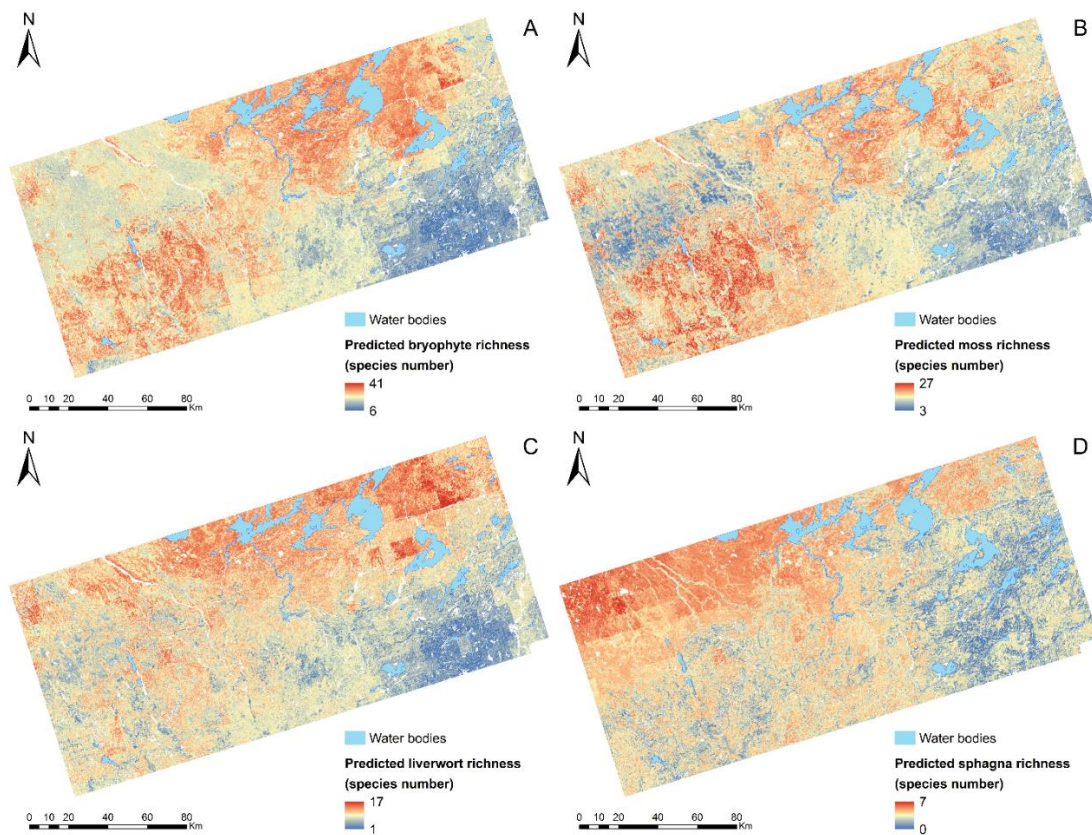


Figure 2.4 Predictive cartography of (A) total bryophyte, (B) moss, (C) liverwort, and (D) sphagna richness for the study area at 30m resolution. Red colors correspond to areas predicted to be species rich, while yellow and blue colours correspond to areas predicted to harbour intermediate and low levels of richness. White areas on maps correspond to non-forest areas for which soil information was not available (Ministère des Forêts, de la Faune et des Parcs du Québec, 2018).

Table 2.3 Coefficient of variation statistics associated to the predictive mapping of total bryophyte, moss, liverwort and sphagna richness shown in Figure 2.4 (see Figure 2.5 for coefficient of variation maps).

	Coefficient of variation statistics				
	Min.	1 st quantile	Median	3 rd quantile	Max.
Bryophytes	0.14	0.33	0.38	0.45	0.97
Mosses	0.10	0.48	0.55	0.62	1.26
Liverworts	0.19	0.51	0.60	0.71	1.63
Sphagna	0.11	0.47	0.58	0.75	2.16

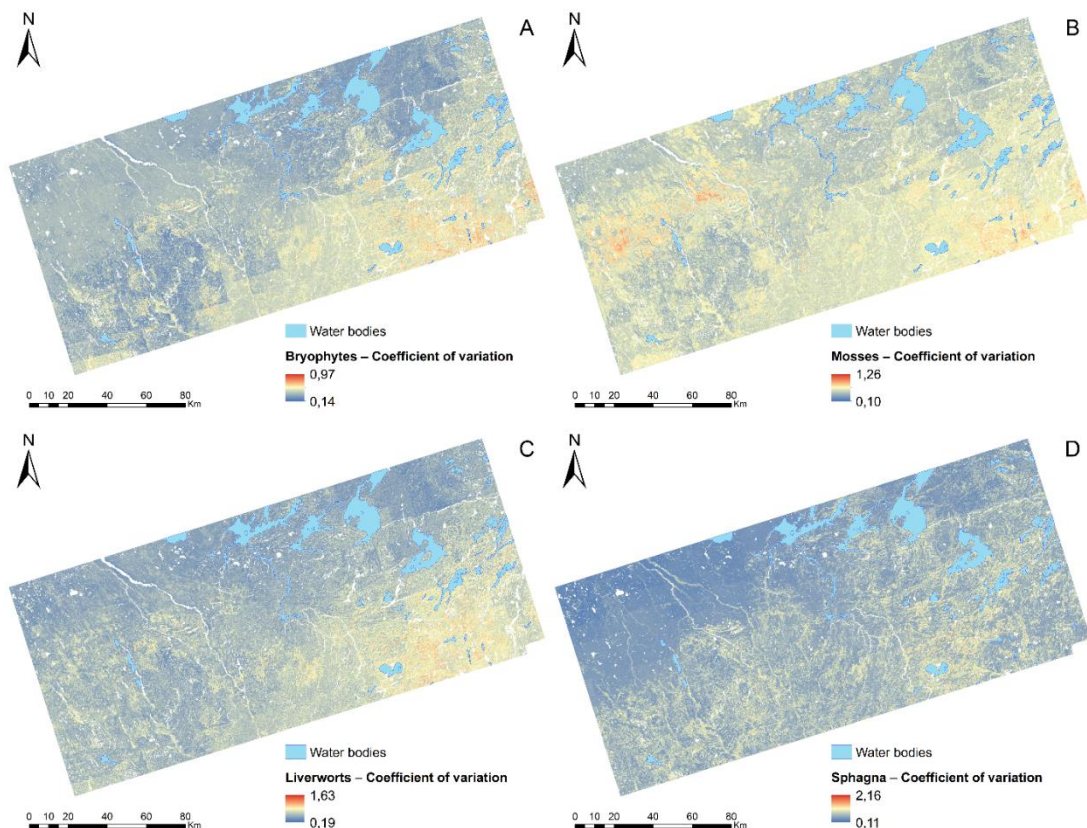


Figure 2.5 Maps of coefficient of variation associated to the predictive mapping of (A) total bryophyte, (B) moss, (C) liverwort, and (D) sphagna richness. Measures were derived from predictions of individual Random Forest trees at each pixel.

2.6 Discussion

2.6.1 Predicting bryophyte richness patterns

The present study demonstrates the efficacy of combining remote sensing data and SDMs to model and assess the richness patterns of bryophytes in boreal forest. Recent studies have used the same approach to model and understand the spatial patterns of total bryophyte diversity (Bartels *et al.*, 2018; Moeslund *et al.*, 2019). However, our study was also able to develop a predictive cartography at the guild level and therefore

offer a potential repeatable methodology for conservation purposes of these species groups.

Our models explained a significant fraction of the variation in total bryophyte and guild level richness, both in the calibration (42 to 52%) and validation sets (38 to 48%). However, a substantial part of the variation remained unexplained, which can be due to several causes: i) errors inherent to the geolocation of the plots, which can affect the performance of the models (Moudrý and Šímová, 2012); ii) variables describing important environmental features that drive bryophyte richness patterns were missing, especially at the microhabitat scale, since local conditions, such as quantity and decay class of rotting logs, affect bryophyte assemblages more directly (Cole *et al.*, 2008; Hespanhol *et al.*, 2011; Pócs, 1996); iii) variables that explicitly integrate information on anthropogenic pressure on the territory (such as harvest intensity), which considerably influence the dynamics of boreal forests, were not included in our models; iv) the mismatch between the size of the sampling plots (50m²) and image pixels (900m²) used in the modeling can introduce errors that result in a decrease in model accuracy (Xu *et al.*, 2009). Despite these potential limitations, we consider that our results based solely on remote sensing data are significant, specifically at the guild level. Lower fits to the calibration data were achieved by the total bryophyte diversity models developed in similar studies. Bartels *et al.* (2018) were able to explain up to 16% and 11% of the variation in diversity and richness, respectively, while a 32% variance in richness was explained by Moeslund *et al.* (2019).

2.6.2 Remote sensing predictors

Despite variable resolution, remote sensing predictors offer valuable information in understanding the relationships between bryophytes and their environment, and thus for protection and management purposes. Since “bryophytes” are composed of different guilds presenting differences in ecological and physiological terms (Aranda

et al., 2014; Chen *et al.*, 2015a; Fenton and Bergeron, 2008), the discussion in the present section is mainly addressed at the guild level.

This study demonstrated the importance of climatic factors, especially Temperature and Precipitation, in generating richness patterns of the different bryophyte guilds. This result agrees with those obtained in earlier studies, both for total bryophytes (Aragón *et al.*, 2012; Pharo *et al.*, 2005; Zechmeister *et al.*, 2003) and for bryophytes guilds (Chen *et al.*, 2015a, 2015b). Both Temperature and Precipitation show a consistent negative effect throughout the three guilds (Figure 2.6) as previously reported (Chen *et al.*, 2015a, 2015b; Zechmeister *et al.*, 2003). Although the variation of Temperature presented in our study area is around 1.0°C, the effect of this annual variable may be reflecting the masked effect of temperatures of the warmest months which can limit the persistence of bryophytes according to their tolerance to desiccation. The results obtained for Precipitation, however, may seem contradictory. In boreal black spruce forests, where precipitation is primarily intercepted by the first canopy layers (Liu and Liu, 2008), most of bryophyte species appear to be more dependent on other moisture sources such as fog, dew, high humidity (Lüttge *et al.*, 2011) or the water table (Bartels *et al.*, 2018, 2019). The negative effect of Precipitation could be explained based on the spatial pattern that it shows in our study area. Precipitation shows an east west gradient with higher values spatially coinciding with high fire activity areas outside the Clay Belt region close to the Fire Triangle Area (Le Goff *et al.*, 2007, 2008). These more frequently disturbed areas are characterized by well drained sandy soils poor in nutrients (Mansuy *et al.*, 2011). Therefore, we argue that the lower observed bryophyte richness in areas of higher Precipitation may be due to factors related to the natural disturbance regime and the composition and drainage capacity of soils of those areas rather than to the effect of Precipitation as a moisture source.

Days_30degrees was also negatively correlated with the richness of the different bryophyte guilds. This result is directly related to the poikilohydric physiology of these

organisms (Gignac, 2001; Huttunen *et al.*, 2018; Raven, 1995). Days of extreme heat may exceed the desiccation tolerance of these species (as well as of their propagules), particularly in the case of liverworts that generally have a lower tolerance to stress induced by desiccation (Proctor *et al.*, 2007; Wood, 2007). Although liverworts can resist desiccation periods under determined conditions (Proctor *et al.*, 2007; Wood, 2007), stable humid environments are required, among other factors, to harbor and maintain high levels of their richness.

The richness of the different guilds was also influenced by the Freeze-thaw variable. It showed a positive effect for mosses and sphagna and a negative effect for liverworts. Although many bryophytes show physiological response mechanisms to freezing which allow them to withstand freeze-thaw cycles without suffering severe damage (Lenne *et al.*, 2010; Takezawa, 2018), the positive influence of Freeze-Thaw events on moss and sphagna richness remains unclear. Liverworts, conversely, are species generally more sensitive to freezing (Longton, 1988), especially in the case of thalloid liverworts which can suffer frost-induced irreversible damage (Clausen, 1964; Dilks and Proctor, 1975). This fact would explain the lower richness of liverwort species in areas exposed to more frequent freeze-thaw cycles.

NDVI also appeared as a very important predictor, positively correlated in particular with moss and liverwort richness (Figure 2.6). The usefulness of this vegetation index, as well as of its combination with climatic variables (Li *et al.*, 2020), as predictors of bryophyte biodiversity-related aspects are consistent with previous studies (Jiang *et al.*, 2013, 2014). NDVI relates to the absorption of photosynthetically active radiation carried out by plants (Rouse *et al.*, 1974) and therefore to the presence of vegetation, which increases with time since disturbance as regeneration advances. Diversity of substrates as well as their quality and quantity also increases with time since disturbance, which are factors that favour a higher diversity of bryophytes, particularly of liverworts (Barbé *et al.*, 2017; Boudreault *et al.*, 2018; Paquette *et al.*, 2016).

Likewise, the long ecological continuity of forests with high NDVI values increases their probability of being colonized by new species (Nordén *et al.*, 2014), especially for potentially dispersal-limited species, such as rare bryophytes found in managed environments (Söderström and During, 2005). The influence of disturbance regimes, both natural and anthropogenic, on the dynamics and spatial patterns of boreal forests (Castonguay, 2016; Cyr *et al.*, 2009; Grandpré *et al.*, 2011; Lecomte *et al.*, 2006), as well as the ability of NDVI to capture disturbance-derived differences in important forest attributes that affect moss and liverwort richness, explain the importance of this index.

B4, as NDVI, is sensitive to the presence of vegetation, which can explain that both predictors show similar importance for, and relationships with, those observed richness values of mosses and sphagna (Figure 2.3). However, these results contrast with those obtained for liverworts, in which we observe a significantly importance of NDVI with respect to B4. Although we ignore the cause of this disparity, it is likely that B4 is also providing information on vegetation structural features (Ewalda *et al.*, 2019; Huete *et al.*, 1997) that can be more determinant for the richness of mosses and sphagna than for liverworts richness.

Regarding the sphagna guild, a higher richness was found in sites showing poor drainage capacity, low relative elevation, high soil moisture content and flat relief. These are features normally associated with paludified sites (Laamrani *et al.*, 2015; Mansuy *et al.*, 2018), habitats in which feathermosses are naturally replaced by sphagna (Fenton and Bergeron, 2006; Simard *et al.*, 2007) and that are known for harboring a high diversity of these latter species (Boudreault *et al.*, 2002). In fact, the areas predicted as the richest in sphagna species correspond to those predicted by Mansuy *et al.* (2018) within our study area to have thicker organic layers as a result of the paludification process.

While bryophytes also respond to microhabitat conditions (Cole *et al.*, 2008; Pócs, 1996), larger-scale environmental factors, such as climate (Medina *et al.*, 2014) or overstorey vegetation (Weibull and Rydin, 2005) can substantially influence their diversity patterns by shaping local conditions. The differences found among guilds in terms of relevant variables as well as of their relative importance highlight the importance of focussing at the guild level. This permits the identification of the environmental features that influence each guild in order to develop management and conservation strategies adapted to their ecophysiological specificities (Baldwin and Bradfield, 2007; Fenton and Bergeron, 2008; Raabe *et al.*, 2010).

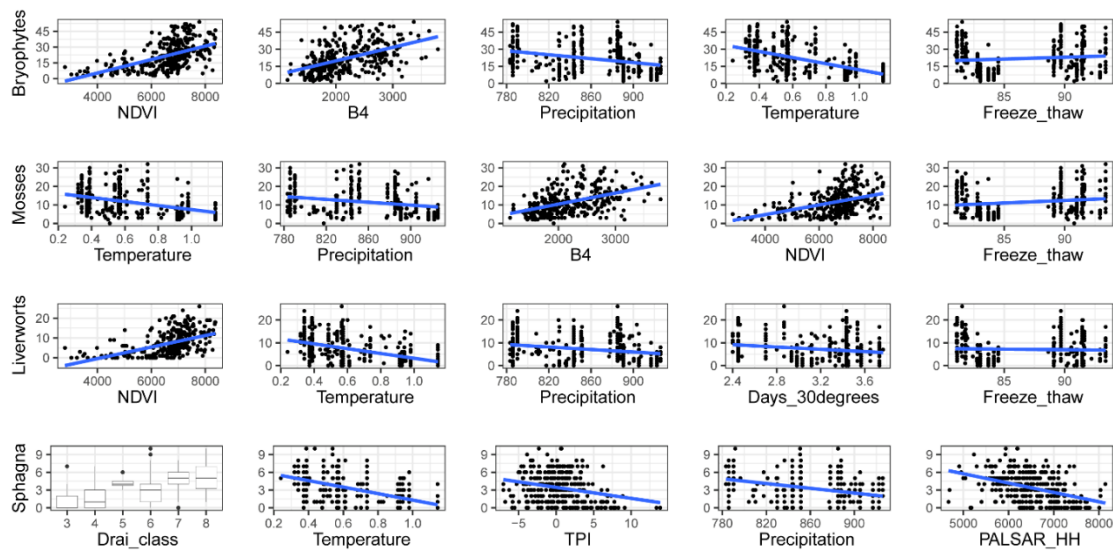


Figure 2.6 Relationship between the observed richness of total bryophytes, mosses, liverworts, and sphagna and their five best predictors (in decreasing order of importance from left to right; see Table 2.1 for predictor description).

2.6.3 Implications for conservation strategies

Boreal forests are poor in tree species diversity (Turetsky *et al.*, 2012) and show an overall species richness inferior to that found in lower latitude forests (Gentry, 1986; Gower *et al.*, 2001; Myers, 1988). Bryophytes therefore represent a significant

proportion of the diversity in boreal forests (i.e. 207 different species included in the present study against 10 tree species recorded in the boreal black spruce forest of Quebec; Gagnon, 2004). Bryophytes are also well known indicators of environmental changes (Frego, 2007; Hylander *et al.*, 2002; Vellak and Ingerpuu, 2005) and their monitoring and mapping can be used to track the impacts of natural and anthropogenic disturbances in the landscape. As 99% of the study area experiences some form of forestry or mining related activities, the bryophyte richness predictive map provided here could be integrated in land use management as well as in a decision support tool for government and industries operating in this region. Understanding the main drivers of bryophyte richness patterns at a large scale is also crucial to the development of conservation strategies and the maintenance of ecosystem functions. Other biodiversity indicators such as dissimilarity measures (beta diversity) could be added to the baseline provided by our study to support conservation planning processes in boreal forests.

2.7 Conclusion

At the scale of the study (about 30,000 km²), the predictive performance of the model encompassing total bryophyte species was acceptable. However, predictive mapping of bryophyte richness at the guild level allowed us to identify important variables determining the richness of a myriad of bryophyte species with singular environmental requirements. This distinction among guilds remains hidden when bryophytes are considered as a homogeneous plant group. Independent guild-level models also produced more accurate predictions, since they were better adapted, in terms of predictors and their relative contribution, to the specific ecological preferences and tolerances of each guild. This study highlights the importance of working, not only with bryophytes as a whole, but also at the guild level.

The 30m spatial resolution remote sensing data used in our study were able to capture biophysical features driving the assemblage of different bryophyte species. This

ultimately allowed the explanation of a significant fraction of richness variations in all models in both training and validation datasets. Therefore, the indirect remote sensing approach provides a valuable tool for assessing bryophyte diversity and to make predictions on biodiversity distribution across the landscape. However, more research on remote sensing-derived indicators of bryophyte diversity is needed. While more accurate and reliable predictive models could be developed in the future using high-resolution data, this study clearly underlines the potential of remote sensing tools in the field of predictive modeling of bryophyte biodiversity. Our work also lays the basis for eventual inclusion of bryophytes, until now overlooked, into the sustainable industrial development planning in northern Canada.

2.8 Acknowledgements

We greatly thank Philippe Marchand for his assistance in the initial phases of this work, especially during the predictor selection procedure. We also thank Chafi Chaieb and Joëlle Castonguay for providing part of the bryophyte field data, and Julie Arseneault for her help in identifying bryophyte samples. We also thank André Beaudoin and Luc Guindon from NRcan for the valuable contribution in Radar and remote sensing database. This research was funded by Environmental Damages Fund, Environment and Climate Change Canada.

CHAPTER III

SMALL BUT VISIBLE: PREDICTING RARE BRYOPHYTE DISTRIBUTION AND RICHNESS PATTERNS USING REMOTE SENSING-BASED ENSEMBLES OF SMALL MODELS

Carlos Cerrejón^{1,*}, Osvaldo Valeria^{1,2}, Jesús Muñoz³ and Nicole J. Fenton¹

¹ Institut de recherche sur les forêts, Université du Québec en Abitibi-Témiscamingue, 445 boul. de l'Université, Rouyn-Noranda, Québec, J9X 5E4, Canada

² Hémera Centro de Observación de la Tierra, Escuela de Ingeniería Forestal, Facultad de Ciencias, Universidad Mayor, Camino La Pirámide 5750, Huechuraba, Santiago 8580745, Chile

³ Real Jardín Botánico (RJB-CSIC), Plaza de Murillo 2, 28014 Madrid, España

* Corresponding author: carlos.cerrejonlozano@uqat.ca

Plos One, 17(1), e0260543

3.1 Abstract

In Canadian boreal forests, bryophytes represent an essential component of biodiversity and play a significant role in ecosystem functioning. Despite their ecological importance and sensitivity to disturbances, bryophytes are overlooked in conservation strategies due to knowledge gaps on their distribution, which is known as the Wallacean shortfall. Rare species deserve priority attention in conservation as they are at a high risk of extinction. This study aims to elaborate predictive models of rare bryophyte species in Canadian boreal forests using remote sensing-derived predictors in an Ensemble of Small Models (ESMs) framework. We hypothesize that high ESMs-based prediction accuracy can be achieved for rare bryophyte species despite their low number of occurrences. We also assess if there is a spatial correspondence between rare and overall bryophyte richness patterns. The study area is located in western Quebec and covers 72,292 km². We selected 52 bryophyte species with < 30 occurrences from a presence-only database (214 species, 389 plots in total). ESMs were built from Random Forest and Maxent techniques using remote sensing-derived predictors related to topography and vegetation. Lee's L statistic was used to assess and map the spatial relationship between rare and overall bryophyte richness patterns. ESMs yielded poor to excellent prediction accuracy (AUC > 0.5) for 73% of the modeled species, with AUC values > 0.8 for 19 species, which confirmed our hypothesis. In fact, ESMs provided better predictions for the rarest bryophytes. Likewise, our study revealed a spatial concordance between rare and overall bryophyte richness patterns in different regions of the study area, which has important implications for conservation planning. This study demonstrates the potential of remote sensing for assessing and making predictions on inconspicuous and rare species across the landscape and lays the basis for the eventual inclusion of bryophytes into sustainable development planning.

3.2 Résumé

Dans les forêts boréales canadiennes, les bryophytes représentent une composante essentielle de la biodiversité et jouent un rôle important dans le fonctionnement des écosystèmes. Malgré leur importance écologique et leur sensibilité aux perturbations, les bryophytes sont négligées dans les stratégies de conservation en raison de lacunes dans les connaissances sur leur distribution, connue sous le nom de déficit de Wallacéen. Les espèces rares méritent une attention prioritaire dans la conservation car elles présentent un risque élevé d'extinction. Cette étude vise à élaborer des modèles prédictifs d'espèces de bryophytes rares dans les forêts boréales canadiennes à l'aide de prédicteurs dérivés de la télédétection dans un cadre des ensemble de petits modèles. Nous émettons l'hypothèse qu'une grande précision de prédiction basée sur les ensembles de petits modèles peut être obtenue pour les espèces de bryophytes rares malgré leur faible nombre d'occurrences. Nous évaluons également s'il existe une correspondance spatiale entre les patrons de richesse en bryophytes rares et totaux. La zone d'étude est située dans l'ouest du Québec et couvre 72,292 km². Nous avons sélectionné 52 espèces de bryophytes avec < 30 occurrences à partir d'une base de données de présence uniquement (214 espèces, 389 parcelles au total). Les ensembles de petits modèles ont été construits à partir des techniques de Random Forest et Maxent en utilisant des prédicteurs dérivés de la télédétection liés à la topographie et à la végétation. La statistique L de Lee a été utilisée pour évaluer et cartographier la relation spatiale entre les patrons de richesse en bryophytes rares et totaux. Les ensembles de petits modèles ont donné une précision de prédiction faible à excellente (AUC > 0.5) pour 73% des espèces modélisées, avec des valeurs d'AUC > 0.8 pour 19 espèces, ce qui a confirmé notre hypothèse. En fait, les ensembles de petits modèles ont fourni de meilleures prédictions pour les bryophytes les plus rares. De même, notre étude a révélé une concordance spatiale entre les patrons de richesse en bryophytes rares et totaux dans différentes régions de la zone d'étude, ce qui a des implications importantes pour

la planification de la conservation. Cette étude démontre le potentiel de la télédétection pour évaluer et faire des prédictions sur les espèces discrètes et rares à travers le paysage et jette les bases pour l'inclusion éventuelle des bryophytes dans la planification du développement durable.

3.3 Introduction

Canadian boreal forests represent 24% of the world's boreal forest (Natural Resources Canada, 2017). In these forests, anthropogenic disturbances pose serious threats for boreal flora (Ficken *et al.*, 2019; Newmaster and Bell, 2002). This is particularly true for sensitive plant species such as bryophytes, which have been recognized as reliable indicators of environmental changes (Frego, 2007; Hylander *et al.*, 2002; Vellak and Ingerpuu, 2005). Bryophytes are key constituents of biodiversity in Canadian boreal forests, promoting species richness (Möls *et al.*, 2013; Turetsky *et al.*, 2012) and supporting important ecosystem functions (Bond-Lamberty and Gower, 2007; Turetsky, 2003; Turetsky *et al.*, 2012).

Forest management pressure is however affecting bryophyte diversity and community composition in the boreal biome, either through direct species removal or by altering habitat conditions originally suitable for bryophytes (Caners *et al.*, 2013). Forestry practices are also reducing the ecological continuity of forests, jeopardizing the recolonization processes after disturbance events (Boudreault *et al.*, 2018; Frego, 2007). Highly habitat-specific and/or dispersal-limited bryophyte species harbored by old-growth boreal forests may therefore be at risk (Boudreault *et al.*, 2018). Despite their ecological importance and sensitivity to disturbances, bryophytes are part of the vast unseen biodiversity that is currently ignored in most conservation plans (Rowntree *et al.*, 2011; Vanderpoorten and Hallingbäck, 2009).

Less known and represented in natural history collections than other groups such as birds, mammals or flowering plants, the large contribution of inconspicuous taxonomic

groups to diversity is difficult to assess, and thus commonly operationalized using diversity measures of these other groups as surrogates (Austin and Margules, 1986; Pimm *et al.*, 2014). However, these better-known taxonomic groups are poor surrogates for highly diverse but less showy or studied taxa (Rodrigues and Brooks, 2007). Including inconspicuous species groups, such as bryophytes (e.g. Cerrejón *et al.*, 2020), representativeness in systematic conservation planning assessments would lead to more robust conservation measures (Delso *et al.*, 2021).

From a conservation perspective, rare species deserve priority attention as they are at a high risk of extinction (Lomba *et al.*, 2010; Zhang, 2019). However, because of their own nature, many rare species of unseen biodiversity groups (Delso *et al.*, 2021) suffer from a lack of information on environmental requirements or their distribution (Hortal *et al.*, 2015; Whittaker *et al.*, 2005). Species Distribution Models (SDMs), which allow to quantify the statistical relationships between species observations and environmental conditions from known locations, can provide useful tools for assessing ecological preferences of rare species or predicting their distributions (Guillera-Arroita *et al.*, 2015; Mateo *et al.*, 2011). More precisely, SDM-based predictions are achieved by using the relevant environmental conditions as proxies of species occurrence. However, the ability of traditional SDMs to predict rare species has been strongly limited by the number of occurrences available, with increases in prediction accuracy with increased sample size (Guisan *et al.*, 2007; Wisz *et al.*, 2008). Furthermore, modeling species with low prevalence often results in a high predictors/occurrences ratio, which can lead to model overfitting and reduced applicability to new data (Breiner *et al.*, 2015; Vaughan and Ormerod, 2005). Fortunately, recent advances in modeling techniques and approaches such as Ensembles of Small Models (ESMs) have been shown to provide robust predictions for rare plants (Amirkhiz *et al.*, 2021; Breiner *et al.*, 2015; Lomba *et al.*, 2010). ESMs are ensembles of bivariate models generated from all pairwise predictor combinations from a larger set of predictors (Breiner *et al.*, 2015;

Lomba *et al.*, 2010). ESMs can produce more accurate predictions than traditional SDMs and reduce model overfitting for rare species (Breiner *et al.*, 2015). In parallel, remote sensing (RS) offers a powerful tool to derive and integrate environmental information into SDMs and generate predictions on species distribution over large areas (Cerrejón *et al.*, 2020; He *et al.*, 2015; Turner *et al.*, 2003). Although a considerable number of studies have successfully integrated RS predictors into SDMs (Jiang *et al.*, 2013; Saatchi *et al.*, 2008; Zimmermann *et al.*, 2007), no study has generated ESMs using only RS predictors, nor has used this approach to generate SDMs of inconspicuous organisms such as bryophytes, much less of their rare species.

In this paper we use RS-derived predictors in an ESMs framework to produce predictive models of rare bryophyte species in Eastern Canadian boreal forests. Bryophyte rare species were selected based on their prevalence in the study area (< 30 occurrences; Barbé *et al.*, 2018). This rare species selection approach was chosen because of the lack of knowledge on bryophytes related to their distribution, ecological preferences and abundance in the region (Barbé *et al.*, 2018), which make it difficult to apply more informative approaches such as multicriteria rare species classification methods (e.g. Rabinowitz, 1981). In fact, the most complete rare bryophyte species list published to date for the region used species' prevalence as the only criterion for rare species classification (Faubert *et al.*, 2010, 2011, 2012). It should be noted that rare bryophytes from (Faubert *et al.*, 2010, 2011, 2012) were not targeted here as their low prevalence (≤ 5 occurrences) greatly restricts the development of SDMs. We hypothesize that high ESMs-based prediction accuracy can be achieved for rare bryophyte species despite their low number of occurrences (Breiner *et al.*, 2015). Our specific objectives are to assess i) if there is a relationship between the number of occurrences and the predictive performance of ESMs, ii) if the predictive performance of models varies by the modeled bryophyte guild (mosses, liverworts and sphagna), and iii) if there is a spatial relationship between the richness patterns of rare bryophyte

species and overall bryophyte species both for bryophytes as a whole and at the guild level (Cerrejón *et al.*, 2020). A total of 52 rare bryophyte species were targeted in the present study, including 33 mosses, 14 liverworts and 5 sphagna

3.4 Materials and methods

3.4.1 Bryophyte field data set

We used a 389-plot database of presences-only including the field data from three studies previously conducted in our study area (Barbé *et al.*, 2017; Castonguay, 2016; Chaieb *et al.*, 2015), which integrated young, mature and old-growth forests and both recent fires and cut-blocks. The study area of 72,292 km² is located in the southwest of the Nord-du-Québec administrative region of western Quebec (48° 51' to 50° 42'N and 74° 31' to 79° 26'W; Figure 3.1), within the Black spruce–feathermoss forest bioclimatic domain (Saucier *et al.*, 2003). Natural dynamics of these forests are primarily driven by stand-replacing fires, whose cycle has been estimated at 398 years after 1920 (Bergeron *et al.*, 2004). The region is characterized by a flat topography, dominance of poorly drained clay soils and a moderately humid and cold climate (927.8 mm annual precipitation and 1.0°C annual mean temperature) (Environment Canada, 2010). These conditions favor the accumulation of organic layer between fires, which is known as the paludification process (Bergeron *et al.*, 2007; Boudreault *et al.*, 2002).

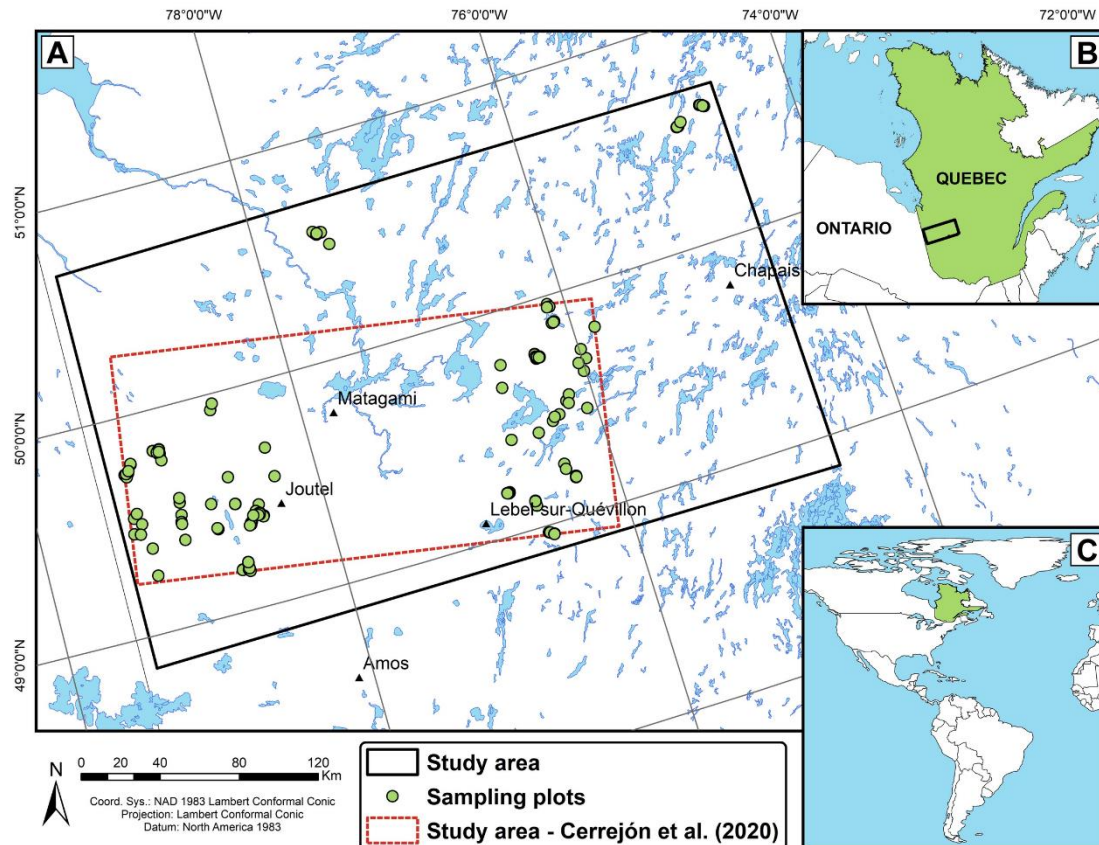


Figure 3.1 A: Study area and sampling plots ($n=389$) in the boreal black spruce forest of western Quebec. B: Location of the study area within Quebec. C: Location of Quebec (eastern Canada).

Bryophytes were collected following a “floristic habitat sampling” method, which consists in collecting all bryophytes found in all microhabitats within 5 x 10m plots (Newmaster *et al.*, 2005). Rare bryophyte species were selected based on their prevalence within the study area (< 30 occurrences) (Barbé *et al.*, 2018). From an initial set of 214 species, 142 rare species were pre-selected, and among them, only those with a minimum of 5 occurrences were retained for modeling, since meaningful predictions can be achieved at this sample size (Hernandez *et al.*, 2006, Pearson *et al.*, 2007; Spiers *et al.*, 2018). A total of 52 rare bryophyte species (33 mosses, 14 liverworts and 5

sphagna; Appendix B) were finally selected for modeling (species occurrence coordinates are shown in Appendix C).

3.4.2 Remote sensing environmental predictors

The selection of RS-derived predictors was carried out based on their sensitivity to environmental factors known to influence bryophyte distribution, namely topography, canopy cover and structure, and vegetation and soil moisture (Cerrejón *et al.*, 2020; Couvreur *et al.*, 2016; Jiang *et al.*, 2014; Raabe *et al.*, 2010). Climatic variables were not included due to their coarse spatial resolution ($\geq 1\text{km}$) and low spatial variability across the study area (annual mean temperature and total precipitation with an approximate variability range of 1 °C and 150 mm respectively; Cerrejón *et al.*, 2020), which could lead us to overestimate the distribution of rare species. In addition, the climatic variability that could be integrated into the individual models of our rare species would be even more limited by the low number of available occurrences. It should be noted that climate variables also present lower reliability compared to RS variables at the scale of our study. This is because climatic variables are based on interpolation methods with high uncertainty, especially in northern latitudes where weather stations are scarce, while RS information is spatially continuous by nature. Therefore, we selected RS variables showing higher variability across the study area and capable of detecting changes in local conditions more closely related to bryophyte occurrence.

RS-derived environmental data were acquired using Google Earth Engine (GEE; Gorelick *et al.*, 2017). The initial set of 6 predictors included topographic position index (TPI), 2-band enhanced vegetation index (EVI2), normalized difference water index (NDWI1), vegetation continuous fields (VCF), PALSAR HV/HH polarization index (PALSAR_HVHH), and bare soil index (BSI; see Table 3.1 for predictor descriptions). TPI was derived from the Shuttle Radar Topography Mission (SRTM)

digital elevation model in ArcGIS v.10.5 (ESRI, 2016) using an annulus neighborhood with inner and outer radius of 15 and 20 pixels, respectively. EVI2, NDWI1, and BSI predictors were derived from Sentinel-2 spectral bands. For each band, a mosaic was built from the images available for the summer season (July 1-August 31) between 2015-2019 to ensure homogeneity in the reflectance values (Franch *et al.*, 2019). Cloudy pixels were masked in all selected images using the Sentinel-2 QA60 band, which allows to identify pixels with opaque clouds and cirrus clouds. Mosaics were performed by applying the median of the overlapping pixel values. We chose EVI2 instead of EVI since EVI2 does not require the blue band, which is sensitive to the presence of residual clouds and aerosols (Jiang *et al.*, 2007). VCF represents percent tree cover at 30m resolution, after rescaling the 250 m MODIS VCF Tree Cover layer using circa-2010 and 2015 Landsat images and incorporating the MODIS Cropland Layer to improve accuracy in agricultural areas (<https://catalog.data.gov/dataset/global-forest-cover-change-tree-cover-multi-year-global-30m-v003>) (Sexton *et al.*, 2013). The VCF predictor presented pixels (0.1% of the total) with missing values in the study area. PALSAR_HVHH was calculated as the ratio of HV-polarized to HH-polarized L-bands from the Advanced Land Observing Satellite (ALOS) Phased Arrayed L-band Synthetic Aperture Radar (SAR) (Mansuy *et al.*, 2018). HV-polarized and HH-polarized L-bands were averaged from yearly mosaics between 2015 and 2017. All predictors were generated and standardized at a 30m spatial resolution (see Table 3.1 for original spatial resolutions). Pearson correlation coefficient was used to identify pairs of highly correlated predictors ($|r| > 0.7$) from a set of 10,000 random background points. Only the NDWI1-BSI predictor pair showed a high correlation ($r = -0.87$). We retained NDWI1 which is sensitive to vegetation and soil moisture (Gao, 1996), since bryophytes are poikilohydric organisms whose distribution is highly dependent on available moisture (Bartels *et al.*,

2018; Gignac, 2001). This resulted in a final set of 5 uncorrelated predictors to run the models (Table 3.1).

Table 3.1 Description of predictors by category and source. Uncorrelated predictors finally selected to model bryophyte distribution are shown in bold.

Predictors	Description	Category	Data source	Source spatial resolution (m)
TPI	Topographic position index; relative elevation at one point compared to its surrounding environment (m); indicative of microclimate conditions (Bennie <i>et al.</i> , 2008)	Topography	SRTM	30m
EVI2	2-band enhanced vegetation index ($2.5 * (NIR - RED) / (NIR + 2.4 * RED + 1)$); sensitive to photosynthetic active biomass (Jiang <i>et al.</i> , 2007; Moreira <i>et al.</i> , 2017)	Vegetation	Sentinel-2	10m
NDWI1	Normalized difference water index ($(NIR - SWIR1) / (NIR + SWIR1)$); sensitive to soil and vegetation moisture (Gao, 1996)	Vegetation	Sentinel-2	10m; 20 m
VCF	Vegetation continuous fields; percent tree cover (%) (Townsend and DiMiceli, 2015)	Vegetation	MODIS	250 m
PALSAR HVHH	PALSAR HV/HH polarization index; indicative of forest structure (Mansuy <i>et al.</i> , 2018)	Vegetation	ALOS PALSAR	25 m
BSI	Bare soil index ($((SWIR1 + RED) - (NIR + BLUE)) / ((SWIR1 + RED) + (NIR + BLUE))$); sensitive to bare soil areas and vegetated areas with different background (Roy <i>et al.</i> , 1996)	Soil	Sentinel-2	10m; 20 m

3.4.3 Modeling approach: Ensembles of Small Models

ESMs based on bivariate models were developed to spatially predict 52 rare bryophyte species (5–29 occurrences) using two modeling machine-learning techniques: Maxent (Phillips *et al.*, 2006) and Random Forest (RF) (Breiman, 2001). Both Maxent and RF techniques can provide robust predictions when few occurrences are available (Hernandez *et al.*, 2006; Pouteau *et al.*, 2012; Williams *et al.*, 2009). Maxent estimates the probability distribution for a given species by finding the probability distribution of maximum entropy according to a set of constraints representing the input known locations (Phillips *et al.*, 2006). RF uses a bootstrap aggregation technique to provide mean predictions from a multitude of independent decision trees built from randomly selected subsamples from the training dataset (Breiman, 2001). A random subset of candidate predictors is assessed to split each node of each individual tree, selecting the predictor that provides the most information in each case (Liaw and Wiener, 2002).

ESMs were generated in R v.3.6.3 (R Development Core Team, 2020) using the *biomod2* package v.3.4.6 (Thuiller *et al.*, 2020). As we used presence-only data, 10,000 background points were randomly generated within the study area and used as pseudo-absences for all species. Presences and pseudo-absences were weighted equally for training the ESMs. The pairwise combinations of our 5 final predictors resulted in 10 candidate bivariate models per modeling technique (Maxent and RF) for each species. We used default settings of the *biomod2* package for computing Maxent and RF models. Predictive performance of each bivariate model was assessed via 10-fold cross-validation procedure, using 80% of the data to train the model and 20% for its validation. While we acknowledge that validation would be optimal using an external dataset, this is hardly available when dealing with rare species. The Somers' D metric was used to identify and select bivariate models better than random (Somers' D score > 0, i.e. AUC > 0.5). Maxent-ESMs and RF-ESMs were then performed using a weighted mean of predicted probabilities from their corresponding retained bivariate models

based on their Somers' D scores (Breiner *et al.*, 2015; Lomba *et al.*, 2010). The contribution of each bivariate model was thus proportional to its predictive accuracy. The final ESMs selected for each species was generated by weighted averaging predictions from Maxent-ESMs and RF-ESMs. Predictive performance of final ESMs was evaluated using the area under the receiver operating characteristic curve (AUC), and the true skills statistic (TSS). AUC is not dependent on a threshold and ranges from 0.5 for an uninformative model to 1 for a perfect fit model, while TSS ranges from -1 to 1 and was chosen instead of kappa because it is not affected by prevalence (Allouche *et al.*, 2006). Since AUC and TSS values were highly correlated (Pearson $r > 0.95$), the results and discussion on models' overall predictive performance will be based on the AUC statistics, following (Breiner *et al.*, 2015) and Allouche *et al.* (2006). The statistic sensitivity was also calculated, which allows the assessment of the proportion of actual presences correctly predicted (Fawcett, 2004). We computed sensitivity for those species whose final ESMs were better than random (AUC > 0.5). Besides of the continuous models (values 0-1000), we generate binary models (presence/absence) using the maximum training sensitivity plus specificity threshold, or TSS optimum (Figure 3.2; predictive mapping of the distribution of the target species is available in Cerrejón *et al.*, 2021b). Finally, we mapped the richness patterns (species number) for total rare bryophyte species, as well as for rare species by guild, by stacking their binary predictions (presence/absence). Missing values associated with the predictions of the three species that included the VCF predictor in their final models were classified as absences before richness computation. We then compared the spatial richness patterns obtained here for rare species with those obtained recently for overall bryophyte species in a smaller region (28,436 km²) but fully included in our study area at the same spatial resolution (30m; Cerrejón *et al.*, 2020). The comparison was performed for bryophytes as a whole (i.e. rare bryophyte richness versus overall bryophyte richness), and between homologous bryophyte guild pairs. This spatial correspondence analysis was carried

out using Lee's L statistic (Lee, 2001) through the *lee()* function from the *spdep* package v.1.1-5. (Bivand *et al.*, 2015). Lee's L statistic, in contrast to non-spatial bivariate association measures such as Pearson's correlation coefficient, integrates and corrects for the spatial autocorrelation of each variable when computing the pixel-to-pixel spatial correlation (Lee, 2001). Due to the high computational requirements to carry out this analysis, the 30m pixels were previously averaged into 300 m pixels through the *aggregate()* function of the *raster* package v.3.4-5 (Hijmans, 2020). Outputs of *lee()* function were centered at 0 and re-scaled to -1 and 1 to facilitate the interpretation of the results by subtracting the overall mean and dividing by the maximum value (Mateo *et al.*, 2016). We then calculated, for each pixel, the quantile associated with its Lee's L value using a Monte Carlo test with 999 simulations in order to identify significant positive (quantile > 0.975) or negative (quantile < 0.025) spatial associations.

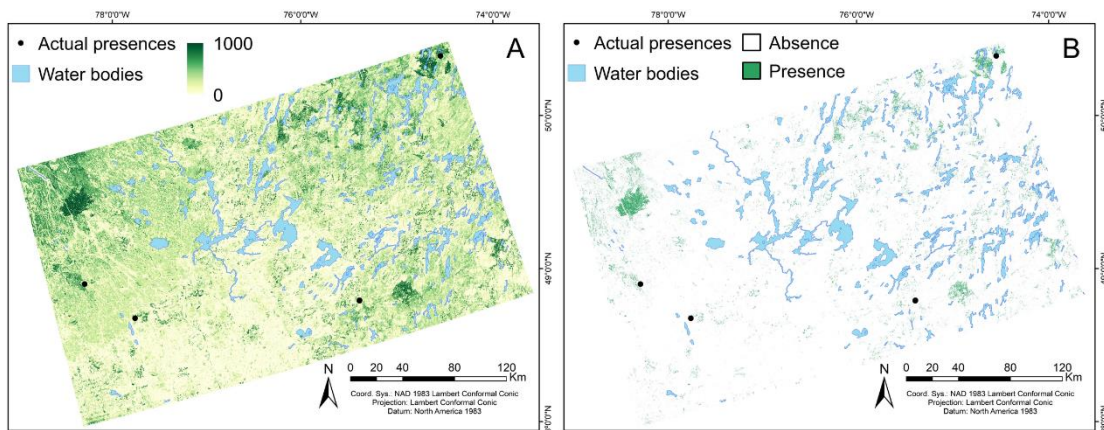


Figure 3.2 Example of (A) continuous and (B) binary predictive mapping of the moss *Trematodon ambiguus* (Hedw.) Hornsch. for the study area at 30m spatial resolution.

3.4.4 Species traits characterization

Species traits can influence the accuracy and therefore the ability of SDMs to predict their occurrence (Chefaoui *et al.*, 2011; McCune *et al.*, 2020). We evaluated the

relationship between ESMs' model performance, as measured by AUC, and rare species traits, namely substrate preference (six categories), reproduction mode (three categories), and spore size (maximum and minimum; Appendix B), as well as their interactions. This assessment was performed using a multiple linear regression through the *lm()* function from the *stats* package v.3.6.3 (R Development Core Team, 2020). Relationships were considered significant at $\alpha = 0.05$.

3.5 Results

3.5.1 ESMs' predictive performance versus number of occurrences and bryophyte guilds

RS-based ESMs provided poor to excellent predictive accuracy for 38 of the 52 modeled rare species, with AUC values ranging from 0.551 to 0.979 and a mean AUC (mAUC) of 0.795 ± 0.132 . Of these 38 species, 19 species were predicted with AUC values greater than 0.8, confirming our hypothesis that high ESMs-based prediction accuracy can be achieved for rare bryophyte species despite their low number of occurrences (< 30). Sensitivity for these 38 species ranged from 0.8 to 1 with an average of 0.959 ± 0.063 , indicating that actual presences were usually accurately predicted. Only predictions for 14 species were not better than random ($AUC \leq 0.5$). Regarding our first specific objective, a negative correlation (Pearson $r = -0.34$) was found between the number of occurrences of the 52 target species and the predictive accuracy as measured by AUC. This negative correlation was also observed at the guild level (Figure 3.3).

To accomplish our second specific objective, we grouped the 52 modeled species by guild and found that predictive accuracy was similar for mosses (mAUC = 0.715 ± 0.167) and liverworts (mAUC = 0.735 ± 0.185), and lower for sphagna (0.663 ± 0.208). No significant relationships were found between ESMs' performance and rare species traits (or their interactions).

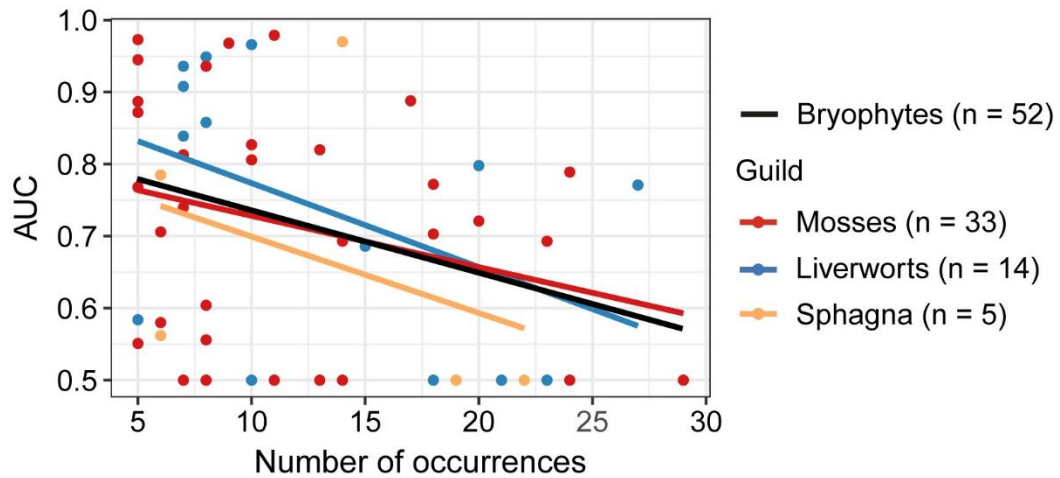


Figure 3.3 AUC values versus number of occurrences (Overall Pearson $r = -0.34$). Bryophyte guilds are indicated.

3.5.2 Richness patterns of rare bryophyte species

Predictive mapping of richness patterns of total rare bryophyte species and rare species at the guild level (mosses, liverworts and sphagna) are presented in Figure 3.4. Predicted richness values ranged from 0 to 30, 21, 9, and 3 species, respectively. The richness pattern of total rare bryophytes was largely structured by the similar richness patterns observed for rare mosses and liverworts, with high richness values mostly found towards the center and southwest of the study area. Conversely, rare sphagna species were concentrated in very specific areas mainly towards the north of the study area with two additional spots towards the southeast.

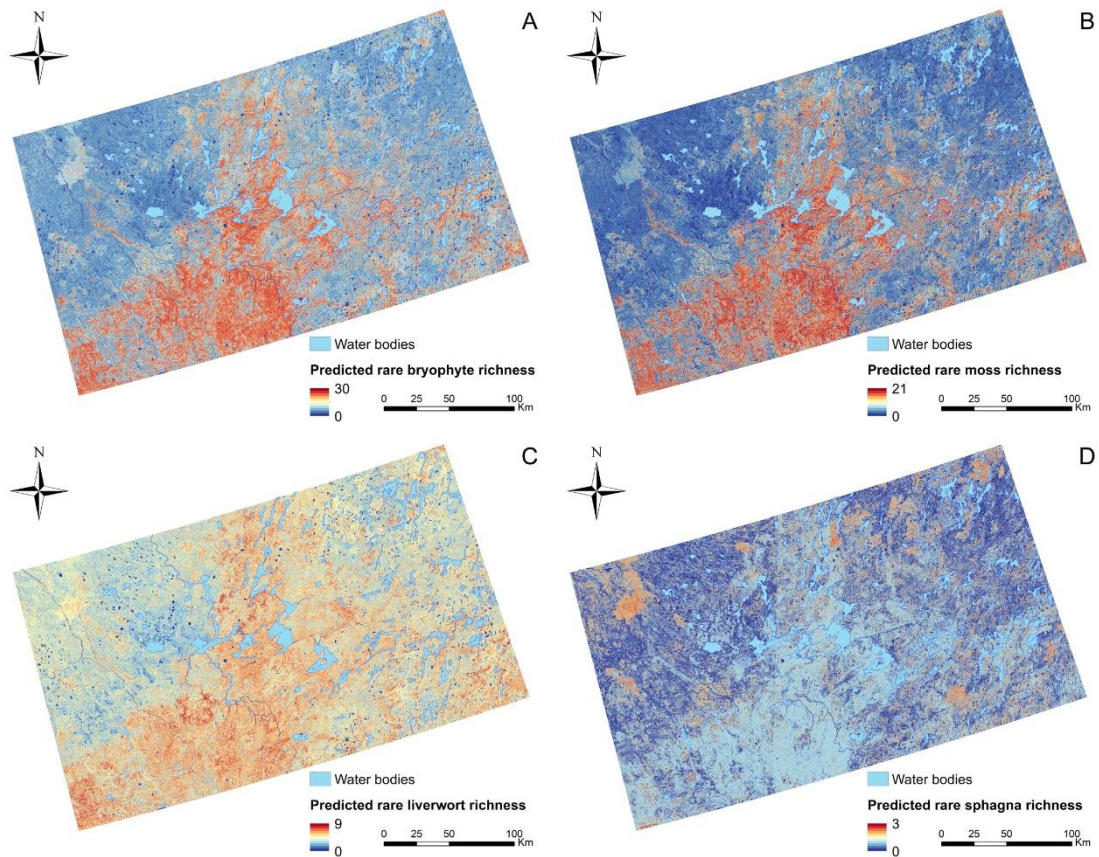


Figure 3.4 Mapping of (A) total rare bryophyte, (B) rare moss, (C) rare liverwort, and (D) rare sphagna richness (species number) for the study area at 30m resolution. Computed from stacked predicted rare species distributions.

Regarding our third specific objective, the Lee's L statistic identified areas of significant positive and negative spatial association between rare and overall species richness for the four homologous bryophyte group pairs (Figure 3.5). Large areas in which the spatial association between the two types of richness was not significant were also consistently observed across pairs.

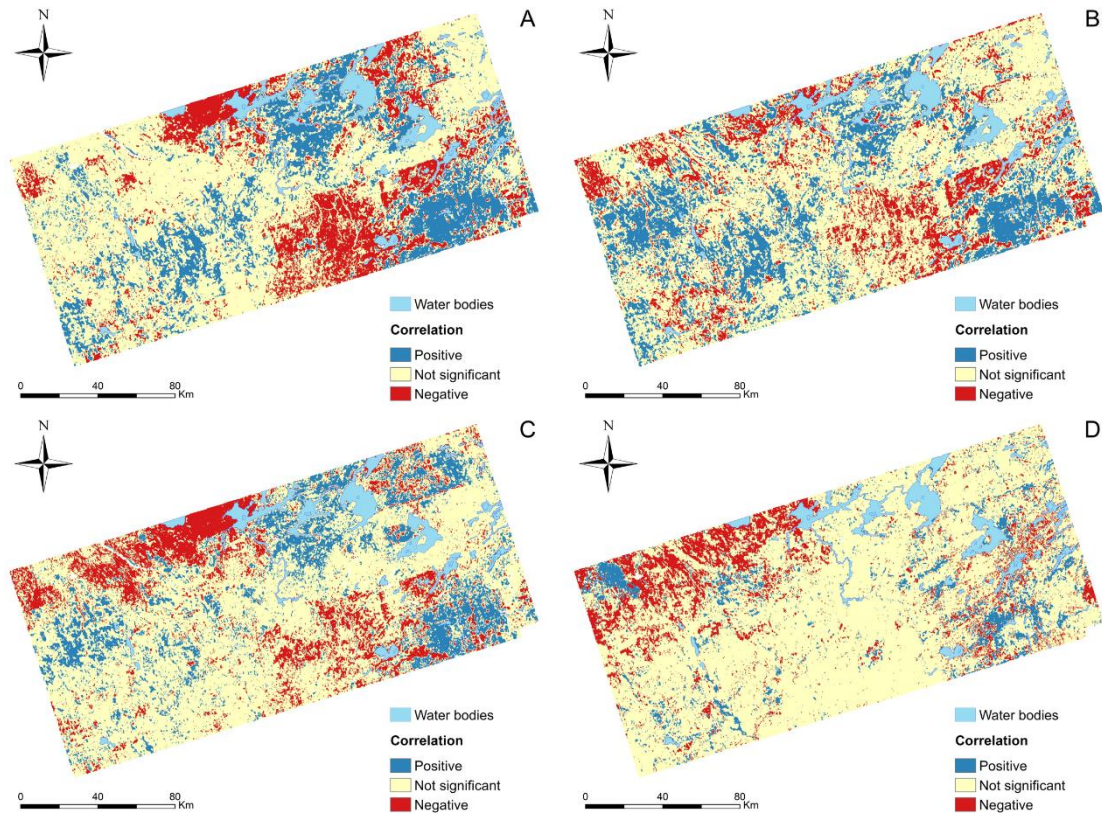


Figure 3.5 Correlation between rare and overall (A) bryophyte, (B) moss, (C) liverwort, and (D) sphagna species richness as measured by re-scaled Lee's L statistic for the study area of Cerrejón *et al.* (2020) at 300 m spatial resolution. "Positive" (blue) and "Negative" (red) indicate significant positive (quantile > 0.975) and negative (quantile < 0.025) Lee's L values derived from Monte Carlo test. Continuous values of the re-scaled Lee's L statistic are shown in Appendix E.

3.6 Discussion

Boreal regions are large areas lacking sharp environmental contrasts, as shown by the low variability of our predictors (Figure 3.6), and thus a habitat where obtaining high-performance SDMs can be challenging. Despite this, our ESMs provided reasonably accurate predictions for rare bryophytes using only 5 uncorrelated RS predictors. Specifically, RS-based ESMs provided poor to excellent predictive accuracy for 73%

of the target species despite their very low number of occurrences. Indeed, 16 species with less than 10 occurrences showed an $AUC > 0.7$. In addition, the computation of the metric sensitivity allowed us to independently show the ability of our ESMs to accurately predict known presences, with high values for the 38 species modeled better than random. Therefore, the combination of RS data at 30m spatial resolution and ESMs proved to be a powerful approach to predict the distribution of rare bryophyte species in Eastern Canadian boreal forests.

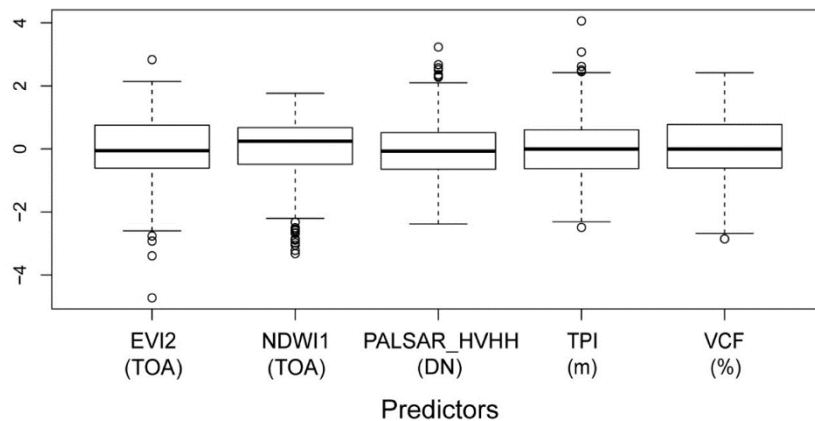


Figure 3.6 Boxplots of standardized uncorrelated predictors used for modeling. See Table 3.1 for predictor descriptions. Measurement units are indicated in parentheses. Unit abbrev.: DN, digital number; TOA, top-of-atmosphere reflectance.

The negative relationship found between models' predictive performance and the number of occurrences of all bryophytes, as well as at the guild level (Figure 3.3), illustrated the suitability of ESMs for predicting the distribution of very rare bryophyte species regardless of guild. This result agrees with those obtained in Breiner *et al.* (2015), who showed a higher predictive performance of ESMs for the rarest vascular plants. Regarding bryophyte species by guild, we consider that the lower overall predictive performance obtained for sphagna species compared to that of mosses and liverworts may be an artifact resulting from the low number of rare sphagna species

modeled ($n = 5$). In fact, the occurrences of two of these five sphagna species were successfully predicted (AUC values of 0.76 and 0.97). However, we do not exclude the possibility that some ecologically meaningful variables that describe the habitat of these species, such as drainage class (Cerrejón *et al.*, 2020), were missing from our models.

In general, our results show that the development of SDMs from RS data allows not only to make predictions of rare species distribution at spatial scales relevant to ecological planning, but also to do so at a level of detail (30m resolution) that can not be achieved using the traditionally used climatic variables at coarse resolutions (1 km). This is particularly important for inconspicuous species such as bryophytes, which interact with their environment at more local scales (Cole *et al.*, 2008; Hespanhol *et al.*, 2011; Pócs, 1996) and for which the use of coarse resolutions can result in a critical loss of information. Likewise, SDMs developed at coarse resolutions can overestimate species distribution (Lawler *et al.*, 2011) and greatly limits the practical utility of derived predictions to subsequently detect species in the field (Guisan *et al.*, 2006). On the other hand, the wide variety of potentially relevant predictors for rare plants that can be derived from RS (related to vegetation, humidity, forest structure, topography, etc.; Annex A; Cerrejón *et al.*, 2021a), can allow a more realistic approach to the environment-species relationship, which can be particularly useful for species with complex ecological niches. Thus, our methodology can play an important role in filling existing knowledge gaps on bryophyte distribution ranges, as well as their ecological preferences, in largely unexplored regions such as boreal forests (Barbé *et al.*, 2018).

The Identification of diversity hotspots has been one of the most used criteria in biodiversity conservation planning in order to locate areas of biological and ecological interest that should be prioritized by decision makers (Hespanhol *et al.*, 2015; Myers *et al.*, 2000; Prendergast *et al.*, 1999). Conservation measures targeting these areas will be more effective if multiple components of biodiversity are spatially concentrated

(Myers *et al.*, 2000; Prendergast *et al.*, 1993; Ricketts *et al.*, 2005). Specifically, both species richness and the presence of rare species have frequently been cited as the main criteria to select areas for conservation (Scott *et al.*, 1993; Usher, 1986), while many rare species might not be represented in species-rich areas (Prendergast *et al.*, 1993). Our study however revealed a spatial concordance between the richness of overall bryophyte species and that of their rare taxa in different regions of the study area (Figure 3.5). While more bryophyte biodiversity components could be subsequently evaluated, this result has important implications for Canadian conservation planning. We consider that the identification of areas harboring high level of both overall and rare bryophyte species diversity, as well as the development of informative tools that serve these purposes, is a significant and necessary step to promote the systematic integration of these species into conservation plans and programs (Hespanhol *et al.*, 2015). Likewise, conservation planning targeting bryophytes and other inconspicuous taxa could further benefit from individual SDMs-based predictions as a basis for assessing their representation in nature reserve networks (Margules and Stein, 1989), to quantify the impact of land use changes on their distribution ranges (Thomas *et al.*, 2004), to inform assessments of their conservation status (Sousa-Silva *et al.*, 2014; Syfert *et al.*, 2014), and to identify suitable areas for their recovery or reintroduction (Pearce and Lindenmayer, 1998).

3.7 Conclusions

Our work demonstrates the ability for RS data to characterize the habitat of rare bryophyte species and predict their distribution patterns across the landscape. This study also reaffirms the effectiveness of ESMs in estimating rare plant distributions (Breiner *et al.*, 2015; Lomba *et al.*, 2010), and highlights, for the first time, the suitability of this modeling approach for making predictions of inconspicuous rare species. We consider that our methods and results provide an important advance in the application of techniques focused on the study of bryophytes, with potential valuable

applications for their management and conservation. In fact, although our study focuses on a particular taxonomic group, the combined use of ESMs and RS would lend useful results for other overlooked inconspicuous taxa lacking information on distribution, which would facilitate their integration in systematic conservation planning.

3.8 Acknowledgements

We thank Marion Barbé, Chafi Chaieb and Joëlle Castonguay for sharing their bryophyte field data, and Julie Arseneault for her help in identifying samples. We thank Rubén G. Mateo for his suggestions and assistance in the preliminary analyzes of the data. We also thank the anonymous reviewers for the constructive comments and suggestions provided on our manuscript. This research was funded by Environmental Damages Fund, Environment and Climate Change Canada.

CHAPTER IV

ASSESSING ALPHA AND BETA DIVERSITY IN INCONSPICUOUS SPECIES USING SATELLITE DATA AT DIFFERENT SPATIAL RESOLUTIONS

Carlos Cerrejón^{1,*}, Osvaldo Valeria^{1,2} and Nicole J. Fenton¹

¹ Institut de recherche sur les forêts, Université du Québec en Abitibi-Témiscamingue,
445 boul. de l'Université, Rouyn-Noranda, Québec, J9X 5E4, Canada

² Hémera Centro de Observación de la Tierra, Escuela de Ingeniería Forestal, Facultad
de Ciencias, Universidad Mayor, Camino La Pirámide 5750, Huechuraba, Santiago
8580745, Chile

* Corresponding author: carlos.cerrejonlozano@uqat.ca

In preparation for *Biological Conservation*

4.1 Abstract

Understanding biodiversity patterns and its environmental drivers is crucial to meet conservation targets and develop effective monitoring tools. Inconspicuous species such as lichens require special attention since they are ecologically important but sensitive species that are often overlooked in conservation planning. Remote sensing (RS) can be particularly beneficial for these species as in combination with modelling techniques it allows planners to assess and better understand biodiversity patterns. This study aims i) to describe and model the lichen alpha diversity (species richness) and beta diversity (species turnover) biodiversity components using high resolution RS variables across a subarctic region in Northern Quebec (~190.25 km²), and ii) to identify habitat types that are lichen biodiversity hotspots. Two sensors, one commercial (WorldView-3, WV3) and another freely accessible (Sentinel-2, S2), at different resolutions (1.2m and 10m, respectively) were tested separately. Lichens were sampled in 45 plots across different habitat types, ranging from forested habitats (coniferous, deciduous) to wetlands (bogs, fens) and rocky outcrops. Two sets of uncorrelated variables (Red and NIR; EVI2) from each sensor were parallelly used to build our alpha and beta diversity models (8 models in total). A total of 116 lichen species were identified. While high lichen richness was generally found across our plots (36.5 ± 9 species), those richer in microhabitats often harbored more species ($R^2 = 0.22$) regardless of the habitat type. Differences in species composition were identified among plots (25.6% explained by PCoA) and habitat types (PERMANOVA $R^2 = 0.35$), both being supported by differences in microhabitat composition (Mantel $R^2 = 0.22$ and PERMANOVA $R^2 = 0.29$, respectively). Rocky outcrops and undisturbed coniferous forests represented the main lichen biodiversity hotspots, while other habitat types were also important for maintaining global biodiversity. Red and NIR variables were useful for modeling the two biodiversity components at both resolutions, while EVI2, especially from WV3, was only informative for assessing beta

diversity. Poisson models explained up to 32% of the variation in lichen richness. Generalized dissimilarity models described well the relationship between beta diversity and spectral dissimilarity (R^2 from 0.25 to 0.30), except for the S2 EVI2 model ($R^2 = 0.07$), confirming that more spectrally and thus environmentally different areas tend to harbor different lichen communities. While WV3 often outperformed the S2 sensor, the latter still provides a powerful tool for the study of lichens and their conservation. This study contributes to improve not only our knowledge of lichen biodiversity in subarctic regions but informs on the use of RS to understand biodiversity patterns of inconspicuous species, which we consider to be an essential step to enhance their representation in conservation planning.

4.2 Résumé

Comprendre les modèles de biodiversité et ses moteurs environnementaux est crucial pour atteindre les objectifs de conservation et développer des outils de surveillance efficaces. Les espèces discrètes telles que les lichens nécessitent une attention particulière car ce sont des espèces écologiquement importantes mais sensibles qui sont souvent négligées dans la planification de la conservation. L'utilisation de la télédétection peut être particulièrement bénéfique pour ces espèces car, en combinaison avec des techniques de modélisation, elle permet aux planificateurs d'évaluer et de mieux comprendre les patrons de biodiversité. Cette étude vise i) à décrire et à modéliser les composantes de la biodiversité de la diversité alpha (richesse des espèces) et de la diversité bêta (changements de la composition des communautés) des lichens à l'aide de variables de télédétection à haute résolution dans une région subarctique du nord du Québec (~190.25 km²), et ii) à identifier les types d'habitats qui sont des points chauds de la biodiversité des lichens. Deux capteurs, un commercial (WorldView-3, WV3) et un autre librement accessible (Sentinel-2, S2), à différentes résolutions (1.2m et 10m, respectivement) ont été testés séparément. Les lichens ont été échantillonnés dans 45 parcelles dans différents types d'habitats, allant des habitats forestiers

(conifères, feuillus) aux milieux humides (tourbières, fens) et aux affleurements rocheux. Deux ensembles de variables non corrélées (Red et NIR; EVI2) de chaque capteur ont été utilisés en parallèle pour construire nos modèles de diversité alpha et bêta (8 modèles au total). Au total, 116 espèces de lichens ont été identifiées. Alors qu'une grande richesse en lichens était généralement observée dans nos parcelles (36.5 ± 9 espèces), les parcelles les plus riches en microhabitats abritaient souvent plus d'espèces ($R^2 = 0.22$) quel que soit le type d'habitat. Des différences dans la composition des espèces ont été identifiées entre les parcelles (25.6% expliquées par la PCoA) et les types d'habitats (PERMANOVA $R^2 = 0.35$), tous deux étayés par des différences dans la composition des microhabitats (Mantel $r = 0.22$ et PERMANOVA $R^2 = 0.29$, respectivement). Les affleurements rocheux et les forêts de conifères non perturbées représentaient les principaux points chauds de la biodiversité des lichens, tandis que d'autres types d'habitats étaient également importants pour le maintien de la biodiversité totale. Les variables Red et NIR étaient utiles pour modéliser les deux composantes de la biodiversité aux deux résolutions, tandis que EVI2, soit de WV3 ou S2, n'était informatif que pour évaluer la diversité bêta. Les modèles de Poisson expliquaient jusqu'à 32% de la variation de la richesse en lichens. Les modèles de dissimilarité généralisée décrivaient bien la relation entre la diversité bêta et la dissimilarité spectrale (R^2 de 0.25 à 0.30), sauf pour le modèle S2 EVI2 ($R^2 = 0.07$), confirmant que des zones plus spectralement et donc environnementales différentes ont tendance à abriter différentes communautés de lichens. Alors que WV3 a souvent surpassé le capteur S2, ce dernier fournit toujours un outil puissant pour l'étude des lichens et leur conservation. Cette étude contribue non seulement à améliorer nos connaissances sur la biodiversité des lichens dans les régions subarctiques, mais nous renseigne sur l'utilisation de la télédétection pour comprendre les modèles de biodiversité des espèces discrètes, que nous considérons comme une étape essentielle pour améliorer leur représentation dans la planification de la conservation.

4.3 Introduction

Currently biodiversity is in a continuous decline worldwide (Brondizio *et al.*, 2019) and understanding its spatial patterns as well as its environmental drivers is essential to efficiently meet conservation targets and elaborate effective monitoring tools (Barnosky *et al.*, 2011). Two major components of biodiversity, namely alpha and beta diversity, are especially informative to identify and prioritize areas of high ecological interest for conservation planning and to ensure appropriate ecosystem management (Socolar *et al.*, 2016). Alpha diversity refers to the diversity within sampling units, while beta diversity describes community composition changes or species turnover between those units (Whittaker, 1960, 1972).

The study of biodiversity is however often limited by the constraints associated with traditional field surveys, especially in remote or inaccessible areas. Remote sensing (RS) can greatly assist in assessing biodiversity and understanding its environmental drivers in remote areas (Pettorelli *et al.* 2014; Rocchini *et al.* 2005), by providing continuous spatial information on a wide variety of biophysical conditions at multiple spatial, spectral and temporal resolutions (He *et al.*, 2015; Rocchini *et al.*, 2015). This information could be used in combination with spatially explicit statistical methods or modelling techniques to better understand and map spatial patterns of biodiversity components (e.g. Rocchini *et al.*, 2010). While the use of RS for the study of alpha diversity has been largely documented in the literature (e.g. Camathias *et al.*, 2013; Waser *et al.* 2004), studies focusing on beta diversity have been much less frequent (Feilhauer and Schmidtlein, 2009; Rocchini *et al.*, 2009). The assessment of both alpha and beta diversity is however required to achieve the most complete and unbiased view of biodiversity (Socolar *et al.*, 2016). RS data can effectively help in this regard, increasing the robustness of biodiversity models for conservation purposes.

RS techniques can be especially beneficial for the conservation of inconspicuous species such as lichens, which suffer from an important lack of knowledge on their distribution and are often neglected in conservation planning (Allen *et al.*, 2019; Hunter and Webb, 2002). Lichens are ubiquitous species that dominate in around 8% of the land surface of the Earth as the main vegetation component (Ahmadjian, 1995; Nash, 2008) and contribute significantly to global biodiversity with a total of approximately 20 000 species (Hawksworth and Lücking 2017; Lücking *et al.*, 2017). They perform key ecological roles in many diverse environments, supporting ecosystem functioning from local (Asplund and Wardle, 2017) to global scales (Elbert *et al.*, 2012; Porada *et al.*, 2014). Specifically, lichens play a major role in nitrogen and carbon cycles as well as in chemical weathering (Asplund and Wardle, 2017; Elbert *et al.*, 2012; Nash, 2008). They provide substrate and microhabitats for a high diversity of micro- and macroorganisms and constitute a food source for herbivores and invertebrates (Boertje, 1984; Nash, 2008). Lichens are also reliable bioindicators of atmospheric and substrate pollution as well as of forest ecological continuity (McMullin and Wiersma, 2019; Seaward, 2004; Tibell, 1992). Therefore, due to their significative ecological contribution, but also their high sensitivity to disturbances (Czerepko *et al.*, 2021), understanding the relationships between lichen communities and their environment is a crucial issue.

Lichens are especially sensitive to local conditions (e.g. air humidity, temperature, light conditions, substrate type and pH) due to their poikilohydric physiology and the influence of those conditions on the photosynthetic efficiency and fitness of their photobiont partner (Lakatos, 2011; Peksa and Škaloud, 2011). Therefore, RS data at high spatial resolution (< 30m; Corbane *et al.*, 2015) can provide useful information that accurately characterizes the environmental drivers potentially shaping their diversity and composition patterns (Keim *et al.*, 2017; Sahu *et al.*, 2019). However, the high costs normally associated with the acquisition of high resolution RS data strongly

limit its systematic use in conservation. Fortunately, satellite sensors such as Sentinel-2 currently provide freely accessible high resolution RS data (10 to 20m), although their resolutions are still coarser compared to those of commercial sensors such as WorldView, Pléiades or GeoEye-1 ($\leq 2\text{m}$ spatial resolution).

In this paper, we aim i) to describe and model the lichen alpha diversity (in terms of species richness) and beta diversity (species turnover) biodiversity components using high resolution RS-derived variables across a subarctic region in Northern Quebec, and ii) to identify which habitat types represent lichen biodiversity hotspots. To model lichen alpha and beta diversity, RS data from two different high resolution sensors, one commercial (WorldView-3; hereafter “WV3”) and another freely accessible (Sentinel-2; hereafter “S2”), at two different resolutions (1.2m and 10m, respectively) will be tested separately. Consequently, we assess the performance of both open access and commercial high resolution RS data for biodiversity estimates for inconspicuous species, which would have important implications for their conservation. The habitat types included in this study range from forested habitats (coniferous, deciduous) to wetlands (bogs, fens) and rocky outcrops, which provide a good representation of the habitat variability found in subarctic boreal landscapes. The hypotheses of this study are:

(1) Sampling units and habitat types that are richer in microhabitats (e.g. tree trunks, snags, logs) will host higher lichen species richness, since different microhabitats can support different inconspicuous species (Barbé *et al.*, 2017; Cole *et al.* 2008; Malíček *et al.*, 2019).

(2) Sampling units and habitat types that are more different in their microhabitat composition will differ more in their species composition (Barbé *et al.*, 2017; Cole *et al.* 2008; Malíček *et al.*, 2019).

(3) As lichens are primarily related to their immediate microenvironment (Keim *et al.*, 2017; Sahu *et al.*, 2019), RS data at higher resolution from WV3 will allow more accurate estimates of this microenvironment than those at lower resolution from S2 and result in better estimation of both alpha and (4) beta diversity.

(5) Regarding beta diversity, a higher spectral dissimilarity between sampling units as well as between habitat types, which is assumed to derive from differences in environmental features, will lead to a higher dissimilarity in terms of the species they host (He *et al.*, 2009; Rocchini *et al.*, 2009).

This study will contribute to improve the knowledge on lichen biodiversity in subarctic boreal regions as well as on the use of RS technologies for understanding biodiversity spatial patterns of inconspicuous species. We consider this to be an essential step to enhance the representation of these species in conservation planning.

4.4 Materials and methods

4.4.1 Study area

The study area is primarily delimited by the boundaries of the Goldcorp Eleonore Mine property (52° 42' 16.49"N, 76° 04' 15.82"W), which is located in the northeast corner of the Opinaca Reservoir within the Eeyou-Istchee James Bay region in Northern Quebec (Figure 4.1). The region is about 250-250m above sea level and is characterized by a subarctic climate with long cold winters and short cool summers (daily average temperatures range from -20°C in January to 17°C in July; Lauzier and Pelletier, 2016). Snow and ice cover the region from approximately November to April, however there is no permafrost. Homogeneous sets of low hills and depressions shape the landscapes, which are composed by gneissic and granitic rocks of the Canadian Precambrian Shield. This region shows one of the most active fire regimes in the North American boreal forest, with an averaged burn rate of 2.4% of the land area per year over the last century (Enri *et al.*, 2017). Fires are not suppressed. The region is thus dominated by even-aged

Picea mariana (Mill.) B.S.P. and *Pinus banksiana* Lamb. forest stands, which are fire adapted species that can quickly recover after fire due to their serotinous cones (Héon *et al.*, 2014). *Betula papyrifera* Marshall and *Populus tremuloides* Michx stands are also present, while their prevalence in the landscape is less than 5%. No logging or agricultural activities are carried out in this region. There is a dense hydrographic network composed by numerous lakes and rivers flowing to James Bay. Peatlands are also abundant in the region, covering around 10–20% of the landscape (Enri *et al.*, 2017). The high diversity of habitats characteristic of the James Bay region, as well as their fire-driven dynamics, are well represented in the study area. Specifically, our study area is composed of a mosaic of *P. mariana* and *P. banksiana* forests interspersed with islets of *B. papyrifera* and *P. tremuloides*, swamps, peatlands, and regenerating sites after recent fires (Lauzier and Pelletier, 2016).

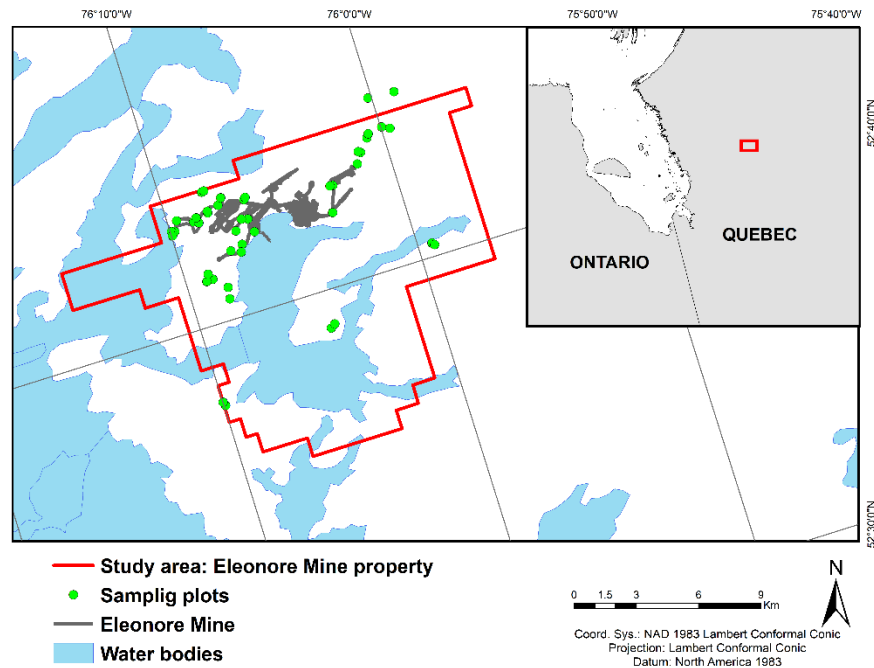


Figure 4.1 Study area and sampling plots (n = 45) within the Eeyou Istchee James Bay region in Northern Quebec. Two plots were located outside the Eleonore Mine property.

4.4.2 Lichen field data set

Field surveys were conducted in 2018 (August 8 to September 2). The lichen community was sampled in a total of 45 plots of 5 x 10m (50m²) using the modified “floristic habitat sampling” method. This method consists in sampling all lichens found in all microhabitats within plots (Newmaster *et al.*, 2005). These plots were selected to represent the variability of habitat types found within the study area. The selection of most of the sampling plots was carried out using classified vegetation maps developed by the Eleonore Mine environmental team, traditional color (RGB) composite imagery derived from Landsat and WorldView-2 satellites, and freely accessible cartography from Google Earth. Table 4.1 shows the different habitat types sampled, their abbreviation codes (used hereafter), and the number of plots per habitat type, which depended on their prevalence in the study area and accessibility. Lichen species were

identified by the lichenologist Mireille Martel in the bryology laboratory of the Université du Québec en Abitibi-Témiscamingue (UQAT). Problematic specimens were verified by a second expert and by thin layer chromatography. Among crustose lichen species, only *Icmadophila ericetorum* (L.) Zahlbr. was identified at the species level, while the rest of the crustose specimens were identified at the "crustose lichen" level. Thus, and to be conservative, species identified as "crustose lichen" were only counted as a species in plots where *I. ericetorum* was not present. Specimen vouchers are stored in the UQAT herbarium (Rouyn-Noranda, Canada). Nomenclature follows Brodo (2016), except for *Bryoria*, *Melanohalea* and *Usnea* genera (Thell and Moberg, 2011). Lichen species at the microhabitat level were aggregated at the plot level to obtain the community species richness and composition per plot. The final database included a total of 116 different lichen species (Appendix F). The rarefaction curve showed good coverage of the lichen species according to the number of plots sampled (Appendix J).

Table 4.1 Habitat types sampled, abbreviation codes used in this study, number of plots, total number of species and description. Numbers in parentheses indicate the number of plots used for alpha and beta diversity analyses after removing outliers (see methods section).

Habitat types	Codes	# of plots sampled (n = 45)	# of species	Description
Bog	B	4	48	Peat-accumulating wetland fed primarily by water from precipitation, with acid pH and low in nutrients. Dominated by <i>Sphagnum</i> mosses and Ericaceae species (<i>Rhododendron groenlandicum</i> , <i>Chamaedaphne calyculata</i> , <i>Kalmia angustifolia</i>). Small coniferous trees (<i>P. mariana</i>) sometimes present.
Bog burned	B_B	6	53	Similar to the bog habitat type but with some evidence of burned soils and/or burned <i>P. mariana</i> trees, which has been replaced by small trees of <i>P. banksiana</i> .
Fen	Fen	5 (3)	28	Peat-accumulating wetland fed by ground or surface water, with basic pH and rich in nutrients. Dominated by <i>Sphagnum</i> mosses and sedges species (mainly <i>Carex</i> sp.). <i>Larix Laricina</i> also present.
Rock	R	5	76	Rocky outcrops. Small coniferous trees (<i>P. mariana</i> or <i>P. banksiana</i>) sometimes present.
Deciduous forest	DF	5	61	Broadleaf forests composed of <i>B. papyrifera</i> and/or <i>P. tremuloides</i> , with mainly bare or litter-covered soils. Some shrubs (<i>Alnus</i> sp., <i>Ribes rubrum</i> , <i>R. groenlandicum</i>) also present.
Coniferous forest	CF	15 (14)	85	Evergreen forests composed of <i>P. mariana</i> and/or <i>P. banksiana</i> . Soils mainly dominated by mosses and/or lichens along with Ericaceae species (<i>R. groenlandicum</i> , <i>C. calyculata</i> , <i>K.angustifolia</i>). <i>Alnus</i> sp. sometimes present.
Coniferous forest burned	CF_B	5	48	Similar to coniferous forest habitat type but with some evidence of burned trees and/or soils.

4.4.3 Environmental characterization of plots through remote sensing variables

Satellite data from two different sensors (WV3, S2) at different spatial resolutions, were used to carry out the environmental characterization of the plots. To compare the results from the two resolutions, we selected the same spectral bands for each satellite as explanatory variables. Since WV3 imagery only spanned the visible and near-infrared spectrum, we chose two bands of ecological interest from that spectral region, namely red and near-infrared (hereafter “Red” and “NIR”, respectively). The blue band was not selected because it is sensitive to atmospheric conditions, and thus is normally used for atmospheric corrections (Xu *et al.*, 2019; Zhang *et al.*, 2013). Green was also not included because of its ability to emphasize peak vegetation (Kerr and Marsha, 2003; Mansuy *et al.*, 2018) is not due to green light reflection by vegetation, as chlorophyll does not reflect green light, but to the absorption of chlorophyll in the blue and Red regions (Virtanen *et al.*, 2020). In fact, compared to green leaves, chlorophyll-deficient leaves are more efficient reflecting green light but also less efficient absorbing Red light. This implies that the potential information that can be derived from green and Red is very similar, as supported by their high correlation (Appendix G). Specifically, Red is particularly effective in distinguishing forested from rocky habitats, due to the high reflection of Red on bare soil and its high absorption by vegetation. Likewise, Red can be informative in discriminating disturbed (burned in our case) from undisturbed habitat types. This is because undisturbed vegetated habitats show higher chlorophyll levels, which absorbs strongly in the Red region (Evans *et al.*, 2004), while the amount of chlorophyll decreases in disturbed habitats, leading to a lower absorption and thus a higher reflection. In addition, this band can be useful for the identification of different vegetation and habitat types, since vegetation differences results in differences in Red absorption and reflection (Kerr and Marsha, 2003). For instance, Red has proved to be informative for discriminating bog habitats from other wetlands classes (Amani *et al.*, 2018). NIR, on the other hand, is indicative of forest structure,

as it can penetrate forest canopy and provide information on foliage vertical profile (Hall *et al.*, 2006; Ma *et al.*, 2019). For instance, NIR is able to detect differences between coniferous and deciduous forests based on the shape and arrangement of the leaves (Cavender-Bares *et al.*, 2020). NIR has also proved to be useful to discriminate among wetland classes (Amani *et al.*, 2018) or disturbed and undisturbed habitats (Ranson *et al.*, 2003). Additionally, we developed the 2-band enhanced vegetation index (EVI2; $2.5 * (NIR - Red) / (NIR + 2.4 * Red + 1)$), which is sensitive to photosynthetic active biomass and thus to the presence of green vegetation and disturbance-induced changes (Jiang *et al.*, 2007; Moreira *et al.*, 2017).

The WV3 imagery consisted in two cloud-free orthorectified scenes corrected atmospherically at Bottom of Atmosphere (BOA) to provide surface reflectance values. Both scenes were captured on July 9, 2020, to ensure that the presence of snow did not influence reflectance values. This date was the closest to the field data collection date for which cloud-free images covering all our sample plots were available. WV3 spectral bands and EVI2 were then extracted and developed, respectively, using the 2020 PCI Geomatics software. Sentinel-2 data was acquired using Google Earth Engine (GEE; Gorelick *et al.* 2017). We used S2 Level 2A images freely available for the study area, which were also atmospherically corrected to provide BOA reflectance values. Images from the summer season (July 1 to August 31) of 2020 were used to match the acquisition date of the WV3 imagery. The S2 QA60 band, which allows the identification of pixels with dense clouds (bit 10) and cirrus clouds (bit 11), was used to mask cloud pixels from the imagery. A mosaic was then performed by applying the median of the overlapping pixel values from each selected image. Finally, spectral variables (including bands and EVI2) were developed at 10m resolution, which is the original resolution provided by S2 for the visible and NIR bands. The spectral variables developed at both resolutions were standardized before statistical analyses

4.4.4 Statistical analyses

The analyses on lichen alpha and beta diversity were performed individually at each resolution in order to compare their performance. All statistical analyses were performed in R v.1.1.456 (R Development Core Team, 2018) and considered significant at $\alpha = 0.05$.

4.4.4.1 Describing lichen alpha diversity

Lichen richness both across all plots and per habitat type was assessed. Plots identified as outliers were removed from all statistical analyses (see Poisson models below). The Tukey test was used to assess if habitat types in pairwise combinations differed significantly in terms of their mean lichen richness values. The Tukey test is a conservative method for unequal sample sizes and thus suitable for comparing our habitat types which were differently represented. We also evaluated the relationship between lichen species richness and microhabitat richness using linear regression. The microhabitats included encompassed 14 different classes (e.g., soil, snags, or logs; Appendix H). The Tukey test was then used to identify potential differences in microhabitat richness among habitat types.

In order to model lichen species richness, Poisson regressions were used. Since Poisson regression is sensitive to multicollinearity, the Pearson correlation coefficient was used to identify highly correlated variables ($|r| > 0.7$) at both pixel resolutions (see Appendix G for correlations coefficients). Regarding the WV3 variables, a high correlation was found between Red and EVI2, while the NIR band was not highly correlated with any other. For the S2 variables, the NIR-EVI2 pair showed a high correlation, while Red was uncorrelated with any other variable. Based on this, two different sets of variables allowed us to generate equivalent lichen richness models from WV3 and S2 and to compare their performances: i) Red + NIR and ii) EVI2. Since Red and NIR raw spectral bands and EVI2 are sensitive to different environmental features, independent

models were computed from each set of variables at both resolutions. This resulted in a total of four models including WV3 and S2 spectral band models, hereinafter referred to as “WV3 band” and “S2 band” respectively, and EVI2 models, referred to as “WV3 EVI2” and “S2 EVI2”. The interaction between Red and NIR bands was also integrated in the band models (Table 4.2).

Table 4.2 Remote sensing-based Poisson models of lichen richness (alpha diversity) tested in the present study. Significant variables are shown in bold. Models were computed from 42 plots after removing outliers.

Model ID	Sensor (resolution)	Variables	Disp.	R²	AICc
WV3 band	WorldView-3 (1.2m)	Red + NIR + Red:NIR	1.65	0.32	188.08
WV3 EVI2	WorldView-3 (1.2m)	EVI2	2.20	0.03	195.71
S2 band	Sentinel-2 (10m)	Red + NIR + Red:NIR	2.05	0.19	199.86
S2 EVI2	Sentinel-2 (10m)	EVI2	2.23	0.03	200.13

Preliminary Poisson regression models were performed to identify potential outliers by visual assessment of the normal Q-Q plots. Three outliers (plots), two located in the Fen habitat type and the third one in the CF_B habitat type, were identified in three of our models, while the S2 band model only shared two of them (Appendices K-N). To ensure model comparability, the three outliers were removed from all models. These outliers showed extremely low richness values (mean richness of 4 ± 1 species; Figure 4.2) compared to the other plots belonging to their corresponding habitat types (mean richness of Fen and CF_B of 19 ± 3.6 and 34.5 ± 3.9 species, respectively). The final Poisson regression models were then fitted using the remaining 42 plots. The Q-Q plots showed that residuals from our models were normally distributed (Appendices O-R), with dispersion coefficients from 1.65 to 2.23 (Table 4.2). To take into account this overdispersion models were corrected through quasi-likelihood adjustments, known as Quasi-Poisson regression models. All Poisson models were performed using the *glm2()* function from the *glm2* package v1.2.1 (Marschner, 2011).

The performance of RS at the two targeted resolutions to estimate lichen richness was assessed through i) the significance level of the corresponding variables, ii) the coefficient of determination (R^2), which refers to the amount of variation explained by a given model, and iii) the Akaike Information Criterion (AIC), which allows the ranking of models based on a trade-off between their goodness of fit and complexity (Burnham and Anderson, 2002). More specifically, we used the second-order AIC (AICc), which is recommended for small sample sizes, i.e., where the ratio between the number of observations (n) and the number of variables (k) is less than 40 (Burnham and Anderson, 2002). Models' AICc were computed using the *aictab()* function of the *AICcmodavg* package v.2.3-1 (Mazerolle, 2020). To correct for overdispersion when computing Models' AICc, the lowest dispersion coefficient from our four candidate models was used (Table 4.2), which was implemented through the *c-hat* parameter.

4.4.4.2 Describing lichen beta diversity

Lichen beta diversity was assessed through a principal coordinates analysis (PCoA). A dissimilarity matrix was first computed from the species presence/absence data using the Sørensen's dissimilarity index with the *dist.binary()* function from the *ade4* package v.1.7-16 (Dray and Dufour, 2007). Sørensen's index was chosen since it gives double weight to double presences, which is a strong indication of resemblance, while the absence of one species at one sampling unit is not necessarily determined by differences in the environmental conditions (Legendre and Legendre, 2012). We confirmed the Euclidean nature of the produced dissimilarity matrix using the *is.euclid()* function, and thus no correction method for negative eigenvalues was applied. A preliminary PCoA was performed using the initial set of 45 plots to identify potential outliers using the *cmdscale()* function from the *stats* package v.2.6.3 (R Development Core Team, 2018). PCoA visualization was carried out through the *ordiplot()* function from the *vegan* package v.2.7-5 (Oksanen *et al.*, 2020). The same three outliers identified from alpha diversity analyzes were identified in the PCoA and thus removed

from further beta diversity analyses (Appendix S). The final PCoA was then performed using the remaining 42 plots. The Mantel regression test was then used to evaluate the relationship between lichen beta diversity, as measured by the Sørensen dissimilarity index, and microhabitat-based dissimilarity, as measured by Euclidean dissimilarity. The Mantel test is based on the Pearson's correlation in which two independent dissimilarity matrices are used as input variables (He *et al.*, 2009). This test allowed us to assess if differences in microhabitat composition between our plots result in different species composition. The Mantel tests were performed through the *mantel()* function from the *vegan* package, using the Monte Carlo test with 999 simulations to estimate the significance of the results.

Lichen beta diversity was modeled through generalized dissimilarity modelling (GDM; Ferrier *et al.*, 2007), using spectral (Euclidean) dissimilarity estimated from the two sets of variables (Red + NIR; EVI2) at both targeted spatial resolutions (1.2m, 10m). With this modeling method we assessed if spectral differences resulting from different environmental conditions lead to different species composition among our plots. GDMs were carried out with the *gdm()* function of the *gdm* package v1.5.0-3 (Fitzpatrick *et al.*, 2020). The parameter *geo* of this function was set to TRUE to include the geographic distance as an additional explanatory variable. We anticipate a negligible effect of the geographic distance in all beta diversity models (sum of coefficients ranging from 0 to 0.028).

Finally, the PERMANOVA test was used to assess if the different habitat types differ significantly from each other in terms of species composition (beta diversity), microhabitat composition, and spectral dissimilarity. The PERMANOVA test was performed using the previously computed dissimilarity matrices and 9999 permutations, through the *adonis2()* function from the *vegan* package.

4.5 Results

4.5.1 Describing lichen alpha diversity

We identified a total of 116 lichen species in our study area, belonging to 33 genera and 14 families. The total number of different species found in each habitat type is shown in Table 4.1, which ranged from 28 to 85 species occurring in Fen and CF, respectively. A mean richness of 36.5 ± 9 species was found across all plots included in the present study, excluding the three outliers previously identified. At the habitat type level, CF and R plots presented the highest mean species richness, followed by CF_B, DF, B_B, and B with intermediate values, and lastly by Fen, which presented the lowest mean species richness (Figure 4.2A). Fen differed significantly in its species richness from all other habitat types according to the Tukey test. Significant differences in species richness were also found between the habitat type pairs CF-B_B and CF-DF (Figure 4.2A). The greatest variability in species richness values was found in R, with a standard deviation of 12 species, while the other habitat types showed more homogenous values, with a standard deviation ranging from approximately 4 to 6 species. A significant positive relationship was found between lichen richness and microhabitat richness across our study area (Figure 4.2B), which confirmed our hypothesis (1), while no significant differences in microhabitat richness were found between habitat types (Appendix T).

Among the lichen species included in the present study, almost 50% occurred in only one or two habitat types, while the remaining species appeared in three to seven different habitat types (Appendix U). Species associated with one habitat type were the most abundant (39 species), of which 17, 13, 7, 1 and 1 species were exclusive of R, CF, DF, CF_B and B_B, respectively. There were no species occurring exclusively in B or Fen. Species occurring in 3 to 5 habitat types were the least frequent, representing 19.8% of the total, while 31% occurred in 6 to 7 (all) habitat types.

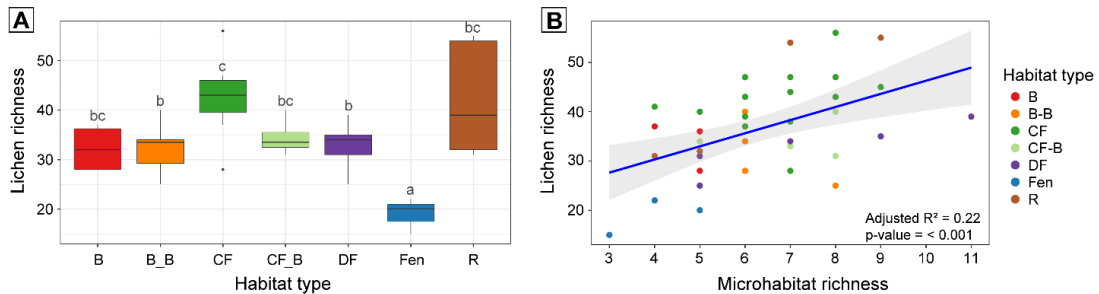


Figure 4.2 A: Boxplots of lichen richness per habitat type; different letters indicate significant differences in lichen richness among habitat types based on the Tukey test. B: Linear regression between lichen richness and microhabitat richness. Outliers were not included. Habitat type abbrev.: B, bog; B_B, bog burned; CF, coniferous forest; CF_B, coniferous forest burned; DF, deciduous forest; Fen, Fen; R, Rock.

Results from Poisson models on lichen richness showed higher R^2 and AICc values for the WV3 band compared to the S2 band model (Table 4.2). The WV3 band model also presented a lower dispersion value, indicating a better fit to a Poisson distribution. The significant variables varied between these two models, with NIR and the Red:NIR interaction being significant in the WV3 band model, and only Red in the S2 band model. EVI2 models at the two targeted resolutions showed very low performance ($R^2 = 0.3$), close AICc ($\Delta AICc = 4.42$) and similar dispersion, with the variable EVI2 being non significant in both cases (Table 4.2). Therefore, our hypothesis (3) that RS variables at higher resolution (1.2m) allow more accurate estimates of alpha diversity than those at 10m resolution was accepted only for the band models (see discussion section for more details).

All variables, namely, Red, NIR and EVI2, showed a negative relationship with lichen richness at the two targeted resolutions (Figure 4.3). Regarding both WV3 and S2 Red values, a transition was found from close to open canopy habitat types (Figure 4.3; Appendix V). More specifically, the lowest Red values, which were indicative of high lichen species richness, were mainly represented by undisturbed forested habitat types (CF and DF). Intermediated Red values were associated with a lower species richness

and represented by disturbed forested (CF_B) and either disturbed or undisturbed wetland habitat types (B, B_B, and Fen). R, which was the best differentiated habitat type in this spectral region, showed the highest Red values despite generally showing high richness. Concerning NIR at both resolutions, the lowest spectral values were generally associated with CF, CF_B and R habitat types, while the highest values were indicative of DF, which was the best discriminated habitat type. The other habitat types, namely B, B_B and Fen, often showed intermediate NIR values, particularly at the higher resolution of WV3. For EVI2, different patterns were observed for WV3 and S2. WV3 EVI2 was able to spectrally discriminate DF and R, which showed the highest and the lowest spectral values, respectively, while the rest of habitat types presented intermediate values. S2 EVI2 differentiated DF well, while it was unable to discriminate the other habitat types, which appeared intermingled through low and intermediate EVI2 values.

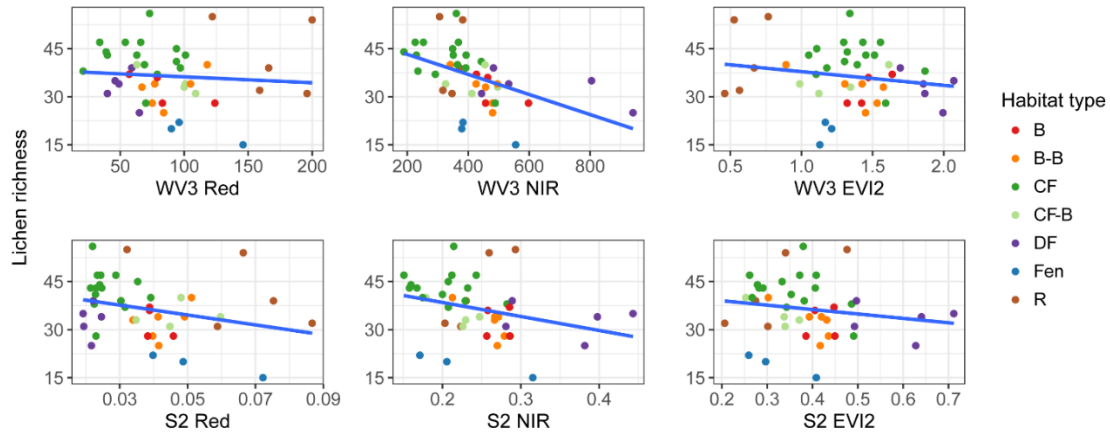


Figure 4.3 Linear relationship between the observed lichen richness and the explanatory variables included in the models at both targeted spatial resolutions (WV3, WorldView-3 at 1.2m resolution; S2, Sentinel-2 at 10m resolution). Units of explanatory variables are expressed in digital numbers. See section 4.4.3 for explanatory variable description. Habitat type abbrev.: B, bog; B_B, bog burned; CF, coniferous forest; CF_B, coniferous forest burned; DF, deciduous forest; Fen, Fen; R, Rock.

4.5.2 Describing lichen beta diversity

Regarding lichen beta diversity, the PCoA explained 25.6% of the total variance in species composition changes between plots (PC1: 13.5%, PC2: 12.1%; Figure 4.4). The habitat types studied showed significant differences in their species composition (Table 4.3). More specifically, Rock and Fen clearly differed in their species composition both between them and from the other habitat types. Plots belonging to forested habitat types, namely DF, CF and CF_B, were clustered close but generally separated, indicating differences in their species composition. These plots were however interposed with those of B and B_B, which showed a high variability in terms of species composition. The differences in species composition found here were supported by significant differences in microhabitat composition across both our plots (Figure 4.5) and habitat types (Table 4.3), confirming our hypothesis (2).

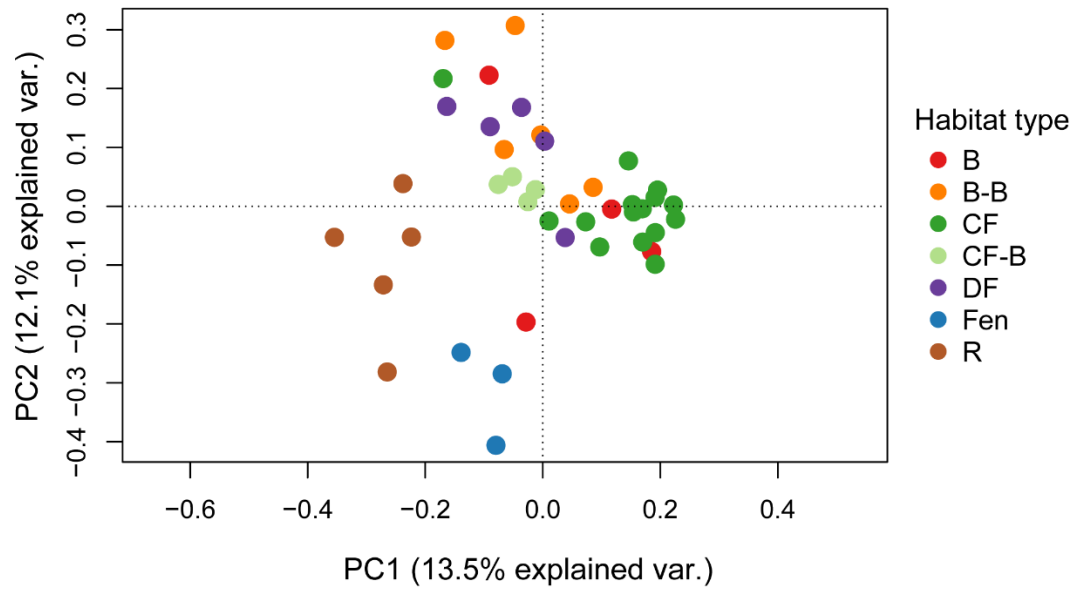


Figure 4.4 Principal coordinates analysis (PCoA) on lichen community composition based on the Sørensen's dissimilarity index. Habitat type abbrev.: B, bog; B_B, bog burned; CF, coniferous forest; CF_B, coniferous forest burned; DF, deciduous forest; Fen, Fen; R, Rock.

Table 4.3 Results of PERMANOVA for lichen species composition (Sørensen's dissimilarity), microhabitat-based and spectral dissimilarities (based on both set of variables – Red + NIR; EVI2 – from both sensors – WV3, WorldView-3; S2, Sentinel-2) according to the habitat type based on 999 permutations. Groups of sampling units were defined by habitat type.

Dissimilarity matrix	R ²	Significance
Species composition	0.35	< 0.001
Microhabitats	0.29	< 0.001
WV3 Red + NIR	0.61	< 0.001
WV3 EVI2	0.76	< 0.001
S2 Red + NIR	0.64	< 0.001
S2 EVI2	0.60	< 0.001

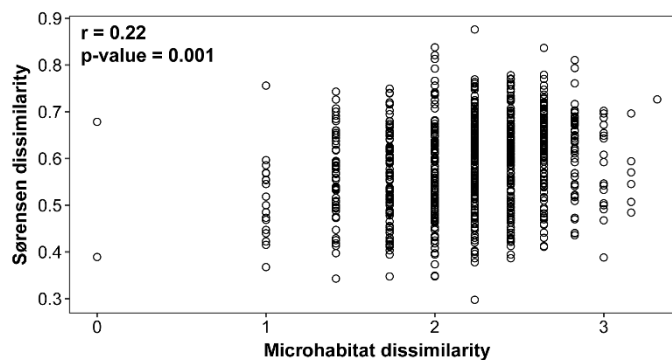


Figure 4.5 Relationship between lichen species composition (Sørensen's dissimilarity) and microhabitat-based dissimilarity. Mantel coefficients (r and p -value) resulting from 999 permutations are indicated. See Appendix I for Mantel upper confidence limits.

GDMs showed significant positive relationships between lichen beta diversity, as measured by the Sørensen dissimilarity, and the spectral dissimilarity at both targeted spatial resolutions for the two different set of variables tested (Figure 4.6). These models explained a significant fraction of the variation in beta diversity ($R^2 = 0.27 \pm 0.03$), except for the spectral dissimilarity computed only from S2-derived EVI2 ($R^2 = 0.07$). Therefore, our hypothesis (3) that RS variables at higher resolution (1.2m) allow more accurate estimates of beta diversity than those at 10m resolution was accepted

when spectral dissimilarity was computed from EVI2 and rejected when estimated from raw spectral bands. The PERMANOVA showed that the habitat types, beyond being significantly different in species composition, also differed significantly in their spectral characteristics, showing relatively high R^2 values for the two different set of variables at both spatial resolutions (Table 4.3). Therefore, GDM and PERMANOVA results consistently confirmed our hypothesis (4) that a higher spectral dissimilarity between plots, as well as between habitat types, leads to a higher dissimilarity in terms of the species they host.

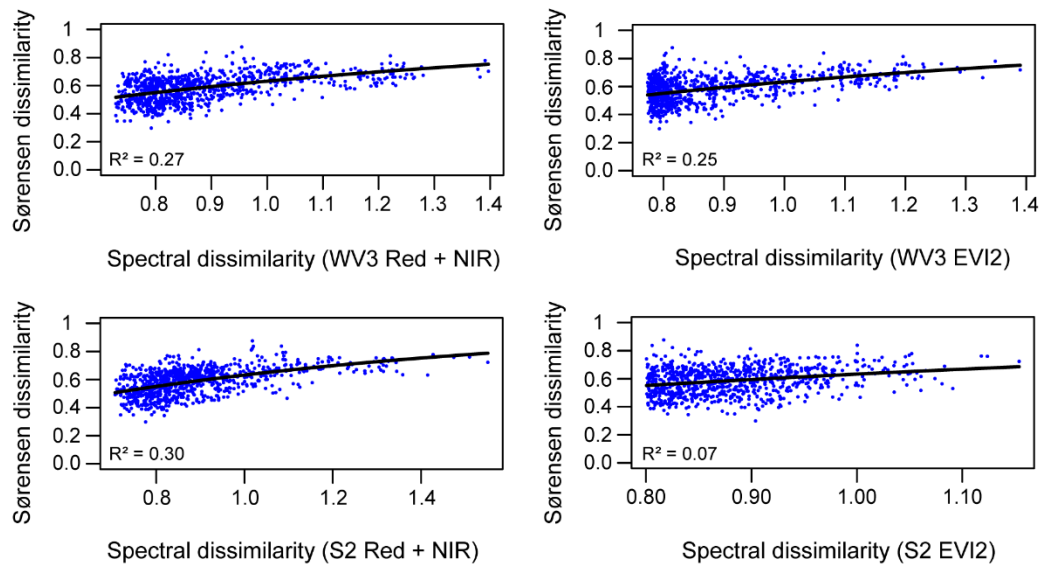


Figure 4.6 Generalized dissimilarity models of lichen beta diversity (Sørensen's dissimilarity) using spectral dissimilarity from the two different set of variables (Red + NIR; EVI2) at both targeted spatial resolutions (WV3, WorldView-3 at 1.2m resolution; S2, Sentinel-2 at 10m resolution). See section 4.4.3 for variable description.

4.6 Discussion

4.6.1 Lichen biodiversity and the influence of environmental variability at different scales

This study put in evidence that high lichen biodiversity can be hosted even in small areas of subarctic boreal regions. This was supported by the 116 lichen species identified, despite the limited number of sampling plots ($n = 45$) and extension of the study area (Eleonore Mine property area of 190.25 km²). Similar results were found by Chagnon *et al.* (2021), who found 94 lichen species in 42 plots distributed across a subarctic to arctic region of Northern Quebec, and Androsova *et al.* (2018), who recorded 158 lichen species in 68 plots in Russian boreal forests.

In our study region, overall lichen biodiversity is promoted by the wide variety of habitat types present, which harbor different species (Figure 4.4; Table 4.3) as a result of their varying environmental characteristics and microhabitats they provide (Table 4.1; Table 4.3). More specifically, higher microhabitat richness promotes higher species richness across all habitat types, while differences in microhabitat composition support different lichen species among both sampling plots and habitat types. These relationships between lichen biodiversity and both microhabitat diversity and composition have been previously shown in the literature (Gignac and Dale, 2005; Peck *et al.*, 2004). This highlights the important role played by environmental variability at different scales (habitat type and microhabitat level) to maintain lichen biodiversity in subarctic regions.

4.6.2 Assessing habitat types as lichen's biodiversity hotspots

The Eeyou Istchee Bay James Region, as many other subarctic boreal regions, represent areas rich in natural resources where the human footprint, while still light or absent, is expected to increase in the future (Boucher *et al.*, 2017; Grondin *et al.*, 2018; Kuuluvainen and Gauthier, 2018; Venier *et al.*, 2018). Thus, the study of biodiversity in these almost intact regions and the identification of hotspots offer an ideal context to inform and promote effective conservation planning, particularly in the case of under-known species such as lichens. In this respect, alpha and beta biodiversity components provide crucial complementary information (Socolar *et al.*, 2016). In this study, the assessment of alpha diversity revealed certain differences in lichen richness among habitat types, while that of beta diversity allowed to identify differences and similarities in species composition among them. Based on these biodiversity components, two environmentally contrasting habitat types were identified as lichen biodiversity hotspots, namely R and CF. While the importance of these habitat types for lichen biodiversity and conservation have already been showed in the literature (Androsova *et al.*, 2018; Boudreault *et al.*, 2002; McMullin and Lendemer, 2013;

Peterson and McCune, 2003), to our knowledge, this is the first time that this has been put in evidence in subarctic ecosystems. Here, R and CF showed the highest species richness, both in overall (Table 4.1) and across their plots (Figure 4.2A). Regarding species composition, R harbored the most differentiated lichen community, showing the highest proportion of exclusive species (17 species) and with its plots differing well from plots belonging to other habitat types (Figure 4.4). CF, which also showed a high number of exclusive species (13 species), shared a higher proportion of species with other habitat types, as shown by the distributions of its plots in the PCoA. Therefore, in terms of species representativeness and potential conservation, these two habitat types can be seen as complementary, since actions or decisions focused on them can maximize the proportion of species benefited throughout the study region. This however does not detract from the other habitat types included in the present study, such as DF or wetland habitat types, which not only harbor relatively high lichen richness but also either exclusive or redundant species. Exclusive species help to maintain the global species pool, as illustrated by the 8 species found only in DF, while redundant species facilitate species persistence in the face of disturbances that could lead to their extirpation. Thus, both exclusive and redundant species, as well as the habitat types harboring them, are also very valuable from a conservation perspective. Given that beta diversity is based on species identity, and that different species can support both unique and redundant functions (Hector and Bagchi, 2007; Isbel *et al.*, 2011; Zavaleta *et al.*, 2010), we consider the assessment of this component as essential not only to identify and preserve biodiversity hotspots, but also to ensure the maintenance of the functioning and ecological stability of ecosystems across the landscape.

4.6.3 Assessing lichen alpha and beta diversity and habitat types through remote sensing

RS variables were reasonably efficient in assessing both lichen alpha and beta diversity at both targeted resolutions (1.2m, 10m). Red and NIR bands were consistently useful for modeling both lichen biodiversity components, while the derived vegetation index EVI2 was only informative when evaluating beta diversity.

Regarding alpha diversity, raw spectral bands at higher resolution (WV3 band model) provided the best performance, explaining up to 32% of the variation in lichen species richness, while the S2 band model performed relatively well ($R^2 = 0.19$). EVI2 models at both targeted resolutions however lacked explanatory power ($R^2 = 0.03$). Raw spectral bands (Red, NIR) thus showed to be able to detect environmental features shaping lichen richness patterns. Specifically, Red captured the transition from closed to open canopy habitat types, which were generally related to high and intermediate/low lichen richness values, respectively. Only the open habitat type R, while being well distinguished in the Red region, did not follow this relationship, since it showed both high Red and richness values (Figure 4.3). S2 Red however performed better than WV3 Red mainly because the reflectance of the close canopy CF habitat type was less variable in this spectral region and thus more consistent across its plots than that of WV3, resulting in a stronger S2 Red-lichen richness relationship (Figure 4.3; Appendix V). The higher variability of WV3 Red in CF plots can be attributed to its higher resolution (1.2m) that can lead the reflectance of conifer stands to be further influenced by more local features such as percent cover, background reflectance or shadow (Walthall *et al.*, 1997). In contrast, the lower resolution of S2 (10m) probably decreases the influence of these factors, giving a more representative spectral characterization of these plots. NIR, on the other hand, was able to successfully detect differences in structure across our plots at both resolutions (Appendix V). This was supported, for example, by the good discrimination achieved for plots belonging to CF

(or CF_B) and DF in this spectral region. The spectral differentiation of these habitat types based on their different structural attributes has been well documented in the literature (e.g., Cavender-Bares *et al.*, 2020; Kuusinen *et al.*, 2016; Zheng *et al.*, 2004). The habitat types richest in lichen species, namely CF and R, while structurally different, often showed similarly low NIR values, reinforcing the lichen richness-NIR reflectance relationship. On the other hand, the less species-rich wetland habitat types (B, B_B, Fen) showed close higher NIR values, particularly at higher resolution, which also supported the performance of this variable. This result agrees the similar structure of the wetland habitat types included here, as being open ecosystems mainly dominated by *Sphagnum* species often with a few small coniferous trees. Similarly to Red, WV3 EVI2 detected the transition from open to closed canopy habitats defined by the minimum and maximum spectral values associated with R and DF, respectively. This agrees with the environmental features of which it is indicative, the presence of photosynthetic active green vegetation (Jiang *et al.*, 2007; Moreira *et al.*, 2017). However, its poor performance at this resolution for modeling lichen richness can mainly be explained by its inability to distinguish between other vegetated habitat types beyond DF that showed different lichen richness, particularly regarding CF (or CF_B) versus wetland habitat types (Figure 4.3; Appendix V). Likewise, as in the case of Red, while WV3 EVI2 was able to spectrally discriminate plots belonging to R, this habitat did not follow the same relationship with lichen richness as other open habitat types, which also influenced its performance. In regard to S2 EVI2, this variable was unable to distinguish between habitats as different in terms of vegetation as R and either CF (or CF_B) or wetland habitat types, which also resulted in a poor lichen richness model. These results regarding EVI2 are in concordance with recent studies which showed the underperformance of vegetation indices compared to raw spectral bands for estimating forest parameters and differentiating habitat types (Grabska *et al.*, 2020; Hallik *et al.*, 2019).

In relation to beta diversity, raw spectral bands at both target resolutions and WV3 EVI2 allowed relatively accurate estimates on the relationship between lichen beta diversity and spectral dissimilarity, while S2 EVI2 showed low performance. Specifically, we demonstrated that more spectrally and thus environmentally different areas tend to host different lichen communities, and that those environmental differences can be detected through high resolution RS (Figure 4.6). These results are in concordance with those from previous studies assessing plant beta diversity using a spectral dissimilarity approach (He *et al.*, 2009; Rocchini *et al.*, 2009). At the habitat type level, these differences in lichen composition and spectral features were also highlighted (Table 4.3). These results underscored that, despite the very small set of RS variables used to compute spectral dissimilarities, either i) Red and NIR or ii) EVI2, they generally well represent ecologically important environmental features shaping lichen beta diversity regardless of the resolution. Therefore, the spectral dissimilarity approach has a high potential for the identification of sites complementary in species composition using spectral dissimilarity as proxies, which can be especially informative to enhance biodiversity assessments and conservation planning. In our case, the combination of Red and NIR would be privileged as potential indicator of the spectral variability found in the study area due to its consistent results (Figure 4.6). While this work was focused on boreal subarctic regions, we are confident in the effectiveness of this approach for beta diversity assessments in other, even contrasting, ecosystem types. In fact, the high diversity of remote sensing variables that can currently be computed (e.g., Cerrejón *et al.*, 2021) can allow to develop larger sets of complementary variables to be jointly used in the estimation of spectral dissimilarities, which would maximize the detection of environmental differences potentially governing species turnover across the landscape.

The commercial WV3 sensor data at 1.2m resolution generally provided better estimates of lichen biodiversity than the open access S2 data at 10m resolution using

the two tested set of variables (Table 4.2; Figure 4.6). However, S2-based modeling of alpha and beta diversity was also acceptable, and even the most accurate when assessing the relationship between beta diversity and spectral dissimilarity through Red and NIR bands. Based on this, and despite its underperformance in the present study, S2 provides a very useful tool for the study of the biodiversity of lichens and other inconspicuous species (Cerrejón *et al.*, 2022). Conservation efforts focused on these often-overlooked species can thus especially benefit from these freely available RS data, especially when financial resources are limited. However, further studies including variables from multiple sensors at different spatial resolutions and covering a broader range of the electromagnetic spectrum are needed to better understand the influence of these RS-related factors on biodiversity estimates of inconspicuous species.

To our knowledge, this is the first study offering an assessment of lichen beta diversity based fully on RS information (Cerrejón *et al.*, unpublished). Regarding alpha diversity, however, two previous studies have modeled lichen richness using RS variables alone (Cerrejón *et al.*, unpublished). In both cases, the authors were able to explain up to a 68% of the variation in lichen richness an alpine region in the Swiss Pre-Alps using the same small set of RS variables at 0.5m spatial resolution (Waser *et al.*, 2004, 2007). These final variables were however selected as the best performing from a larger set of 29 and 32 variables, respectively, covering a wider range of environmental features, which can explain the higher model performance. In our work, the objective of comparing the performance of sensors at different resolutions greatly restricted the selection of RS variables used for modeling and presumably the variability explained for alpha and beta diversity (Marzialetti *et al.*, 2021; Schmidtlein *et al.*, 2017). Therefore, we expect that the use of a more diversified set of RS variables potentially shaping lichen biodiversity, such as topographic, surface temperature, snow persistence or humidity indices, could further enhance future assessments both in our study area and in similar subarctic landscapes. Likewise, the combination of RS variables with other

ecological meaningful non-remotely sensed variables such as climatic or geological, if available, could improve estimates of lichen biodiversity (Camathias *et al.*, 2013; Niittynen and Luoto, 2018), and more particularly when the acquisition of RS variables is limited.

4.7 Conclusions

In this paper we described lichen alpha and beta diversity patterns in a subarctic boreal region of Northern Quebec, highlighting the high lichen biodiversity harbored by these areas, as well as the importance of the environmental variability at the habitat type and microhabitat levels for its maintenance. R and CF habitat types were identified as the main lichen biodiversity hotspots in our study area, while the importance of other habitat types for species conservation and ecosystem functioning was also underscored.

This work also put in evidence the ability for RS to describe and model lichen biodiversity at two different high spatial resolutions (1.2m, 10m). RS variables, especially Red and NIR, captured well ecologically meaningful environmental features shaping both alpha and beta diversity components. While the WV3 commercial sensor often outperformed the S2 open data sensor, the latter still provides a powerful and very promising tool for the study of lichen and other inconspicuous species, with great potential for conservation purposes.

This study not only contributes to enrich the knowledge on lichen biodiversity in subarctic boreal regions but also on the use of RS-based modeling approaches for understanding biodiversity spatial patterns of inconspicuous species. While further studies on lichen biodiversity should be conducted to test a broader range of RS variables, sensors, and spatial resolutions, we hope our work to promote the use of RS technology for the study of inconspicuous species as well as their representation in conservation planning.

4.8 Acknowledgements

We greatly thank Mireille Martel for collecting and identifying the lichen field data used in this study, Yacine Bouroubi for his valuable suggestions on the use of WorldView-3 imagery, Enrique Hernández-Rodríguez for his useful comments on the preliminary version of this manuscript, and Maxence Martin for providing helpful references on boreal forests. We also thank Goldcorp Éléonore mine for collaborating in the development of this study and Environmental Damages Fund, Environment and Climate Change Canada for funding our research.

CHAPTER V

CONCLUSION

Biodiversity assessments are essential in order to avoid and/or mitigate the increasing adverse effects of human-induced global climate and land use changes. The development and application of new approaches allowing to accelerate the acquisition of knowledge on biodiversity patterns and their environmental drivers have thus become crucial, and more particularly in the case of lesser-known, inconspicuous species. Hence the present thesis was focused on evaluating the potential of RS as a source of information to acquire and generate knowledge on biodiversity patterns of cryptogams in regions where this information is deficient such as in Canadian boreal forests. Specifically, this thesis demonstrated the ability for RS to i) characterize the habitat of inconspicuous cryptogam species, namely bryophytes and lichens, and capture meaningful ecological features shaping their distribution, and thus ii) to better understand and/or predict their biodiversity patterns. Overall, various biodiversity components were successfully estimated, ranging from alpha and beta diversity (Chapters II and IV) to the distribution of rare species and their richness patterns (Chapter III). This was possible even when the information available on the species of interest or their biodiversity components was limited, as in Chapters III and IV, where either the number of rare bryophyte species' observations (5 to 29 occurrences) or the plots available for assessing lichen alpha and beta diversity ($n = 43$), respectively, were very low. This thesis thus highlights that RS-based modeling frameworks are informative and thus particularly useful for the study of lesser-known taxa for which baseline information is deficient.

The ability of RS to identify the environmental drivers of species biodiversity patterns depends on the scale in which species interact with their environment and, therefore, on the spatial resolution of RS data, which must be able to detect variation at that scale.

This scale depends ultimately on the particular taxa under study. Cryptogams are sensitive to local conditions (Cole *et al.*, 2008; Keim *et al.*, 2017; Sahu *et al.*, 2019), and RS at high spatial resolution can thus be needed to capture them. Here, however, the usefulness for RS to identify environmental factors shaping their biodiversity patterns was highlighted not only at high (1.2m and 10m; Chapter IV) but also at medium spatial resolution (30m; Chapters II and III; Corbane *et al.*, 2015). In fact, larger-scale environmental features, such as overstory vegetation type and forest structure (Weibull and Rydin, 2005), can significantly affect local conditions (e.g. humidity; substrate composition; litter deposition) and, ultimately, the biodiversity patterns of these species. Likewise, while the results of Chapter IV on lichen alpha and beta diversity generally showed a better performance of the higher resolution (1.2m) commercial WV3 sensor compared to that of open access S2 sensor (10m), this assessment was carried out using only three RS variables (Red, NIR and EVI2) as model's inputs and a limited number of plots. These results can thus be considered preliminary and further studies including a broader range of RS variables at different resolutions are required to confirm whether an increase in the spatial resolution of RS variables translates into an increase in the performance of the models they feed.

The usefulness of a wide range of RS-derived variables for assessing and understanding cryptogam biodiversity patterns was also underscored across the different chapters included in this thesis. These variables, either in the form of raw spectral bands or indices, represented environmental factors as diverse as the presence of vegetation, percent tree cover, stand structure, vegetation and soil moisture content, and topographic features ranging from elevation or slope to relative topographic position, drainage water collection or incident solar radiation, and so on. Likewise, the efficacy of RS variables to feed biodiversity models of cryptogam species was highlighted both in combination with non-remotely sensed variables, such as climatic or soil-related (Chapter II), and alone (Chapters III and IV). A novel and very promising approach

that could improve cryptogam biodiversity assessments and predictions is the development of time series-derived RS variables describing ecosystem functioning attributes to characterize species habitat dynamics, such as energy balance, primary production and CO₂ fluxes, or vegetation or soil water content dynamics (Regos *et al.*, 2022). The usefulness of this approach for prediction purposes has already been demonstrated in different taxa such as birds and vascular plants, including herbaceous and trees (Arenas-Castro *et al.*, 2018, 2022; Vila-Viçosa *et al.*, 2020). Another interesting RS variable to be tested in future boreal cryptogam studies is snow persistence, which influences the duration of the growth session and the time of exposure of species to winter conditions and can therefore have a significant effect on plant growth and survival and thus on their distribution. The performance for predicting cryptogam distribution has already been put in evidence in tundra ecosystems (Niittynen and Luoto, 2018). In addition, the inclusion of other non-remotely sensed variables (e.g., geological) could also be beneficial for cryptogam biodiversity estimates (Camathias *et al.*, 2013), as long as data spatial resolution allows capturing enough environmental variability in the region of interest.

5.1 Remote sensing as a tool to inform conservation actions in cryptogams: Possibilities for improvement are at hand

This thesis unequivocally underscores the high potential of RS technology for conservation purposes of cryptogams, and more specifically of a RS-based modeling framework (RS indirect approach). Interesting insights have been provided on the environmental drivers of cryptogam biodiversity throughout the different scientific chapters, which can guide specific management actions focused on the maintenance or reestablishment of the conditions suitable, e.g. in terms of humidity or forest structure, to conserve biodiversity. Likewise, the ability for RS data to map cryptogam biodiversity patterns across the landscape at a high level of detail, as highlighted in Chapters II and III, makes the resulting predictive cartography very valuable tools to

fill biodiversity data gaps and inform conservation planning for these often neglected species (Delso *et al.*, 2021). This is despite the limitations and uncertainty associated with the use of SDMs for conservation, which is related to the representativeness of the actual distribution, type and geolocation of the biodiversity data used (Aranda and Lobo, 2011; Moudrý and Šímová, 2012; Rondinini *et al.*, 2006; Underwood *et al.*, 2010), the approach employed to assess these biodiversity data (Mateo *et al.*, 2013), and the absence from models of meaningful environmental factors, ecophysiological (e.g., biotic interactions, anthropogenic pressure) and evolutionary or historical processes (e.g. speciation processes, geographic barriers; Cerrejón *et al.*, 2020; Delso *et al.*, 2021; Guisan and Zimmermann, 2000). On the other hand, RS information, continuous by nature and with a source spatial resolution close to that used in our analyses, allows the user to obtain more accurate environmental information (moisture, vegetation attributes, etc.), particularly in relatively flat regions such as ours, and thus to increase model reliability compared to coarse resolution variables, such as climatic or soil attribute variables, which are generally based on interpolation methods and introduce higher uncertainty into the models (Guisan and Zimmermann, 2000).

Specifically, the predictive mapping elaborated in Chapters II and III allowed to geolocate, for the first time, overall and rare bryophyte biodiversity hotspots, respectively, as well as their spatial correspondence, within the Eeyou-Istchee James Bay region, contributing to overcome current knowledge gaps on cryptogam biodiversity patterns (Barbé *et al.*, 2018). The identification of these hotspots provides very useful information for prioritizing areas to preserve and prevent species loss. In total, 46 predictive maps were produced, including one map on overall bryophyte richness (Figure 2.4A), three maps on guild-level bryophyte richness (Figure 2.4B-D), 38 maps on individual rare bryophyte species distribution (Cerrejón *et al.*, 2021b), one map on rare bryophyte richness (Figure 3.4A), and three maps on guild-level rare bryophyte richness (Figure 3.4B-D). An eventual modeling and spatial prediction of

the bryophyte beta diversity component in the study region of Chapters II and III would allow to identify complementary area in terms of species composition, providing very valuable information to be integrated in the hotspot identification process. On the other hand, while lichen biodiversity hotspots were not mapped in Chapter IV, the habitat types representing their main biodiversity hotspots were identified.

If the lack of knowledge of the cryptogams in general can put their perpetuation at risk in the face of the increasing magnitude of industrial development activities in the boreal regions, this poses an even greater threat to their rare species. Therefore, rare species monitoring has become a conservation priority (Guisan *et al.*, 2006; Lomba *et al.*, 2010; Zhang, 2019). Bearing this in mind, the predictive mapping of rare species distribution elaborated in Chapter III represents a significant progress in the application of techniques focused on the study and conservation of cryptogams. Despite its high potential as decision support tools, no previous studies have used RS-based modeling approaches for assessing and mapping the presence of rare species of cryptogams and their richness patterns (Cerrejón *et al.*, unpublished). Although the knowledge on the performance of stacked SDMs in inconspicuous species is deficient and more data need to be collected from insufficiently surveyed areas (Hespanhol *et al.*, 2015), particularly in the case of rare species characterized by low prevalence, our predictive mapping, as developed at 30m spatial resolution, have a great potential to guide future field surveys and discover new populations of the mapped rare species (Annex A; Cerrejón *et al.*, 2021; Guisan *et al.*, 2006). This would allow us to provide an independent validation assessment of rare species model performance, to check for possible overprediction instances either of single species distributions (Cayuela *et al.*, 2009; Guisan and Thuiller, 2005; Trotta-Moreu and Lobo, 2010) or derived richness patterns (Dubuis *et al.*, 2011; Mateo *et al.*, 2012), and to improve these models and their predictions by integrating the new observations. Likewise, this new information on species occurrence can better inform the actual environmental variability in which rare species occurs

(Guisan *et al.*, 2006), which is deficiently documented (Barbé *et al.*, 2018). This knowledge on species' ecological niches can ultimately help understand the causes of their rarity, review their conservation status, and facilitate either the discovery of new populations and the development of effective management and conservation measures (Annex A; Cerrejón *et al.*, 2021; Söderström *et al.*, 1992).

The promising results obtained in the present thesis using freely accessible satellite data with global coverage at high and medium spatial resolutions (S2 and Landsat, respectively) support the suitability of RS-based modeling approaches as a tool to promote the systematic integration of cryptogams in conservation planning. This is especially relevant for regions or countries where resources devoted to conservation issues are limited and/or where increasing anthropogenic pressure makes biodiversity assessments critical, particularly regarding lesser-known, inconspicuous species. Although economic and logistical resources were used for the collection of the cryptogam field data used across the scientific chapters included in this thesis, the increasing availability of open access biodiversity data from digitization of natural history collection and herbarium sheet data or citizen science initiatives and programs (Rocchetti *et al.*, 2021; Andrew *et al.*, 2017; Beaman and Cellinese, 2012; Chandler *et al.*, 2017; Paton *et al.*, 2020; www.gbif.org), which are typically in presence-only data format (Guillera-Arroita, 2017), provides a unique opportunity to perform biodiversity assessments through a RS indirect approach without cost associated to either species or satellite data acquisition. The usefulness of these freely accessible biodiversity data to feed SDMs have been put in evidence (Feldman *et al.*, 2021; Henckel *et al.*, 2020). Therefore, a modeling framework combining open access RS and species data can be key for rapid biodiversity assessments of cryptogam species and their future preservation across the world. Furthermore, our results and methodologies could be useful for other lesser-known, inconspicuous species facing underrepresentation in conservation planning (e.g. fungi, arthropods, etc.; Delso *et al.*, 2021; Dunn, 2005;

Senn-Irlet *et al.*, 2007). Following a similar approach of that used in Chapter III based on Lee's L statistic (Lee, 2001), future multi-taxon studies could be directed at assessing and mapping the spatial relationships among hotspots of these different inconspicuous taxonomic groups, which represent most of the biodiversity in any given region (Delso *et al.*, 2021). This type of cartography would be of great interest to planners and other stakeholders in order to identify exclude sites of high ecological interest from growing industrial development and facilitate its coexistence with the conservation of biodiversity and the ecological functions it supports.

ANNEX A

NO PLACE TO HIDE: RARE PLANT DETECTION THROUGH REMOTE
SENSING

Carlos Cerrejón^{1,*}, Osvaldo Valeria¹, Philippe Marchand¹, Richard T. Caners² and
Nicole J. Fenton¹

¹ Institut de recherche sur les forêts, Université du Québec en Abitibi-Témiscamingue,
445 boul. de l'Université, Rouyn-Noranda, Québec, J9X 5E4, Canada

² Royal Alberta Museum, 9810 103a Ave NW, Edmonton, AB, T5J 0G2, Canada

* Corresponding author: carlos.cerrejonlozano@uqat.ca

Diversity and Distributions, 27(6), 948-961

A.1 Abstract

Aim. Detection of rare species is limited by their intrinsic nature and by the constraints associated with traditional field surveys. Remote sensing (RS) provides a powerful alternative to traditional detection methods through the increasing availability of RS products. Here we assess the capacity of RS at high and medium resolution to detect rare plants with direct and indirect approaches, and how the performance of RS can be influenced by the characteristics of species.

Methods. An extensive literature review was conducted to synthesize the use of RS to detect or predict rare plant occurrence at high and medium resolution (<30m and 30–300m, respectively). The concept of “rarity” was based on Rabinowitz’s rare species classification. The literature review was performed in Scopus for the period 1990–2020.

Results. While direct detection is often limited, it is possible with high and very high spatial resolution data for rare plants with distinctive traits. RS is also able to capture biophysical conditions driving rare plant distributions, which can indirectly provide accurate predictions for them. Both approaches have the potential to discover new populations of rare plants. RS can also feed SAMs of rare plants, which combined with SDMs can provide a valuable approach for rare plant detection. While direct detection is limited by the space occupied by a species within its habitat and its morphological, phenological, and physiological characteristics, the predictive performance of RS-based SDMs (indirect detection) can be influenced by habitat size, habitat specificity, and phenological features of rare plants. Similarly, model predictive performance can be influenced by the rarity form of the target species according to the rarity classification criteria.

Main conclusions. With this synthesis, the strong potential of RS for the purposes of detection and prediction of rare plant has been highlighted, with practical applications for conservation and management.

Keywords: Direct detection; Endemism; New populations; Predictive models; Rarity; Remote sensing predictors; Sensor; SDMs; Spatial resolution.

A.2 Résumé

Objectif. La détection des espèces rares est limitée par leur nature intrinsèque et par les contraintes associées aux enquêtes de terrain traditionnelles. La télédétection offre une alternative puissante aux méthodes de détection traditionnelles grâce à la disponibilité croissante des produits de télédétection. Ici, nous évaluons la capacité de la télédétection à haute et moyenne résolution à détecter des plantes rares avec des approches directes et indirectes, et comment les performances de la télédétection peuvent être influencées par les caractéristiques des espèces.

Méthodes. Une revue approfondie de la littérature a été menée pour synthétiser l'utilisation de la télédétection pour détecter ou prédire la présence de plantes rares à haute et moyenne résolution (<30 m et 30–300 m, respectivement). Le concept de “rareté” était basé sur la classification des espèces rares de Rabinowitz. La revue de la littérature a été réalisée dans Scopus pour la période 1990-2020.

Résultats. Bien que la détection directe soit souvent limitée, elle est possible avec des données à haute et très haute résolution spatiale pour les plantes rares aux traits distinctifs. La télédétection est également capable de capturer les conditions biophysiques qui déterminent la distribution des plantes rares, ce qui peut indirectement fournir des prédictions précises pour celles-ci. Les deux approches ont le potentiel de découvrir de nouvelles populations de plantes rares. La télédétection peut également alimenter les modèles d'abondance d'espèces de plantes rares, qui, combinés aux SDMs, peuvent fournir une approche précieuse pour la détection des plantes rares. Alors que la détection directe est limitée par l'espace occupé par une espèce dans son habitat et ses caractéristiques morphologiques, phénologiques et physiologiques, la performance prédictive des SDMs basés sur la télédétection (détection indirecte) peut être influencée par la taille de l'habitat, la spécificité de l'habitat et les caractéristiques phénologiques des plantes rares. De même, la

performance prédictive du modèle peut être influencée par la forme de rareté de l'espèce cible selon les critères de classification de la rareté.

Conclusions principales. Avec cette synthèse, le fort potentiel de la télédétection à des fins de détection et de prédiction de plantes rares a été mis en évidence, avec des applications pratiques pour la conservation et la gestion.

Mots clés: Capteur; Détection directe; Endémisme; Modèles prédictifs; Nouvelles populations; Prédicteurs de télédétection; Rareté; Résolution spatiale; SDMs.

A.3 Introduction

Rare plants are recognized as a conservation priority as they are key components of biodiversity, increasing and promoting species richness and functional diversity at different scales (Bracken and Low, 2012; Kearsley *et al.*, 2019; Leitao *et al.*, 2016; Mouillot *et al.*, 2013; Patykowski *et al.*, 2018; Rejžek *et al.*, 2016; Umaña *et al.*, 2017) and supporting ecosystem functioning and services (Dee *et al.*, 2019; Hooper *et al.*, 2012; Jolls *et al.*, 2019; Soliveres *et al.*, 2016; Xu *et al.*, 2020; Zavaleta and Hulvey, 2004). While rare plants are especially vulnerable to extinction (Sykes *et al.*, 2019; Weisser *et al.*, 2017; Zhang, 2019), implementing effective conservation measures is limited by the quality and quantity of data available on them. The low detectability often associated with rare plants due to their low prevalence (Lomba *et al.*, 2010) and/or sparse and small populations (Guisan *et al.*, 2006; Menon *et al.*, 2010) results in notable knowledge gaps on important aspects of their ecology (Lyons *et al.*, 2005; Wu and Smeins, 2000) or spatial distribution patterns (Gogol-Prokurat, 2011; MacDougall and Loo, 2002). Furthermore, remoteness of terrain, as well as economic and logistic constraints, can make field studies of rare plants unfeasible (Le Lay *et al.*, 2010). Remote sensing (hereafter “RS”; see Glossary Box) has become an important tool for the scientific community in addressing these field survey issues, offering an inexpensive method to assess biodiversity characteristics over large areas at regular intervals (Corbane *et al.*, 2015; Kerr and Ostrovsky, 2003;). RS allows both i) detection of individual biological entities, species assemblages, or ecological communities (direct approach) and ii) acquisition of biodiversity-related information from environmental proxies (indirect approach; Turner *et al.*, 2003). The indirect approach provides a powerful alternative that, in combination with species distribution models (hereafter “SDMs”), enables users to infer species’ habitat preferences or predict species distributions (Buechling and Tobalske, 2011; Guillera-Arroita *et al.*, 2015).

Glossary Box. Remote sensing (RS)-related terms and abbreviations

Active sensor: Emits radiation and measures the energy returned after being reflected.

Hyperspectral sensor: Discriminates many narrow spectral bands across the electromagnetic spectrum.

Multispectral sensor: Discriminates a few relatively broad spectral bands across the electromagnetic spectrum.

Multi-temporal imagery: Multiple images of the same location acquired on different dates.

Passive sensor: Measures energy emitted or reflected by the earth's surface without emitting radiation.

Remote sensing: Methods of detecting the electromagnetic radiation coming from the Earth's surface via aircraft or satellite sensors (Campbell and Wynne, 2011; Turner *et al.*, 2003).

Spatial resolution: Basic unit of captured information that corresponds to pixel or grain size and determines the minimum spatial scale at which variation can be observed. Categories of spatial resolution in this paper follow Corbane *et al.* (2015): very high resolution <3m; high resolution 3–29m; medium resolution 30–300m; low resolution >300m.

Spectral resolution: Width (and thus number) of bands into which the electromagnetic spectrum is divided.

Temporal resolution: Measure of the revisit frequency of the sensor at the same location.

Sensors abbrev.: AISA, Airborne Imaging Spectrometer for Applications; AMSR-E, Advanced Microwave Scanning Radiometer for Earth Observing System; ASTER, Advanced Spaceborne Thermal Emission and Reflection Radiometer; CMOS, Complementary Metal Oxide Semiconductor; HiFIS, High Fidelity Imaging Spectroscopy; LiDAR, Light Detection and Ranging; LISS, Linear Imaging and Self Scanning; MERIS, Medium Resolution Imaging Spectrometer; MODIS, Moderate-Resolution Imaging Spectroradiometer; SPOT, Satellite for Observation of Earth; SRTM, Shuttle Radar Topography Mission; SSM/I, Special Sensor Microwave Imager; TMI, TRMM Microwave Imager.

RS data/predictor abbrev.: EVI, Enhanced Vegetation Index; GCC, Green Chromatic Coordinate; mNDWI, modified Normalized Difference Water Index; NCVI, Normalized Coastal Vegetation Index; NDVI, Normalized Difference Vegetation Index; NDWI, Normalized Difference Water Index; NGVI, Normalized Green Vegetation Index; NIR band, Near Infrared band; PRI, Photochemical Reflectance Index; REVDVI, Red Edge Normalized Difference Vegetation Index; SAVI, Soil-Adjusted Vegetation Index; SIPI, Structurally Insensitive Pigment Index; SWIR band, Shortwave Infrared band; Thermal IR band, Thermal Infrared band; TNDVI, Transformed Normalized Difference Vegetation Index.

RS has become a widely applied tool in plant studies (e.g. Asner, Hughes, *et al.*, 2008; Asner, Jones, *et al.*, 2008; Kopeć *et al.*, 2020; Wan *et al.*, 2020) with the increasing availability of RS products that capture a wide variety of environmental features (Corbane *et al.*, 2015; Kerr and Ostrovsky, 2003; Turner *et al.*, 2003). Studies using RS to focus specifically on rare plants remain uncommon, although their number has been growing in recent years (e.g. Arenas-Castro *et al.*, 2019; Gonçalves *et al.*, 2016; Zhu *et al.*, 2016). As an emerging research field, the potential benefits of RS for the detection of rare plants remain unclear. In this context, the objectives of this synthesis were i) to evaluate the capacity for RS to detect and predict the occurrence of rare plants, and ii) to assess how the main characteristics of rare plants influence the performance of RS. Our concept of “rarity” is based on Rabinowitz’s rare species classification (Rabinowitz, 1981), which discerns seven rarity types based on three dichotomous criteria: geographic distribution range (large vs. restricted), habitat specificity (wide vs. narrow), and local population size (large vs. small). Since these criteria are characterized by a continuous transition among the different rarity categories (absence of defined thresholds) and make abstraction of causes of rarity, it is a flexible concept for the continuous and complex nature of rarity. While we will discuss the capacity for RS to feed into and improve SDMs of rare plants, a comparative evaluation of the performance of different modeling techniques is beyond the scope of this synthesis and has been addressed in the literature (e.g. Elith and Burgman, 2002; Williams *et al.*, 2009; Wiser *et al.*, 1998). We will discuss the suitability of predictive performance measures for rare plant modeling studies, as well as the potential influence of rarity types on RS effectiveness and the detection of target species in the field (hereafter “practical utility”).

A.4 Methods

An extensive literature review was conducted to synthesize the use of RS to detect or predict rare plant distributions. Although the term "remote sensing" is defined precisely in the literature, the concept of "remote sensing variables or predictors" remains ambiguous. Henceforth, RS predictors refer to i) continuous spectral information obtained from aircraft or satellite sensors, either as raw spectral bands or as indices; ii) landcover products developed from the classification of spectral information; and iii) digital elevation models ("DEMs") developed from satellite or airborne sensor information as well as derived topographic indices. In cases where the information on the origin or generation process of the predictors were not provided nor accessible, they were considered as non-RS predictors, except for DEM-derived topographic indices. DEMs are commonly generated through RS techniques and their direct survey is rare; therefore, when the DEM source is other than RS, it is usually stated in the literature (e.g. Padalia *et al.*, 2010; Sperduto and Congalton, 1996).

A literature review of peer-reviewed articles was carried out using the search engine Scopus by combining terms related to plant with keywords related to RS and rarity or species at risk for the period 1990–2020. Studies targeting species at risk were included since they can be considered rare according to Rabinowitz's rarity classification (Rabinowitz, 1981). Specifically, the search was carried out using the following combination of keywords: (plant OR tree OR bryophyte OR moss) AND (rare OR endemic OR "at risk" OR endangered OR threatened OR red-list) AND ("remote sensing" OR "remotely sensed" OR sensor OR satellite OR drone OR "unmanned aerial vehicle" OR spectral OR lidar OR radar OR airborne OR aircraft). A total of 1112 articles matched our search criteria. These articles were reviewed individually to identify and keep only those relevant for our topic, i.e., articles using RS data for the purpose of detecting or modeling and predicting the presence of rare plant species. We excluded i) articles that model richness distribution patterns of rare plants as they do

not evaluate the capacity for RS to predict individual species, nor the influence of species' characteristics on RS performance, and ii) those studies performed at low spatial resolutions (>300m) since SDMs at these pixel sizes hinder the identification of local environmental factors driving species occurrence patterns (Engler *et al.*, 2004), can result in large areas predicted as suitable habitat of limited practical use to detect rare species through field surveys (Guisan *et al.*, 2006), and normally provide less accurate predictions for sessile species (Guisan and Thuiller, 2005). A total of 43 articles were selected for the development of this study. These articles were first classified by RS approach (direct or indirect) and then by spatial resolution used (Table A.1).

Table A.1 Reviewed literature using remote sensing at very high, high, or medium resolutions to detect or predict the occurrence of rare plants. See Glossary Box for sensor and RS data/predictor abbreviations.

Reference study	Location on map ^a	# and type of rare species ^b	Sensor(s) ^c	Pixel size (m) ^d	Data/Predictors ^e		Practical utility ^h
					Remote sensing ^f	Non-remote sensing ^g	
Direct approach (detection)							
Very high spatial resolution (<3m)							
Landenberger <i>et al.</i> (2003)	1	1: S	Airborne optical sensor (Nikon N90s)	0.04 to 0.05	Traditional colour imagery	NA	No
Jones <i>et al.</i> (2011)	2	1: T	LiDAR; Airborne optical sensor (AISA)	2	Structural (Canopy height; Canopy volume profiles); Spectral bands	NA	No
Fletcher and Erskine (2012)	3	1: H	Airborne optical sensor (Sony NEX5)	0.041 x 0.096	Traditional colour imagery	NA	Yes
Chávez <i>et al.</i> (2013)	4	1: T	WorldView-2	0.5	Panchromatic band	NA	No
Omer <i>et al.</i> (2015)	5	6: T	WorldView-2	2	Spectral bands	NA	No
Chávez <i>et al.</i> (2016)	6	1: T	Quickbird2	0.6	Panchromatic band	NA	No

Table A.1 continued

Murfitt <i>et al.</i> (2016)	7	1: T	WorldView-2	0.5	Spectral bands; Panchromatic band	NA	No
Leduc and Knudby (2018)	8	1: H	Airborne optical sensor (CMOS)	0.05	Vegetation index (GCC)	NA	No
Liu <i>et al.</i> (2018)	9	1: T	Airborne optical sensor (Sony A6000)	0.12	Topographic; Spectral bands; Vegetation indices (NDVI; PRI; RENDVI; SIPI); Texture indices; Geometric indices	NA	No
Paz-Kagan <i>et al.</i> (2018)	10	1: T	LiDAR; HiFIS	2	Structural (Canopy height; Canopy volume profiles); Spectral bands	NA	No
Poursanidis <i>et al.</i> (2018)	11	1: H	WorldView-2	0.46	Spectral bands; Panchromatic band; Wetness index (NDWI); Water transparency	NA	No
López-Jiménez <i>et al.</i> (2019)	12	1: T	Airborne optical sensor (CMOS)	0.1 to 0.15	Traditional colour imagery	NA	No

Table A.1 continued

Maděra <i>et al.</i> (2019)	13	1: T	Pleiades	0.5 to 1	Vegetation index (NDVI)	NA	No
Meiforth <i>et al.</i> (2019)	14	1: T	Airborne optical sensor (AISA)	1	Spectral bands; Wetness indices (mNDWI)	NA	No
Rominger and Meyer (2019)	15	1: H	Airborne optical sensor (CMOS)	0.0191; 0.0232	Traditional colour imagery	NA	No
Slingsby and Slingsby (2019)	16	1: T	Pleiades	0.5	Traditional colour imagery	NA	No
Lobo Torres <i>et al.</i> (2020)	17	1: T	Airborne optical sensor (CMOS)	0.01	Traditional colour imagery	NA	No
High spatial resolution (3–29m)							
Pasqualini <i>et al.</i> (1998)	18	1: H	Airborne optical sensor	5	Traditional colour imagery	NA	No
Zhao <i>et al.</i> (2016)	19	1: T	SPOT	5	Topographic; Spectral bands	NA	No

Indirect approach (prediction)

Very high spatial resolution (<3m)

Table A.1 continued

Ishii <i>et al.</i> (2009)	20	8: H	Airborne optical sensor (AISA)	1.5	Spectral bands; Vegetation index (NDVI)	NA	No
Robinson <i>et al.</i> (2019)	21	5: H; S	LiDAR	2	Topographic	NA	No
Cursach <i>et al.</i> (2020)	22	1: H	LiDAR; Airborne optical sensor (camera)	2	Topographic; Vegetation index (NDVI);	Soil type	No
High spatial resolution (3–29m)							
Sellars and Jolls (2007)	23	1: H	LiDAR	3	Topographic	NA	No
Varghese <i>et al.</i> (2010)	24	8: T	LISS IV	5.8	Topographic; Vegetation type	Soil	No
Pouteau <i>et al.</i> (2012)	25	3: S, T	Quickbird	5	Topographic; Vegetation type	NA	No

Table A.1 continued

Baker <i>et al.</i> (2016)	26	1: S	LiDAR; Landsat	9.327	Topographic; Spectral bands; Band ratio; Normalized band ratios; Vegetation indices (NDVI; Greenness); Soil (Brightness; Yellownes); Wetness index	NA	No
Traganos and Reinartz (2018)	27	1: H	Sentinel-2	10	Bathymetry; Spectral bands; Water transparency	NA	No

Medium spatial resolution (30–300m)

Table A.1 continued

Lauver and Whistler (1993)	28	2: H	Landsat	30	Vegetation indices (NDVI; Greenness); Soil brightness index; Wetness indices (including raw SWIR1 and SWIR2 bands)	NA	Yes
Sperduto and Congalton (1996)	29	1: H	Landsat	30	Topographic; Vegetation index (raw NIR band)	Topographic; Soil; Land-use	Yes
Wu and Smeins (2000)	30	8: H, S	Airborne optical sensor	30	Topographic; Vegetation type	Soil	No

Table A.1 continued

<i>Crase et al. (2006)</i>	31	2: S	Airborne optical sensor (Exploranium GR-820); Airborne optically pumped magnetometer sensor (Scintrex CS2)	100; 250	Topographic; Geological (Radiometric data)	NA	No
<i>Zimmermann et al. (2007)</i>	32	12: T	SRTM; Landsat	90	Topographic; Spectral bands*; Vegetation indices* (NDVI; Greenness); Surface temperature index*; Soil brightness index*; Wetness index*	Climatic	No

Table A.1 continued

Williams <i>et al.</i> (2009)	33	6: H, S	MODIS	150	Topographic; Vegetation index (NDVI)	Climatic; Geological	Yes
Ishihama <i>et al.</i> (2010)	34	4: H	Airborne optical sensors (ADS40; RC30)	100	Topographic; Spectral bands*; Vegetation index (Vegetation height*)	NA	No
Padalia <i>et al.</i> (2010)	35	1: T	LISS IV	150	Vegetation type; NDVI-derived density class; Land-use	Topographic; Soil; Geological	No
Buechling and Tobalske (2011)	36	4: H	Landsat	30	Topographic; Spectral bands*; Vegetation indices * (TNDVI; Greenness); Soil brightness index*; Wetness index*	Climatic; Soil	Yes

Table A.1 continued

de Queiroz <i>et al.</i> (2012)	37	6: H	Landsat	30	Topographic; Geological (Gypsum springmound occurrence probability)	NA	Yes
Zucchettaa <i>et al.</i> (2016)	38	1: H	SRTM30_PLUS; MERIS; MODIS; SSM/I; TMI; AMSR-E; SeaWinds	300	Bathymetry; Surface temperature index; Water transparency; Wind induced disturbance (Relative Exposure Index)	Water salinity	No
Adhikari <i>et al.</i> (2018)	39	1: T	MODIS	250	Vegetation index (EVI*)	NA	Yes
Kim <i>et al.</i> (2018)	40	1: H	LiDAR; Landsat	30	Topographic; Vegetation index (NDVI); Wetness index (NDWI)	Climatic; Soil; Flood area	No

Table A.1 continued

Attanayake <i>et al.</i> (2019)	41	9: H; S	Landsat	30	Spectral bands	NA	No
Borfecchia <i>et al.</i> (2019)	42	1: H	Landsat	30	Bathymetry; Vegetation indices (NCVI; NGVI)	NA	No
Hernández-Lambrano <i>et al.</i> (2020)	43	1: H	LiDAR; Landsat	30	Topographic; Vegetation index (SAVI); Surface temperature index; Wetness index	NA	Yes

^aThe number indicates the location of the reference study in Figure A.1.

^bTotal number of target rare plants with capital letters indicating the type of species based on their growth form (H: herbaceous; S: shrub; T: tree).

^cSensors from which remote sensing information was extracted.

^dSpatial resolution of analysis

^eOnly data/predictors used for detection/prediction purposes are included.

^fVegetation indices refer to continuous spectral information, while vegetation type refers to classified information.

A.5 Remote sensing direct approach— Detection of rare plants

The direct detection of rare plants and their traits through RS requires previous knowledge of a species' ecology and distribution, as well as the use of high spatial resolution imagery. Despite these constraints, 19 articles following this RS approach were found (Table A.1; Figure A.1). Direct detection can be carried out either by visual identification or by image classification methods that allow the detection of distinctive spectral features of the target species. Specifically, Fletcher and Erskine (2012) and Rominger and Meyer (2019) showed the usefulness of very high spatial resolution traditional color aerial imagery for the visual detection of the rare plant *Boronia deanei* Maiden & Betche (Deane's Boronia) and the endangered and gypsophile endemic plant *Arctomecon humilis* Coville (dwarf bear-poppy), respectively. The uniqueness of the morphological characteristics exhibited by these two species at detection was key to their identification. Likewise, the classification of traditional color aerial imagery allowed the detection of the endemic cactus *Neobuxbaumia tetetzo* (F.A.C. Weber ex K. Schum.) Backeb. in the Tehuacan-Cuicatlan Valley in Mexico with high validation accuracy (0.95; López-Jiménez *et al.*, 2019). When morphological features extracted from traditional color imagery are not enough to discriminate rare plants, spectral bands and derived indices, either alone or in combination with other types of RS indices, has proven to be an effective alternative approach for their direct detection (Liu *et al.*, 2018). For instance, the endangered *Allium tricoccum* Aiton (wild leek) and the endemic *Agathis australis* (D.Don) Lindl. ex Loudon (kauri) were successfully detected using vegetation and wetness indices derived from multi- and hyperspectral airborne sensors, respectively (Leduc and Knudby, 2018; Meiforth *et al.*, 2019). Likewise, the rare plant *Firmiana danxiaensis* H.H.Hsue & H.S.Kiu, J. S. was detected in Danxia Mountain (China) using multispectral bands and RS-derived vegetation, topographic, texture and geometric indices (Liu *et al.*, 2018).

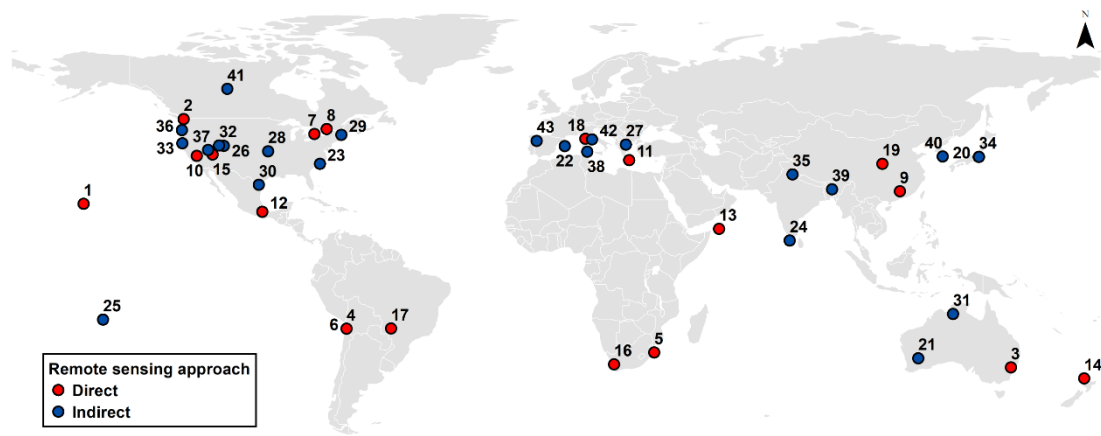


Figure A.1 Distribution map of reviewed studies. Numbers correspond to those appearing in the column "location on map" in Table A.1.

The utility of high and very high spatial resolution satellite sensors for direct detection of rare plants has also been highlighted. Omer *et al.* (2015) detected with high accuracy 5 of the 6 target endangered tree species in Dukuduku forest in South Africa using WorldView-2 satellite spectral imagery at 2m spatial resolution. Similarly, the use of 5m resolution SPOT imagery allowed to map the endangered and endemic alpine tree *Larix chinensis* Beissn. (Shaanxi larch) on Mount Taibai in China (Zhao *et al.*, 2016). Other studies have also tested the combined use of RS data from passive and active sensors for direct detection purposes. This combination provides a powerful approach, since active sensors, which allow the assessment of rare plant structural properties, can provide valuable information complementary to the optical information derived from passive sensors. Specifically, the use of hyperspectral information along with LiDAR-derived structural data, namely canopy height and canopy volume profiles, allowed a successful detection of the rare trees *Quercus garryana* Douglas ex Hook. (Garry oak) in southern Gulf Islands (British Columbia) and *Sequoiadendron giganteum* (Lindl.) J. Buchholz (giant sequoia) in the western Sierra Nevada of California (Jones *et al.*, 2011; Paz-Kagan *et al.*, 2018). On the other hand, RS has also allowed the direct detection of rare plants in aquatic environments, as demonstrated by Pasqualini *et al.* (1998) and

Poursanidis *et al.* (2018), who detected and mapped the species *Posidonia oceanica* (L.) Delile (Neptune grass) endemic to the Mediterranean Sea using aerial traditional colour imagery and WorldView-2-derived information, respectively.

The RS direct approach not only offers the possibility to detect and map rare plants but also to assess their status (e.g. water stress, health; Chávez *et al.*, 2013, 2016; Murfitt *et al.*, 2016). This ability may allow the implementation of monitoring systems for these species, which can provide valuable additional information for management and conservation purposes. The studies reviewed here well exemplify the potential of a direct RS approach not only to detect rare plants, but also to monitor them in space and time (Landenberger *et al.*, 2003; McGraw *et al.*, 1998), or even to discover new populations (Fletcher and Erskine, 2012).

A.6 Remote sensing indirect approach— Prediction of rare plant distributions

The indirect RS approach allows the prediction of rare plants under environmental conditions where their direct detection is not possible (Levin *et al.*, 2007). Most of the studies included in this section were performed in the Northern Hemisphere, while only three were conducted in the Southern Hemisphere (Figure A.1). RS has been used to spatially characterize different biophysical conditions at multiple spatial, spectral, and temporal resolutions related to topography, vegetation, structure, climate, soil, geology, moisture, bathymetry, and water transparency, as well as to anthropogenic and natural disturbances (Table A.1). RS information have been acquired primarily from passive satellite sensors, although active satellite sensors, and airborne sensors both active and passive, have also been used.

Only three studies have used very high resolution RS to model the distribution of rare plants, being limited exclusively to LiDAR-derived topographic predictors, NDVI and hyperspectral data. The usefulness of 2m resolution topographic predictors alone to predict rare plants was proven by achieving excellent accuracies (AUC = 0.99–1) for

five rare plants modeled in semiarid south-western Australia (Robinson *et al.*, 2019). Similarly, high predictive performance (AUC = 97) was obtained for the endemic plant *Euphorbia fontqueriana* Greuter by combining 2m resolution topographic and NDVI predictors, with almost no contribution from the non-RS soil type variable (Cursach *et al.*, 2020). More modest predictions were however obtained in the mapping of habitat types for 8 threatened species in Watarase wetland (Japan) using hyperspectral data (Ishii *et al.*, 2009).

A higher diversity of RS predictors has been tested in models developed at high resolution, while topographic (or bathymetric) variables have been the common element in all of them. One example used LiDAR-derived elevation at 3m resolution to predict up to 88% of *Amaranthus pumilus* Raf. (seabeach amaranth) occurrences across the North Carolina coastline (Sellars and Jolls, 2007). The integration of a Quickbird-derived vegetation type map along with topographic variables also provided accurate predictions (AUC = 89–97.9) for three endangered or endemic plant species on the island of Moorea (Pouteau *et al.*, 2012). Likewise, the endemic plant *Schoenocrambe suffrutescens* (Rollins) S.L. Welsh & Chatterley (shrubby reed-mustard) was successfully mapped (AUC = 0.85) by combining a wide variety of RS predictors, including topographic variables, spectral bands (and ratios), as well as vegetation, wetness and soil indices (Baker *et al.*, 2016).

Rare plant studies using medium resolution RS are more common and have used a much wider diversity of RS predictors than those developed at high and very high resolutions (Table A.1). The variety of RS predictors that can be successfully integrated into rare plant models at this resolution was exemplified by Zimmermann *et al.* (2007). The authors modeled 19 tree species distributions ranging from rare to common and found that models combining RS and non-RS predictors consistently provided better performance for all species, and more so for rare species. Medium resolution RS-only SDMs are also very useful for predicting rare plant occurrences. Suitable habitats for

the endemic tree *Adinandra griffithii* Dyer were accurately predicted (AUC = 0.99) by using EVI time series (Adhikari *et al.*, 2018). Similarly, robust predictions were achieved for the narrow-range endemic species *Antirrhinum lopesianum* Rothm. in the Iberian Peninsula using RS-derived topographic, vegetation, surface temperature and wetness indices (Hernández-Lambraño *et al.*, 2020). RS can also provide useful geology-related information for predicting rare plants. The Landsat-derived geological predictor “Gypsum springmound occurrence probability” alone was able to successfully predict habitat suitability (AUC = 0.92) for 6 edaphic endemic plants in White River Valley, Nevada (de Queiroz *et al.*, 2012). Robust models were also developed for the rare sandstone shrubs *Melaleuca triumphalis* Craven and *Stenostegia congesta* A.R. Bean using a RS radiometric map representing thorium, uranium and potassium in combination with two and one topographic predictors, respectively (Crase *et al.*, 2006). Likewise, the usefulness of the indirect RS approach to characterize aquatic habitats of rare plants has been demonstrated by several studies (Borfecchia *et al.*, 2019; Traganos and Reinartz, 2018; Zucchettaa *et al.*, 2016). While all these studies focused on the same species, the endemic plant *P. oceanica*, they exemplify the variety of RS predictors that can be employed for predictive mapping purposes in aquatic environments (Table A.1).

Overall, RS has provided valuable information on rare plant niches with good predictability at high and medium resolution. These results highlight the potential of RS to not only characterize the habitats of rare plants but also to monitor them spatially and temporally (Bartel and Sexton, 2009; Neumann *et al.*, 2015). Several authors have also demonstrated the practical utility of predictive models built partially (Buechling and Tobalske, 2011; Sperduto and Congalton, 1996; Williams *et al.*, 2009) or completely (e.g. de Queiroz *et al.*, 2012; Hernández-Lambraño *et al.*, 2020; Lauver and Whistler, 1993) with RS predictors at those resolutions by discovering previously unknown populations of rare plants (Table A.1). While SDMs-based predictions are

valuable tools to guide the search for rare plants in the field, the integration of abundance estimates derived from species abundance models (“SAMs”) could further facilitate their detection. Likewise, when probability of occurrence estimated from SDMs and predicted abundance are uncorrelated and determined by different sets of predictors, SAMs can provide valuable additional information on habitat quality or ecological species preferences (Duff *et al.*, 2012). Since RS also has the ability to feed SAMs (e.g. Arenas-Castro *et al.*, 2019; Duff *et al.*, 2012; Guarino *et al.*, 2012), abundance estimates can also be obtained at high or medium resolutions. Therefore, the combination of both RS-based SDM and SAM model types may represent a new and strong practical approach for detection of rare plants, by guiding field search efforts towards predicted habitats where higher plant abundance makes them more detectable.

A.6.1 Considerations of predictive performance measures for rare plants

Currently there is still no consensus on which are the most suitable metrics to evaluate the predictive performance of SDMs, which has the use of multiple metrics as the best solution (Amini Tehrani *et al.*, 2020; Breiner *et al.*, 2015). However, since each accuracy metric provides a type of information, the choice should ideally be based on their intended use (Fielding and Bell, 1997) rather than on the arbitrary selection of different metrics. As rare plants typically show low prevalence (i.e. high absences/presences ratio), overall predictive performance metrics (e.g. accuracy or AUC) can lead to overly optimistic results about model accuracy (Buechling and Tobalske, 2011; Lobo *et al.*, 2008). Furthermore, those metrics are not sensitive to overprediction, which can be common for rare plant presence. Based on these drawbacks, we propose the use of two complementary metrics to evaluate in isolation the ability of the model to predict presences of rare plants, namely sensitivity and precision. Sensitivity is the proportion of true positives correctly predicted, while precision is the proportion of positive predictions corresponding to true positives (Fawcett, 2004). The use of both metrics provides information on the proportion of

actual presences correctly predicted and possible instances of overestimation. Therefore, sensitivity and precision are ultimately metrics indicative of the practical utility of models to find new localities of rare plants.

A.7 Remote sensing based on the characteristics of rare plants

Rare plants, like all plant species, have distinct features that allow their differentiation and identification, but is it possible to capture some of the distinguishing features of rare plants through RS? Can these features influence the performance of RS to detect or predict rare plants? In this section, rare plant features related to morphology, phenology, physiology, and ecological niche are discussed. Since rare and common plants are not categorized as such based on the plant features presented, we are aware that some aspects of our discussion may also apply to common plants.

A.7.1 Morphology

Morphological features of rare plants can provide decisive information for their direct detection. Two conditions must be met to ensure the success of this approach (also applicable to common plants): i) very high spatial resolution is required to capture morphological characters considered important, and ii) the date on which RS imagery is taken must correspond to a time when the target plant exhibits distinctive morphological characters that allow its discrimination. The direct detection of the rare shrub *Boronia deanei* based on its pink flowers and growth form exemplifies these criteria (Fletcher and Erskine, 2012).

A.7.2 Phenology

Multi-temporal RS imagery at high temporal resolution has the potential to capture phenological traits of rare plants, such as flowering, fruiting, or leaf growth/fall (Campbell and Wynne, 2011; Turner *et al.*, 2003). This phenological information can be advantageous for both RS approaches. Direct detection can benefit from

phenological processes as long as the conditions mentioned in the previous subsection are met. However, multi-temporal imagery can only provide useful information when morphologically and phenologically similar target and cohabitating species display these features at different times. By contrast, single-date images provide similar information if the detection date captures the uniqueness of morphological characters derived from phenological features.

In the indirect approach, the spectral radiation associated with phenological features of rare plants can directly influence the information captured from remote sensors during the characterization process of their ecological niche, which is subsequently used to model rare plant occurrence. This fact has been defined as a source of unintentional bias when predicting potentially suitable habitats of plants, since the captured information is associated with their actual distribution (Bradley *et al.*, 2012). However, this type of bias can be considered advantageous when RS-based predictions are used to locate actual rare plant occurrences. For instance, predictions of rare trees improved with the inclusion of multi-temporal predictors whose spectral information was directly influenced by their leaf phenological features (Zimmermann *et al.*, 2007). Similarly, the detection of leaf phenological changes in the Watarase wetland allowed to accurately predict the occurrence of two of four rare plants studied (Ishihama *et al.*, 2010). The authors highlighted that one of these species, *Ophioglossum namegatae* Nish. & Kurita, because of its sprouting period (early spring) and rapid growth, could directly contribute to the spectral information captured in early May, which was one of the most important predictors for both species. Likewise, the flowering phenological stage of the endemic tree *A. griffithii* played an important role in predicting its distribution, since the EVI for the periods of June and July were the most influential predictors (Adhikari *et al.*, 2018).

A.7.3 Physiology

Plant spectral information is influenced by plant physiological traits such as concentration and distribution of biochemical components (Peñuelas and Filella, 1998), which can be identifiable and quantifiable based on their spectral absorption features (Asner and Vitousek, 2005; Blackburn, 1998; Sims and Gamon, 2003). The use of multispectral bands and physiological indices at high spatial resolution have been shown to significantly contribute to the detection of rare tree species (Liu *et al.*, 2018; Omer *et al.*, 2015). However, the detection of rare plants could also benefit from hyperspectral bands and LiDAR sensors, which have the capacity to assess plant physiological traits in more detail (Andrew and Ustin, 2006; Asner, Jones, *et al.*, 2008; Ustin and Gamon, 2010).

A.7.4 Ecological niche

The vertical position occupied by rare plants in their respective habitats (e.g. overstory or understory) influences their direct detection by RS. Active airborne sensors (e.g. LiDAR) are required to detect subcanopy plants (Asner, Hughes, *et al.*, 2008; Hernandez-Santin *et al.*, 2019). On the other hand, the effectiveness of the RS indirect approach in characterizing species' ecological niches depends on two conditions. First, sensor spatial resolution must be adapted to habitat size. This is especially important for rare plants that are associated with small habitat patches (e.g. de Queiroz *et al.*, 2012), which can remain indistinguishable if they are smaller than the RS imagery pixel (Luoto *et al.*, 2002). Secondly, habitat specificity of rare plants has been shown to influence prediction accuracy (Buechling and Tobalske, 2011; Parviainen *et al.*, 2013). Prediction accuracy of rare plants can increase when their habitat specialization increases (Hernandez *et al.*, 2006), making habitats where they occur more distinct than habitats where they are absent. For rare plants with wider habitat specificity and few occurrences, insufficient prior knowledge seems to be the main limiting factor rather

than capacity of RS to successfully discriminate between suitable and unsuitable habitats.

A.8 Relating rarity forms with model predictive performance

The rare species classification developed by Rabinowitz (1981) suggests that predictive performance of models could vary by type of rare species. This section addresses this assumption starting at the criterion level.

The geographic distribution of species has an indirect rather than direct effect on model predictive performance through the acquisition of RS products. Availability and cost of RS imagery could restrict analyses to coarser spatial resolutions unable to capture species-environment relationships, especially when dealing with widely distributed rare plants. A practical solution to this drawback would be to guide modeling studies to smaller areas within a species' distribution range where their conservation status is most critical or their study is more urgently required.

Habitat specificity can positively influence model predictive performance, with increases in model predictive performance as habitat specificity increases. Local population size can also strongly affect model predictive performance. Species with smaller populations are more vulnerable to demographic, environmental, and genetic stochastic events as well as anthropic pressure, which can reduce their probability of persistence (Fischer and Stöcklin, 1997; Matthies *et al.*, 2004; Ouborg, 1993; Thomas, 1994). This can result in lower proportion of occupied suitable sites or “fidelity”, which can lead to an increase in false positives and thus decrease model predictive accuracy. In contrast, species with larger populations are more resistant to stochastic events and therefore more stable over time, which would increase their probability of presence and fidelity.

Summarizing the previous ideas regarding the influence of Rabinowitz's rarity classification criteria on model predictive performance, predictive performance can be negatively influenced by geographic distribution range and positively influenced by habitat specificity and local population size (Figure A.2). Nonetheless, predicting widely distributed rare plants throughout their entire distribution range is not practical for their detection; thus, the effect of the geographic distribution range on model performance becomes negligible when prioritizing smaller areas for predictions. At this point and using the same classification as Rabinowitz (1981), better results in terms of predictive performance can be expected for predictable and endemic rarity forms showing large local population size (Figure A.2). However, because the assumption initially raised in this section has been only theoretically addressed, the veracity of these final conjectures must be tested empirically.

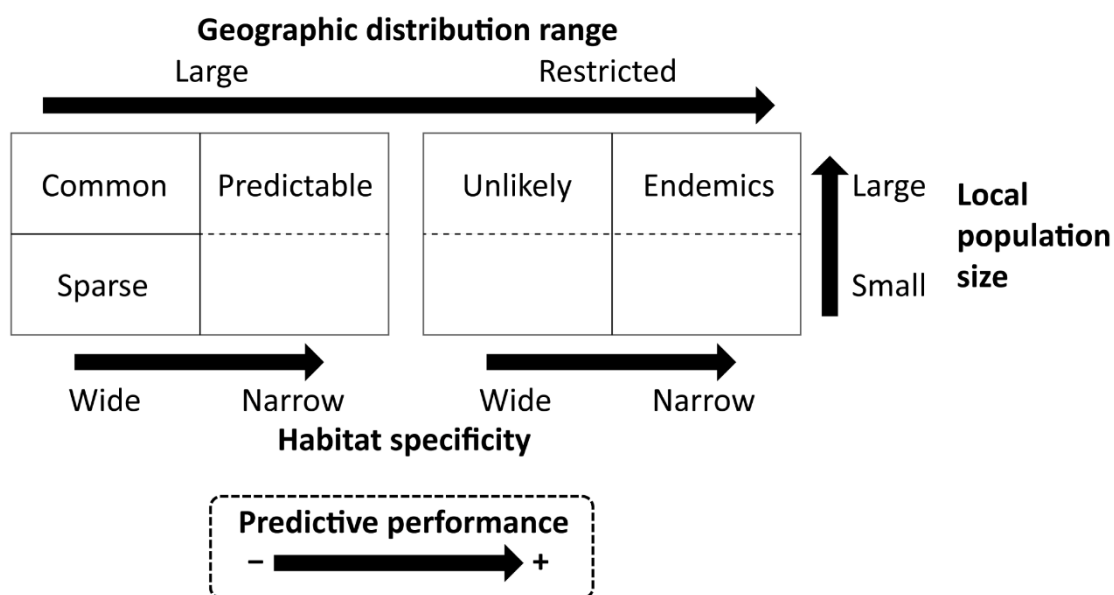


Figure A.2 Classification of rarity forms showing the potential changes in model predictive performance (solid arrows), based on the three criteria used for such classification: geographic distribution range, habitat specificity, and local population size. The arrowhead indicates the direction of improvement (+) in predictive performance. Adapted from Rabinowitz (1981).

A.9 Conclusion

Direct and indirect RS provide great potential for the detection and prediction of rare plants in both terrestrial and aquatic environments. While direct detection is often limited, it was shown to be possible with high and very high spatial resolution data for species with distinctive traits. Remote sensors were also able to capture important biophysical conditions that drive rare plant distributions at very high to medium resolutions. Generally, RS predictors contributed positively to the predictive performance of SDMs when they were combined with non-RS predictors. RS predictors by themselves also provided accurate predictions of rare plant occurrences and allowed the discovery of new locations, highlighting the practical utility of these tools for conservation purposes. Likewise, the capacity for RS to feed SAMs and provide abundance estimates at high resolutions can offer, in combination with

traditional SDMs, a valuable approach to guide future field surveys and facilitate the detection of new populations, as well as for monitoring these species and their populations in space and time. Additionally, accuracy metrics were proposed for future modeling studies that focus on predicting actual rare plant occurrences.

Some characters of rare plants can influence the capacity for direct RS to detect them. The effectiveness of this RS approach will depend on the space occupied by a species within its habitat and the distinctive morphological, phenological, and/or physiological features that facilitate its identification. On the other hand, the predictive performance of RS-based SDMs can be influenced by the habitat size, habitat specificity, and phenological features of rare plants. The spatial resolution of RS imagery must match the habitat size occupied by species; otherwise, small habitats can remain indistinguishable at coarse resolutions. Likewise, higher habitat specificity for rare species facilitates the capture and integration of environmental variability associated with the species, and better discrimination between suitable and unsuitable habitats. In addition, the influence of phenological features of rare plants on the spectral information captured by remote sensors can improve SDM performance for predicting actual occurrences. Similarly, model predictive performance can be influenced by the rarity form of the target species according to the rarity classification criteria, but this requires empirical testing.

In conclusion, RS is a powerful information source to generate predictions and guide the discovery of new rare plant populations. New rare plant occurrences can subsequently be used as inputs for improving predictive models, to acquire better knowledge on ecological requirements and restrictions of species to help understand the causes of their rarity, and to review and update when necessary their conservation status. With this synthesis we have highlighted the strong potential of RS for the purposes of detection and prediction of rare plants, with practical applications for rare species conservation and management.

A.10 Acknowledgements

We greatly thank Sandra Fernández Fariñas and Milka for their valuable comments and support in the initial phases of this study. We thank Annie Desrochers for reviewing the first version of the manuscript. Also, we are very grateful for the constructive comments and suggestions provided by the anonymous reviewers, which greatly helped to improve the quality of our manuscript. We also thank Environmental Damages Fund, Environment and Climate Change Canada for funding this research.

A.11 References

- Adhikari, D., Mir, A. H., Upadhaya, K., Iralu, V., & Roy, D. K. (2018). Abundance and habitat-suitability relationship deteriorate in fragmented forest landscapes: a case of *Adinandra griffithii* Dyer, a threatened endemic tree from Meghalaya in northeast India. *Ecological processes*, 7(1), 1-9.
- Amini Tehrani, N., Naimi, B., & Jaboyedoff, M. (2020). Toward community predictions: Multi-scale modelling of mountain breeding birds' habitat suitability, landscape preferences, and environmental drivers. *Ecology and evolution*, 10(12), 5544-5557.
- Andrew, M. E., & Ustin, S. L. (2006). Spectral and physiological uniqueness of perennial pepperweed (*Lepidium latifolium*). *Weed Science*, 54(6), 1051-1062.
- Arenas-Castro, S., Regos, A., Gonçalves, J. F., Alcaraz-Segura, D., & Honrado, J. (2019). Remotely sensed variables of ecosystem functioning support robust predictions of abundance patterns for rare species. *Remote Sensing*, 11(18), 2086.
- Asner, G. P., & Vitousek, P. M. (2005). Remote analysis of biological invasion and biogeochemical change. *Proceedings of the National Academy of Sciences*, 102(12), 4383-4386.
- Asner, G. P., Hughes, R. F., Vitousek, P. M., Knapp, D. E., Kennedy-Bowdoin, T., Boardman, J., ... & Green, R. O. (2008). Invasive plants transform the three-dimensional structure of rain forests. *Proceedings of the National Academy of Sciences*, 105(11), 4519-4523.

- Asner, G. P., Jones, M. O., Martin, R. E., Knapp, D. E., & Hughes, R. F. (2008). Remote sensing of native and invasive species in Hawaiian forests. *Remote sensing of Environment*, 112(5), 1912-1926.
- Attanayake, A. U., Xu, D., Guo, X., & Lamb, E. G. (2019). Long-term sand dune spatio-temporal dynamics and endemic plant habitat extent in the Athabasca sand dunes of northern Saskatchewan. *Remote Sensing in Ecology and Conservation*, 5(1), 70-86.
- Baker, J. B., Fonnesebeck, B. B., & Boettinger, J. L. (2016). Modeling rare endemic shrub habitat in the Uinta Basin using soil, spectral, and topographic data. *Soil Science Society of America Journal*, 80(2), 395-408.
- Bartel, R. A., & Sexton, J. O. (2009). Monitoring habitat dynamics for rare and endangered species using satellite images and niche-based models. *Ecography*, 32(5), 888-896.
- Blackburn, G. A. (1998). Quantifying chlorophylls and carotenoids at leaf and canopy scales: An evaluation of some hyperspectral approaches. *Remote sensing of environment*, 66(3), 273-285.
- Borfecchia, F., Consalvi, N., Micheli, C., Carli, F. M., Cognetti De Martiis, S., Gnisci, V., ... & Marcelli, M. (2019). Landsat 8 OLI satellite data for mapping of the *Posidonia oceanica* and benthic habitats of coastal ecosystems. *International Journal of Remote Sensing*, 40(4), 1548-1575.
- Bracken, M. E., & Low, N. H. (2012). Realistic losses of rare species disproportionately impact higher trophic levels. *Ecology letters*, 15(5), 461-467.
- Bradley, B. A., Olsson, A. D., Wang, O., Dickson, B. G., Pelech, L., Sesnie, S. E., & Zachmann, L. J. (2012). Species detection vs. habitat suitability: are we biasing habitat suitability models with remotely sensed data?. *Ecological Modelling*, 244, 57-64.
- Breiner, F. T., Guisan, A., Bergamini, A., & Nobis, M. P. (2015). Overcoming limitations of modelling rare species by using ensembles of small models. *Methods in Ecology and Evolution*, 6(10), 1210-1218.
- Buechling, A., & Tobalske, C. (2011). Predictive habitat modeling of rare plant species in Pacific Northwest forests. *Western Journal of Applied Forestry*, 26(2), 71-81.

- Campbell, J. B., & Wynne, R. H. (2011). Introduction to remote sensing. Guilford Press.
- Chávez, R. O., Clevers, J. G., Herold, M., Acevedo, E., & Ortiz, M. (2013). Assessing water stress of desert tamarugo trees using in situ data and very high spatial resolution remote sensing. *Remote Sensing*, 5(10), 5064-5088.
- Chávez, R. O., Clevers, J. G. P. W., Decuyper, M., De Bruin, S., & Herold, M. (2016). 50 years of water extraction in the Pampa del Tamarugal basin: Can *Prosopis tamarugo* trees survive in the hyper-arid Atacama Desert (Northern Chile)? *Journal of Arid Environments*, 124, 292-303.
- Corbane, C., Lang, S., Pipkins, K., Alleaume, S., Deshayes, M., Millán, V. E. G., ... & Michael, F. (2015). Remote sensing for mapping natural habitats and their conservation status—New opportunities and challenges. *International Journal of Applied Earth Observation and Geoinformation*, 37, 7-16.
- Cruse, B., Cowie, I. D., & Michell, C. R. (2006). Distribution and conservation status of the rare plants *Melaleuca triumphalis* and *Stenostegia congesta* (Myrtaceae), Victoria River district, northern Australia. *Australian Journal of Botany*, 54(7), 641-653.
- Cursach, J., Far, A. J., & Ruiz, M. (2020). Geospatial analysis to assess distribution patterns and predictive models for endangered plant species to support management decisions: a case study in the Balearic Islands. *Biodiversity and Conservation*, 29(11), 3393-3410.
- de Queiroz, T. F., Baughman, C., Baughman, O., Gara, M., & Williams, N. (2012). Species distribution modeling for conservation of rare, edaphic endemic plants in White River Valley, Nevada. *Natural Areas Journal*, 32(2), 149-158.
- Dee, L. E., Cowles, J., Isbell, F., Pau, S., Gaines, S. D., & Reich, P. B. (2019). When do ecosystem services depend on rare species?. *Trends in Ecology & Evolution*, 34(8), 746-758.
- Duff, T. J., Bell, T. L., & York, A. (2011). Patterns of plant abundances in natural systems: is there value in modelling both species abundance and distribution?. *Australian Journal of Botany*, 59(8), 719-733.
- Elith, J., & Burgman, M. A. (2002). Predictions and their validation: rare plants in the Central Highlands, Victoria, Australia. Predicting species occurrences: issues of accuracy and scale, 303-314.

- Engler, R., Guisan, A., & Rechsteiner, L. (2004). An improved approach for predicting the distribution of rare and endangered species from occurrence and pseudo-absence data. *Journal of applied ecology*, 41(2), 263-274.
- Fawcett, T. (2004). ROC graphs: Notes and practical considerations for researchers. *Machine learning*, 31(1), 1-38.
- Fielding, A. H., & Bell, J. F. (1997). A review of methods for the assessment of prediction errors in conservation presence/absence models. *Environmental conservation*, 24(1), 38-49.
- Fischer, M., & Stöcklin, J. (1997). Local Extinctions of Plants in Remnants of Extensively Used Calcareous Grasslands 1950–1985: Extinciones Locales de Plantas en Remanentes de Pastizales Calcáreos de Uso extensivo entre 1950 y 1985. *Conservation Biology*, 11(3), 727-737.
- Fletcher, A. T., & Erskine, P. D. (2012). Mapping of a rare plant species (*Boronia deanei*) using hyper-resolution remote sensing and concurrent ground observation. *Ecological Management & Restoration*, 13(2), 195-198.
- Gogol-Prokurat, M. (2011). Predicting habitat suitability for rare plants at local spatial scales using a species distribution model. *Ecological Applications*, 21(1), 33-47.
- Gonçalves, J., Alves, P., Pôças, I., Marcos, B., Sousa-Silva, R., Lomba, Â., & Honrado, J. P. (2016). Exploring the spatiotemporal dynamics of habitat suitability to improve conservation management of a vulnerable plant species. *Biodiversity and Conservation*, 25(14), 2867-2888.
- Guarino, E. D. S. G., Barbosa, A. M., & Waechter, J. L. (2012). Occurrence and abundance models of threatened plant species: Applications to mitigate the impact of hydroelectric power dams. *Ecological Modelling*, 230, 22-33.
- Guillera-Arroita, G., Lahoz-Monfort, J. J., Elith, J., Gordon, A., Kujala, H., Lentini, P. E., ... & Wintle, B. A. (2015). Is my species distribution model fit for purpose? Matching data and models to applications. *Global Ecology and Biogeography*, 24(3), 276-292.
- Guisan, A., & Thuiller, W. (2005). Predicting species distribution: offering more than simple habitat models. *Ecology letters*, 8(9), 993-1009.

- Guisan, A., Broennimann, O., Engler, R., Vust, M., Yoccoz, N. G., Lehmann, A., & Zimmermann, N. E. (2006). Using niche-based models to improve the sampling of rare species. *Conservation biology*, 20(2), 501-511.
- Hernandez, P. A., Graham, C. H., Master, L. L., & Albert, D. L. (2006). The effect of sample size and species characteristics on performance of different species distribution modeling methods. *Ecography*, 29(5), 773-785.
- Hernández-Lambrano, R. E., Carbonell, R., & Sánchez-Agudo, J. Á. (2020). Making the most of scarce data: Mapping distribution range and variation in population abundance of a threatened narrow-range endemic plant. *Journal for Nature Conservation*, 57, 125889.
- Hernandez-Santin, L., Rudge, M. L., Bartolo, R. E., & Erskine, P. D. (2019). Identifying species and monitoring understorey from uas-derived data: a literature review and future directions. *Drones*, 3(1), 9.
- Hooper, D. U., Adair, E. C., Cardinale, B. J., Byrnes, J. E., Hungate, B. A., Matulich, K. L., ... & O'Connor, M. I. (2012). A global synthesis reveals biodiversity loss as a major driver of ecosystem change. *Nature*, 486(7401), 105-108.
- Ishihama, F., Takeda, T., Oguma, H., & Takenaka, A. (2010). Comparison of effects of spatial autocorrelation on distribution predictions of four rare plant species in the Watarase wetland. *Ecological research*, 25(6), 1057-1069.
- Ishii, J., Lu, S., Funakoshi, S., Shimizu, Y., Omasa, K., & Washitani, I. (2009). Mapping potential habitats of threatened plant species in a moist tall grassland using hyperspectral imagery. *Biodiversity and conservation*, 18(9), 2521-2535.
- Jolls, C. L., Inkster, J. N., Scholtens, B. G., Vitt, P., & Havens, K. (2019). An endemic plant and the plant-insect visitor network of a dune ecosystem. *Global Ecology and Conservation*, 18, e00603.
- Jones, T. G., Coops, N. C., & Sharma, T. (2011). Exploring the utility of hyperspectral imagery and LiDAR data for predicting *Quercus garryana* ecosystem distribution and aiding in habitat restoration. *Restoration Ecology*, 19(201), 245-256.
- Kearsley, E., Hufkens, K., Verbeeck, H., Bauters, M., Beckman, H., Boeckx, P., & Huygens, D. (2019). Large-sized rare tree species contribute disproportionately to functional diversity in resource acquisition in African tropical forest. *Ecology and evolution*, 9(8), 4349-4361.

- Kerr, J. T., & Ostrovsky, M. (2003). From space to species: ecological applications for remote sensing. *Trends in ecology & evolution*, 18(6), 299-305.
- Kim, J. Y., Kim, G. Y., Do, Y., Park, H. S., & Joo, G. J. (2018). Relative importance of hydrological variables in predicting the habitat suitability of *Euryale ferox* Salisb. *Journal of Plant Ecology*, 11(2), 169-179.
- Kopeć, D., Sabat-Tomala, A., Michalska-Hejduk, D., Jarocińska, A., & Niedzielko, J. (2020). Application of airborne hyperspectral data for mapping of invasive alien *Spiraea tomentosa* L.: A serious threat to peat bog plant communities. *Wetlands Ecology and Management*, 28(2), 357-373.
- Landenberger, R. E., McGraw, J. B., Warner, T. A., & Brandtberg, T. (2003). Potential of digital color imagery for censusing Haleakala silverswords in Hawaii. *Photogrammetric Engineering & Remote Sensing*, 69(8), 915-923.
- Lauver, C. L. (1993). A hierarchical classification of Landsat TM imagery to identify natural grassland areas and rare species habitat. *Photogrammetric Engineering & Remote Sensing*, 59(5), 627-634.
- Le Lay, G., Engler, R., Franc, E., & Guisan, A. (2010). Prospective sampling based on model ensembles improves the detection of rare species. *Ecography*, 33(6), 1015-1027.
- Leduc, M. B., & Knudby, A. J. (2018). Mapping wild leek through the forest canopy using a UAV. *Remote sensing*, 10(1), 70.
- Leitão, R. P., Zuanon, J., Villéger, S., Williams, S. E., Baraloto, C., Fortunel, C., ... & Moullot, D. (2016). Rare species contribute disproportionately to the functional structure of species assemblages. *Proceedings of the Royal Society B: Biological Sciences*, 283(1828), 20160084.
- Levin, N., Shmida, A., Levanoni, O., Tamari, H., & Kark, S. (2007). Predicting mountain plant richness and rarity from space using satellite-derived vegetation indices. *Diversity and Distributions*, 13(6), 692-703.
- Liu, C., Ai, M., Chen, Z., Zhou, Y., & Wu, H. (2018). Detection of *Firmiana danxiaensis* canopies by a customized imaging system mounted on an UAV platform. *Journal of Sensors*, 2018.
- Lobo Torres, D., Queiroz Feitosa, R., Nigri Happ, P., Elena Cué La Rosa, L., Marcato Junior, J., Martins, J., ... & Liesenberg, V. (2020). Applying fully convolutional

architectures for semantic segmentation of a single tree species in urban environment on high resolution UAV optical imagery. *Sensors*, 20(2), 563.

- Lobo, J. M., Jiménez-Valverde, A., & Real, R. (2008). AUC: a misleading measure of the performance of predictive distribution models. *Global ecology and Biogeography*, 17(2), 145-151.
- Lomba, A., Pellissier, L., Randin, C., Vicente, J., Moreira, F., Honrado, J., & Guisan, A. (2010). Overcoming the rare species modelling paradox: A novel hierarchical framework applied to an Iberian endemic plant. *Biological conservation*, 143(11), 2647-2657.
- López-Jiménez, E., Vasquez-Gomez, J. I., Sanchez-Acevedo, M. A., Herrera-Lozada, J. C., & Uriarte-Arcia, A. V. (2019). Columnar cactus recognition in aerial images using a deep learning approach. *Ecological Informatics*, 52, 131-138.
- Luoto, M., Toivonen, T., & Heikkinen, R. K. (2002). Prediction of total and rare plant species richness in agricultural landscapes from satellite images and topographic data. *Landscape Ecology*, 17(3), 195-217.
- Lyons, K. G., Brigham, C. A., Traut, B. H., & Schwartz, M. W. (2005). Rare species and ecosystem functioning. *Conservation biology*, 19(4), 1019-1024.
- MacDougall, A. S., & Loo, J. A. (2002). Predicting occurrences of geographically restricted rare floral elements with qualitative habitat data. *Environmental Reviews*, 10(3), 167-190.
- Maděra, P., Volařík, D., Patočka, Z., Kalivodová, H., Divín, J., Rejžek, M., ... & Vahalík, P. (2019). Sustainable land use management needed to conserve the dragon's blood tree of Socotra Island, a vulnerable endemic umbrella species. *Sustainability*, 11(13), 3557.
- Matthies, D., Bräuer, I., Maibom, W., & Tschardtke, T. (2004). Population size and the risk of local extinction: empirical evidence from rare plants. *Oikos*, 105(3), 481-488.
- McGraw, J. B., Warner, T. A., & Key, T. L. (1998). High spatial resolution remote sensing of forest trees. *Trends in Ecology & Evolution*, 13(8), 300-301.
- Meiforth, J. J., Buddenbaum, H., Hill, J., Shepherd, J., & Norton, D. A. (2019). Detection of New Zealand Kauri trees with AISA aerial hyperspectral data for use in multispectral monitoring. *Remote Sensing*, 11(23), 2865.

- Menon, S., Choudhury, B. I., Khan, M. L., & Peterson, A. T. (2010). Ecological niche modeling and local knowledge predict new populations of *Gymnocladus assamicus* a critically endangered tree species. *Endangered Species Research*, 11(2), 175-181.
- Mouillot, D., Bellwood, D. R., Baraloto, C., Chave, J., Galzin, R., Harmelin-Vivien, M., ... & Thuiller, W. (2013). Rare species support vulnerable functions in high-diversity ecosystems. *PLoS biology*, 11(5), e1001569.
- Murfitt, J., He, Y., Yang, J., Mui, A., & De Mille, K. (2016). Ash decline assessment in emerald ash borer infested natural forests using high spatial resolution images. *Remote Sensing*, 8(3), 256.
- Neumann, C., Weiss, G., Schmidlein, S., Itzerott, S., Lausch, A., Doktor, D., & Brell, M. (2015). Gradient-based assessment of habitat quality for spectral ecosystem monitoring. *Remote Sensing*, 7(3), 2871-2898.
- Omer, G., Mutanga, O., Abdel-Rahman, E. M., & Adam, E. (2015). Performance of support vector machines and artificial neural network for mapping endangered tree species using WorldView-2 data in Dukuduku forest, South Africa. *IEEE Journal of Selected Topics in Applied Earth Observations and Remote Sensing*, 8(10), 4825-4840.
- Ouborg, N. J. (1993). Isolation, population size and extinction: the classical and metapopulation approaches applied to vascular plants along the Dutch Rhine-system. *Oikos*, 298-308.
- Padalia, H., Bharti, R. R., Pundir, Y. P. S., & Sharma, K. P. (2010). Geospatial multiple logistic regression approach for habitat characterization of scarce plant population: A case study of *Pittosporum eriocarpum* Royle (an endemic species of Uttarakhand, India). *Journal of the Indian Society of Remote Sensing*, 38(3), 513-521.
- Parviainen, M., Zimmermann, N. E., Heikkinen, R. K., & Luoto, M. (2013). Using unclassified continuous remote sensing data to improve distribution models of red-listed plant species. *Biodiversity and Conservation*, 22(8), 1731-1754.
- Pasqualini, V., Pergent-Martini, C., & Pergent, G. (1998). Use of remote sensing for the characterization of the Mediterranean coastal environment—the case of *Posidonia oceanica*. *Journal of Coastal Conservation*, 4(1), 59-66.

- Patykowski, J., Dell, M., Wevill, T., & Gibson, M. (2018). Rarity and nutrient acquisition relationships before and after prescribed burning in an Australian box-ironbark forest. *AoB Plants*, 10(3), ply032.
- Paz-Kagan, T., Vaughn, N. R., Martin, R. E., Brodrick, P. G., Stephenson, N. L., Das, A. J., ... & Asner, G. P. (2018). Landscape-scale variation in canopy water content of giant sequoias during drought. *Forest Ecology and Management*, 419, 291-304.
- Penuelas, J., & Filella, I. (1998). Visible and near-infrared reflectance techniques for diagnosing plant physiological status. *Trends in plant science*, 3(4), 151-156.
- Poursanidis, D., Topouzelis, K., & Chrysoulakis, N. (2018). Mapping coastal marine habitats and delineating the deep limits of the Neptune's seagrass meadows using very high resolution Earth observation data. *International journal of remote sensing*, 39(23), 8670-8687.
- Pouteau, R., Meyer, J. Y., Taputuarai, R., & Stoll, B. (2012). Support vector machines to map rare and endangered native plants in Pacific islands forests. *Ecological Informatics*, 9, 37-46.
- Rabinowitz, D. (1981) Seven forms of rarity. In *The Biological Aspects of Rare Plant Conservation* (Synge, H. ed). Wiley, Hoboken, USA. pp. 205-217.
- Rejžek, M., Svátek, M., Šebesta, J., Adolt, R., Maděra, P., & Matula, R. (2016). Loss of a single tree species will lead to an overall decline in plant diversity: Effect of *Dracaena cinnabari* Balf. f. on the vegetation of Socotra Island. *Biological Conservation*, 196, 165-172.
- Robinson, T. P., Di Virgilio, G., Temple-Smith, D., Hesford, J., & Wardell-Johnson, G. W. (2018). Characterisation of range restriction amongst the rare flora of Banded Ironstone Formation ranges in semiarid south-western Australia. *Australian Journal of Botany*, 67(3), 234-247.
- Rominger, K., & Meyer, S. E. (2019). Application of UAV-based methodology for census of an endangered plant species in a fragile habitat. *Remote Sensing*, 11(6), 719.
- Sellars, J. D., & Jolls, C. L. (2007). Habitat modeling for *Amaranthus pumilus*: an application of light detection and ranging (LIDAR) data. *Journal of Coastal Research*, 23(5), 1193-1202.

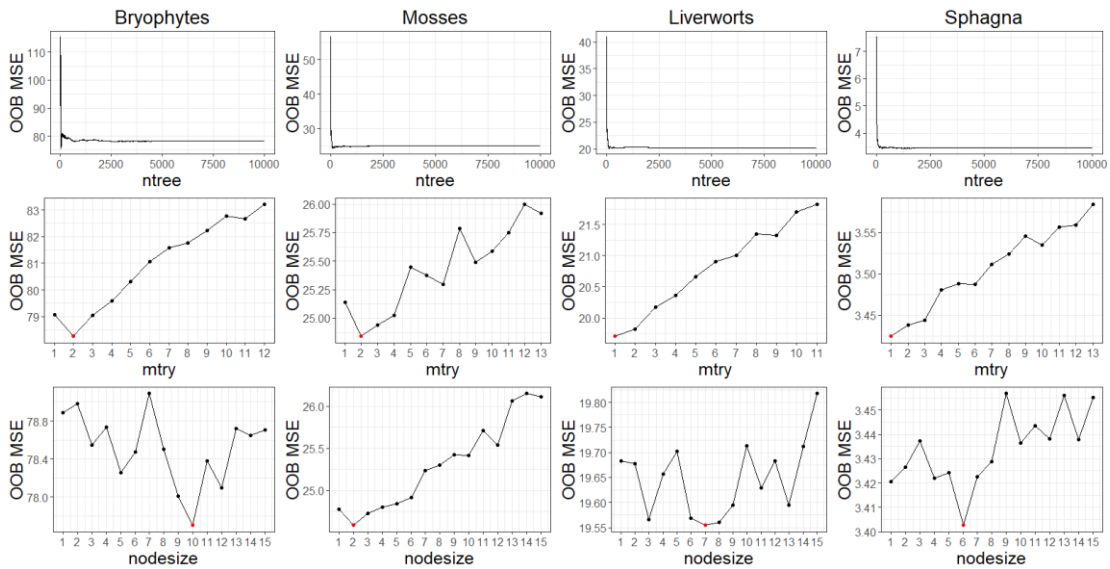
- Sims, D. A., & Gamon, J. A. (2003). Estimation of vegetation water content and photosynthetic tissue area from spectral reflectance: a comparison of indices based on liquid water and chlorophyll absorption features. *Remote sensing of environment*, 84(4), 526-537.
- Slingsby, J. A., & Slingsby, P. W. (2019). Monitoring the critically endangered Clanwilliam cedar with freely available Google Earth imagery. *PeerJ*, 7, e7005.
- Soliveres, S., Manning, P., Prati, D., Gossner, M. M., Alt, F., Arndt, H., ... & Allan, E. (2016). Locally rare species influence grassland ecosystem multifunctionality. *Philosophical Transactions of the Royal Society B: Biological Sciences*, 371(1694), 20150269.
- Sperduto, M. B., & Congalton, R. G. (1996). Predicting rare orchid (small whorled pogonia) habitat using GIS. *Photogrammetric Engineering and Remote Sensing*, 62(11), 1269-1279.
- Sykes, L., Santini, L., Etard, A., & Newbold, T. (2020). Effects of rarity form on species' responses to land use. *Conservation Biology*, 34(3), 688-696.
- Thomas, C. (1994) Extinction, colonization, and metapopulations: environmental tracking by rare species. *Conservation Biology*, 8, 373–378.
- Traganos, D., & Reinartz, P. (2018). Machine learning-based retrieval of benthic reflectance and *Posidonia oceanica* seagrass extent using a semi-analytical inversion of Sentinel-2 satellite data. *International Journal of Remote Sensing*, 39(24), 9428-9452.
- Turner, W., Spector, S., Gardiner, N., Fladeland, M., Sterling, E., & Steininger, M. (2003). Remote sensing for biodiversity science and conservation. *Trends in ecology & evolution*, 18(6), 306-314.
- Umaña, M. N., Mi, X., Cao, M., Enquist, B. J., Hao, Z., Howe, R., ... & Swenson, N. G. (2017). The role of functional uniqueness and spatial aggregation in explaining rarity in trees. *Global Ecology and Biogeography*, 26(7), 777-786.
- Ustin, S. L., & Gamon, J. A. (2010). Remote sensing of plant functional types. *New Phytologist*, 186(4), 795-816.
- Varghese, A. O., Joshi, A. K., & Krishna Murthy, Y. V. N. (2010). Mapping of realized and fundamental niches of threatened tree species using geoinformatics: a

- species level approach for sustaining biodiversity. *Journal of the Indian Society of Remote Sensing*, 38(3), 523-534.
- Wan, L., Lin, Y., Zhang, H., Wang, F., Liu, M., & Lin, H. (2020). GF-5 hyperspectral data for species mapping of mangrove in Mai Po, Hong Kong. *Remote Sensing*, 12(4), 656.
- Weisser, W. W., Roscher, C., Meyer, S. T., Ebeling, A., Luo, G., Allan, E., ... & Eisenhauer, N. (2017). Biodiversity effects on ecosystem functioning in a 15-year grassland experiment: Patterns, mechanisms, and open questions. *Basic and applied ecology*, 23, 1-73.
- Williams, J. N., Seo, C., Thorne, J., Nelson, J. K., Erwin, S., O'Brien, J. M., & Schwartz, M. W. (2009). Using species distribution models to predict new occurrences for rare plants. *Diversity and Distributions*, 15(4), 565-576.
- Wiser, S. K., Peet, R. K., & White, P. S. (1998). Prediction of rare-plant occurrence: a southern Appalachian example. *Ecological Applications*, 8(4), 909-920.
- Wu, X. B., & Smeins, F. E. (2000). Multiple-scale habitat modeling approach for rare plant conservation. *Landscape and Urban Planning*, 51(1), 11-28.
- Xu, G., Zhang, Y., Zhang, S., & Ma, K. (2020). Biodiversity associations of soil fauna and plants depend on plant life form and are accounted for by rare taxa along an elevational gradient. *Soil Biology and Biochemistry*, 140, 107640.
- Zavaleta, E. S., & Hulvey, K. B. (2004). Realistic species losses disproportionately reduce grassland resistance to biological invaders. *Science*, 306(5699), 1175-1177.
- Zhang, P. (2019). Effective predictors of herbaceous plant diversity responses to changes in nutrient availability and herbivory (Doctoral dissertation, Utrecht University).
- Zhao, X., Meng, H., Wang, W., & Yan, B. (2016). Prediction of the distribution of alpine tree species under climate change scenarios: *Larix chinensis* in Taibai Mountain (China). *Polish Journal of Ecology*, 64(2), 200-212.
- Zhu, G. P., Li, H. Q., Zhao, L., Man, L., & Liu, Q. (2016). Mapping the ecological dimensions and potential distributions of endangered relic shrubs in western Ordos biodiversity center. *Scientific Reports*, 6(1), 1-9.

- Zimmermann, N. E., Edwards Jr, T. C., Moisen, G. G., Frescino, T. S., & Blackard, J. A. (2007). Remote sensing-based predictors improve distribution models of rare, early successional and broadleaf tree species in Utah. *Journal of applied ecology*, 44(5), 1057-1067.
- Zucchetto, M., Venier, C., Taji, M. A., Mangin, A., & Pastres, R. (2016). Modelling the spatial distribution of the seagrass *Posidonia oceanica* along the North African coast: Implications for the assessment of Good Environmental Status. *Ecological Indicators*, 61, 1011-1023.

APPENDIX A

Out-of-bag mean square error OOB MSE versus ntree, mtry and nodesize parameter values of the Random Forest regression models for bryophytes, mosses, liverworts and sphagna



Evolution of the out-of-bag mean square error (OOB MSE) in function of the values of the ntree, mtry and nodesize parameters of the Random Forest algorithm (first, second and third row, respectively) for each of the regression models (from left to right: total bryophytes, mosses, liverworts and sphagna).

APPENDIX B

Modeled rare bryophyte species including their number of occurrences, ESMs' predictive performance, and species traits

Modeled rare bryophyte species (n = 52) indicating the number of available occurrences as well as the predictive performance of ESMs as measured by AUC, TSS and Sensitivity. Bryophyte species traits, namely substrate preference, reproduction mode, and spore size are also included.

Species	# of occurrences	AUC	TSS	Sensitivity	Substrate preference	Reproduction mode	Spore size (µm)
Liverworts (n = 14)							
<i>Anastrophyllum minutum</i>	8	0.858	0.767	0.8	R	V	12-14
<i>Barbilophozia attenuata</i>	23	0.5	0	0	G	V	10-14
<i>Bazzania trilobata</i>	7	0.936	0.933	1	T	NA	12-17
<i>Calypogeia integristipula</i>	7	0.839	0.834	1	G	V	10-13
<i>Calypogeia suecica</i>	5	0.584	0.384	1	EO	V	9-11
<i>Cephaloziella elachista</i>	15	0.686	0.494	1	G	S	9-11
<i>Cephaloziella spinigera</i>	10	0.966	0.962	0.95	G	S	7-10

<i>Chiloscyphus coadunatus</i>	21	0.5	0	0	G	S	15-20
<i>Gymnocolea inflata</i>	10	0.5	0	0	G	VS	12-18
<i>Jungermannia leiantha</i>	18	0.5	0	0	G	S	12-15
<i>Lophozia ascendens</i>	20	0.798	0.657	0.975	EO	V	9.5-10.5
<i>Lophozia bicrenata</i>	8	0.949	0.93	0.9	G	VS	12-16
<i>Plagiochila porelloides</i>	7	0.908	0.705	1	G	S	14-20
<i>Tritomaria exsectiformis</i>	27	0.771	0.523	0.84	G	V	9-12
Mosses (n = 33)							
<i>Amblystegium serpens</i>	17	0.888	0.842	0.8668	G	S	8-15
<i>Brachythecium erythrorrhizon</i>	5	0.973	0.968	1	R	S	14-20
<i>Brachythecium populeum</i>	5	0.872	0.871	1	G	S	12-20
<i>Brachythecium rutabulum</i>	18	0.772	0.734	0.975	G	S	12-18
<i>Brachythecium velutinum</i>	20	0.721	0.487	0.8	G	S	13-16

<i>Breidleria pratensis</i>	7	0.5	0	0	G	S	10-13
<i>Brotherella recurvans</i>	14	0.693	0.496	0.8668	G	S	13-18
<i>Bryum caespiticium</i>	5	0.887	0.882	1	T	S	10-18
<i>Callicladium haldanianum</i>	23	0.693	0.449	1	G	S	10-18
<i>Calliargon richardsonii</i>	6	0.706	0.555	1	P	S	17-31
<i>Campyliadelphus chrysophyllus</i>	7	0.813	0.81	1	G	S	14-14
<i>Campylophyllum hispidulum</i>	13	0.5	0	0	G	S	9-13
<i>Campylium stellatum</i>	5	0.551	0.538	1	P	S	12-18
<i>Drepanocladus aduncus</i>	13	0.82	0.646	0.9667	P	S	16-16
<i>Hygroamblystegium varium</i>	8	0.5	0	0	G	S	10-16
<i>Isopterygiopsis muelleriana</i>	7	0.74	0.739	1	R	VS	8-12
<i>Leptodictyum riparium</i>	8	0.556	0.323	0.9	G	S	12-16
<i>Mnium spinulosum</i>	10	0.827	0.718	1	G	S	16-24

<i>Plagiomnium cuspidatum</i>	10	0.806	0.703	0.9	G	S	18-31
<i>Plagiomnium drummondii</i>	5	0.945	0.943	1	T	S	18-25
<i>Plagiomnium medium</i>	8	0.604	0.415	0.9	T	S	20-36
<i>Plagiothecium denticulatum</i>	29	0.5	0	0	EF	S	9-13
<i>Platygyrium repens</i>	18	0.703	0.623	0.85	G	V	13-18
<i>Platydictya subtilis</i>	6	0.58	0.527	1	EO	S	9-13
<i>Pogonatum dentatum</i>	8	0.936	0.892	1	G	S	18-24
<i>Polytrichastrum longisetum</i>	9	0.968	0.95	1	P	S	18-28
<i>Polytrichastrum pallidisetum</i>	5	0.768	0.761	1	G	S	12-16
<i>Rhizomnium pseudopunctatu m</i>	24	0.5	0	0	T	S	40-50
<i>Rhizomnium punctatum</i>	11	0.5	0	0	G	S	29-41
<i>Sarmentypnum exannulatum</i>	19	0.5	0	0	P	S	16-20
<i>Tomentypnum falcifolium</i>	24	0.789	0.578	0.98	P	S	NA

<i>Tomentypnum nitens</i>	14	0.5	0	0	P	S	16-20
<i>Trematodon ambiguus</i>	11	0.979	0.973	1	T	S	30-36
Sphagna (n = 5)							
<i>Sphagnum cuspidatum</i>	6	0.785	0.743	1	P	S	29-38
<i>Sphagnum pulchrum</i>	6	0.562	0.517	1	P	S	25-28
<i>Sphagnum squarrosum</i>	19	0.5	0	0	G	S	17-30
<i>Sphagnum subtile</i>	22	0.5	0	0	T	S	19-29
<i>Sphagnum tenerum</i>	14	0.97	0.937	0.9667	P	S	22-25

Substrate preference abbrev.: EF, facultative epixylic; EO, obligate epixylic; G, generalist; P, peatland; R, rock; T, terricolous. Reproduction mode abbrev.: S, sexual; V, vegetative; VS, vegetative and sexual. Information on bryophyte species traits was found in Faubert (2012, 2013, 2014), Boudreault *et al.* (2018), Barbé *et al.* (2017), Crum & Anderson (1981), BFNA (http://www.efloras.org/flora_page.aspx?flora_id=50), BRYOATT (Hill *et al.*, 2007), and based on personal experience (laboratory of N.J. Fenton).

APPENDIX C

Species occurrence coordinates used for modeling

Rare bryophyte species occurrence coordinates used for modeling.

Species	x lon	y lat
<i>Anastrophyllum minutum</i>	-77.569253	50.5843075
<i>Anastrophyllum minutum</i>	-76.108279	49.8784826
<i>Anastrophyllum minutum</i>	-77.514714	50.5721486
<i>Anastrophyllum minutum</i>	-79.3088	49.7410387
<i>Anastrophyllum minutum</i>	-76.28157	49.7427071
<i>Anastrophyllum minutum</i>	-76.119009	49.9550212
<i>Anastrophyllum minutum</i>	-76.10822	49.8780001
<i>Anastrophyllum minutum</i>	-78.46555	49.41563
<i>Barbilophozia attenuata</i>	-76.300497	49.7434854
<i>Barbilophozia attenuata</i>	-77.51246	50.5725778
<i>Barbilophozia attenuata</i>	-74.62631	50.6013069
<i>Barbilophozia attenuata</i>	-74.853916	50.5504147
<i>Barbilophozia attenuata</i>	-74.845739	50.5523812
<i>Barbilophozia attenuata</i>	-76.30754	49.7619118
<i>Barbilophozia attenuata</i>	-76.300875	49.7429968
<i>Barbilophozia attenuata</i>	-77.512402	50.5723798
<i>Barbilophozia attenuata</i>	-74.855167	50.5500158
<i>Barbilophozia attenuata</i>	-76.281295	49.7423701
<i>Barbilophozia attenuata</i>	-77.514714	50.5721486
<i>Barbilophozia attenuata</i>	-74.856373	50.5494175
<i>Barbilophozia attenuata</i>	-79.030797	49.8150734
<i>Barbilophozia attenuata</i>	-76.307396	49.7628233
<i>Barbilophozia attenuata</i>	-77.514346	50.5719872
<i>Barbilophozia attenuata</i>	-74.856909	50.5492466
<i>Barbilophozia attenuata</i>	-78.771267	49.395417
<i>Barbilophozia attenuata</i>	-79.075046	49.8157375
<i>Barbilophozia attenuata</i>	-78.46555	49.41563
<i>Barbilophozia attenuata</i>	-76.28373	49.17232
<i>Barbilophozia attenuata</i>	-78.48627	49.43067

<i>Barbilophozia attenuata</i>	-76.77185	49.19325
<i>Barbilophozia attenuata</i>	-76.54262	48.95425
<i>Bazzania trilobata</i>	-76.119675	49.9624052
<i>Bazzania trilobata</i>	-76.307947	49.7622753
<i>Bazzania trilobata</i>	-76.108494	49.8783377
<i>Bazzania trilobata</i>	-76.75473	49.19441
<i>Bazzania trilobata</i>	-78.6312	49.21166
<i>Bazzania trilobata</i>	-78.63873	49.18228
<i>Bazzania trilobata</i>	-78.54087	49.38384
<i>Calypogeia integristipula</i>	-76.109693	49.9486279
<i>Calypogeia integristipula</i>	-76.108494	49.8783377
<i>Calypogeia integristipula</i>	-76.2802	49.7449718
<i>Calypogeia integristipula</i>	-76.119009	49.9550212
<i>Calypogeia integristipula</i>	-76.282069	49.7431831
<i>Calypogeia integristipula</i>	-79.306981	49.7387841
<i>Calypogeia integristipula</i>	-78.68008	49.18813
<i>Calypogeia suecica</i>	-77.569253	50.5843075
<i>Calypogeia suecica</i>	-76.120026	49.9508003
<i>Calypogeia suecica</i>	-76.304391	49.7432298
<i>Calypogeia suecica</i>	-76.067417	49.457733
<i>Calypogeia suecica</i>	-76.119042	49.9546511
<i>Cephaloziella elachista</i>	-76.127196	49.9489462
<i>Cephaloziella elachista</i>	-76.305678	49.7499746
<i>Cephaloziella elachista</i>	-76.121271	49.9497325
<i>Cephaloziella elachista</i>	-79.282351	49.747359
<i>Cephaloziella elachista</i>	-79.30808	49.7421242
<i>Cephaloziella elachista</i>	-76.118985	49.9556754
<i>Cephaloziella elachista</i>	-79.074728	49.8147542
<i>Cephaloziella elachista</i>	-74.62582	50.6008219
<i>Cephaloziella elachista</i>	-74.63809	50.6083907
<i>Cephaloziella elachista</i>	-79.041715	49.796027
<i>Cephaloziella elachista</i>	-75.970933	49.67545
<i>Cephaloziella elachista</i>	-79.249474	49.7807209
<i>Cephaloziella elachista</i>	-79.287476	49.7463647
<i>Cephaloziella elachista</i>	-76.12017	49.9598684
<i>Cephaloziella elachista</i>	-79.041687	49.7957438
<i>Cephaloziella spinigera</i>	-79.249693	49.7841002
<i>Cephaloziella spinigera</i>	-77.517366	50.5744163
<i>Cephaloziella spinigera</i>	-76.120981	49.9503332

<i>Cephaloziella spinigera</i>	-77.56931	50.5845054
<i>Cephaloziella spinigera</i>	-74.63809	50.6083907
<i>Cephaloziella spinigera</i>	-79.041715	49.796027
<i>Cephaloziella spinigera</i>	-79.321583	49.538067
<i>Cephaloziella spinigera</i>	-74.857981	50.5486199
<i>Cephaloziella spinigera</i>	-79.041687	49.7957438
<i>Cephaloziella spinigera</i>	-78.46555	49.41563
<i>Chiloscyphus coadunatus</i>	-79.276028	49.7545564
<i>Chiloscyphus coadunatus</i>	-74.820354	50.5661632
<i>Chiloscyphus coadunatus</i>	-76.279988	49.7438949
<i>Chiloscyphus coadunatus</i>	-77.512402	50.5723798
<i>Chiloscyphus coadunatus</i>	-76.108279	49.8784826
<i>Chiloscyphus coadunatus</i>	-76.280171	49.7441196
<i>Chiloscyphus coadunatus</i>	-77.51706	50.5731419
<i>Chiloscyphus coadunatus</i>	-76.126576	49.874086
<i>Chiloscyphus coadunatus</i>	-76.307396	49.7628233
<i>Chiloscyphus coadunatus</i>	-76.2802	49.7449718
<i>Chiloscyphus coadunatus</i>	-74.624256	50.6003918
<i>Chiloscyphus coadunatus</i>	-78.475667	49.410383
<i>Chiloscyphus coadunatus</i>	-76.1915	49.516483
<i>Chiloscyphus coadunatus</i>	-76.10822	49.8780001
<i>Chiloscyphus coadunatus</i>	-76.304278	49.7437714
<i>Chiloscyphus coadunatus</i>	-78.46626	49.41651
<i>Chiloscyphus coadunatus</i>	-78.46809	49.4109
<i>Chiloscyphus coadunatus</i>	-78.44347	49.39995
<i>Chiloscyphus coadunatus</i>	-78.44025	49.40106
<i>Chiloscyphus coadunatus</i>	-78.63749	49.18093
<i>Chiloscyphus coadunatus</i>	-78.63873	49.18228
<i>Gymnocolea inflata</i>	-79.308487	49.7418214
<i>Gymnocolea inflata</i>	-79.30808	49.7421242
<i>Gymnocolea inflata</i>	-79.30478	49.7399919
<i>Gymnocolea inflata</i>	-74.62582	50.6008219
<i>Gymnocolea inflata</i>	-79.304844	49.7401884
<i>Gymnocolea inflata</i>	-76.108494	49.8783377
<i>Gymnocolea inflata</i>	-79.011967	49.386433
<i>Gymnocolea inflata</i>	-79.277217	49.505117
<i>Gymnocolea inflata</i>	-78.46926	49.41026
<i>Gymnocolea inflata</i>	-78.67995	49.18873
<i>Jungermannia leiantha</i>	-79.282574	49.7482319

<i>Jungermannia leiantha</i>	-79.30468	49.7398824
<i>Jungermannia leiantha</i>	-79.30478	49.7399919
<i>Jungermannia leiantha</i>	-76.108279	49.8784826
<i>Jungermannia leiantha</i>	-79.030805	49.814703
<i>Jungermannia leiantha</i>	-76.280171	49.7441196
<i>Jungermannia leiantha</i>	-79.304844	49.7401884
<i>Jungermannia leiantha</i>	-77.51706	50.5731419
<i>Jungermannia leiantha</i>	-76.307396	49.7628233
<i>Jungermannia leiantha</i>	-79.282744	49.7456616
<i>Jungermannia leiantha</i>	-79.305078	49.7403205
<i>Jungermannia leiantha</i>	-79.287277	49.7461456
<i>Jungermannia leiantha</i>	-76.119009	49.9550212
<i>Jungermannia leiantha</i>	-78.511483	49.414583
<i>Jungermannia leiantha</i>	-78.771267	49.395417
<i>Jungermannia leiantha</i>	-76.280434	49.7453947
<i>Jungermannia leiantha</i>	-79.287476	49.7463647
<i>Jungermannia leiantha</i>	-78.63873	49.18228
<i>Lophozia ascendens</i>	-76.307785	49.7613967
<i>Lophozia ascendens</i>	-76.300497	49.7434854
<i>Lophozia ascendens</i>	-76.279581	49.7435313
<i>Lophozia ascendens</i>	-79.286547	49.7454659
<i>Lophozia ascendens</i>	-74.845739	50.5523812
<i>Lophozia ascendens</i>	-76.119467	49.9628343
<i>Lophozia ascendens</i>	-76.30754	49.7619118
<i>Lophozia ascendens</i>	-77.512402	50.5723798
<i>Lophozia ascendens</i>	-79.287044	49.7460135
<i>Lophozia ascendens</i>	-76.118885	49.9552786
<i>Lophozia ascendens</i>	-76.108494	49.8783377
<i>Lophozia ascendens</i>	-78.771267	49.395417
<i>Lophozia ascendens</i>	-76.282069	49.7431831
<i>Lophozia ascendens</i>	-78.46546	49.41556
<i>Lophozia ascendens</i>	-78.46555	49.41563
<i>Lophozia ascendens</i>	-78.46809	49.4109
<i>Lophozia ascendens</i>	-78.44467	49.3983
<i>Lophozia ascendens</i>	-78.44347	49.39995
<i>Lophozia ascendens</i>	-78.44261	49.40078
<i>Lophozia ascendens</i>	-78.54163	49.37795
<i>Lophozia bicrenata</i>	-79.036254	49.8048529
<i>Lophozia bicrenata</i>	-74.633589	50.6041966

<i>Lophozia bicrenata</i>	-76.127196	49.9489462
<i>Lophozia bicrenata</i>	-74.646849	50.6110259
<i>Lophozia bicrenata</i>	-79.282574	49.7482319
<i>Lophozia bicrenata</i>	-76.121271	49.9497325
<i>Lophozia bicrenata</i>	-74.623676	50.6000774
<i>Lophozia bicrenata</i>	-76.119042	49.9546511
<i>Plagiochila porelloides</i>	-79.282574	49.7482319
<i>Plagiochila porelloides</i>	-79.249734	49.7836428
<i>Plagiochila porelloides</i>	-79.282351	49.747359
<i>Plagiochila porelloides</i>	-79.287044	49.7460135
<i>Plagiochila porelloides</i>	-78.308983	49.69765
<i>Plagiochila porelloides</i>	-76.282069	49.7431831
<i>Plagiochila porelloides</i>	-78.68008	49.18813
<i>Tritomaria exsectiformis</i>	-79.03065	49.814026
<i>Tritomaria exsectiformis</i>	-76.300497	49.7434854
<i>Tritomaria exsectiformis</i>	-79.286547	49.7454659
<i>Tritomaria exsectiformis</i>	-74.653244	50.6122043
<i>Tritomaria exsectiformis</i>	-76.120981	49.9503332
<i>Tritomaria exsectiformis</i>	-76.305454	49.7409978
<i>Tritomaria exsectiformis</i>	-76.30754	49.7619118
<i>Tritomaria exsectiformis</i>	-76.300875	49.7429968
<i>Tritomaria exsectiformis</i>	-76.28098	49.7421188
<i>Tritomaria exsectiformis</i>	-76.307947	49.7622753
<i>Tritomaria exsectiformis</i>	-76.281295	49.7423701
<i>Tritomaria exsectiformis</i>	-79.282337	49.7459642
<i>Tritomaria exsectiformis</i>	-77.569271	50.584592
<i>Tritomaria exsectiformis</i>	-79.287044	49.7460135
<i>Tritomaria exsectiformis</i>	-77.514714	50.5721486
<i>Tritomaria exsectiformis</i>	-77.558361	50.5758474
<i>Tritomaria exsectiformis</i>	-76.307396	49.7628233
<i>Tritomaria exsectiformis</i>	-76.28157	49.7427071
<i>Tritomaria exsectiformis</i>	-79.282744	49.7456616
<i>Tritomaria exsectiformis</i>	-79.287277	49.7461456
<i>Tritomaria exsectiformis</i>	-76.119009	49.9550212
<i>Tritomaria exsectiformis</i>	-78.308983	49.69765
<i>Tritomaria exsectiformis</i>	-78.771267	49.395417
<i>Tritomaria exsectiformis</i>	-76.011517	49.622833
<i>Tritomaria exsectiformis</i>	-75.8473	49.799767
<i>Tritomaria exsectiformis</i>	-76.440733	49.415333

<i>Tritomaria exsectiformis</i>	-78.45592	49.45592
<i>Amblystegium serpens</i>	-77.558902	50.5766025
<i>Amblystegium serpens</i>	-76.280171	49.7441196
<i>Amblystegium serpens</i>	-76.120454	49.9604903
<i>Amblystegium serpens</i>	-78.308983	49.69765
<i>Amblystegium serpens</i>	-76.636883	49.419817
<i>Amblystegium serpens</i>	-79.306981	49.7387841
<i>Amblystegium serpens</i>	-78.46546	49.41556
<i>Amblystegium serpens</i>	-78.46758	49.41831
<i>Amblystegium serpens</i>	-78.44261	49.40086
<i>Amblystegium serpens</i>	-76.6013	49.10045
<i>Amblystegium serpens</i>	-78.61356	49.48611
<i>Amblystegium serpens</i>	-78.61349	49.48624
<i>Amblystegium serpens</i>	-78.6119	49.48584
<i>Amblystegium serpens</i>	-78.63095	49.21301
<i>Amblystegium serpens</i>	-78.63873	49.18228
<i>Amblystegium serpens</i>	-78.63735	49.1809
<i>Amblystegium serpens</i>	-78.55132	49.37499
<i>Brachythecium erythrorrhizon</i>	-79.039665	49.7975361
<i>Brachythecium erythrorrhizon</i>	-77.514714	50.5721486
<i>Brachythecium erythrorrhizon</i>	-76.307396	49.7628233
<i>Brachythecium erythrorrhizon</i>	-78.63873	49.18228
<i>Brachythecium erythrorrhizon</i>	-78.55132	49.37499
<i>Brachythecium populeum</i>	-76.280171	49.7441196
<i>Brachythecium populeum</i>	-76.2802	49.7449718
<i>Brachythecium populeum</i>	-76.280434	49.7453947
<i>Brachythecium populeum</i>	-78.46668	49.41376
<i>Brachythecium populeum</i>	-78.55118	49.37511
<i>Brachythecium rutabulum</i>	-76.279297	49.7429102
<i>Brachythecium rutabulum</i>	-79.308487	49.7418214
<i>Brachythecium rutabulum</i>	-76.279581	49.7435313
<i>Brachythecium rutabulum</i>	-79.30468	49.7398824
<i>Brachythecium rutabulum</i>	-77.569271	50.584592
<i>Brachythecium rutabulum</i>	-76.2802	49.7449718
<i>Brachythecium rutabulum</i>	-79.305078	49.7403205
<i>Brachythecium rutabulum</i>	-79.306981	49.7387841
<i>Brachythecium rutabulum</i>	-78.46626	49.41651
<i>Brachythecium rutabulum</i>	-78.46926	49.41026
<i>Brachythecium rutabulum</i>	-78.46668	49.41376

<i>Brachythecium rutabulum</i>	-78.61347	49.48646
<i>Brachythecium rutabulum</i>	-78.61338	49.48572
<i>Brachythecium rutabulum</i>	-78.63095	49.21301
<i>Brachythecium rutabulum</i>	-78.63746	49.18096
<i>Brachythecium rutabulum</i>	-78.63873	49.18228
<i>Brachythecium rutabulum</i>	-78.67911	49.18961
<i>Brachythecium rutabulum</i>	-78.54903	49.37536
<i>Brachythecium velutinum</i>	-76.115411	49.8757773
<i>Brachythecium velutinum</i>	-76.119476	49.9631186
<i>Brachythecium velutinum</i>	-79.30468	49.7398824
<i>Brachythecium velutinum</i>	-77.51246	50.5725778
<i>Brachythecium velutinum</i>	-76.127015	49.8740661
<i>Brachythecium velutinum</i>	-79.286781	49.745598
<i>Brachythecium velutinum</i>	-77.512402	50.5723798
<i>Brachythecium velutinum</i>	-76.108279	49.8784826
<i>Brachythecium velutinum</i>	-76.119675	49.9624052
<i>Brachythecium velutinum</i>	-79.032495	49.795755
<i>Brachythecium velutinum</i>	-77.51706	50.5731419
<i>Brachythecium velutinum</i>	-76.120297	49.9611178
<i>Brachythecium velutinum</i>	-76.307396	49.7628233
<i>Brachythecium velutinum</i>	-79.282744	49.7456616
<i>Brachythecium velutinum</i>	-76.120454	49.9604903
<i>Brachythecium velutinum</i>	-78.511483	49.414583
<i>Brachythecium velutinum</i>	-79.282953	49.7451398
<i>Brachythecium velutinum</i>	-78.46546	49.41556
<i>Brachythecium velutinum</i>	-78.46555	49.41563
<i>Brachythecium velutinum</i>	-78.54073	49.38416
<i>Breidleria pratensis</i>	-79.282574	49.7482319
<i>Breidleria pratensis</i>	-79.249734	49.7836428
<i>Breidleria pratensis</i>	-79.282351	49.747359
<i>Breidleria pratensis</i>	-74.638088	50.6086755
<i>Breidleria pratensis</i>	-78.308983	49.69765
<i>Breidleria pratensis</i>	-78.61347	49.48646
<i>Breidleria pratensis</i>	-78.55132	49.37499
<i>Brotherella recurvans</i>	-76.300497	49.7434854
<i>Brotherella recurvans</i>	-76.280171	49.7441196
<i>Brotherella recurvans</i>	-76.118885	49.9552786
<i>Brotherella recurvans</i>	-76.108494	49.8783377
<i>Brotherella recurvans</i>	-76.28157	49.7427071

<i>Brotherella recurvans</i>	-77.569368	50.5847034
<i>Brotherella recurvans</i>	-78.308983	49.69765
<i>Brotherella recurvans</i>	-78.771267	49.395417
<i>Brotherella recurvans</i>	-76.011517	49.622833
<i>Brotherella recurvans</i>	-79.306981	49.7387841
<i>Brotherella recurvans</i>	-76.10822	49.8780001
<i>Brotherella recurvans</i>	-78.46555	49.41563
<i>Brotherella recurvans</i>	-76.6013	49.10045
<i>Brotherella recurvans</i>	-78.46668	49.41376
<i>Bryum caespiticium</i>	-76.28194	49.17344
<i>Bryum caespiticium</i>	-78.63749	49.18093
<i>Bryum caespiticium</i>	-78.63735	49.1809
<i>Bryum caespiticium</i>	-78.55132	49.37499
<i>Bryum caespiticium</i>	-78.53313	49.38706
<i>Callicladium haldanianum</i>	-77.558651	50.5761817
<i>Callicladium haldanianum</i>	-76.307396	49.7628233
<i>Callicladium haldanianum</i>	-74.624256	50.6003918
<i>Callicladium haldanianum</i>	-76.119009	49.9550212
<i>Callicladium haldanianum</i>	-76.108312	49.8781126
<i>Callicladium haldanianum</i>	-76.011517	49.622833
<i>Callicladium haldanianum</i>	-78.44261	49.40078
<i>Callicladium haldanianum</i>	-78.44261	49.40086
<i>Callicladium haldanianum</i>	-78.46069	49.41317
<i>Callicladium haldanianum</i>	-78.46668	49.41376
<i>Callicladium haldanianum</i>	-78.6136	49.48602
<i>Callicladium haldanianum</i>	-78.61349	49.48624
<i>Callicladium haldanianum</i>	-78.61347	49.48646
<i>Callicladium haldanianum</i>	-78.63091	49.21284
<i>Callicladium haldanianum</i>	-78.63095	49.21301
<i>Callicladium haldanianum</i>	-78.63749	49.18093
<i>Callicladium haldanianum</i>	-78.63746	49.18096
<i>Callicladium haldanianum</i>	-78.6363	49.18156
<i>Callicladium haldanianum</i>	-78.63735	49.1809
<i>Callicladium haldanianum</i>	-78.67995	49.18873
<i>Callicladium haldanianum</i>	-78.63079	49.17515
<i>Callicladium haldanianum</i>	-78.63248	49.18825
<i>Callicladium haldanianum</i>	-78.53313	49.38706
<i>Calliargon richardsonii</i>	-79.282574	49.7482319
<i>Calliargon richardsonii</i>	-79.282267	49.7461382

<i>Calliergon richardsonii</i>	-79.287044	49.7460135
<i>Calliergon richardsonii</i>	-79.282744	49.7456616
<i>Calliergon richardsonii</i>	-78.68008	49.18813
<i>Calliergon richardsonii</i>	-78.67995	49.18873
<i>Campyliadelphus chrysophyllus</i>	-79.03065	49.814026
<i>Campyliadelphus chrysophyllus</i>	-77.558651	50.5761817
<i>Campyliadelphus chrysophyllus</i>	-76.108279	49.8784826
<i>Campyliadelphus chrysophyllus</i>	-76.280434	49.7453947
<i>Campyliadelphus chrysophyllus</i>	-79.282953	49.7451398
<i>Campyliadelphus chrysophyllus</i>	-78.46555	49.41563
<i>Campyliadelphus chrysophyllus</i>	-78.55132	49.37499
<i>Campylophyllum hispidulum</i>	-77.558902	50.5766025
<i>Campylophyllum hispidulum</i>	-74.653244	50.6122043
<i>Campylophyllum hispidulum</i>	-77.517486	50.5735012
<i>Campylophyllum hispidulum</i>	-79.040682	49.7971522
<i>Campylophyllum hispidulum</i>	-76.280171	49.7441196
<i>Campylophyllum hispidulum</i>	-79.287277	49.7461456
<i>Campylophyllum hispidulum</i>	-77.517217	50.5727958
<i>Campylophyllum hispidulum</i>	-78.5876	49.954517
<i>Campylophyllum hispidulum</i>	-76.1617	49.540967
<i>Campylophyllum hispidulum</i>	-79.249474	49.7807209
<i>Campylophyllum hispidulum</i>	-78.46555	49.41563
<i>Campylophyllum hispidulum</i>	-78.63749	49.18093
<i>Campylophyllum hispidulum</i>	-78.63746	49.18185
<i>Campylium stellatum</i>	-79.298405	49.7290824
<i>Campylium stellatum</i>	-79.30808	49.7421242
<i>Campylium stellatum</i>	-79.282267	49.7461382
<i>Campylium stellatum</i>	-78.774567	49.513567
<i>Campylium stellatum</i>	-78.67995	49.18873
<i>Drepanocladus aduncus</i>	-79.249734	49.7836428
<i>Drepanocladus aduncus</i>	-79.282351	49.747359
<i>Drepanocladus aduncus</i>	-79.30478	49.7399919
<i>Drepanocladus aduncus</i>	-79.304844	49.7401884
<i>Drepanocladus aduncus</i>	-76.28157	49.7427071
<i>Drepanocladus aduncus</i>	-79.282744	49.7456616
<i>Drepanocladus aduncus</i>	-79.305078	49.7403205
<i>Drepanocladus aduncus</i>	-79.303017	49.460617
<i>Drepanocladus aduncus</i>	-76.282069	49.7431831
<i>Drepanocladus aduncus</i>	-77.517063	50.5724864

<i>Drepanocladus aduncus</i>	-78.46926	49.41026
<i>Drepanocladus aduncus</i>	-78.67995	49.18873
<i>Drepanocladus aduncus</i>	-78.67911	49.18961
<i>Hygroamblystegium varium</i>	-76.284811	49.7426038
<i>Hygroamblystegium varium</i>	-76.279297	49.7429102
<i>Hygroamblystegium varium</i>	-76.279988	49.7438949
<i>Hygroamblystegium varium</i>	-79.308999	49.7412577
<i>Hygroamblystegium varium</i>	-76.280171	49.7441196
<i>Hygroamblystegium varium</i>	-76.2802	49.7449718
<i>Hygroamblystegium varium</i>	-76.280434	49.7453947
<i>Hygroamblystegium varium</i>	-79.041687	49.7957438
<i>Isopterygiopsis muelleriana</i>	-79.30468	49.7398824
<i>Isopterygiopsis muelleriana</i>	-79.30478	49.7399919
<i>Isopterygiopsis muelleriana</i>	-79.287044	49.7460135
<i>Isopterygiopsis muelleriana</i>	-76.108494	49.8783377
<i>Isopterygiopsis muelleriana</i>	-76.28157	49.7427071
<i>Isopterygiopsis muelleriana</i>	-76.282069	49.7431831
<i>Isopterygiopsis muelleriana</i>	-79.287476	49.7463647
<i>Leptodictyum riparium</i>	-77.51246	50.5725778
<i>Leptodictyum riparium</i>	-77.557502	50.5770955
<i>Leptodictyum riparium</i>	-77.569271	50.584592
<i>Leptodictyum riparium</i>	-79.287044	49.7460135
<i>Leptodictyum riparium</i>	-79.030797	49.8150734
<i>Leptodictyum riparium</i>	-76.301722	49.742132
<i>Leptodictyum riparium</i>	-79.287476	49.7463647
<i>Leptodictyum riparium</i>	-78.54073	49.38407
<i>Mnium spinulosum</i>	-76.2802	49.7449718
<i>Mnium spinulosum</i>	-76.28157	49.7427071
<i>Mnium spinulosum</i>	-76.282069	49.7431831
<i>Mnium spinulosum</i>	-76.6013	49.10045
<i>Mnium spinulosum</i>	-76.2812	49.1744
<i>Mnium spinulosum</i>	-76.28233	49.17467
<i>Mnium spinulosum</i>	-78.61349	49.48624
<i>Mnium spinulosum</i>	-78.63749	49.18093
<i>Mnium spinulosum</i>	-78.63873	49.18228
<i>Mnium spinulosum</i>	-78.53313	49.38706
<i>Plagiomnium cuspidatum</i>	-77.512402	50.5723798
<i>Plagiomnium cuspidatum</i>	-76.307396	49.7628233
<i>Plagiomnium cuspidatum</i>	-76.1617	49.540967

<i>Plagiomnium cuspidatum</i>	-79.282953	49.7451398
<i>Plagiomnium cuspidatum</i>	-78.6136	49.48602
<i>Plagiomnium cuspidatum</i>	-78.61349	49.48624
<i>Plagiomnium cuspidatum</i>	-78.61347	49.48646
<i>Plagiomnium cuspidatum</i>	-78.61128	49.4858
<i>Plagiomnium cuspidatum</i>	-78.63873	49.18228
<i>Plagiomnium cuspidatum</i>	-78.55132	49.37499
<i>Plagiothecium denticulatum</i>	-79.286547	49.7454659
<i>Plagiothecium denticulatum</i>	-77.51246	50.5725778
<i>Plagiothecium denticulatum</i>	-76.279988	49.7438949
<i>Plagiothecium denticulatum</i>	-79.282267	49.7461382
<i>Plagiothecium denticulatum</i>	-77.512402	50.5723798
<i>Plagiothecium denticulatum</i>	-77.558651	50.5761817
<i>Plagiothecium denticulatum</i>	-79.282337	49.7459642
<i>Plagiothecium denticulatum</i>	-76.307396	49.7628233
<i>Plagiothecium denticulatum</i>	-76.2802	49.7449718
<i>Plagiothecium denticulatum</i>	-76.28157	49.7427071
<i>Plagiothecium denticulatum</i>	-79.305078	49.7403205
<i>Plagiothecium denticulatum</i>	-77.569368	50.5847034
<i>Plagiothecium denticulatum</i>	-79.287277	49.7461456
<i>Plagiothecium denticulatum</i>	-76.120454	49.9604903
<i>Plagiothecium denticulatum</i>	-76.304391	49.7432298
<i>Plagiothecium denticulatum</i>	-78.5876	49.954517
<i>Plagiothecium denticulatum</i>	-78.308983	49.69765
<i>Plagiothecium denticulatum</i>	-76.1617	49.540967
<i>Plagiothecium denticulatum</i>	-76.011517	49.622833
<i>Plagiothecium denticulatum</i>	-76.440733	49.415333
<i>Plagiothecium denticulatum</i>	-76.282069	49.7431831
<i>Plagiothecium denticulatum</i>	-79.282953	49.7451398
<i>Plagiothecium denticulatum</i>	-78.46546	49.41556
<i>Plagiothecium denticulatum</i>	-78.44261	49.40086
<i>Plagiothecium denticulatum</i>	-78.61338	49.48572
<i>Plagiothecium denticulatum</i>	-78.63091	49.21284
<i>Plagiothecium denticulatum</i>	-78.55132	49.37499
<i>Plagiothecium denticulatum</i>	-78.54073	49.38407
<i>Plagiothecium denticulatum</i>	-78.53313	49.38706
<i>Plagiomnium drummondii</i>	-78.61356	49.48611
<i>Plagiomnium drummondii</i>	-78.61349	49.48624
<i>Plagiomnium drummondii</i>	-78.63873	49.18228

<i>Plagiomnium drummondii</i>	-78.54073	49.38407
<i>Plagiomnium drummondii</i>	-78.54073	49.38416
<i>Plagiomnium medium</i>	-76.119467	49.9628343
<i>Plagiomnium medium</i>	-79.305078	49.7403205
<i>Plagiomnium medium</i>	-76.6013	49.10045
<i>Plagiomnium medium</i>	-76.28389	49.17217
<i>Plagiomnium medium</i>	-78.46668	49.41376
<i>Plagiomnium medium</i>	-78.61349	49.48624
<i>Plagiomnium medium</i>	-78.55132	49.37499
<i>Plagiomnium medium</i>	-78.54073	49.38407
<i>Platygyrium repens</i>	-76.279988	49.7438949
<i>Platygyrium repens</i>	-76.28098	49.7421188
<i>Platygyrium repens</i>	-76.108279	49.8784826
<i>Platygyrium repens</i>	-76.280171	49.7441196
<i>Platygyrium repens</i>	-76.2802	49.7449718
<i>Platygyrium repens</i>	-76.28157	49.7427071
<i>Platygyrium repens</i>	-77.558318	50.577245
<i>Platygyrium repens</i>	-79.307145	49.7390901
<i>Platygyrium repens</i>	-76.119009	49.9550212
<i>Platygyrium repens</i>	-76.280434	49.7453947
<i>Platygyrium repens</i>	-76.282069	49.7431831
<i>Platygyrium repens</i>	-79.249474	49.7807209
<i>Platygyrium repens</i>	-78.46546	49.41556
<i>Platygyrium repens</i>	-78.46933	49.41018
<i>Platygyrium repens</i>	-78.46926	49.41026
<i>Platygyrium repens</i>	-78.46255	49.41814
<i>Platygyrium repens</i>	-76.6013	49.10045
<i>Platygyrium repens</i>	-78.63873	49.18228
<i>Platydictya subtilis</i>	-79.303017	49.460617
<i>Platydictya subtilis</i>	-78.44467	49.3983
<i>Platydictya subtilis</i>	-76.6013	49.10045
<i>Platydictya subtilis</i>	-78.63873	49.18228
<i>Platydictya subtilis</i>	-78.68089	49.18738
<i>Platydictya subtilis</i>	-78.55132	49.37499
<i>Pogonatum dentatum</i>	-74.633589	50.6041966
<i>Pogonatum dentatum</i>	-76.127196	49.9489462
<i>Pogonatum dentatum</i>	-76.119042	49.9546511
<i>Pogonatum dentatum</i>	-76.28112	49.17339
<i>Pogonatum dentatum</i>	-76.28126	49.17422

<i>Pogonatum dentatum</i>	-76.2812	49.1744
<i>Pogonatum dentatum</i>	-76.77223	49.19369
<i>Pogonatum dentatum</i>	-78.61168	49.48597
<i>Polytrichastrum longisetum</i>	-79.305078	49.7403205
<i>Polytrichastrum longisetum</i>	-76.28126	49.17422
<i>Polytrichastrum longisetum</i>	-76.2812	49.1744
<i>Polytrichastrum longisetum</i>	-76.2836	49.17248
<i>Polytrichastrum longisetum</i>	-76.77221	49.19354
<i>Polytrichastrum longisetum</i>	-76.75454	49.1938
<i>Polytrichastrum longisetum</i>	-76.75452	49.19384
<i>Polytrichastrum longisetum</i>	-78.61232	49.48579
<i>Polytrichastrum longisetum</i>	-78.54073	49.38416
<i>Polytrichastrum pallidisetum</i>	-76.28098	49.7421188
<i>Polytrichastrum pallidisetum</i>	-76.108279	49.8784826
<i>Polytrichastrum pallidisetum</i>	-76.108494	49.8783377
<i>Polytrichastrum pallidisetum</i>	-76.75454	49.1938
<i>Polytrichastrum pallidisetum</i>	-78.61169	49.48649
<i>Rhizomnium pseudopunctatum</i>	-79.30468	49.7398824
<i>Rhizomnium pseudopunctatum</i>	-79.30478	49.7399919
<i>Rhizomnium pseudopunctatum</i>	-77.512402	50.5723798
<i>Rhizomnium pseudopunctatum</i>	-76.108279	49.8784826
<i>Rhizomnium pseudopunctatum</i>	-79.304844	49.7401884
<i>Rhizomnium pseudopunctatum</i>	-79.287044	49.7460135
<i>Rhizomnium pseudopunctatum</i>	-76.108494	49.8783377
<i>Rhizomnium pseudopunctatum</i>	-79.282744	49.7456616
<i>Rhizomnium pseudopunctatum</i>	-79.305078	49.7403205
<i>Rhizomnium pseudopunctatum</i>	-79.287277	49.7461456
<i>Rhizomnium pseudopunctatum</i>	-74.638088	50.6086755
<i>Rhizomnium pseudopunctatum</i>	-76.304391	49.7432298
<i>Rhizomnium pseudopunctatum</i>	-78.5876	49.954517
<i>Rhizomnium pseudopunctatum</i>	-78.511483	49.414583
<i>Rhizomnium pseudopunctatum</i>	-76.302633	49.46265
<i>Rhizomnium pseudopunctatum</i>	-76.1617	49.540967
<i>Rhizomnium pseudopunctatum</i>	-76.334683	49.24555
<i>Rhizomnium pseudopunctatum</i>	-79.282953	49.7451398
<i>Rhizomnium pseudopunctatum</i>	-79.287476	49.7463647
<i>Rhizomnium pseudopunctatum</i>	-78.61349	49.48624
<i>Rhizomnium pseudopunctatum</i>	-78.61347	49.48646
<i>Rhizomnium pseudopunctatum</i>	-78.61173	49.48665

<i>Rhizomnium pseudopunctatum</i>	-78.67995	49.18873
<i>Rhizomnium pseudopunctatum</i>	-78.53313	49.38706
<i>Rhizomnium punctatum</i>	-79.282574	49.7482319
<i>Rhizomnium punctatum</i>	-79.249734	49.7836428
<i>Rhizomnium punctatum</i>	-79.282351	49.747359
<i>Rhizomnium punctatum</i>	-79.282267	49.7461382
<i>Rhizomnium punctatum</i>	-77.558651	50.5761817
<i>Rhizomnium punctatum</i>	-79.282337	49.7459642
<i>Rhizomnium punctatum</i>	-79.304844	49.7401884
<i>Rhizomnium punctatum</i>	-78.511483	49.414583
<i>Rhizomnium punctatum</i>	-79.321583	49.538067
<i>Rhizomnium punctatum</i>	-78.308983	49.69765
<i>Rhizomnium punctatum</i>	-78.61338	49.48572
<i>Sarmentypnum exannulatum</i>	-79.282267	49.7461382
<i>Sarmentypnum exannulatum</i>	-77.558167	50.5756246
<i>Sarmentypnum exannulatum</i>	-79.307145	49.7390901
<i>Sarmentypnum exannulatum</i>	-79.277217	49.505117
<i>Sarmentypnum exannulatum</i>	-78.511483	49.414583
<i>Sarmentypnum exannulatum</i>	-78.308983	49.69765
<i>Sarmentypnum exannulatum</i>	-79.305346	49.7403656
<i>Sarmentypnum exannulatum</i>	-76.11962	49.9519427
<i>Sarmentypnum exannulatum</i>	-79.034623	49.8123807
<i>Sarmentypnum exannulatum</i>	-78.46926	49.41026
<i>Sarmentypnum exannulatum</i>	-76.6013	49.10045
<i>Sarmentypnum exannulatum</i>	-76.28098	49.17384
<i>Sarmentypnum exannulatum</i>	-78.46668	49.41376
<i>Sarmentypnum exannulatum</i>	-78.45592	49.45592
<i>Sarmentypnum exannulatum</i>	-78.61347	49.48646
<i>Sarmentypnum exannulatum</i>	-78.61352	49.48655
<i>Sarmentypnum exannulatum</i>	-78.63873	49.18228
<i>Sarmentypnum exannulatum</i>	-78.6363	49.18156
<i>Sarmentypnum exannulatum</i>	-78.67911	49.18961
<i>Tomentypnum falcifolium</i>	-79.03338	49.7646841
<i>Tomentypnum falcifolium</i>	-79.249693	49.7841002
<i>Tomentypnum falcifolium</i>	-79.249734	49.7836428
<i>Tomentypnum falcifolium</i>	-79.282351	49.747359
<i>Tomentypnum falcifolium</i>	-79.30808	49.7421242
<i>Tomentypnum falcifolium</i>	-79.074728	49.8147542
<i>Tomentypnum falcifolium</i>	-79.040244	49.7971704

<i>Tomentypnum falcifolium</i>	-79.282267	49.7461382
<i>Tomentypnum falcifolium</i>	-77.517486	50.5735012
<i>Tomentypnum falcifolium</i>	-77.557813	50.5770588
<i>Tomentypnum falcifolium</i>	-76.301171	49.7426799
<i>Tomentypnum falcifolium</i>	-79.074685	49.8152115
<i>Tomentypnum falcifolium</i>	-79.249901	49.7814427
<i>Tomentypnum falcifolium</i>	-74.624256	50.6003918
<i>Tomentypnum falcifolium</i>	-74.638088	50.6086755
<i>Tomentypnum falcifolium</i>	-76.301702	49.7415639
<i>Tomentypnum falcifolium</i>	-79.282953	49.7451398
<i>Tomentypnum falcifolium</i>	-79.287476	49.7463647
<i>Tomentypnum falcifolium</i>	-74.650785	50.6114883
<i>Tomentypnum falcifolium</i>	-78.44444	49.39832
<i>Tomentypnum falcifolium</i>	-78.67995	49.18873
<i>Tomentypnum falcifolium</i>	-78.67911	49.18961
<i>Tomentypnum falcifolium</i>	-78.67906	49.18966
<i>Tomentypnum falcifolium</i>	-78.63079	49.17515
<i>Tomentypnum nitens</i>	-79.03338	49.7646841
<i>Tomentypnum nitens</i>	-79.282574	49.7482319
<i>Tomentypnum nitens</i>	-79.282351	49.747359
<i>Tomentypnum nitens</i>	-79.282337	49.7459642
<i>Tomentypnum nitens</i>	-79.287277	49.7461456
<i>Tomentypnum nitens</i>	-74.638088	50.6086755
<i>Tomentypnum nitens</i>	-78.6097	49.928
<i>Tomentypnum nitens</i>	-79.321583	49.538067
<i>Tomentypnum nitens</i>	-76.302633	49.46265
<i>Tomentypnum nitens</i>	-76.1617	49.540967
<i>Tomentypnum nitens</i>	-79.249474	49.7807209
<i>Tomentypnum nitens</i>	-79.287476	49.7463647
<i>Tomentypnum nitens</i>	-78.44347	49.39995
<i>Tomentypnum nitens</i>	-78.44261	49.40086
<i>Trematodon ambiguus</i>	-79.036254	49.8048529
<i>Trematodon ambiguus</i>	-74.654047	50.6126612
<i>Trematodon ambiguus</i>	-76.2812	49.1744
<i>Trematodon ambiguus</i>	-76.28381	49.17203
<i>Trematodon ambiguus</i>	-76.28389	49.17217
<i>Trematodon ambiguus</i>	-76.2836	49.17248
<i>Trematodon ambiguus</i>	-76.28363	49.17254
<i>Trematodon ambiguus</i>	-76.28185	49.17398

<i>Trematodon ambiguus</i>	-76.28429	49.17241
<i>Trematodon ambiguus</i>	-76.28233	49.17467
<i>Trematodon ambiguus</i>	-78.61189	49.48665
<i>Sphagnum cuspidatum</i>	-79.03338	49.7646841
<i>Sphagnum cuspidatum</i>	-78.6097	49.928
<i>Sphagnum cuspidatum</i>	-78.771267	49.395417
<i>Sphagnum cuspidatum</i>	-78.9936	49.500967
<i>Sphagnum cuspidatum</i>	-76.60106	49.12339
<i>Sphagnum cuspidatum</i>	-78.54171	49.37817
<i>Sphagnum pulchrum</i>	-79.074728	49.8147542
<i>Sphagnum pulchrum</i>	-77.514714	50.5721486
<i>Sphagnum pulchrum</i>	-77.557871	50.5772568
<i>Sphagnum pulchrum</i>	-76.282069	49.7431831
<i>Sphagnum pulchrum</i>	-76.119042	49.9546511
<i>Sphagnum pulchrum</i>	-78.67995	49.18873
<i>Sphagnum squarrosum</i>	-79.276028	49.7545564
<i>Sphagnum squarrosum</i>	-77.547936	50.5683146
<i>Sphagnum squarrosum</i>	-77.512149	50.5726143
<i>Sphagnum squarrosum</i>	-76.127015	49.8740661
<i>Sphagnum squarrosum</i>	-77.517486	50.5735012
<i>Sphagnum squarrosum</i>	-77.558361	50.5758474
<i>Sphagnum squarrosum</i>	-76.301722	49.742132
<i>Sphagnum squarrosum</i>	-76.119009	49.9550212
<i>Sphagnum squarrosum</i>	-79.346317	49.4696
<i>Sphagnum squarrosum</i>	-76.12017	49.9598684
<i>Sphagnum squarrosum</i>	-78.46926	49.41026
<i>Sphagnum squarrosum</i>	-78.44342	49.39977
<i>Sphagnum squarrosum</i>	-76.28381	49.17203
<i>Sphagnum squarrosum</i>	-76.28363	49.17254
<i>Sphagnum squarrosum</i>	-76.28185	49.17398
<i>Sphagnum squarrosum</i>	-78.61347	49.48646
<i>Sphagnum squarrosum</i>	-78.61169	49.48649
<i>Sphagnum squarrosum</i>	-78.55132	49.37499
<i>Sphagnum squarrosum</i>	-78.54166	49.37768
<i>Sphagnum subtile</i>	-79.276028	49.7545564
<i>Sphagnum subtile</i>	-79.03338	49.7646841
<i>Sphagnum subtile</i>	-74.654047	50.6126612
<i>Sphagnum subtile</i>	-74.853514	50.5506141
<i>Sphagnum subtile</i>	-79.249734	49.7836428

<i>Sphagnum subtile</i>	-79.249745	49.7829019
<i>Sphagnum subtile</i>	-74.855167	50.5500158
<i>Sphagnum subtile</i>	-79.074756	49.8150377
<i>Sphagnum subtile</i>	-79.032495	49.795755
<i>Sphagnum subtile</i>	-74.638045	50.6084761
<i>Sphagnum subtile</i>	-76.118885	49.9552786
<i>Sphagnum subtile</i>	-76.108494	49.8783377
<i>Sphagnum subtile</i>	-76.120297	49.9611178
<i>Sphagnum subtile</i>	-79.074685	49.8152115
<i>Sphagnum subtile</i>	-79.282744	49.7456616
<i>Sphagnum subtile</i>	-74.638088	50.6086755
<i>Sphagnum subtile</i>	-74.856909	50.5492466
<i>Sphagnum subtile</i>	-79.074883	49.8154311
<i>Sphagnum subtile</i>	-76.011517	49.622833
<i>Sphagnum subtile</i>	-79.282953	49.7451398
<i>Sphagnum subtile</i>	-79.075046	49.8157375
<i>Sphagnum subtile</i>	-79.034623	49.8123807
<i>Sphagnum tenerum</i>	-79.050741	49.8045359
<i>Sphagnum tenerum</i>	-77.512149	50.5726143
<i>Sphagnum tenerum</i>	-74.654047	50.6126612
<i>Sphagnum tenerum</i>	-74.847035	50.5521816
<i>Sphagnum tenerum</i>	-74.653244	50.6122043
<i>Sphagnum tenerum</i>	-74.63809	50.6083907
<i>Sphagnum tenerum</i>	-79.032495	49.795755
<i>Sphagnum tenerum</i>	-79.032396	49.7956452
<i>Sphagnum tenerum</i>	-79.032467	49.7954714
<i>Sphagnum tenerum</i>	-77.557702	50.5753519
<i>Sphagnum tenerum</i>	-74.650785	50.6114883
<i>Sphagnum tenerum</i>	-74.623676	50.6000774
<i>Sphagnum tenerum</i>	-74.844308	50.5499899
<i>Sphagnum tenerum</i>	-79.032537	49.7952976

APPENDIX D

Standardized predictor values used for modeling

Standardized predictor values used for modeling the distribution of the rare bryophytes species.

Predictors				
EVI2	NDWI1	PALSAR HVHH	TPI	VCF
1.39696237	0.3300764	1.414159117	0.89753846	-0.5212923
1.66387272	0.75854119	-0.701438562	1.07762694	-0.8667483
1.96414687	0.60019551	0.073221727	0.75019333	-0.3485643
1.35247731	0.33939085	-0.516998591	0.25904291	-0.8667483
1.35247731	0.33939085	-0.516998591	0.25904291	-0.8667483
1.25794656	0.24624633	-0.427195837	0.29178628	-1.9031164
1.21902213	0.32076195	1.378609361	0.09532611	-2.4213005
1.21902213	0.32076195	1.378609361	0.09532611	-2.4213005
1.5915845	0.78648455	-0.476217874	1.12674198	-0.5212923
1.6249483	0.67471113	-0.581759372	1.17585702	-0.3485643
1.6249483	0.67471113	-0.581759372	1.17585702	-0.3485643
1.19121897	0.24624633	0.10681625	1.38868887	-0.6940203
1.19121897	0.24624633	0.10681625	1.38868887	-0.6940203
1.13005201	0.33939085	-0.14519338	0.25904291	-0.4349283
2.09204142	0.89825797	0.296023874	0.48824644	-0.3485643
1.05220316	0.14378736	-0.268536203	0.48824644	-0.3485643
2.05867762	0.81442791	-0.524302623	0.22629955	-0.3485643
2.83160553	1.25220715	-1.026357692	0.47187476	-0.3485643
1.4358868	-0.1449606	-1.60704238	-1.0670632	0.08325579
-0.2100604	-0.7504	0.133793695	0.17718451	-0.6940203
0.57954941	-0.6945133	-0.107165316	1.04488358	-0.3485643
-0.9551851	-1.6911597	-0.836068798	0.50461812	-0.3485643
-0.9551851	-1.6911597	-0.836068798	0.50461812	-0.3485643
-1.033034	-1.8495054	-0.770689299	0.09532611	0.60143984
-0.4936526	-1.4396695	-1.14572124	-0.1011341	0.60143984
-0.7939268	-1.7097886	0.025057164	0.04621107	-0.4349283
-0.7939268	-1.7097886	0.025057164	0.04621107	-0.4349283

-0.5548196	-1.4117261	0.082845901	-1.1980367	-0.0031082
-0.5548196	-1.4117261	0.082845901	-1.1980367	-0.0031082
-0.9051394	-1.0950348	-1.309542327	-1.0506915	0.42871183
-0.3045911	-0.3871364	-0.325420239	-0.821488	0.51507584
0.56842814	0.22761743	-0.367174314	-0.870603	-0.0894722
-0.2267423	-0.7597145	-1.316347726	-0.5431694	-0.0894722
-1.3777932	-1.719103	0.449808372	0.55373316	0.51507584
-1.3777932	-1.719103	0.449808372	0.55373316	0.51507584
-0.6771535	0.0599573	-0.084714424	-0.002904	0.60143984
-0.1933785	-0.1822185	-0.517243682	-0.0356473	-0.0894722
-0.3490762	-0.5361676	-0.204833505	-0.1011341	-0.6076563
-0.3490762	-0.5361676	-0.204833505	-0.1011341	-0.6076563
0.9910362	0.78648455	0.470461689	-0.002904	0.42871183
0.2347902	1.15906263	-0.657132375	-0.002904	1.72417196
-0.0488021	0.37664866	-0.745751745	-0.870603	0.25598381
0.57954941	0.61882441	0.153027562	-0.5431694	-0.0894722
0.57954941	0.61882441	0.153027562	-0.5431694	-0.0894722
-0.3935613	-0.0425017	-0.496415931	-0.0356473	1.03325989
-0.6104259	0.24624633	2.075911996	0.24267123	1.63780795
0.46833676	1.34535167	-0.159950555	0.89753846	0.1696198
0.31263905	1.33603722	-0.034850284	1.1103703	0.1696198
1.25238593	1.76450201	1.366417036	0.5209898	1.37871592
1.13561265	1.475754	0.379016214	0.79930837	1.29235191
0.26259336	1.62478523	0.691802622	1.06125526	1.55144394
0.16806261	0.91688688	1.062477392	1.01214022	1.81053597
0.42941233	1.35466612	2.305795659	0.60284821	1.55144394
0.42941233	1.35466612	2.305795659	0.60284821	1.55144394
-0.065484	1.28946496	0.334546923	-1.0179482	1.37871592
0.87982356	1.67135749	1.655566325	-0.461311	1.46507993
-1.4723239	0.5443088	0.070511909	1.55240568	1.72417196
-0.9551851	0.89825797	0.908678308	1.6997508	1.55144394
-0.443607	0.34870531	0.121833914	2.42010475	1.20598791
-0.5047739	0.5443088	-0.085111642	2.09267113	1.29235191
-0.3991219	0.51636544	0.327594526	-0.2812225	1.03325989
-0.7271992	0.17173072	1.434224168	-0.1011341	2.41508403
-0.8717756	0.45116428	0.848872505	0.40638804	1.37871592
1.30799225	-0.1822185	-0.947810529	1.01214022	-2.1622084
1.77508537	0.0599573	-2.313334154	1.94532601	-1.8167524
1.58602387	0.15310182	-0.95340749	-0.2812225	-0.9531123

0.40160917	-0.4243942	-2.261917682	1.29045879	-2.2485724
0.40160917	-0.4243942	-2.261917682	1.29045879	-2.2485724
0.62403447	-0.5175387	-2.178437859	1.536034	-2.3349364
-0.443607	-0.9460035	-2.133204374	0.84842341	-2.6803925
-0.7661236	-1.2626949	-2.380132126	0.88116678	-2.8531205
1.58602387	0.15310182	-0.95340749	-0.2812225	-0.9531123
1.13561265	-0.0890739	-0.34386703	-0.0192757	-1.0394763
1.13561265	-0.0890739	-0.34386703	-0.0192757	-1.0394763
-0.4992133	0.5443088	-1.092550259	-0.3958243	-2.6803925
0.56842814	-0.3498786	0.61868657	-0.2157358	-2.3349364
1.69723652	0.38596311	-2.359646181	-0.5759128	-1.2122043
2.14208711	0.50705099	-1.96835003	-0.3958243	-1.8167524
1.46368996	-0.0611306	-1.272076125	0.34090132	-1.1258403
1.46368996	-0.0611306	-1.272076125	0.34090132	-1.1258403
1.46368996	-0.0611306	-1.272076125	0.34090132	-1.1258403
-1.2999443	-2.1941401	0.512431743	1.22497207	-0.9531123
-2.4231921	-3.2187298	-0.871148661	1.0285119	-0.6076563
-2.4787984	-2.976554	-0.135483659	3.07497197	-0.2622002
-2.4787984	-2.976554	-0.135483659	3.07497197	-0.2622002
-1.2610199	-1.2720093	-0.235121771	2.50196315	0.08325579
-0.3323943	-0.070445	-0.665086179	2.50196315	-0.0031082
1.01883937	-0.1635896	-1.458056206	2.45284811	-0.5212923
1.33023478	-0.2008474	-0.108556477	2.32187466	-0.8667483
-1.5279303	-2.501517	-0.741357184	1.15948534	-0.4349283
-1.5279303	-2.501517	-0.741357184	1.15948534	-0.4349283
-0.6271078	0.05064284	-1.754156045	1.30683047	-0.1758362
-0.5603802	0.0972151	0.639437215	0.5209898	0.42871183
-1.6669461	-2.2034545	1.700187092	-0.2484792	-0.0031082
-2.2396912	-3.0510697	0.059022356	-0.7560013	-0.5212923
-1.1442466	-1.2999527	-0.565092394	0.47187476	-0.7803843
-1.6447036	-1.4489839	-0.203220681	0.45550308	-0.1758362
-1.1275647	-0.7131422	-1.419752896	0.19355619	-0.6076563
-0.4158038	0.23693188	-1.398712908	-0.2812225	0.42871183
-2.0728722	-2.3245424	-0.891948928	0.17718451	0.86053187
-2.923649	-2.6598627	-0.645112494	0.45550308	-0.0031082
0.41829107	0.38596311	-0.041610263	-0.870603	0.60143984
0.55730688	0.81442791	-0.800283359	2.35461802	0.68780385
1.02996063	1.41986728	0.741099915	-0.9852048	1.46507993
0.35156348	-0.7597145	1.717280037	0.25904291	-1.2122043

-1.2721412	-1.6818452	-0.66290734	-0.1502491	-0.8667483
-1.3666719	-1.327896	-0.930575105	-0.6741429	-0.9531123
-0.9162607	-1.3930972	-0.604909725	0.12806947	-0.9531123
-1.6780673	-2.1475678	-0.073995419	0.06258275	-0.7803843
-1.2999443	-1.8960776	-0.036133962	0.04621107	-0.6940203
-0.8550938	-1.3930972	-0.127360866	-0.2157358	-0.8667483
-0.8550938	-1.3930972	-0.127360866	-0.2157358	-0.8667483
0.47945802	-0.7783434	-0.676983648	-0.052019	-0.6076563
-0.8328512	-1.4024117	-1.431921736	-0.002904	-1.0394763
-0.9885489	-1.7563608	-0.492475567	-0.6741429	-0.7803843
-0.9885489	-1.4955562	-1.079183441	-0.8378597	-1.2985683
-0.0988477	0.28350414	0.45265312	1.91258265	0.1696198
-0.6715929	-1.5700718	0.414102642	-1.1980367	-0.6076563
-0.6715929	-1.5700718	0.414102642	-1.1980367	-0.6076563
0.42941233	-0.4802809	-0.44973931	-1.590957	-0.5212923
1.69167589	0.61882441	-0.182374727	-1.5745853	-0.6940203
0.42941233	-0.4802809	-0.44973931	-1.590957	-0.5212923
-1.7948406	-2.5480893	0.110816666	0.78293669	-0.5212923
0.46277613	-0.9646324	-0.033368312	0.16081283	0.25598381
-2.0673116	-2.6784916	-0.363970601	0.68470661	-0.4349283
-1.2498987	-1.5048706	-1.604589979	1.04488358	0.42871183
-0.6215472	-0.6572555	-2.104669517	1.09399862	0.34234782
-1.3333081	-0.5454821	-0.226801421	2.3709897	0.34234782
-0.9496245	-0.2474196	-0.438002772	4.0572728	1.20598791
-0.0599233	-0.7876578	-0.06819984	2.61656491	-0.2622002
-0.0599233	-0.7876578	-0.06819984	2.61656491	-0.2622002
-0.9885489	-2.1941401	-0.608178333	0.45550308	-0.3485643
-0.3935613	-0.461652	0.105019565	0.09532611	0.42871183
1.07444569	0.75854119	-1.760470689	-0.6741429	-0.0031082
-0.4658495	-1.4489839	-0.04022116	-0.9852048	-0.2622002
-0.4658495	-1.4489839	-0.04022116	-0.9852048	-0.2622002
-0.1322115	-0.66657	0.226865383	-2.4913994	0.42871183
-0.1322115	-0.66657	0.226865383	-2.4913994	0.42871183
-0.9607458	0.25556079	0.479377578	-1.6073287	1.81053597
-0.6493504	-0.4895954	-0.912983758	-0.3139659	1.46507993
-2.6011323	-2.8554662	-0.760312235	-0.4449393	0.1696198
-1.4667633	-2.5946615	-0.418980318	-0.2648509	-0.1758362
0.07909249	0.14378736	-0.037971196	0.93028182	-0.1758362
1.24126466	1.23357824	-0.132416407	-1.0179482	0.34234782

0.95211178	1.14974818	-0.807532534	-0.6250278	0.77416786
0.78529281	1.31740831	0.245711315	-0.2975942	1.1196239
1.33579541	1.41055283	1.108911199	-0.2321075	1.1196239
-0.0098776	0.67471113	0.885883724	0.68470661	1.46507993
-0.0098776	0.67471113	0.885883724	0.68470661	1.46507993
-0.321273	0.14378736	1.38572041	0.9466535	0.77416786
-0.0209989	0.27418969	1.638396255	0.42275972	-0.0031082
0.47389739	0.795799	0.551671212	0.04621107	1.03325989
-0.0265595	0.3114475	1.39944184	-0.1666208	1.1196239
-0.3657581	0.0599573	0.48489349	-0.3958243	1.20598791
0.0290468	0.64676777	0.591727395	-0.4285677	1.63780795
1.0244	1.13111927	1.623309562	-1.4436119	0.51507584
1.03552126	1.12180482	1.599580389	-1.6564437	0.60143984
-0.4769707	0.45116428	-0.381843826	1.04488358	-0.6940203
0.41273044	0.84237126	-0.221667558	0.9466535	-0.5212923
0.29039652	1.14043372	1.978747741	1.35594551	1.20598791
0.45165486	0.96345914	-0.175814897	0.75019333	1.1196239
0.76305028	1.38260948	-0.728858414	0.11169779	1.20598791
0.72412585	1.63409968	0.181576535	-0.3467093	1.20598791
0.72968648	1.0100314	1.633846504	-0.1829925	0.86053187
0.56286751	-0.1356462	1.322234542	-1.6891871	-0.6076563
-0.171136	-0.275363	0.099601307	0.83205173	-0.8667483
0.69632269	0.72128339	0.931273144	0.4391314	-0.3485643
-0.0432414	-0.3126208	-1.32287031	0.25904291	-0.4349283
0.05684996	0.46979318	1.258612204	-0.1175057	-0.6076563
-0.0543627	0.82374236	-1.356647277	0.61921989	-1.9894804
1.50261439	0.86100017	0.068555996	0.20992787	-0.8667483
1.74728221	1.14043372	0.61318175	0.2754146	1.1196239
1.06888506	1.33603722	0.639444919	-0.870603	0.51507584
-0.3768794	0.01338504	2.050455014	-0.1011341	0.08325579
0.26815399	0.72128339	0.340875118	-0.6905146	-0.6076563
0.86870229	0.44184983	-0.596297583	0.71744997	-0.4349283
-0.109969	-0.4709665	1.605506389	0.61921989	-1.2122043
1.49705375	0.49773654	1.061417386	-2.3113109	-0.6076563
-2.2674944	-2.892724	-0.732521225	-2.049364	-0.4349283
-0.215621	-0.66657	0.501840002	-1.1489216	-0.6940203
-0.6048653	-1.1695504	0.657359373	-0.3467093	-0.6940203
-0.1210903	-0.3964509	-0.156918444	-0.4285677	-0.6940203
0.8353385	-0.070445	-0.055514195	-0.002904	-1.9894804

1.58602387	1.05660366	-1.617051167	-0.870603	-1.2985683
0.16250198	-0.0425017	-1.557933647	-0.772373	-1.6440244
0.0123649	0.18104517	0.780813678	-1.5745853	-0.0031082
0.5962313	-0.3126208	-0.892341848	0.19355619	-1.2122043
0.91874798	0.86100017	0.430116384	-0.1175057	-0.3485643
-3.3907421	-3.3211888	0.498101338	-0.4940544	0.42871183
0.49613992	0.88894352	-0.355796492	0.02983939	0.25598381
1.49705375	1.39192393	1.967980254	1.14311366	-0.0031082
0.91874798	0.73059784	-1.098708823	-1.0670632	-0.5212923
0.49057929	0.21830298	0.055975785	-0.6577712	-0.6076563
-0.6104259	0.81442791	0.242189587	0.14444115	1.20598791
-0.654911	0.74922674	0.736055619	0.39001636	1.20598791
0.00680427	0.36733421	0.997044357	-1.0343198	1.46507993
-0.6604716	0.11584401	0.508693242	0.4391314	0.25598381
-0.7661236	-0.5827399	-0.057232223	-0.7232579	1.03325989
-0.7661236	0.00407058	0.182273144	0.86479509	0.86053187
-0.0488021	0.89825797	2.046892718	-1.4436119	1.81053597
-0.1933785	0.62813887	1.526867411	-2.0657357	1.1196239
0.17918387	0.78648455	0.109291897	-0.870603	1.63780795
-0.4658495	0.92620133	-0.00489879	0.16081283	1.03325989
-0.7216386	0.39527757	-0.601707697	-1.9675056	1.29235191
0.14582008	0.46047873	1.23704472	-0.9360898	0.51507584
-0.321273	0.94483023	-0.029333511	-0.4285677	1.37871592
-1.0663978	0.21830298	-1.272974128	1.1103703	0.08325579
-0.2323029	-0.5734254	0.007294597	0.30815796	0.86053187
-0.1377722	0.39527757	0.316391025	-0.4285677	1.81053597
-0.6271078	0.76785565	1.794719133	-0.6250278	1.72417196
-0.5715015	0.16241627	0.58353495	-0.870603	1.03325989
-1.0441553	0.30213305	-0.940089547	1.0285119	1.55144394
0.03460743	-0.0518161	0.473439059	-1.2798951	-0.4349283
-0.3435156	-0.0983884	-0.658187557	-0.3467093	-0.6940203
-0.5158952	0.44184983	-1.636271655	-0.1502491	-1.9031164
-0.9607458	0.02269949	-0.038346737	-0.2321075	1.20598791
-0.488092	0.94483023	-0.076700156	0.55373316	1.89689997
-0.6104259	0.13447291	1.620549022	-1.23078	1.72417196
-0.004317	0.87031462	1.896670898	0.17718451	1.20598791
-0.7438811	0.29281859	-0.260200723	0.68470661	1.46507993
-0.6604716	0.46979318	1.21996702	-0.5267978	1.29235191
-0.6048653	0.36733421	0.013922586	-0.3303376	0.86053187

-4.7252939	-1.8960776	0.037977028	0.9466535	0.51507584
-0.6771535	-0.0890739	-0.271371055	-0.412196	1.63780795
-0.9941096	-0.1170173	0.768365314	-0.0847624	0.68780385
-1.138686	-0.0983884	-0.402192019	0.63559157	0.42871183
-1.2554593	-0.2194763	-0.465219412	0.02983939	-0.2622002
-0.593744	0.3114475	-0.798832174	-0.002904	-1.0394763
1.20234024	0.65608222	2.276221256	-0.9033464	-0.0894722
-0.9774277	-0.0983884	0.286805971	0.73382165	0.77416786
-0.6827141	-0.275363	-1.321083578	-0.6905146	-0.7803843
0.57954941	1.58752742	-1.568385167	-0.3630809	-1.8167524
-0.5826228	0.26487524	1.565642346	0.29178628	0.77416786
-0.3268337	0.55362325	-0.975590323	0.04621107	0.60143984
0.78529281	0.60950996	-0.852317496	-1.7546738	-0.3485643
-0.4158038	-0.4709665	0.207166207	0.79930837	-0.6940203
0.26259336	0.68402558	-0.532110626	0.50461812	0.86053187
-0.4158038	-0.6386266	-0.96569744	0.48824644	-0.2622002
0.35156348	0.85168571	-0.89167393	0.11169779	0.1696198
-0.3546368	0.44184983	-1.507287207	0.12806947	-1.9031164
1.07444569	0.97277359	-0.466353778	0.19355619	0.08325579
1.0244	0.73059784	1.650204569	1.04488358	0.86053187
1.16341581	1.19632044	0.365810777	-0.412196	0.34234782
1.55822071	1.2801505	0.588407568	-0.002904	0.60143984
-0.0321202	0.41390647	-0.068960225	-0.5922845	0.86053187
-0.7383205	-0.564111	3.230880674	0.32452964	0.34234782
0.11245629	0.14378736	-0.821990547	0.71744997	-0.0894722
1.08556696	0.42322092	0.636869044	-1.9347623	-0.8667483
-1.6280217	-1.8588198	0.789037552	-2.0821074	-0.5212923
-0.2934699	-0.5268532	-0.976137284	-1.3781251	0.25598381
-0.0932871	-0.3964509	-0.186257335	-0.9852048	0.34234782
0.35712411	0.46979318	-1.218877477	-0.4285677	-0.3485643
0.89650545	0.25556079	0.077420427	-0.3139659	-0.8667483
1.05220316	1.0286603	0.234852548	-0.4449393	-0.9531123
0.05684996	0.08790065	0.322206491	-0.5595411	-0.6076563
0.11245629	0.33939085	-0.818816214	-1.5745853	0.51507584
0.5962313	-0.3126208	-0.892341848	0.19355619	-1.2122043
-0.3713187	0.26487524	-0.117152063	0.24267123	0.77416786
-1.1053222	-0.4337087	-0.734938638	-0.5922845	0.94689588
0.70744395	0.74922674	1.503155493	0.04621107	0.77416786
1.78620664	1.61547077	2.3549051	1.07762694	0.1696198

-0.0154383	0.51636544	-0.524942405	-1.0343198	0.51507584
1.78620664	1.42918174	2.089354485	-0.821488	-0.2622002
-1.0385946	0.40459202	0.334486899	-0.1829925	0.25598381
0.36824538	0.38596311	-1.099109486	-1.3290101	-0.1758362
-0.3546368	-0.5082243	-1.352460971	1.06125526	-0.7803843
-0.4491676	0.89825797	-0.659459302	0.73382165	0.1696198
-0.4825314	-0.461652	-0.30534066	0.47187476	-0.2622002
-0.3935613	0.38596311	0.54704893	-0.002904	-0.0031082
-0.3435156	-0.1077028	-0.325932345	0.12806947	-0.8667483
-0.2601061	0.80511345	-0.203090738	-0.5759128	1.37871592
0.99659684	0.78648455	0.522567019	1.38868887	0.60143984
1.16341581	1.19632044	0.365810777	-0.412196	0.34234782
0.29595716	1.27083605	0.336984576	-0.2484792	1.89689997
-0.654911	0.50705099	-1.323002655	-0.3467093	0.77416786
-2.0506297	-2.11031	0.219329994	0.50461812	1.03325989
-0.3713187	0.27418969	0.349254678	0.55373316	1.03325989
-0.0710446	0.55362325	0.608448492	-1.951134	0.68780385
-0.9551851	-1.4117261	-0.172997214	-2.0657357	-0.7803843
0.36824538	0.39527757	1.921698134	-1.2635234	0.77416786
-0.8384119	-0.4243942	0.4364677	-1.4436119	1.20598791
0.27371463	0.39527757	-0.169761403	-0.412196	-0.0894722
0.8353385	0.37664866	-0.538511324	-0.3467093	-0.6076563
0.08465312	0.75854119	1.454894692	-0.3139659	0.1696198
-0.1433328	0.23693188	2.095714998	-0.5922845	0.42871183
-0.2378636	-0.2008474	-0.372941901	-1.5418419	0.68780385
0.74636838	0.01338504	1.96425496	-0.0192757	-1.2122043
-0.4992133	0.50705099	0.895930983	0.24267123	1.20598791
-0.760563	-0.0890739	-0.631890701	-0.2321075	1.03325989
0.41273044	1.11249037	0.746000171	-0.052019	1.03325989
-0.4992133	0.35801976	0.028249143	1.7816092	1.81053597
-0.1488934	0.19967408	-0.12204452	-0.821488	0.77416786
-0.1322115	0.81442791	-0.072777047	-0.6086562	1.1196239
-0.9162607	0.45116428	2.300348537	-0.1829925	1.37871592
0.19030514	0.23693188	-1.195912028	-1.1161783	0.51507584
-0.3546368	-0.5082243	-1.352460971	1.06125526	-0.7803843
-0.549259	0.28350414	-1.26589265	0.79930837	0.08325579
-0.3435156	0.03201394	0.601387781	0.4391314	0.08325579
-0.488092	0.19035962	0.934364197	0.14444115	0.08325579
-0.3435156	-0.1077028	-0.325932345	0.12806947	-0.8667483

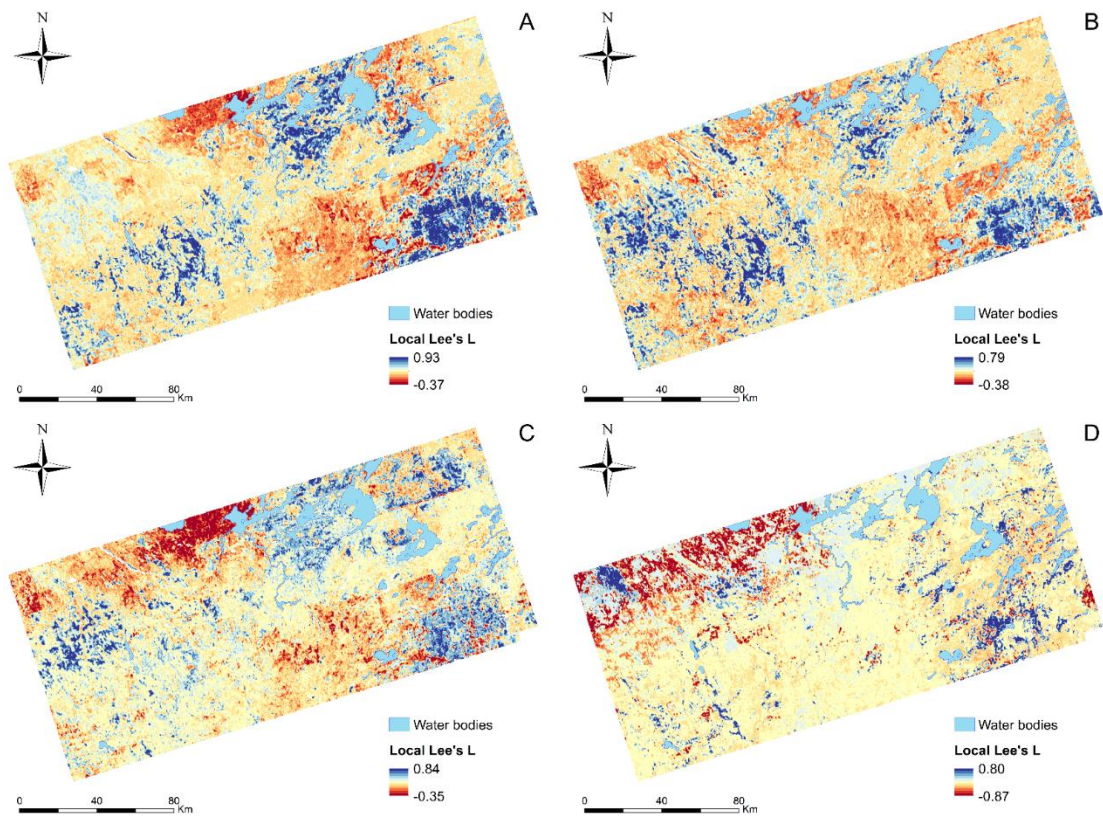
0.85758103	1.08454701	2.57355901	0.02983939	1.63780795
0.99659684	0.78648455	0.522567019	1.38868887	0.60143984
1.25794656	1.07523256	-0.087144096	0.07895443	0.1696198
0.29595716	1.27083605	0.336984576	-0.2484792	1.89689997
0.04016806	0.61882441	2.509788373	-0.1502491	0.42871183
-2.7623907	-2.6598627	-0.47487176	0.89753846	1.37871592
-0.5603802	0.32076195	-1.942576	1.45417559	1.03325989
-0.4658495	0.61882441	-0.148444819	-1.4599835	1.29235191
-0.9551851	-1.4117261	-0.172997214	-2.0657357	-0.7803843
-0.7939268	-0.6386266	0.577890483	-1.2635234	-0.8667483
-0.9329426	-0.8808024	-0.952471801	-1.1489216	-0.9531123
0.80753534	0.28350414	-1.362227682	-0.5922845	0.1696198
0.8353385	0.28350414	-0.547531097	-0.3630809	-0.2622002
-0.0877265	0.48842209	-0.115806523	-0.1666208	0.51507584
0.38492727	0.42322092	-0.349427539	-0.6577712	0.60143984
0.03460743	0.48842209	-0.073345934	-1.3126384	-0.0894722
0.74636838	0.01338504	1.96425496	-0.0192757	-1.2122043
-0.6271078	0.41390647	0.425768103	-0.2812225	0.68780385
-0.9774277	-0.1077028	0.130893604	0.47187476	0.94689588
0.85758103	1.41986728	0.279747949	0.01346771	0.60143984
0.17362324	1.27083605	-0.266972446	1.45417559	1.55144394
-0.065484	0.41390647	-0.489760304	-0.8051163	0.94689588
0.09577439	0.58156661	0.800217501	-1.0179482	0.86053187
0.01792554	0.40459202	0.104235839	-0.5431694	1.1196239
0.36824538	0.49773654	-0.780921395	-1.0343198	0.25598381
-0.7105173	-0.7783434	-0.136961583	0.83205173	-0.4349283
-0.549259	0.28350414	-1.26589265	0.79930837	0.08325579
0.34044221	0.36733421	0.509518474	0.09532611	-0.3485643
-0.5659409	0.0972151	0.058860822	0.24267123	-0.0894722
-0.0543627	0.0599573	-1.45240436	0.12806947	-0.3485643
0.34600285	0.95414468	0.807170443	0.61921989	0.42871183
0.19586577	0.65608222	-0.259563306	1.48691895	0.60143984
1.35803794	1.43849619	0.402824513	-0.7232579	0.51507584
0.59067067	0.73991229	-0.337635216	-0.0192757	-0.3485643
0.06241059	0.3114475	-0.489842626	-0.2812225	-0.6076563
-2.000584	-1.8122476	-0.518905716	0.63559157	1.37871592
0.86314166	0.61882441	-0.334707103	2.22364458	0.86053187
-0.3935613	-0.564111	-0.371058405	-1.0343198	0.08325579
-0.4380463	-1.2068082	-1.23030224	-2.2785676	-1.3849324

-1.1609285	-0.6293122	0.165412246	-1.7710455	0.86053187
0.84645976	-0.1635896	0.680031344	-1.5090986	0.42871183
0.11801692	-0.5454821	0.008614049	-0.2812225	-1.6440244
0.51282182	-0.1635896	0.933767625	-0.3794526	-0.9531123
-0.3713187	-0.7038278	-0.022613659	-0.2648509	-0.5212923
1.34691668	1.0100314	-0.429131432	-0.412196	-0.2622002
0.30707842	0.3300764	1.926519494	-1.2962667	0.1696198
0.0457287	-0.275363	1.972063452	-0.002904	-1.5576604
-0.5548196	-0.1077028	0.253251748	-0.3794526	0.1696198
-0.1155296	0.42322092	1.380804009	0.16081283	0.68780385
1.48037186	1.19632044	2.672163127	0.12806947	0.51507584
0.68520142	1.19632044	1.067282253	1.19222871	1.55144394
-0.3768794	0.05064284	1.146139076	-0.9688331	-0.1758362
1.0077181	1.17769153	1.615683745	-1.1980367	0.25598381
-0.7049567	0.67471113	0.655431778	-0.002904	1.20598791
0.53506435	0.53499435	-1.229258044	-1.0506915	-0.0031082
-0.7550024	-0.5734254	-0.823269	0.81568005	-1.0394763
0.78529281	0.18104517	-0.282056871	0.17718451	-0.9531123
-0.0710446	0.28350414	0.341834876	0.34090132	-0.3485643
1.20790087	1.60615632	-0.007792613	0.81568005	-0.0894722
1.39140174	0.50705099	-0.182111692	-0.461311	-0.0894722
-0.8161693	-0.9646324	0.26418565	1.40506055	-2.1622084
-0.0209989	-0.5454821	-1.087351673	-0.9524614	-0.6076563
-0.8439725	-0.7876578	1.698420189	-1.4436119	-0.0894722
0.21254767	-0.6106832	0.221222466	-1.181665	-1.1258403
-0.4324857	-0.9460035	-0.233619109	-0.002904	-1.2122043
1.36359858	0.99140249	-0.553165659	-0.3958243	-0.4349283
1.0244	0.69334003	-1.123024032	-0.002904	-1.1258403
-0.2823486	0.10652956	0.171151974	-0.1829925	-0.0894722
0.72412585	0.95414468	0.445787859	0.9466535	0.34234782
0.77417154	0.32076195	0.558906941	-0.9197181	-0.4349283
0.89094482	0.42322092	0.646546619	-1.3617535	-0.1758362
-0.1377722	0.62813887	-0.387447238	0.70107829	-1.6440244
-1.7614768	-1.8867632	0.094387553	-0.9033464	-0.5212923
0.75748964	0.0785862	-0.359002234	-0.461311	-0.3485643
0.31263905	0.0599573	-0.895386917	0.37364468	-1.7303884
0.96323304	0.47910763	-0.581103541	0.61921989	-0.7803843
0.4071698	-0.5082243	-1.078260833	0.17718451	-1.3849324
-0.1377722	0.5443088	0.000547748	0.17718451	0.34234782

1.96970751	0.17173072	0.514870545	-1.0834349	-0.9531123
-0.654911	-0.7690289	-1.997197859	1.27408711	-2.4213005
-0.2823486	-0.4243942	-0.692161334	-1.4436119	-0.0031082
1.10780948	0.83305681	0.316853128	0.34090132	-1.8167524
-0.2434242	0.00407058	-0.265089132	-0.1175057	-1.4712964
1.0244	1.00071694	-1.179514458	-0.6413995	-0.6076563
1.10224885	-0.1170173	1.033181882	2.04355609	-1.6440244
0.86870229	0.04132839	-1.541671504	-0.1175057	-1.3849324
1.58046324	1.08454701	0.97051223	-0.7887446	-0.2622002
0.75192901	0.38596311	1.681517346	-1.2798951	-0.6940203
0.57398877	-0.1915329	0.489614718	1.48691895	-1.4712964

APPENDIX E

Re-scaled Lee's L bivariate spatial association between rare and overall bryophyte, moss, liverwort, and sphagna species richness



Re-scaled Lee's L bivariate spatial association between rare and overall (A) bryophyte, (B) moss, (C) liverwort, and (D) sphagna species richness for the study area of Cerrejón *et al.* (2020) at 300 m spatial resolution.

APPENDIX F

Lichen species identified and used for modeling

Lichen species identified in the present study and used for modeling (n = 116).

Lichen species	
<i>Arctoparmelia centrifuga</i>	<i>Evernia mesomorpha</i>
<i>Bryoria americana</i>	<i>Heterodermia galactophylla</i>
<i>Bryoria furcellata</i>	<i>Hypogymnia bitteri</i>
<i>Bryoria fuscescens</i>	<i>Hypogymnia incurvoides</i>
<i>Bryoria nadvornikiana</i>	<i>Hypogymnia physodes</i>
<i>Bryoria pikei</i>	<i>Hypogymnia pulverata</i>
<i>Bryoria simplicior</i>	<i>Hypogymnia vittata</i>
<i>Bryoria trichodes</i>	<i>Icmadophila ericetorum</i>
<i>Calicium glaucellum</i>	<i>Imshaugia aleurites</i>
<i>Calicium parvum</i>	<i>Imshaugia placorodia</i>
<i>Calicium trabinellum</i>	<i>Melanelia hepatizon</i>
<i>Cetraria ericetorum</i>	<i>Melanelia sorediata</i>
<i>Cetraria islandica</i>	<i>Melanelia stygia</i>
<i>Chaenotheca balsamconensis</i>	<i>Melanohalea olivacea</i>
<i>Chaenotheca chrysocephala</i>	<i>Melanohalea septentrionalis</i>
<i>Chaenothecopsis nana</i>	<i>Montanelia panniformis</i>
<i>Cladonia amaurocraea</i>	<i>Nephroma arcticum</i>
<i>Cladonia arbuscula</i>	<i>Nephroma bellum</i>
<i>Cladonia bacilliformis</i>	<i>Parmelia sulcata</i>
<i>Cladonia bellidiflora</i>	<i>Parmeliopsis ambigua</i>
<i>Cladonia borealis</i>	<i>Parmeliopsis capitata</i>
<i>Cladonia botrytes</i>	<i>Parmeliopsis hyperopta</i>
<i>Cladonia carneola</i>	<i>Peltigera aphthosa</i>
<i>Cladonia cenotea</i>	<i>Peltigera didactyla</i>
<i>Cladonia chlorophaea</i>	<i>Peltigera elisabethae</i>
<i>Cladonia coccifera</i>	<i>Peltigera extenuata</i>
<i>Cladonia coniocraea</i>	<i>Peltigera neopolydactyla</i>
<i>Cladonia cornuta</i>	<i>Peltigera polydactylon</i>
<i>Cladonia crispata</i>	<i>Peltigera scabrosa</i>
<i>Cladonia cristatella</i>	<i>Phaeocalicium compressulum</i>

<i>Cladonia_cyanipes</i>	<i>Phaeophyscia_orbicularis</i>
<i>Cladonia_deformis</i>	<i>Physcia_adscendens</i>
<i>Cladonia_digitata</i>	<i>Physcia_aipolia</i>
<i>Cladonia_fimbriata</i>	<i>Physciella_chloantha</i>
<i>Cladonia_glauca</i>	<i>Platismatia_glauca</i>
<i>Cladonia_gracilis</i>	<i>Ramalina_roesleri</i>
<i>Cladonia_grayi</i>	<i>Stenocybe_major</i>
<i>Cladonia_macilenta</i>	<i>Stereocaulon_alpinum</i>
<i>Cladonia_macrophylla</i>	<i>Stereocaulon_dactylophyllum</i>
<i>Cladonia_merochlorophaea</i>	<i>Stereocaulon_grande</i>
<i>Cladonia_multiformis</i>	<i>Stereocaulon_paschale</i>
<i>Cladonia_norvegica</i>	<i>Stereocaulon_tomentosum</i>
<i>Cladonia_phyllophora</i>	<i>Tuckermannopsis_americana</i>
<i>Cladonia_pleurota</i>	<i>Tuckermannopsis_orbata</i>
<i>Cladonia_pyxidata</i>	<i>Tuckermannopsis_sepincola</i>
<i>Cladonia_rangiferina</i>	<i>Umbilicaria_deusta</i>
<i>Cladonia_rei</i>	<i>Umbilicaria_hyperborea</i>
<i>Cladonia_squamosa</i>	<i>Umbilicaria_muehlenbergii</i>
<i>Cladonia_stellaris</i>	<i>Umbilicaria_polyphylla</i>
<i>Cladonia_stricta</i>	<i>Umbilicaria_torrefacta</i>
<i>Cladonia_stygia</i>	<i>Usnea_dasopoga</i>
<i>Cladonia_subulata</i>	<i>Usnea_hirta</i>
<i>Cladonia_sulphurina</i>	<i>Usnea_perplexans</i>
<i>Cladonia_symphycarpa</i>	<i>Usnea_scabrata</i>
<i>Cladonia_uncialis</i>	<i>Usnea_subfloridana</i>
<i>Cladonia_verticillata</i>	<i>Usnea_substerilis</i>
<i>Crustose</i>	<i>Vulpicida_pinastri</i>
<i>Cyphobasidium_hypogymniicola</i>	<i>Xanthomendoza_hasseana</i>

APPENDIX G

Pearson correlation coefficients among variable pairs at both targeted spatial resolutions

Pearson correlation coefficients among variable pairs at both targeted spatial resolutions (WorldView-3 at 1.2m resolution; Sentinel-2 at 10m resolution). Values in bold indicate variables pairs highly correlated ($|\text{Pearson } r| > 0.7$).

WorldView-3	Green	Red	NIR	EVI2	Sentinel-2	Green	Red	NIR	EVI2
Green		0.94	0.19	-0.74	Green		0.92	0.07	-0.28
Red	0.94		0.01	-0.86	Red	0.92		-0.04	-0.41
NIR	0.19	0.01		0.45	NIR	0.07	-0.04		0.92
EVI2	-0.74	-0.86	0.45		EVI2	-0.28	-0.41	0.92	

APPENDIX H

List of microhabitats included

List of different microhabitats included in this study (n = 14).

Microhabitats

Shrub base

Tree base

Rock

Bare soil

Moss

Peat hummock

Root

Dead branch

Snag

Burned snag

Unburned log of decay class 1 and 2

Unburned log of decay class 3, 4 and 5

Burned log of decay class 1 and 2

Burned log of decay class 3, 4 and 5

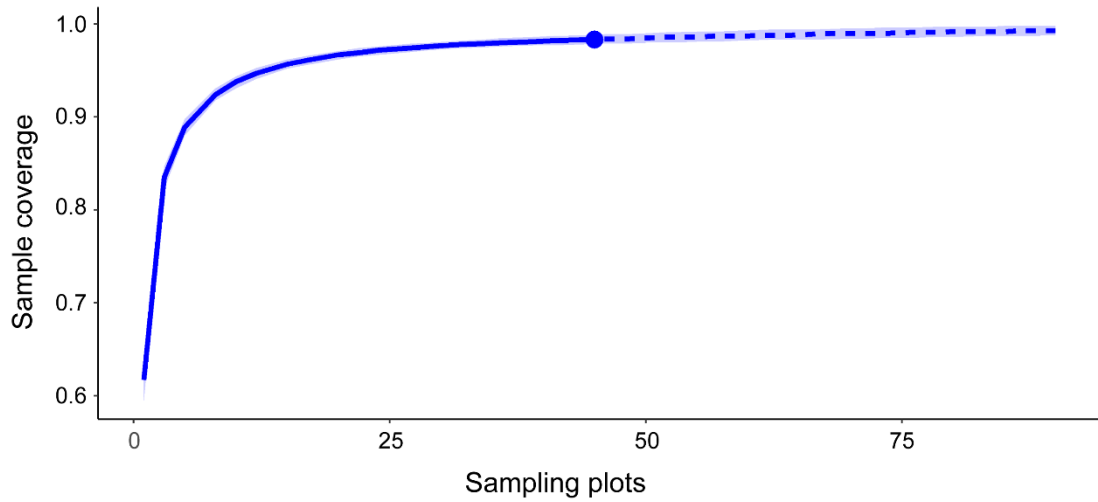
APPENDIX I

Mantel test results between lichen species composition (Sørensen's dissimilarity) and microhabitat-based dissimilarity

Mantel test results based on Pearson's correlation between lichen species composition (Sørensen's dissimilarity) and microhabitat-based dissimilarity.

R²	Sig	90%	95%	97.50%	99%
0.2171	0.001	0.066	0.083	0.0974	0.1145

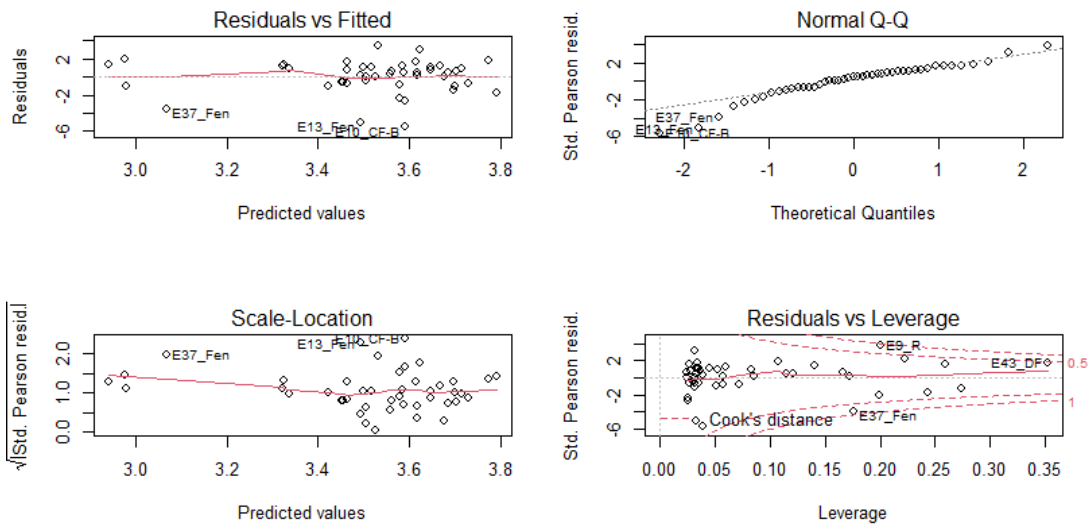
APPENDIX J
Species rarefaction curve



Rarefaction curve showing the sample coverage (percentage of species) as a function of the number of plots sampled ($n = 45$; outliers included).

APPENDIX K

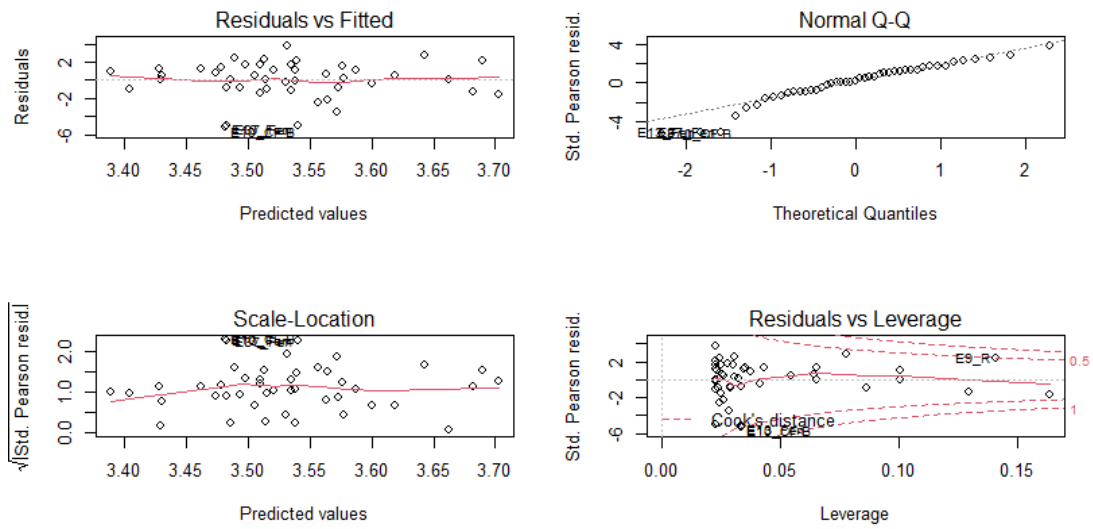
Diagnostic graphs of the WV3 band model including outliers



Diagnostic graphs of the WV3 band model (45 plots including outliers).

APPENDIX L

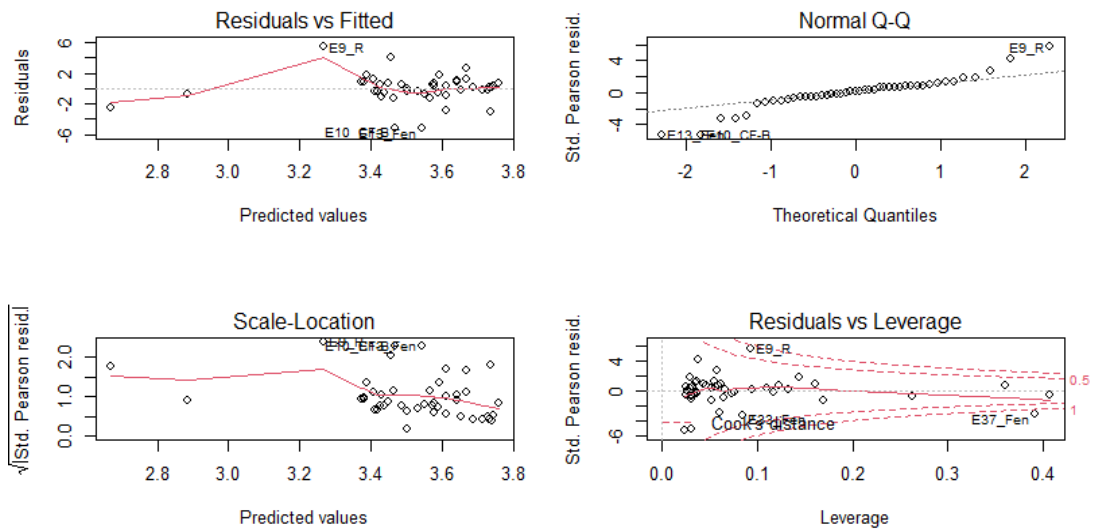
Diagnostic graphs of the WV3 EVI2 model including outliers



Diagnostic graphs of the WV3 EVI2 model (45 plots including outliers).

APPENDIX M

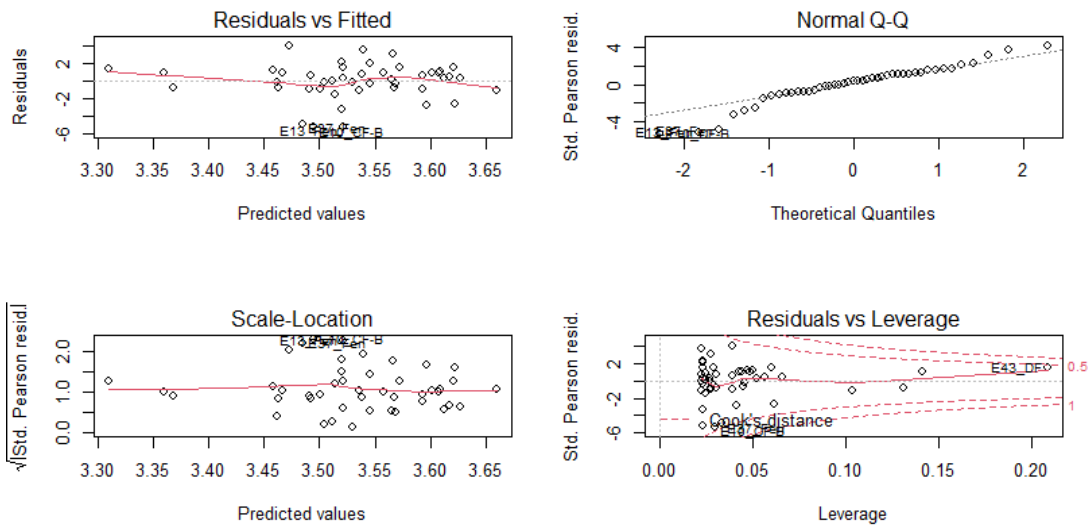
Diagnostic graphs of the S2 band model including outliers



Diagnostic graphs of the S2 band model (45 plots including outliers)

APPENDIX N

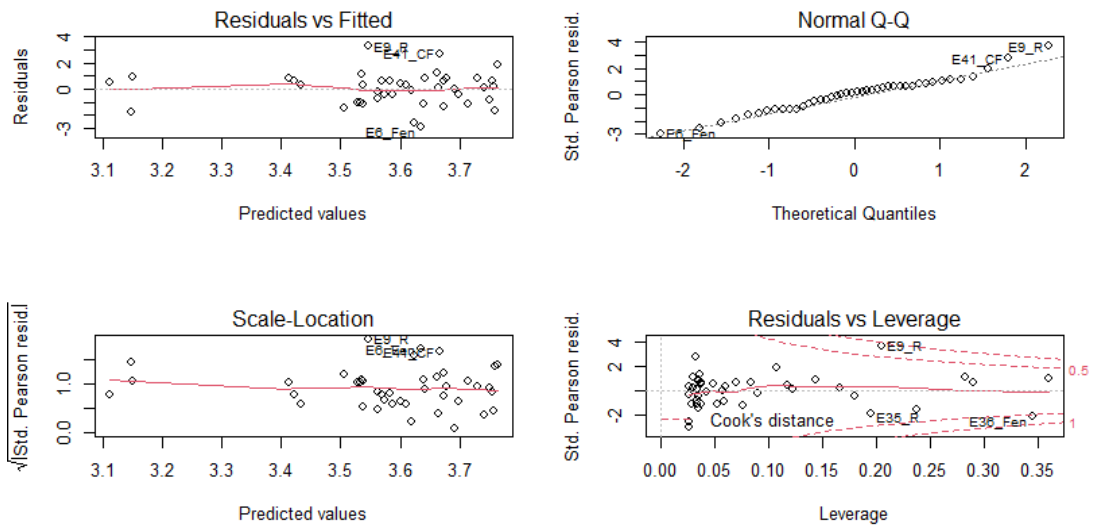
Diagnostic graphs of the S2 EVI2 model including outliers



Diagnostic graphs of the S2 EVI2 model (45 plots including outliers)

APPENDIX O

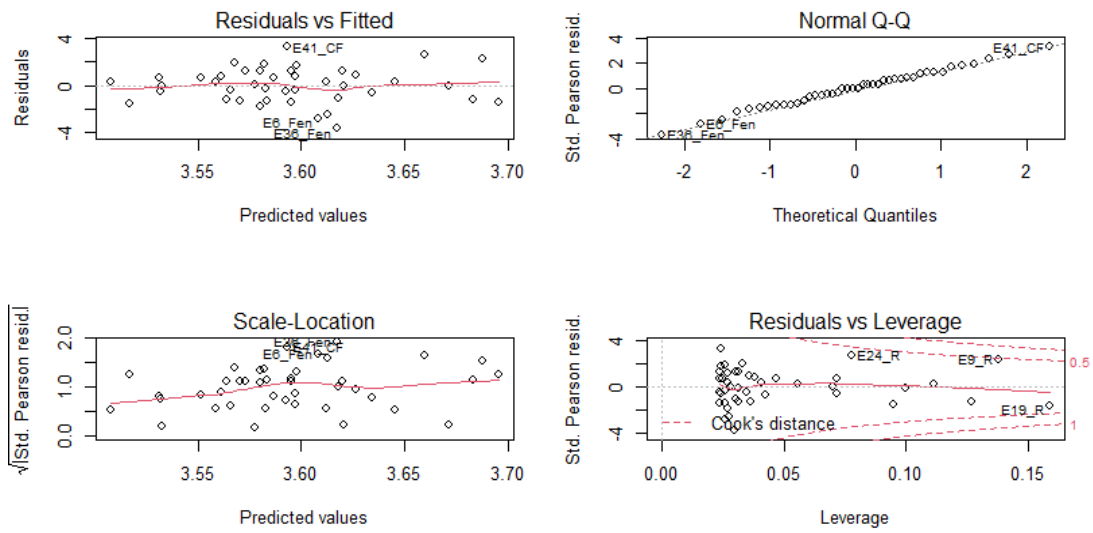
Diagnostic graphs of the WV3 band model excluding outliers



Diagnostic graphs of the WV3 band model (42 plots excluding outliers).

APPENDIX P

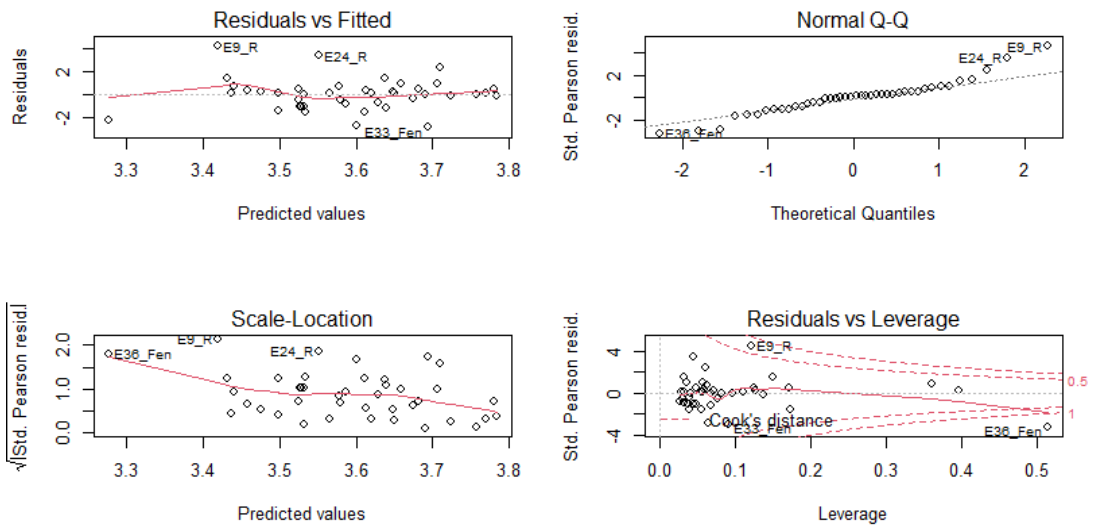
Diagnostic graphs of the WV3 EVI2 model excluding outliers



Diagnostic graphs of the WV3 EVI2 model (42 plots excluding outliers).

APPENDIX Q

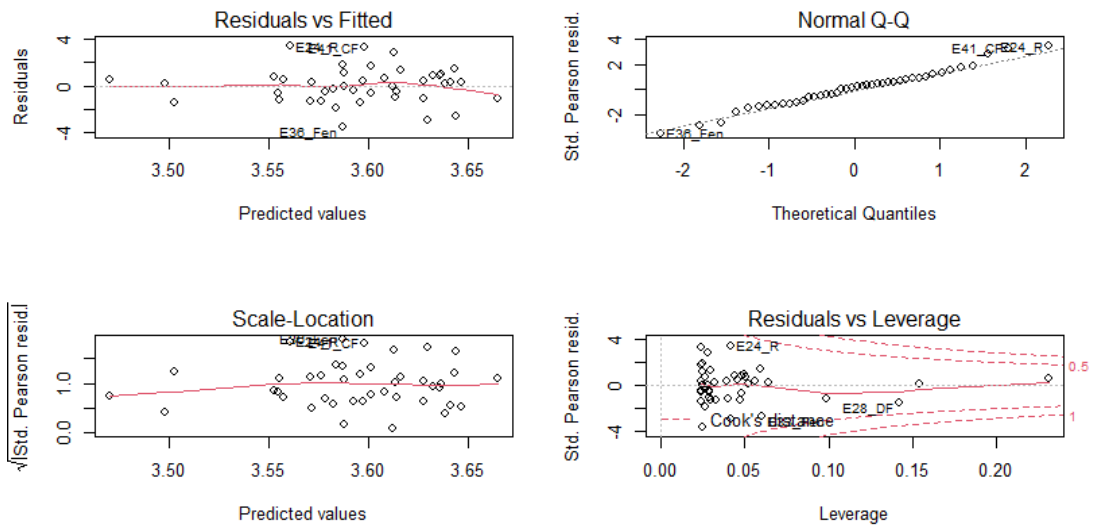
Diagnostic graphs of the S2 band model excluding outliers



Diagnostic graphs of the S2 band model (42 plots excluding outliers)

APPENDIX R

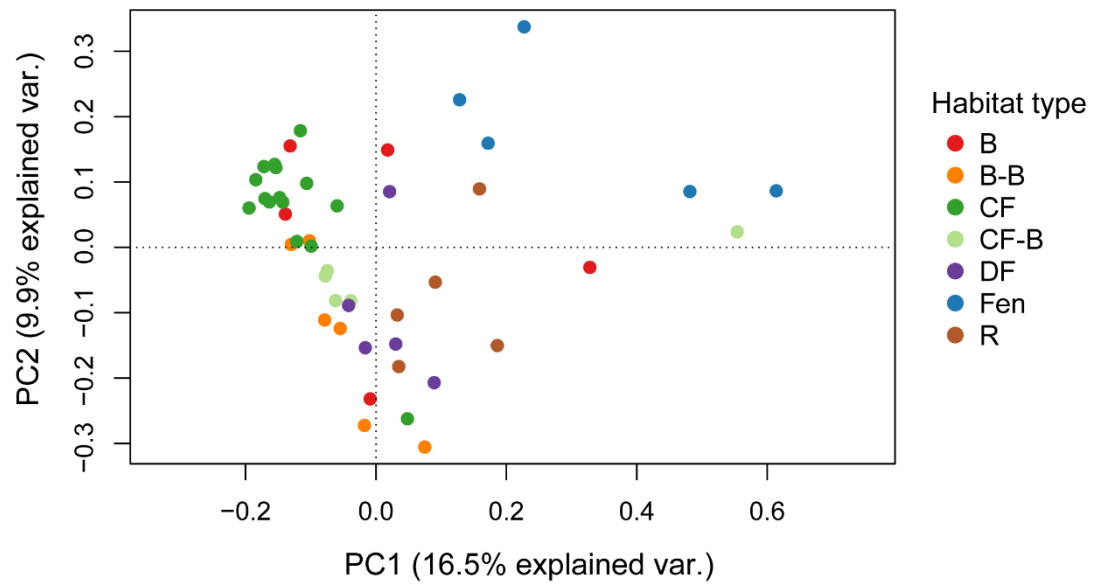
Diagnostic graphs of the S2 EVI2 model excluding outliers



Diagnostic graphs of the S2 EVI2 model (42 plots excluding outliers)

APPENDIX S

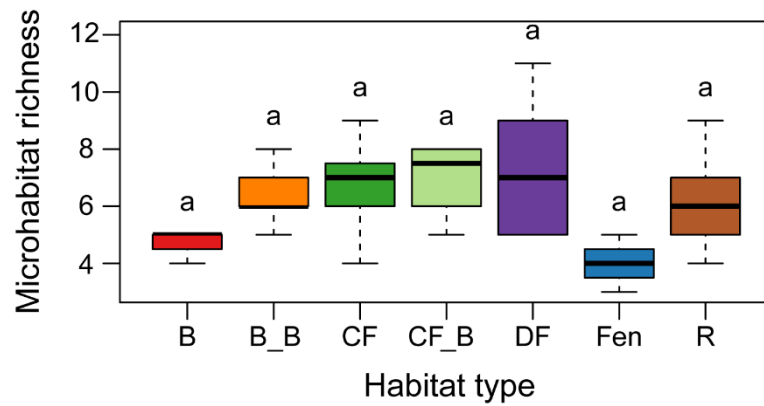
PCoA on lichen community composition (including outliers)



PCoA on lichen community composition (45 plots including outliers). Habitat type abbrev.: B, bog; B_B, bog burned; CF, coniferous forest; CF_B, coniferous forest burned; DF, deciduous forest; Fen, Fen; R, Rock.

APPENDIX T

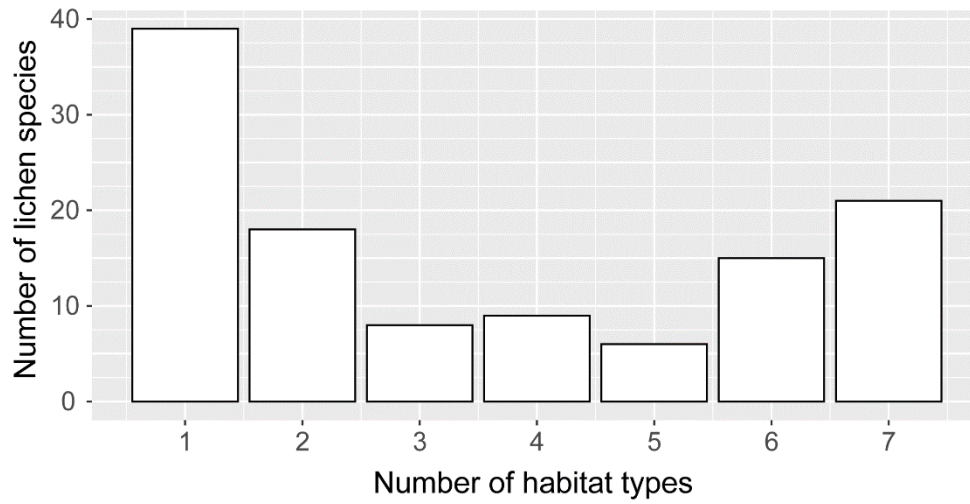
Boxplots of microhabitat richness per habitat type



Boxplots of microhabitat richness per habitat type. Different letters indicate significant differences in microhabitat richness among habitat types based on the Tukey test. Outliers were not included. Habitat type abbrev.: B, bog; B_B, bog burned; CF, coniferous forest; CF_B, coniferous forest burned; DF, deciduous forest; Fen, Fen; R, Rock.

APPENDIX U

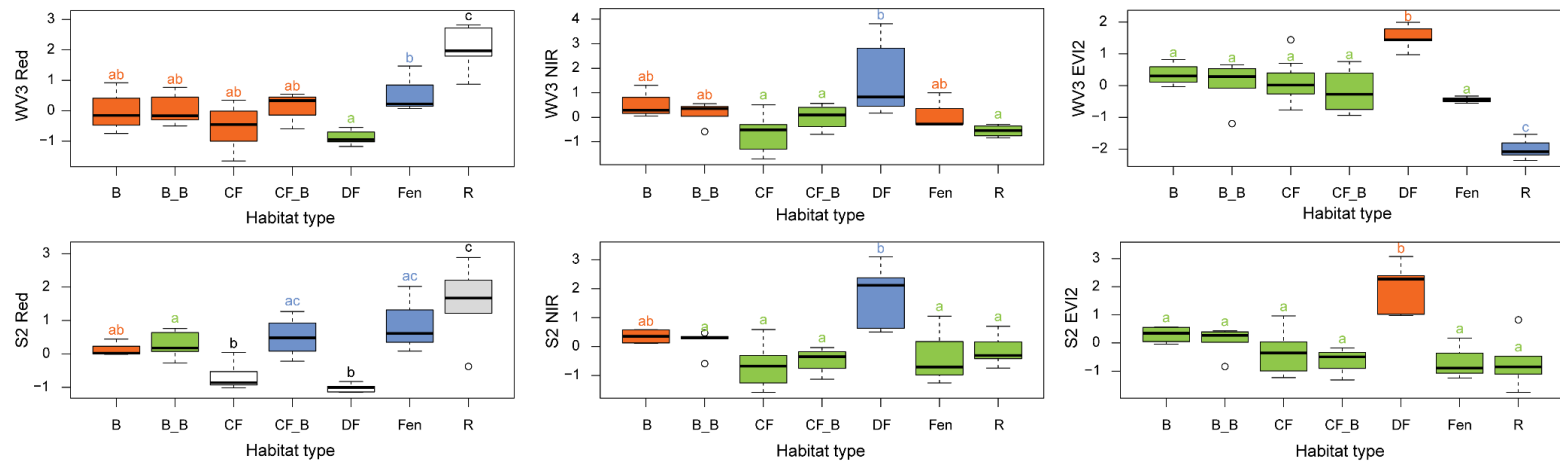
Number of lichen species versus the number of habitat types in which they occur



Number of lichen species versus the number of different habitat types in which they occur.

APPENDIX V

Boxplots of variables included in the models at both targeted spatial resolutions per habitat type



Boxplots of variables included in the models at both targeted spatial resolutions (WW3, WorldView-3 at 1.2m resolution; S2, Sentinel-2 at 10m resolution) per habitat type. Different letters and boxplot colors indicate significant differences in variable values among habitat types based on the Tukey test. Boxplot colors were not associated here to different habitat types to facilitate the visualization of these significant differences. See section 4.4.3 for variable description. Habitat type abbrev.: B, bog; B_B, bog burned; CF, coniferous forest; CF_B, coniferous forest burned; DF, deciduous forest; Fen, Fen; R, Rock.

REFERENCES

- Adamo, P., & Violante, P. (2000). Weathering of rocks and neogenesis of minerals associated with lichen activity. *Applied Clay Science*, 16(5-6), 229-256.
- Ahmadjian, V. (1995). Lichens are more important than you think. *BioScience*, 45(3), 124.
- Ah-Peng, C., Chuah-Petiot, M., Descamps-Julien, B., Bardat, J., Stamenoff, P., & Strasberg, D. (2007). Bryophyte diversity and distribution along an altitudinal gradient on a lava flow in La Réunion. *Diversity and distributions*, 13(5), 654-662.
- Allen, J. L., McMullin, R. T., Tripp, E. A., & Lendemer, J. C. (2019). Lichen conservation in North America: a review of current practices and research in Canada and the United States. *Biodiversity and Conservation*, 28(12), 3103-3138.
- Allouche, O., Tsoar, A., & Kadmon, R. (2006). Assessing the accuracy of species distribution models: prevalence, kappa and the true skill statistic (TSS). *Journal of applied ecology*, 43(6), 1223-1232.
- Amani, M., Salehi, B., Mahdavi, S., & Brisco, B. (2018). Spectral analysis of wetlands using multi-source optical satellite imagery. *ISPRS Journal of Photogrammetry and Remote Sensing*, 144, 119-136.
- Amirikhiz, R. G., Dixon, M. D., Palmer, J. S., & Swanson, D. L. (2021). Investigating niches and distribution of a rare species in a hierarchical framework: Virginia's Warbler (*Leiothlypis virginiae*) at its northeastern range limit. *Landscape Ecology*, 36(4), 1039-1054.
- Andrew, C., Heegaard, E., Kirk, P. M., Bässler, C., Heilmann-Clausen, J., Krisai-Greilhuber, I., ... & Kausarud, H. (2017). Big data integration: Pan-European fungal species observations' assembly for addressing contemporary questions in ecology and global change biology. *Fungal Biology Reviews*, 31(2), 88-98.
- Androsova, V. I., Tarasova, V. N., & Gorshkov, V. V. (2018). Diversity of lichens and allied fungi on Norway spruce (*Picea abies*) in the middle boreal forests of Republic of Karelia (Russia). *Folia Cryptogamica Estonica*, 55, 133-149.

- Aptroot, A. (2009). Lichens as an indicator of climate and global change. In *Climate Change*. Elsevier, Amsterdam, Netherlands. pp. 401-408.
- Aragón, G., Martínez, I., & García, A. (2012). Loss of epiphytic diversity along a latitudinal gradient in southern Europe. *Science of the Total Environment*, 426, 188-195.
- Aranda, S. C., & Lobo, J. M. (2011). How well does presence-only-based species distribution modelling predict assemblage diversity? A case study of the Tenerife flora. *Ecography*, 34(1), 31-38.
- Aranda, S. C., Gabriel, R., Borges, P. A., Santos, A. M., de Azevedo, E. B., Patiño, J., ... & Lobo, J. M. (2014). Geographical, temporal and environmental determinants of bryophyte species richness in the Macaronesian Islands. *PLoS One*, 9(7), e101786.
- Arenas-Castro, S., Gonçalves, J., Alves, P., Alcaraz-Segura, D., & Honrado, J. P. (2018). Assessing the multi-scale predictive ability of ecosystem functional attributes for species distribution modelling. *PLoS One*, 13(6), e0199292.
- Arenas-Castro, S., Regos, A., Martins, I., Honrado, J., & Alonso, J. (2022). Effects of input data sources on species distribution model predictions across species with different distributional ranges. *Journal of Biogeography*, 49:1299-1312.
- Asplund, J., & Wardle, D. A. (2017). How lichens impact on terrestrial community and ecosystem properties. *Biological Reviews*, 92(3), 1720-1738.
- Austin, M. P. , Margules, C. R. (1986). Assessing representativeness, in: Usher, M. B. (ed.). *Wildlife Conservation Evaluation*. Chapman and Hall, London. Pp. 45-67.
- Austrheim, G. (2002). Plant diversity patterns in semi-natural grasslands along an elevational gradient in southern Norway. *Plant Ecology*, 161(2), 193-205.
- Bakkestuen, V., Halvorsen, R., & Heegaard, E. (2009). Disentangling complex fine-scale ecological patterns by path modelling using GLMM and GIS. *Journal of Vegetation Science*, 20(5), 779-790.
- Baldwin, L. K., & Bradfield, G. E. (2005). Bryophyte community differences between edge and interior environments in temperate rain-forest fragments of coastal British Columbia. *Canadian Journal of Forest Research*, 35(3), 580-592.

- Baldwin, L. K., & Bradfield, G. E. (2007). Bryophyte responses to fragmentation in temperate coastal rainforests: a functional group approach. *Biological Conservation*, 136(3), 408-422.
- Barbé, M., Dubois, L., Faubert, J., Lavoie, M., Bergeron, Y., & Fenton, N. J. (2018). Range Extensions of 35 Bryophyte Species in the Black Spruce–Feather Moss Forest of Western Quebec, Canada. *The Canadian Field-Naturalist*, 131(3), 258-269.
- Barbé, M., Fenton, N. J., & Bergeron, Y. (2017). Are post-fire residual forest patches refugia for boreal bryophyte species? Implications for ecosystem based management and conservation. *Biodiversity and Conservation*, 26(4), 943-965.
- Barnosky, A. D., Matzke, N., Tomiya, S., Wogan, G. O., Swartz, B., Quental, T. B., ... & Ferrer, E. A. (2011). Has the Earth's sixth mass extinction already arrived?. *Nature*, 471(7336), 51-57.
- Bartels, S. F., Caners, R. T., Ogilvie, J., White, B., & Macdonald, S. E. (2018). Relating bryophyte assemblages to a remotely sensed depth-to-water index in boreal forests. *Frontiers in plant science*, 9, 858.
- Bartels, S. F., James, R. S., Caners, R. T., & Macdonald, S. E. (2019). Depth-to-water mediates bryophyte response to harvesting in boreal forests. *Journal of Applied Ecology*, 56(5), 1256-1266.
- Beaman, R. S., & Cellinese, N. (2012). Mass digitization of scientific collections: New opportunities to transform the use of biological specimens and underwrite biodiversity science. *ZooKeys*, (209), 7.
- Belland, R. J. (1998). The rare mosses of Canada: a review and first listing. Committee on the Status of Endangered Wildlife in Canada, Environnement Canada, Ottawa, Ontario, Canada. 91 pp.
- Belnap, J. (2001). Biological soil crusts: structure, function, and management (Vol. 150). O. L. Lange (Ed.). Springer, Berlin, Germany. pp. 241-261.
- Benítez, Á., Prieto, M., & Aragón, G. (2015). Large trees and dense canopies: key factors for maintaining high epiphytic diversity on trunk bases (bryophytes and lichens) in tropical montane forests. *Forestry: An International Journal of Forest Research*, 88(5), 521-527.

- Benítez, Á., Prieto, M., González, Y., & Aragón, G. (2012). Effects of tropical montane forest disturbance on epiphytic macrolichens. *Science of the Total Environment*, 441, 169-175.
- Bennie, J., Huntley, B., Wiltshire, A., Hill, M. O., & Baxter, R. (2008). Slope, aspect and climate: spatially explicit and implicit models of topographic microclimate in chalk grassland. *Ecological modelling*, 216(1), 47-59.
- Bergamini, A., Ungricht, S., & Hofmann, H. (2009). An elevational shift of cryophilous bryophytes in the last century—an effect of climate warming?. *Diversity and distributions*, 15(5), 871-879.
- Bergeron, Y., Drapeau, P., Gauthier, S., & Lecomte, N. (2007). Using knowledge of natural disturbances to support sustainable forest management in the northern Clay Belt. *The Forestry Chronicle*, 83(3), 326-337.
- Bergeron, Y., Gauthier, S., Flannigan, M., & Kafka, V. (2004). Fire regimes at the transition between mixedwood and coniferous boreal forest in northwestern Quebec. *Ecology*, 85(7), 1916-1932.
- Bivand, R., Gómez-Rubio, V., & Rue, H. (2015). Spatial data analysis with R-INLA with some extensions. *Journal of statistical software*, 63, 1-31.
- Bobbe, T., Finco, M.V., Quayle, B., Lannom, K., Sohlberg, R., Parsons, A., (2001). Field measurements for the training and validation of burn severity maps from spaceborne, remotely sensed imagery. USDI Joint Fire Science Program Final Project Report JFSP RFP 2.
- Boertje, R. D. (1984). Seasonal diets of the Denali caribou herd, Alaska. *Arctic*, 161-165.
- Bokhorst, S., Bjerke, J. W., Tømmervik, H., Preece, C., & Phoenix, G. K. (2012). Ecosystem response to climatic change: the importance of the cold season. *Ambio*, 41(3), 246-255.
- Bond-Lamberty, B., & Gower, S. T. (2007). Estimation of stand-level leaf area for boreal bryophytes. *Oecologia*, 151(4), 584-592.
- Bond-Lamberty, B., Wang, C., & Gower, S. T. (2004). Net primary production and net ecosystem production of a boreal black spruce wildfire chronosequence. *Global Change Biology*, 10(4), 473-487.

- Boucher, Y., Perrault-Hébert, M., Fournier, R., Drapeau, P., & Auger, I. (2017). Cumulative patterns of logging and fire (1940–2009): consequences on the structure of the eastern Canadian boreal forest. *Landscape ecology*, 32(2), 361-375.
- Boudreault, C., Bergeron, Y., Gauthier, S., & Drapeau, P. (2002). Bryophyte and lichen communities in mature to old-growth stands in eastern boreal forests of Canada. *Canadian Journal of Forest Research*, 32(6), 1080-1093.
- Boudreault, C., Paquette, M., Fenton, N. J., Pothier, D., & Bergeron, Y. (2018). Changes in bryophytes assemblages along a chronosequence in eastern boreal forest of Quebec. *Canadian Journal of Forest Research*, 48(7), 821-834.
- Bourg, N. A., McShea, W. J., & Gill, D. E. (2005). Putting a CART before the search: successful habitat prediction for a rare forest herb. *Ecology*, 86(10), 2793-2804.
- Bourgouin, M., Valeria, O., & Fenton, N. J. (2022). Predictive mapping of bryophyte diversity associated with mature forests using LiDAR-derived indices in a strongly managed landscape. *Ecological Indicators*, 136, 108585.
- Bracken, M. E., & Low, N. H. (2012). Realistic losses of rare species disproportionately impact higher trophic levels. *Ecology letters*, 15(5), 461-467.
- Breiman, L. (2001). Random forests. *Machine learning*, 45(1), 5-32.
- Breiner, F. T., Guisan, A., Bergamini, A., & Nobis, M. P. (2015). Overcoming limitations of modelling rare species by using ensembles of small models. *Methods in Ecology and Evolution*, 6(10), 1210-1218.
- Brodo, I. M. (2016). *Keys to lichens of North America: revised and expanded*. Yale University Press, New Haven and London, USA. 427 pp.
- Brondizio, E. S., Settele, J., Díaz, S., Ngo, H. T., 2019. IPBES (2019): Global assessment report on biodiversity and ecosystem services of the Intergovernmental Science-Policy Platform on Biodiversity and Ecosystem Services. IPBES secretariat, Bonn, Germany.
- Brunialti, G., Frati, L., Aleffi, M., Marignani, M., Rosati, L., Burrascano, S., & Ravera, S. (2010). Lichens and bryophytes as indicators of old-growth features in Mediterranean forests. *Plant Biosystems*, 144(1), 221-233.

- Bruun, H. H., Moen, J., Virtanen, R., Grytnes, J. A., Oksanen, L., & Angerbjörn, A. (2006). Effects of altitude and topography on species richness of vascular plants, bryophytes and lichens in alpine communities. *Journal of Vegetation Science*, 17(1), 37-46.
- Bubier, J. L., Rock, B. N., & Crill, P. M. (1997). Spectral reflectance measurements of boreal wetland and forest mosses. *Journal of Geophysical Research: Atmospheres*, 102(D24), 29483-29494.
- Buermann, W., Saatchi, S., Smith, T. B., Zutta, B. R., Chaves, J. A., Milá, B., & Graham, C. H. (2008). Predicting species distributions across the Amazonian and Andean regions using remote sensing data. *Journal of Biogeography*, 35(7), 1160-1176.
- Burnham, K. P., & Anderson, D. R. (2002). A practical information-theoretic approach. *Model selection and multimodel inference*, 2, 70-71.
- Burton, P. J., Messier, C., Smith, D. W., & Adamowicz, W. L. (2003). Towards sustainable management of the boreal forest. NRC Research Press, Ottawa, Ontario, Canada. 1039 pp.
- Butchart, S. H., Walpole, M., Collen, B., Van Strien, A., Scharlemann, J. P., Almond, R. E., ... & Watson, R. (2010). Global biodiversity: indicators of recent declines. *Science*, 328(5982), 1164-1168.
- Camathias, L., Bergamini, A., Küchler, M., Stofer, S., & Baltensweiler, A. (2013). High-resolution remote sensing data improves models of species richness. *Applied Vegetation Science*, 16(4), 539-551.
- Campbell, J. B., & Wynne, R. H. (2011). Introduction to remote sensing. Guilford Press, New York, USA. 667 pp.
- Caners, R. T., Macdonald, S. E., & Belland, R. J. (2013). Bryophyte assemblage structure after partial harvesting in boreal mixedwood forest depends on residual canopy abundance and composition. *Forest Ecology and Management*, 289, 489-500.
- Cardinale, B. J., Duffy, J. E., Gonzalez, A., Hooper, D. U., Perrings, C., Venail, P., ... & Naeem, S. (2012). Biodiversity loss and its impact on humanity. *Nature*, 486(7401), 59-67.

- Casajus, N., Périé, C., Logan, T., Lambert, M. C., de Blois, S., & Berteaux, D. (2016). An objective approach to select climate scenarios when projecting species distribution under climate change. *PloS one*, 11(3), e0152495.
- Castonguay, J., (2016). Dynamique des communautés de bryophytes dans la pessière à mousses de la forêt boréale: rôle des îlots de rétention après coupe. M.Sc. Thesis. Montreal (Quebec, Canada), Université du Québec à Montréal.
- Cavender-Bares, J., Gamon, J. A., & Townsend, P. A. (2020). Remote sensing of plant biodiversity. Springer Nature, Cham, Switzerland. 581 pp.
- Cayuela, L., Golicher, D. J., Newton, A. C., Kolb, M., De Albuquerque, F. S., Arets, E. J. M. M., ... & Pérez, A. M. (2009). Species distribution modeling in the tropics: problems, potentialities, and the role of biological data for effective species conservation. *Tropical Conservation Science*, 2(3), 319-352.
- Cerrejón, C., Valeria, O., Marchand, P., Caners, R. T., & Fenton, N. J. (2021a). No place to hide: Rare plant detection through remote sensing. *Diversity and Distributions*, 27(6), 948-961.
- Cerrejón, C., Valeria, O., Muñoz, J., Fenton, N. J. (2021b). Mapping of rare bryophyte species distribution. *Mendeley Data* 2021; V3. <https://data.mendeley.com/datasets/9mtcx3jnx/2>
<https://data.mendeley.com/datasets/9mtcx3jnx/3>. doi: 10.17632/9mtcx3jnxz.3
- Cerrejón, C., Valeria, O., Mansuy, N., Barbé, M., & Fenton, N. J. (2020). Predictive mapping of bryophyte richness patterns in boreal forests using species distribution models and remote sensing data. *Ecological Indicators*, 119, 106826.
- Cerrejón, C., Valeria, O., Muñoz, J., & Fenton, N. J. (2022). Small but visible: Predicting rare bryophyte distribution and richness patterns using remote sensing-based ensembles of small models. *Plos one*, 17(1), e0260543.
- Chagnon, C., Simard, M., & Boudreau, S. (2021). Patterns and determinants of lichen abundance and diversity across a subarctic to arctic latitudinal gradient. *Journal of Biogeography*, 48(11), 2742-2754.
- Chaieb, C., Fenton, N. J., Lafleur, B., & Bergeron, Y. (2015). Can we use forest inventory mapping as a coarse filter in ecosystem based management in the black spruce boreal forest?. *Forests*, 6(4), 1195-1207.

- Chandler, M., See, L., Copas, K., Bonde, A. M., López, B. C., Danielsen, F., ... & Turak, E. (2017). Contribution of citizen science towards international biodiversity monitoring. *Biological conservation*, 213, 280-294.
- Chapin Iii, F. S., Zavaleta, E. S., Eviner, V. T., Naylor, R. L., Vitousek, P. M., Reynolds, H. L., ... & Díaz, S. (2000). Consequences of changing biodiversity. *Nature*, 405(6783), 234-242.
- Charron, I., (2016). *A Guidebook on Climate Scenarios: Using Climate Information to Guide Adaptation Research and Decisions*, 2016 Edition. Ouranos, 94.
- Chefaoui, R. M., Lobo, J. M., & Hortal, J. (2011). Effects of species' traits and data characteristics on distribution models of threatened invertebrates. *Animal Biodiversity and Conservation*, 34(2), 229-247.
- Chen, S., Slik, J. W. F., Mao, L., Zhang, J., Sa, R., Zhou, K., & Gao, J. (2015a). Spatial patterns and environmental correlates of bryophyte richness: sampling effort matters. *Biodiversity and conservation*, 24(3), 593-607.
- Chen, S., Slik, J. W. F., Gao, J., Mao, L. F., Bi, M. J., Shen, M. W., & Zhou, K. X. (2015b). Latitudinal diversity gradients in bryophytes and woody plants: Roles of temperature and water availability. *Journal of Systematics and Evolution*, 53(6), 535-545.
- Chuquimarca, L., Gaona, F. P., Iñiguez-Armijos, C., & Benítez, Á. (2019). Lichen responses to disturbance: clues for biomonitoring land-use effects on riparian Andean ecosystems. *Diversity*, 11(5), 73.
- Clausen, E. (1964). The tolerance of hepatics to desiccation and temperature. *The bryologist*, 67(4), 411-417.
- Cole, H. A., Newmaster, S. G., Bell, F. W., Pitt, D., & Stinson, A. (2008). Influence of microhabitat on bryophyte diversity in Ontario mixedwood boreal forest. *Canadian Journal of Forest Research*, 38(7), 1867-1876.
- Corbane, C., Lang, S., Pipkins, K., Alleaume, S., Deshayes, M., Millán, V. E. G., ... & Michael, F. (2015). Remote sensing for mapping natural habitats and their conservation status—New opportunities and challenges. *International Journal of Applied Earth Observation and Geoinformation*, 37, 7-16.
- Cornelissen, J. H. C., Callaghan, T. V., Alatalo, J. M., Michelsen, A., Graglia, E., Hartley, A. E., ... & Aerts, R. (2001). Global change and arctic ecosystems: is

- lichen decline a function of increases in vascular plant biomass?. *Journal of Ecology*, 89(6), 984-994.
- Cornwell, W. K., Pearse, W. D., Dalrymple, R. L., & Zanne, A. E. (2019). What we ('on't) know about global plant diversity. *Ecography*, 42(11), 1819-1831.
- Couvreur, J. M., San Martin, G., & Sotiaux, A. (2016). Factors affecting the presence and the diversity of bryophytes in the petrifying sources habitat (7220) in Wallonia and the Brussels-Capital Region, Belgium. *International Journal of Agronomy*, 2016, 1-18.
- Cutler, N. (2010). Long-term primary succession: a comparison of non-spatial and spatially explicit inferential techniques. *Plant Ecology*, 208(1), 123-136.
- Cyr, D., Gauthier, S., Bergeron, Y., & Carcaillet, C. (2009). Forest management is driving the eastern North American boreal forest outside its natural range of variability. *Frontiers in Ecology and the Environment*, 7(10), 519-524.
- Czerepko, J., Gawryś, R., Szymczyk, R., Pisarek, W., Janek, M., Haidt, A., ... & Cacciatori, C. (2021). How sensitive are epiphytic and epixylic cryptogams as indicators of forest naturalness? Testing bryophyte and lichen predictive power in stands under different management regimes in the Białowieża forest. *Ecological Indicators*, 125, 107532.
- Dee, L. E., Cowles, J., Isbell, F., Pau, S., Gaines, S. D., & Reich, P. B. (2019). When do ecosystem services depend on rare species?. *Trends in Ecology & Evolution*, 34(8), 746-758.
- Delso, Á., Fajardo, J., & Muñoz, J. (2021). Protected area networks do not represent unseen biodiversity. *Scientific Reports*, 11(1), 1-10.
- Dettki, H., & Esseen, P. A. (2003). Modelling long-term effects of forest management on epiphytic lichens in northern Sweden. *Forest ecology and management*, 175(1-3), 223-238.
- Dilks, T. J. K., & Proctor, M. C. F. (1975). Comparative experiments on temperature responses of bryophytes: assimilation, respiration and freezing damage. *Journal of Bryology*, 8(3), 317-336.
- Doetterl, S., Stevens, A., Van Oost, K., Quine, T. A., & Van Wesemael, B. (2013). Spatially-explicit regional-scale prediction of soil organic carbon stocks in

- cropland using environmental variables and mixed model approaches. *Geoderma*, 204, 31-42.
- Dray, S., & Dufour, A. B. (2007). The ade4 package: implementing the duality diagram for ecologists. *Journal of statistical software*, 22, 1-20.
- Drew, C. A., Wiersma, Y. F., Huettmann, F., (2010). Predictive species and habitat modeling in landscape ecology: concepts and applications. Springer Science & Business Media, New York, USA. 313 pp.
- Dubuis, A., Pottier, J., Rion, V., Pellissier, L., Theurillat, J. P., & Guisan, A. (2011). Predicting spatial patterns of plant species richness: a comparison of direct macroecological and species stacking modelling approaches. *Diversity and Distributions*, 17(6), 1122-1131.
- Dunn, R. R. (2005). Modern insect extinctions, the neglected majority. *Conservation biology*, 19(4), 1030-1036.
- Elbert, W., Weber, B., Burrows, S., Steinkamp, J., Büdel, B., Andreae, M. O., & Pöschl, U. (2012). Contribution of cryptogamic covers to the global cycles of carbon and nitrogen. *Nature Geoscience*, 5(7), 459-462.
- Erni, S., Arseneault, D., Parisien, M. A., & Bégin, Y. (2017). Spatial and temporal dimensions of fire activity in the fire-prone eastern Canadian taiga. *Global Change Biology*, 23(3), 1152-1166.
- Environment Canada, (2010). https://climate.weather.gc.ca/climate_normals/ (accessed 28 March 2019).
- ESRI. (2016). ArcGIS Desktop. v. 10.5. Redlands, CA: Environmental Systems Research Institute.
- Evans, J., Terashima, I., Hanba, Y., & Loreto, F. (2004). Chloroplast to leaf, in: Smith, W. K., Vogelmann, T. C., Critchley, C., (eds.). *Photosynthetic adaptation: chloroplast to the landscape*. Springer, New York, USA. pp. 107-132.
- Ewald, M., Skowronek, S., Aerts, R., Lenoir, J., Feilhauer, H., Van De Kerchove, R., ... & Schmidtlein, S. (2020). Assessing the impact of an invasive bryophyte on plant species richness using high resolution imaging spectroscopy. *Ecological Indicators*, 110, 105882.

- Faubert, J., Bastien, D. F., & Gilbert, H. (2011). Mise à jour de la publication Les bryophytes rares du Québec. Espèces prioritaires pour la conservation. Carnets de bryologie, 1, 29-31.
- Faubert, J., Gagnon, J., Tremblay, B., & Couillard, L. (2012). Mise à jour de la publication Les bryophytes rares du Québec. Espèces prioritaires pour la conservation. -2 – Carnets de bryologie ; 2: 53-56.
- Faubert, J. (2012). Flore des bryophytes du Québec-Labrador. Volume 1: Anthocérotes et hépatiques. Société québécoise de bryologie, Saint-Valérien, Québec, Canada, xvii.
- Faubert, J., & Gagnon, J. (2013). Bryophytes nouvelles pour le Québec. Carnets de bryologie, 3, 19-29.
- Faubert, J., Lapointe, M., & Tardif, B. (2010). Les bryophytes rares du Québec: espèces prioritaires pour la conservation. Centre de données sur le patrimoine naturel du Québec, Ministère du développement durable, de l'environnement et des parcs.
- Fawcett, T. (2004). ROC graphs: Notes and practical considerations for researchers. Machine learning, 31(1), 1-38.
- Feilhauer, H., & Schmidtlein, S. (2009). Mapping continuous fields of forest alpha and beta diversity. Applied Vegetation Science, 12(4), 429-439.
- Feldman, M. J., Imbeau, L., Marchand, P., Mazerolle, M. J., Darveau, M., & Fenton, N. J. (2021). Trends and gaps in the use of citizen science derived data as input for species distribution models: A quantitative review. PloS one, 16(3), e0234587.
- Fenton, N. J., & Bergeron, Y. (2006). Facilitative succession in a boreal bryophyte community driven by changes in available moisture and light. Journal of Vegetation Science, 17(1), 65-76.
- Fenton, N. J., & Bergeron, Y. (2008). Does time or habitat make old-growth forests species rich? Bryophyte richness in boreal *Picea mariana* forests. Biological conservation, 141(5), 1389-1399.
- Fenton, N. J., & Bergeron, Y. (2011). Dynamic old-growth forests? A case study of boreal black spruce forest bryophytes. Silva Fennica, 45(5), 983-994.

- Fenton, N. J., & Bergeron, Y. (2013). Stochastic processes dominate during boreal bryophyte community assembly. *Ecology*, 94(9), 1993-2006.
- Fenton, N. J., & Frego, K. A. (2005). Bryophyte (moss and liverwort) conservation under remnant canopy in managed forests. *Biological conservation*, 122(3), 417-430.
- Ferrier, S., Manion, G., Elith, J., & Richardson, K. (2007). Using generalized dissimilarity modelling to analyse and predict patterns of beta diversity in regional biodiversity assessment. *Diversity and distributions*, 13(3), 252-264.
- Fitzpatrick, M., Mokany, K., Manion, G., Lisk, M., Ferrier, S., & Nieto-Lugilde, D. (2022). gdm: Generalized dissimilarity modeling. R package version, 1.5.0-3. <https://CRAN.R-project.org/package=gdm>
- Ficken, C. D., Cobbaert, D., & Rooney, R. C. (2019). Low extent but high impact of human land use on wetland flora across the boreal oil sands region. *Science of the Total Environment*, 693, 133647.
- Flather, C. H., & Sieg, C. H. (2007). Species rarity: definition, causes and classification. *Conservation of rare or little-known species: Biological, social, and economic considerations*, 40-66.
- Frahm, J. P., & Klaus, D. (2001). Bryophytes as indicators of recent climate fluctuations in Central Europe. *Lindbergia*, 97-104.
- Franch, B., Vermote, E., Skakun, S., Roger, J. C., Masek, J., Ju, J., ... & Santamaria-Artigas, A. (2019). A method for Landsat and Sentinel 2 (HLS) BRDF normalization. *Remote Sensing*, 11(6), 632.
- Freeman, E. A., Frescino, T. S., & Moisen, G. G. (2018). ModelMap: an R package for model creation and map production. *R Package Version*, 4.6-12.
- Frego, K. A. (2007). Bryophytes as potential indicators of forest integrity. *Forest ecology and management*, 242(1), 65-75.
- French, N. H., Kasischke, E. S., Hall, R. J., Murphy, K. A., Verbyla, D. L., Hoy, E. E., & Allen, J. L. (2008). Using Landsat data to assess fire and burn severity in the North American boreal forest region: an overview and summary of results. *International Journal of Wildland Fire*, 17(4), 443-462.

- Gagnon, D., (2004). La forêt naturelle du Québec, un survol. Rapport préparé pour la Commission d'étude sur la gestion de la forêt publique québécoise. Groupe de recherche en écologie forestière interuniversitaire Université du Québec à Montréal.
- Gao, B. C. (1996). NDWI—A normalized difference water index for remote sensing of vegetation liquid water from space. *Remote sensing of environment*, 58(3), 257-266.
- Gentry, A. H. (1986). Endemism in tropical versus temperate plant communities, in: M.E. Soulé (ed.). *Conservation biology*. Sinauer Assoc., Sunderland, MA, pp. 153-181.
- Gignac, L. D. (2001). Bryophytes as indicators of climate change. *The bryologist*, 104(3), 410-420.
- Gillis, M. D., Omule, A. Y., & Brierley, T. (2005). Monitoring Can'da's forests: the national forest inventory. *The Forestry Chronicle*, 81(2), 214-221.
- Goffinet, B., & Shaw, A. J. (Eds.). (2000). *Bryophyte biology*. Cambridge University Press, Cambridge, United Kingdom. 486 pp.
- Goguen, M., & Arp, P. A. (2017). Modeling and mapping forest floor distributions of common bryophytes using a LiDAR-derived depth-to-water index. *American Journal of Plant Sciences*, 8(04), 867.
- Gorelick, N., Hancher, M., Dixon, M., Ilyushchenko, S., Thau, D., & Moore, R. (2017). Google Earth Engine: Planetary-scale geospatial analysis for everyone. *Remote sensing of Environment*, 202, 18-27.
- Gould, W. (2000). Remote sensing of vegetation, plant species richness, and regional biodiversity hotspots. *Ecological applications*, 10(6), 1861-1870.
- Goward, T., Brodo, I. M., & Clayden, S. R. (1998). *Rare Lichens of Canada. A Review and Provisional Listing*. Committee on the Status of Endangered Wildlife in Canada Report. Canadian Wildlife Service, Ottawa, Ontario, Canada. 74 pp.
- Gower, S. T., Krankina, O., Olson, R. J., Apps, M., Linder, S., & Wang, C. (2001). Net primary production and carbon allocation patterns of boreal forest ecosystems. *Ecological applications*, 11(5), 1395-1411.

- Gower, S. T., Vogel, J. G., Norman, J. M., Kucharik, C. J., Steele, S. J., & Stow, T. K. (1997). Carbon distribution and aboveground net primary production in aspen, jack pine, and black spruce stands in Saskatchewan and Manitoba, Canada. *Journal of Geophysical Research: Atmospheres*, 102(D24), 29029-29041.
- Grabska, E., Hawryło, P., & Socha, J. (2020). Continuous detection of small-scale changes in scots pine dominated stands using dense sentinel-2 time series. *Remote Sensing*, 12(8), 1298.
- Grandpré, L., Boucher, D., Bergeron, Y., & Gagnon, D. (2011). Effects of small canopy gaps on boreal mixedwood understory vegetation dynamics. *Community Ecology*, 12(1), 67-77.
- Grondin, P., Gauthier, S., Poirier, V., Tardif, P., Boucher, Y., & Bergeron, Y. (2018). Have some landscapes in the eastern Canadian boreal forest moved beyond their natural range of variability?. *Forest Ecosystems*, 5(1), 1-17.
- Guillera-Arroita, G., Lahoz-Monfort, J. J., Elith, J., Gordon, A., Kujala, H., Lentini, P. E., ... & Wintle, B. A. (2015). Is my species distribution model fit for purpose? Matching data and models to applications. *Global Ecology and Biogeography*, 24(3), 276-292.
- Guillera-Arroita, G. (2017). Modelling of species distributions, range dynamics and communities under imperfect detection: advances, challenges and opportunities. *Ecography*, 40(2), 281-295.
- Guisan, A., Graham, C. H., Elith, J., Huettmann, F., & NCEAS Species Distribution Modelling Group (2007). Sensitivity of predictive species distribution models to change in grain size. *Diversity and distributions*, 13(3), 332-340.
- Guisan, A., & Thuiller, W. (2005). Predicting species distribution: offering more than simple habitat models. *Ecology letters*, 8(9), 993-1009.
- Guisan, A., & Zimmermann, N. E. (2000). Predictive habitat distribution models in ecology. *Ecological modelling*, 135(2-3), 147-186.
- Guisan, A., Broennimann, O., Engler, R., Vust, M., Yoccoz, N. G., Lehmann, A., & Zimmermann, N. E. (2006). Using niche-based models to improve the sampling of rare species. *Conservation biology*, 20(2), 501-511.
- Hall, R. J., Skakun, R. S., Arsenault, E. J., & Case, B. S. (2006). Modeling forest stand structure attributes using Landsat ETM+ data: Application to mapping of

aboveground biomass and stand volume. *Forest ecology and management*, 225(1-3), 378-390.

- Hallik, L., Kuusk, A., Lang, M., & Kuusk, J. (2019). Reflectance properties of hemiboreal mixed forest canopies with focus on red edge and near infrared spectral regions. *Remote Sensing*, 11(14), 1717.
- Hallingbäck, T., Hodgetts, N. G. (2000). Mosses, liverworts, and hornworts: status survey and conservation action plan for bryophytes, IUCN/SSC Bryophyte Specialist Group. IUCN. Gland, Switzerland and Cambridge, United Kingdom. 106 pp.
- Hammond, D. H., Strand, E. K., Hudak, A. T., & Newingham, B. A. (2019). Boreal forest vegetation and fuel conditions 12 years after the 2004 Taylor Complex fires in Alaska, USA. *Fire Ecology*, 15(1), 1-19.
- Harris, A., & Baird, A. J. (2019). Microtopographic drivers of vegetation patterning in blanket peatlands recovering from erosion. *Ecosystems*, 22(5), 1035-1054.
- Hawksworth, D. L., & Lücking, R. (2017). Fungal diversity revisited: 2.2 to 3.8 million species. *Microbiology spectrum*, 5(4), 5-4.
- He, K. S., Bradley, B. A., Cord, A. F., Rocchini, D., Tuanmu, M. N., Schmidlein, S., ... & Pettorelli, N. (2015). Will remote sensing shape the next generation of species distribution models?. *Remote Sensing in Ecology and Conservation*, 1(1), 4-18.
- He, K. S., Zhang, J., & Zhang, Q. (2009). Linking variability in species composition and MODIS NDVI based on beta diversity measurements. *acta oecologica*, 35(1), 14-21.
- He, Y., Wang, J., Lek-Ang, S., & Lek, S. (2010). Predicting assemblages and species richness of endemic fish in the upper Yangtze River. *Science of the Total Environment*, 408(19), 4211-4220.
- Hector, A., & Bagchi, R. (2007). Biodiversity and ecosystem multifunctionality. *Nature*, 448(7150), 188-190.
- Henckel, L., Bradter, U., Jönsson, M., Isaac, N. J., & Snäll, T. (2020). Assessing the usefulness of citizen science data for habitat suitability modelling: Opportunistic reporting versus sampling based on a systematic protocol. *Diversity and Distributions*, 26(10), 1276-1290.

- Héon, J., Arseneault, D., & Parisien, M. A. (2014). Resistance of the boreal forest to high burn rates. *Proceedings of the National Academy of Sciences*, 111(38), 13888-13893.
- Hernandez, P. A., Graham, C. H., Master, L. L., & Albert, D. L. (2006). The effect of sample size and species characteristics on performance of different species distribution modeling methods. *Ecography*, 29(5), 773-785.
- Hespanhol, H., Cezón, K., Felicísimo, Á. M., Muñoz, J., & Mateo, R. G. (2015). How to describe species richness patterns for bryophyte conservation?. *Ecology and Evolution*, 5(23), 5443-5455.
- Hespanhol, H., Séneca, A., Figueira, R., & Sérgio, C. (2011). Microhabitat effects on bryophyte species richness and community distribution on exposed rock outcrops in Portugal. *Plant Ecology & Diversity*, 4(2-3), 251-264.
- Hijmans, R. J. (2020). raster: Geographic Data Analysis and Modeling. R package version 3.4-5. 2020. <https://CRAN.R-project.org/package=raster>.
- Honegger, R. (1998). The lichen symbiosis—what is so spectacular about it?. *The Lichenologist*, 30(3), 193-212.
- Hooper, D. U., Adair, E. C., Cardinale, B. J., Byrnes, J. E., Hungate, B. A., Matulich, K. L., ... & O'Connor, M. I. (2012). A global synthesis reveals biodiversity loss as a major driver of ecosystem change. *Nature*, 486(7401), 105-108.
- Hortal, J., de Bello, F., Diniz-Filho, J. A. F., Lewinsohn, T. M., Lobo, J. M., & Ladle, R. J. (2015). Seven shortfalls that beset large-scale knowledge of biodiversity. *Annual Review of Ecology, Evolution, and Systematics*, 46, 523-549.
- Hudak, A. T., Robichaud, P., Evans, J. S., Clark, J., Lannom, K., Morgan, P., Stone, C. (2004). Field validation of Burned Area Reflectance Classification (BARC) products for post fire assessment, in: *Remote sensing for field users: proceedings of the tenth Forest Service Remote Sensing Applications Conference*, Salt Lake City, Utah, April 5-9, 2004, [CD-ROM]. Bethesda, Md. : American Society for Photogrammetry and Remote Sensing. 13 pp.
- Huete, A. R., Liu, H. Q., Batchily, K. V., & Van Leeuwen, W. J. D. A. (1997). A comparison of vegetation indices over a global set of TM images for EOS-MODIS. *Remote sensing of environment*, 59(3), 440-451.

- Hugron, S., Andersen, R., Poulin, M., & Rochefort, L. (2011). Natural plant colonization of borrow pits in boreal forest highlands of eastern Canada. *Botany*, 89(7), 451-465.
- Hunter Jr, M. L., & Webb, S. L. (2002). Enlisting taxonomists to survey poorly known taxa for biodiversity conservation: a lichen case study. *Conservation Biology*, 16(3), 660-665.
- Huttunen, S., Bell, N., & Hedenäs, L. (2018). The evolutionary diversity of mosses—taxonomic heterogeneity and its ecological drivers. *Critical reviews in plant sciences*, 37(2-3), 128-174.
- Hylander, K., Jonsson, B. G., & Nilsson, C. (2002). Evaluating buffer strips along boreal streams using bryophytes as indicators. *Ecological applications*, 12(3), 797-806.
- Isbell, F., Calcagno, V., Hector, A., Connolly, J., Harpole, W. S., Reich, P. B., ... & Loreau, M. (2011). High plant diversity is needed to maintain ecosystem services. *Nature*, 477(7363), 199-202.
- Jenness, J. (2006). Topographic Position Index (tpi_jen.avx) extension for ArcView 3.x, v. 1.2.
- Jiang, Y., De Bie, C. A. J. M., Wang, T., Skidmore, A. K., Liu, X., Song, S., & Shao, X. (2013). Hyper-temporal remote sensing helps in relating epiphyllous liverworts and evergreen forests. *Journal of vegetation science*, 24(2), 214-226.
- Jiang, Y., Wang, T., De Bie, C. A. J. M., Skidmore, A. K., Liu, X., Song, S., ... & Shao, X. (2014). Satellite-derived vegetation indices contribute significantly to the prediction of epiphyllous liverworts. *Ecological Indicators*, 38, 72-80.
- Jiang, Z., Huete, A. R., Kim, Y., & Didan, K. (2007). 2-band enhanced vegetation index without a blue band and its application to AVHRR data. *Proceedings of SPIE*, 6679, 45-53.
- Johansson, P. (2008). Consequences of disturbance on epiphytic lichens in boreal and near boreal forests. *Biological conservation*, 141(8), 1933-1944.
- Jolls, C. L., Inkster, J. N., Scholtens, B. G., Vitt, P., & Havens, K. (2019). An endemic plant and the plant-insect visitor network of a dune ecosystem. *Global Ecology and Conservation*, 18, e00603.

- Jonsson, B. G., & Esseen, P. A. (1990). Treefall disturbance maintains high bryophyte diversity in a boreal spruce forest. *The Journal of Ecology*, 924-936.
- Kearsley, E., Hufkens, K., Verbeeck, H., Bauters, M., Beeckman, H., Boeckx, P., & Huygens, D. (2019). Large-sized rare tree species contribute disproportionately to functional diversity in resource acquisition in African tropical forest. *Ecology and evolution*, 9(8), 4349-4361.
- Keim, J. L., DeWitt, P. D., Fitzpatrick, J. J., & Jenni, N. S. (2017). Estimating plant abundance using inflated beta distributions: Applied learnings from a lichen-caribou ecosystem. *Ecology and evolution*, 7(2), 486-493.
- Keitt, T. H., & Urban, D. L. (2005). Scale-specific inference using wavelets. *Ecology*, 86(9), 2497-2504.
- Kerr, J. T., & Ostrovsky, M. (2003). From space to species: ecological applications for remote sensing. *Trends in ecology & evolution*, 18(6), 299-305.
- Kivinen, S., Moen, J., Berg, A., & Eriksson, Å. (2010). Effects of modern forest management on winter grazing resources for reindeer in Sweden. *Ambio*, 39(4), 269-278.
- Kuenzer, C., Bluemel, A., Gebhardt, S., Quoc, T. V., & Dech, S. (2011). Remote sensing of mangrove ecosystems: A review. *Remote Sensing*, 3(5), 878-928.
- Kuhn, M. (2018). Package 'caret': Classification and regression training. R package version 6.0-80.
- Kursa, M. B., & Rudnicki, W. R. (2010). Feature selection with the Boruta package. *Journal of statistical software*, 36, 1-13.
- Kuuluvainen, T., & Gauthier, S. (2018). Young and old forest in the boreal: critical stages of ecosystem dynamics and management under global change. *Forest Ecosystems*, 5(1), 1-15.
- Kuusinen, N., Stenberg, P., Korhonen, L., Rautiainen, M., & Tomppo, E. (2016). Structural factors driving boreal forest albedo in Finland. *Remote sensing of environment*, 175, 43-51.
- Kuzemko, A. A., Steinbauer, M. J., Becker, T., Didukh, Y. P., Dolnik, C., Jeschke, M., ... & Dengler, J. (2016). Patterns and drivers of phytodiversity in steppe

- grasslands of Central Podolia (Ukraine). *Biodiversity and Conservation*, 25(12), 2233-2250.
- Laamrani, A., Valeria, O., Bergeron, Y., Fenton, N., & Cheng, L. Z. (2015). Distinguishing and mapping permanent and reversible paludified landscapes in Canadian black spruce forests. *Geoderma*, 237, 88-97.
- Lakatos, M. (2011). Lichens and bryophytes: habitats and species. *Plant desiccation tolerance*, 65-87.
- Larraín, J., Alarcón, D., Ardiles, V., & Atala, C. (2019). Hidden in plain sight: how overlooking ephemeral bryophytes can bias biodiversity assessments and conservation actions. *The Bryologist*, 122(2), 260-270.
- Lauzier, S., & Pelletier, P. A. (2016). Till and Boulder Survey on the Opinaca Property, James Bay Area, Quebec, Canada. Submitted to Tashota Resources Inc.
- Lawler, J. J., Wiersma, Y. F., & Huettmann, F. (2011). Using species distribution models for conservation planning and ecological forecasting, in: *Predictive species and habitat modeling in landscape ecology*. Springer, New York, USA. pp. 271-290.
- Le Goff, H., Flannigan, M. D., Bergeron, Y., & Girardin, M. P. (2007). Historical fire regime shifts related to climate teleconnections in the Waswanipi area, central Quebec, Canada. *International Journal of Wildland Fire*, 16(5), 607-618.
- Le Goff, H., Girardin, M. P., Flannigan, M. D., & Bergeron, Y. (2008). Dendroclimatic inference of wildfire activity in Quebec over the 20th century and implications for natural disturbance-based forest management at the northern limit of the commercial forest. *International journal of wildland fire*, 17(3), 348-362.
- Lecomte, N., Simard, M., Fenton, N., & Bergeron, Y. (2006). Fire severity and long-term ecosystem biomass dynamics in coniferous boreal forests of eastern Canada. *Ecosystems*, 9(8), 1215-1230.
- Lee, S. I. (2001). Developing a bivariate spatial association measure: an integration of Pearson's r and Moran's I . *Journal of geographical systems*, 3(4), 369-385.
- Legendre, P., & Legendre, L. (2012). *Numerical ecology*. Elsevier, Amsterdam, Netherlands. 990 pp.

- Lehosmaa, K., Jyväsjärvi, J., Virtanen, R., Ilmonen, J., Saastamoinen, J., & Muotka, T. (2017). Anthropogenic habitat disturbance induces a major biodiversity change in habitat specialist bryophytes of boreal springs. *Biological Conservation*, 215, 169-178.
- Leitão, R. P., Zuanon, J., Villéger, S., Williams, S. E., Baraloto, C., Fortunel, C., ... & Mouillot, D. (2016). Rare species contribute disproportionately to the functional structure of species assemblages. *Proceedings of the Royal Society B: Biological Sciences*, 283(1828), 20160084.
- Lendemer, J. C., Keepers, K. G., Tripp, E. A., Pogoda, C. S., McCain, C. M., & Kane, N. C. (2019). A taxonomically broad metagenomic survey of 339 species spanning 57 families suggests cystobasidiomycete yeasts are not ubiquitous across all lichens. *American Journal of Botany*, 106(8), 1090-1095.
- Lenne, T., Bryant, G., Hocart, C. H., Huang, C. X., & Ball, M. C. (2010). Freeze avoidance: a dehydrating moss gathers no ice. *Plant, cell & environment*, 33(10), 1731-1741.
- Levin, N., Shmida, A., Levanoni, O., Tamari, H., & Kark, S. (2007). Predicting mountain plant richness and rarity from space using satellite-derived vegetation indices. *Diversity and Distributions*, 13(6), 692-703.
- Li, H., & Chang, C. (2021). Evolutionary insight of plant cuticle biosynthesis in bryophytes. *Plant Signaling & Behavior*, 16(10), 1943921.
- Li, R., Wang, Y., Hu, J., Wang, Y., Min, Q., Bergeron, Y., ... & Fu, Y. (2020). Spatiotemporal variations of satellite microwave emissivity difference vegetation index in China under clear and cloudy skies. *Earth and Space Science*, 7(5), e2020EA001145.
- Liaw, A., & Wiener, M. (2002). The randomforest package. *R news*, 2, 18–22.
- Liu, L., & Liu, J. (2008). A rainfall interception model for inhomogeneous forest canopy. *Frontiers of Forestry in China*, 3(1), 50-57.
- Locky, D. A. (2010). Boreal peatlands and plant diversity: what's there and why it matters. *SFM Network Research Note Series*, 58.
- Lomba, A., Pellissier, L., Randin, C., Vicente, J., Moreira, F., Honrado, J., & Guisan, A. (2010). Overcoming the rare species modelling paradox: A novel

- hierarchical framework applied to an Iberian endemic plant. *Biological conservation*, 143(11), 2647-2657.
- Longton, R. E. (1992). Role of bryophytes and lichens in terrestrial ecosystems, in: Bates, J. W., & Farmer, A. M. (eds.). *Bryophytes and lichens in a changing environment*. Clarendon Press, Oxford, United Kingdom. pp. 32-76.
- Longton, R. E. (1988). Adaptations and strategies of polar bryophytes. *Botanical journal of the Linnean Society*, 98(3), 253-268.
- Lucas, R., Armston, J., Fairfax, R., Fensham, R., Accad, A., Carreiras, J., ... & Shimada, M. (2010). An evaluation of the ALOS PALSAR L-band backscatter—Above ground biomass relationship Queensland, Australia: Impacts of surface moisture condition and vegetation structure. *IEEE Journal of selected topics in applied earth observations and remote sensing*, 3(4), 576-593.
- Lücking, R., Hodkinson, B. P., & Leavitt, S. D. (2017). The 2016 classification of lichenized fungi in the Ascomycota and Basidiomycota—Approaching one thousand genera. *The Bryologist*, 119(4), 361-416.
- Lüttge, U., Beck, E., & Bartels, D. (2011). *Plant desiccation tolerance* (Vol. 215). Springer, Heidelberg, Germany. 386 pp.
- Ma, X., Mahecha, M. D., Migliavacca, M., van der Plas, F., Benavides, R., Ratcliffe, S., ... & Wirth, C. (2019). Inferring plant functional diversity from space: the potential of Sentinel-2. *Remote Sensing of Environment*, 233, 111368.
- Maes, D., Bauwens, D., De Bruyn, L., Anselin, A., Vermeersch, G., Van Landuyt, W., ... & Gilbert, M. (2005). Species richness coincidence: conservation strategies based on predictive modelling. *Biodiversity & Conservation*, 14(6), 1345-1364.
- Malíček, J., Palice, Z., Vondrák, J., Kostovčík, M., Lenzová, V., & Hofmeister, J. (2019). Lichens in old-growth and managed mountain spruce forests in the Czech Republic: assessment of biodiversity, functional traits and bioindicators. *Biodiversity and Conservation*, 28(13), 3497-3528.
- Mansuy, N., Burton, P. J., Stanturf, J., Beatty, C., Mooney, C., Besseau, P., ... & Lapointe, R. (2020). Scaling up forest landscape restoration in Canada in an era of cumulative effects and climate change. *Forest Policy and Economics*, 116, 102177.

- Mansuy, N., Gauthier, S., Robitaille, A., & Bergeron, Y. (2010). The effects of surficial deposit–drainage combinations on spatial variations of fire cycles in the boreal forest of eastern Canada. *International Journal of Wildland Fire*, 19(8), 1083-1098.
- Mansuy, N., Gauthier, S., Robitaille, A., & Bergeron, Y. (2012). Regional patterns of postfire canopy recovery in the northern boreal forest of Quebec: interactions between surficial deposit, climate, and fire cycle. *Canadian Journal of Forest Research*, 42(7), 1328-1343.
- Mansuy, N., Valeria, O., Laamrani, A., Fenton, N., Guindon, L., Bergeron, Y., ... & Légaré, S. (2018). Digital mapping of paludification in soils under black spruce forests of eastern Canada. *Geoderma Regional*, 15, e00194.
- Mazerolle, M. J. (2020) AICcmodavg: Model selection and multimodel inference based on (Q)AIC(c). R package version 2.3-1. <https://cran.r-project.org/package=AICcmodavg>.
- Margules, C. R., & Stein, J. L. (1989). Patterns in the distributions of species and the selection of nature reserves: an example from Eucalyptus forests in south-eastern New South Wales. *Biological Conservation*, 50(1-4), 219-238.
- Marschner, I. C. (2011). glm2: Fitting generalized linear models with convergence problems. *The R Journal*, 3(2): 12-15.
- Marzialetti, F., Cascone, S., Frate, L., Di Febbraro, M., Acosta, A. T. R., & Carranza, M. L. (2021). Measuring Alpha and Beta Diversity by Field and Remote-Sensing Data: A Challenge for Coastal Dunes Biodiversity Monitoring. *Remote Sensing*, 13(10), 1928.
- Mateo, R. G., Felicísimo, Á. M., Pottier, J., Guisan, A., & Muñoz, J. (2012). Do stacked species distribution models reflect altitudinal diversity patterns?. *PLoS One*, 7(3), e32586.
- Mateo, R. G., Vanderpoorten, A., Muñoz, J., Laenen, B., & Désamoré, A. (2013). Modeling species distributions from heterogeneous data for the biogeographic regionalization of the European bryophyte flora. *PLoS One*, 8(2), e55648.
- Mateo, R. G., Felicísimo, A. M., & Muñoz, J. (2011). Species distributions models: A synthetic revision. *Revista Chilena de Historia Natural*, 84(2), 217-240.

- Mateo, R. G., Broennimann, O., Normand, S., Petitpierre, B., Araújo, M. B., Svenning, J. C., ... & Vanderpoorten, A. (2016). The mossy north: an inverse latitudinal diversity gradient in European bryophytes. *Scientific Reports*, 6(1), 1-9.
- McCune, J. L., Rosner-Katz, H., Bennett, J. R., Schuster, R., & Kharouba, H. M. (2020). Do traits of plant species predict the efficacy of species distribution models for finding new occurrences?. *Ecology and evolution*, 10(11), 5001-5014.
- McMullin, R. T. (2015). The lichens of Prince Edward Island, Canada: a second checklist, with species ranked for conservation status. *Rhodora*, 117(972), 454-484.
- McMullin, R. T., & Lendemer, J. C. (2013). Lichen biodiversity and conservation status in the Copeland Forest Resources Management Area: a lichen-rich second-growth forest in southern Ontario. *The Canadian Field-Naturalist*, 127(3), 240-254.
- McMullin, R. T., & Wiersma, Y. F. (2019). Out with OLD growth, in with ecological continuity: new perspectives on forest conservation. *Frontiers in Ecology and the Environment*, 17(3), 176-181.
- Medina, N. G., Albertos, B., Lara, F., Mazimpaka, V., Garilleti, R., Draper, D., & Hortal, J. (2014). Species richness of epiphytic bryophytes: drivers across scales on the edge of the Mediterranean. *Ecography*, 37(1), 80-93.
- MFFP (2018). Cartographie du 5e inventaire écoforestier du Québec méridional — Méthodes et données associées, Ministère des Forêts, de la Faune et des Parcs, Secteur des forêts, Direction des inventaires forestiers.
- Millennium Ecosystem Assessment (2005). *Ecosystems and Human Well-being: Synthesis*. Island Press, Washington, DC, USA. 137 pp.
- Mitchard, E. T., Saatchi, S. S., Lewis, S. L., Feldpausch, T. R., Woodhouse, I. H., Sonké, B., ... & Meir, P. (2011). Measuring biomass changes due to woody encroachment and deforestation/degradation in a forest-savanna boundary region of central Africa using multi-temporal L-band radar backscatter. *Remote Sensing of Environment*, 115(11), 2861-2873.
- Moeslund, J. E., Zlinszky, A., Ejrnæs, R., Brunbjerg, A. K., Bøcher, P. K., Svenning, J. C., & Normand, S. (2019). Light detection and ranging explains diversity of plants, fungi, lichens, and bryophytes across multiple habitats and large geographic extent. *Ecological Applications*, 29(5), e01907.

- Möls, T., Vellak, K., Vellak, A., & Ingerpuu, N. (2013). Global gradients in moss and vascular plant diversity. *Biodiversity and conservation*, 22(6), 1537-1551.
- Moreira, E. F., Santos, R. L. D. S., Silveira, M. S., Boscolo, D., Neves, E. L. D., & Viana, B. F. (2017). Influence of landscape structure on Euglossini composition in open vegetation environments. *Biota Neotropica*, 17.
- Moudrý, V., & Šímová, P. (2012). Influence of positional accuracy, sample size and scale on modelling species distributions: a review. *International Journal of Geographical Information Science*, 26(11), 2083-2095.
- Mouillot, D., Bellwood, D. R., Baraloto, C., Chave, J., Galzin, R., Harmelin-Vivien, M., ... & Thuiller, W. (2013). Rare species support vulnerable functions in high-diversity ecosystems. *PLoS biology*, 11(5), e1001569.
- Myers, N., Mittermeier, R. A., Mittermeier, C. G., Da Fonseca, G. A., & Kent, J. (2000). Biodiversity hotspots for conservation priorities. *Nature*, 403(6772), 853-858.
- Myers, N. (1988). Tropical forests and their species: going, going . . . ?, in: Wilson, E. O. (ed.). *Biodiversity*. National Academies Press, Washington, DC, USA. pp. 28-35.
- Nash, T. H. (2008). *Lichen Biology*. Cambridge University Press, Cambridge United Kingdom, 486 pp.
- Natural Resources Canada–Canadian Forest Service (2017). *The State of Canada's Forests: Annual Report 2017*. 84 pp.
- Newbold, T., Hudson, L. N., Hill, S. L., Contu, S., Lysenko, I., Senior, R. A., ... & Purvis, A. (2015). Global effects of land use on local terrestrial biodiversity. *Nature*, 520(7545), 45-50.
- Newmaster, S. G., & Bell, F. W. (2002). The effects of silvicultural disturbances on cryptogam diversity in the boreal-mixedwood forest. *Canadian journal of forest research*, 32(1), 38-51.
- Newmaster, S. G., Belland, R. J., Arsenault, A., Vitt, D. H., & Stephens, T. R. (2005). The ones we left behind: comparing plot sampling and floristic habitat sampling for estimating bryophyte diversity. *Diversity and distributions*, 11(1), 57-72.

- Nguyen, T. T., Huang, J. Z., & Nguyen, T. T. (2015). Unbiased feature selection in learning random forests for high-dimensional data. *The Scientific World Journal*, 2015, 1-18.
- Niittynen, P., & Luoto, M. (2018). The importance of snow in species distribution models of arctic vegetation. *Ecography*, 41(6), 1024-1037.
- Nilsson, M. C., & Wardle, D. A. (2005). Understory vegetation as a forest ecosystem driver: evidence from the northern Swedish boreal forest. *Frontiers in Ecology and the Environment*, 3(8), 421-428.
- Nordén, B., Dahlberg, A., Brandrud, T. E., Fritz, Ö., Ejrnaes, R., & Ovaskainen, O. (2014). Effects of ecological continuity on species richness and composition in forests and woodlands: a review. *Ecoscience*, 21(1), 34-45.
- O'Neill, K. P. (2000). Role of bryophyte-dominated ecosystems in the global carbon budget. *Bryophyte biology*. Cambridge University Press, Cambridge, 344-368.
- Oksanen, J., Blanchet, F. G., Friendly, M., Kindt, R., Legendre, P., McGlinn, D., ... & Solymos, P. (2020). *vegan: Community Ecology Package*. R package version 2.5-7.
- Paquette, M., Boudreault, C., Fenton, N., Pothier, D., & Bergeron, Y. (2016). Bryophyte species assemblages in fire and clear-cut origin boreal forests. *Forest Ecology and Management*, 359, 99-108.
- Paton, A., Antonelli, A., Carine, M., Forzza, R. C., Davies, N., Demissew, S., ... & Dickie, J. (2020). Plant and fungal collections: Current status, future perspectives. *Plants, People, Planet*, 2(5), 499-514.
- Patykowski, J., Dell, M., Wevill, T., & Gibson, M. (2018). Rarity and nutrient acquisition relationships before and after prescribed burning in an Australian box-ironbark forest. *AoB Plants*, 10(3), ply032.
- Pearce, J., & Lindenmayer, D. (1998). Bioclimatic analysis to enhance reintroduction biology of the endangered helmeted honeyeater (*Lichenostomus melanops cassidix*) in southeastern Australia. *Restoration ecology*, 6(3), 238-243.
- Pearson, R. G., Raxworthy, C. J., Nakamura, M., & Townsend Peterson, A. (2007). Predicting species distributions from small numbers of occurrence records: a test case using cryptic geckos in Madagascar. *Journal of biogeography*, 34(1), 102-117.

- Peck, J. E., Grabner, J., Ladd, D., & Larsen, D. R. (2004). Microhabitat affinities of Missouri Ozarks lichens. *The Bryologist*, 107(1), 47-61.
- Peckham, S. D., Ahl, D. E., & Gower, S. T. (2009). Bryophyte cover estimation in a boreal black spruce forest using airborne lidar and multispectral sensors. *Remote Sensing of Environment*, 113(6), 1127-1132.
- Peksa, O., & Škaloud, P. (2011). Do photobionts influence the ecology of lichens? A case study of environmental preferences in symbiotic green alga *Asterochloris* (Trebouxiophyceae). *Molecular Ecology*, 20(18), 3936-3948.
- Pereira, H. M., Leadley, P. W., Proença, V., Alkemade, R., Scharlemann, J. P., Fernandez-Manjarrés, J. F., ... & Walpole, M. (2010). Scenarios for global biodiversity in the 21st century. *Science*, 330(6010), 1496-1501.
- Peterson, E. B., & McCune, B. (2003). The importance of hotspots for lichen diversity in forests of western Oregon. *Bryologist*, 246-256.
- Pettorelli, N., Laurance, W. F., O'Brien, T. G., Wegmann, M., Nagendra, H., & Turner, W. (2014). Satellite remote sensing for applied ecologists: opportunities and challenges. *Journal of Applied Ecology*, 51(4), 839-848.
- Pharo, E. J., Kirkpatrick, J. B., Gilfedder, L., Mendel, L., & Turner, P. A. (2005). Predicting bryophyte diversity in grassland and eucalypt-dominated remnants in subhumid Tasmania. *Journal of Biogeography*, 32(11), 2015-2024.
- Phillips, S. J., Anderson, R. P., & Schapire, R. E. (2006). Maximum entropy modeling of species geographic distributions. *Ecological modelling*, 190(3-4), 231-259.
- Pimm, S. L., Jenkins, C. N., Abell, R., Brooks, T. M., Gittleman, J. L., Joppa, L. N., ... & Sexton, J. O. (2014). The biodiversity of species and their rates of extinction, distribution, and protection. *science*, 344(6187), 1246752.
- Pócs, T. (1996). Epiphyllous liverwort diversity at worldwide level and its threat and conservation. *Anales del Instituto de Biología Serie Botánica*, 67(001), 109-127.
- Porada, P., Ekici, A., & Beer, C. (2016). Effects of bryophyte and lichen cover on permafrost soil temperature at large scale. *The Cryosphere*, 10(5), 2291-2315.
- Porada, P., Van Stan, J. T., & Kleidon, A. (2018). Significant contribution of non-vascular vegetation to global rainfall interception. *Nature Geoscience*, 11(8), 563-567.

- Porada, P., Weber, B., Elbert, W., Pöschl, U., & Kleidon, A. (2014). Estimating impacts of lichens and bryophytes on global biogeochemical cycles. *Global Biogeochemical Cycles*, 28(2), 71-85.
- Porley, R. D. (2013). *England's rare mosses and liverworts: Their history, ecology and conservation*. Princeton University Press, Princeton, New Jersey. United Kingdom. 224 pp.
- Pouteau, R., Meyer, J. Y., Taputuarai, R., & Stoll, B. (2012). Support vector machines to map rare and endangered native plants in Pacific islands forests. *Ecological Informatics*, 9, 37-46.
- Prendergast, J. R., Quinn, R. M., Lawton, J. H., Eversham, B. C., & Gibbons, D. W. (1993). Rare species, the coincidence of diversity hotspots and conservation strategies. *Nature*, 365(6444), 335-337.
- Prendergast, J. R., Quinn, R. M., & Lawton, J. H. (1999). The gaps between theory and practice in selecting nature reserves. *Conservation biology*, 13(3), 484-492.
- Proctor, M. C., Oliver, M. J., Wood, A. J., Alpert, P., Stark, L. R., Cleavitt, N. L., & Mishler, B. D. (2007). Desiccation-tolerance in bryophytes: a review. *The bryologist*, 110(4), 595-621.
- Proisy, C., Mitchell, A., Lucas, R., Fromard, F., & Mougin, E. (2003, May). Estimation of mangrove biomass using multifrequency radar data. Application to mangroves of French Guiana and Northern Australia, in: *Proceedings of the Mangrove 2003 Conference*. pp. 20-24.
- Pykälä, J. (2019). Habitat loss and deterioration explain the disappearance of populations of threatened vascular plants, bryophytes and lichens in a hemiboreal landscape. *Global Ecology and Conservation*, 18, e00610.
- R Development Core Team (2018). *R: A language and environment for statistical computing*. Version 1.1.456. R Foundation for Statistical Computing, Vienna, Austria.
- R Development Core Team (2020). *R: A language and environment for statistical computing*. Version 3.6.3. R Foundation for Statistical Computing, Vienna, Austria.
- Raabe, S., Müller, J., Manthey, M., Dürhammer, O., Teuber, U., Göttlein, A., ... & Bässler, C. (2010). Drivers of bryophyte diversity allow implications for forest

- management with a focus on climate change. *Forest ecology and management*, 260(11), 1956-1964.
- Rabinowitz, D. (1981). Seven forms of rarity, in: Synge, H. (ed.). *The biological aspects of rare plant conservation*. Wiley, London, United Kingdom. pp. 205-217.
- Ranson, K. J., Kovacs, K., Sun, G., & Kharuk, V. I. (2003). Disturbance recognition in the boreal forest using radar and Landsat-7. *Canadian journal of remote sensing*, 29(2), 271-285.
- Rapalee, G., Steyaert, L. T., & Hall, F. G. (2001). Moss and lichen cover mapping at local and regional scales in the boreal forest ecosystem of central Canada. *Journal of Geophysical Research: Atmospheres*, 106(D24), 33551-33563.
- Raven, J. A. (1995). The early evolution of land plants: aquatic ancestors and atmospheric interactions. *Botanical Journal of Scotland*, 47(2), 151-175.
- Regos, A., Gonçalves, J., Arenas-Castro, S., Alcaraz-Segura, D., Guisan, A., & Honrado, J. P. (2022). Mainstreaming remotely sensed ecosystem functioning in ecological niche models. *Remote Sensing in Ecology and Conservation*, 8(4), 431-447.
- Rejžek, M., Svátek, M., Šebesta, J., Adolt, R., Maděra, P., & Matula, R. (2016). Loss of a single tree species will lead to an overall decline in plant diversity: Effect of *Dracaena cinnabari* Balf. f. on the vegetation of Socotra Island. *Biological Conservation*, 196, 165-172.
- Rey Benayas, J. M. (1995). Patterns of diversity in the strata of boreal montane forest in British Columbia. *Journal of Vegetation Science*, 6(1), 95-98.
- Ricketts, T. H., Dinerstein, E., Boucher, T., Brooks, T. M., Butchart, S. H., Hoffmann, M., ... & Wikramanayake, E. (2005). Pinpointing and preventing imminent extinctions. *Proceedings of the National Academy of Sciences*, 102(51), 18497-18501.
- Riffo-Donoso, V., Osorio, F., & Fontúrbel, F. E. (2021). Habitat disturbance alters species richness, composition, and turnover of the bryophyte community in a temperate rainforest. *Forest Ecology and Management*, 496, 119467.

- Robinson, S. A., Wasley, J., & Tobin, A. K. (2003). Living on the edge—plants and global change in continental and maritime Antarctica. *Global Change Biology*, 9(12), 1681-1717.
- Rocchetti, G.A., Armstrong, C. G., Abeli, T., Orsenigo, S., Jasper, C., Joly, S., ... & Vamosi, J. C. (2021). Reversing extinction trends: new uses of (old) herbarium specimens to accelerate conservation action on threatened species. *New Phytologist*, 230(2), 433-450.
- Rocchini, D., Andreini Butini, S., & Chiarucci, A. (2005). Maximizing plant species inventory efficiency by means of remotely sensed spectral distances. *Global Ecology and Biogeography*, 14(5), 431-437.
- Rocchini, D., Balkenhol, N., Carter, G. A., Foody, G. M., Gillespie, T. W., He, K. S., ... & Neteler, M. (2010). Remotely sensed spectral heterogeneity as a proxy of species diversity: recent advances and open challenges. *Ecological Informatics*, 5(5), 318-329.
- Rocchini, D., He, K. S., & Zhang, J. (2009). Is spectral distance a proxy of beta diversity at different taxonomic ranks? A test using quantile regression. *Ecological Informatics*, 4(4), 254-259.
- Rocchini, D., Hernández-Stefanoni, J. L., & He, K. S. (2015). Advancing species diversity estimate by remotely sensed proxies: a conceptual review. *Ecological informatics*, 25, 22-28.
- Rodrigues, A. S., & Brooks, T. M. (2007). Shortcuts for biodiversity conservation planning: the effectiveness of surrogates. *Annu. Rev. Ecol. Evol. Syst.*, 38, 713-737.
- Rondinini, C., Wilson, K. A., Boitani, L., Grantham, H., & Possingham, H. P. (2006). Tradeoffs of different types of species occurrence data for use in systematic conservation planning. *Ecology letters*, 9(10), 1136-1145.
- Root, H. T., Brinda, J. C., & Dodson, E. K. (2017). Recovery of biological soil crust richness and cover 12–16 years after wildfires in Idaho, USA. *Biogeosciences*, 14(17), 3957-3969.
- Ross-Davis, A. L., & Frego, K. A. (2002). Comparison of plantations and naturally regenerated clearcuts in the Acadian Forest: forest floor bryophyte community and habitat features. *Canadian journal of botany*, 80(1), 21-33.

- Rouse Jr, J. W., Haas, R., Schell, J. & Deering, D. (1974). Monitoring vegetation systems in the Great Plains with ERTS, in: Third ERTS Symposium, NASA SP-351, Washington DC, USA. pp. 309-317.
- Route, T. (2020). Facteurs environnementaux influençant la biodiversité des lichens à différentes échelles dans le nord-ouest du Québec. Doctoral dissertation, Université du Québec en Abitibi-Témiscamingue.
- Rowntree, J. K., Pressel, S., Ramsay, M. M., Sabovljevic, A., & Sabovljevic, M. (2011). In vitro conservation of European bryophytes. *In Vitro Cellular & Developmental Biology-Plant*, 47(1), 55-64.
- Roy, P. S., Sharma, K. P., & Jain, A. (1996). Stratification of density in dry deciduous forest using satellite remote sensing digital data—An approach based on spectral indices. *Journal of biosciences*, 21(5), 723-734.
- Rudiyanto, Minasny, B., Setiawan, B. I., Saptomo, S. K., & McBratney, A. B. (2018). Open digital mapping as a cost-effective method for mapping peat thickness and assessing the carbon stock of tropical peatlands. *Geoderma*, 313, 25-40.
- Ryömä, R., & Laaka-Lindberg, S. (2005). Bryophyte recolonization on burnt soil and logs. *Scandinavian Journal of Forest Research*, 20(S6), 5-16.
- Saatchi, S., Buermann, W., Ter Steege, H., Mori, S., & Smith, T. B. (2008). Modeling distribution of Amazonian tree species and diversity using remote sensing measurements. *Remote Sensing of Environment*, 112(5), 2000-2017.
- Sahu, N., Singh, S. N., Singh, P., Mishra, S., Karakoti, N., Bajpai, R., ... & Upreti, D. K. (2019). Microclimatic variations and their effects on photosynthetic efficiencies and lichen species distribution along elevational gradients in Garhwal Himalayas. *Biodiversity and Conservation*, 28(8), 1953-1976.
- Saucier, J. P., Grondin, P., Robitaille, A., & Bergeron, J. F. (2003). Zones de végétation et domaines bioclimatiques du Québec. Publication No. 2003-3015. Ministère des Ressources naturelles, de la Faune et des Parcs (MRNFP), direction des inventaires forestiers. Quebec, Canada. Code de diffusion, 2003, vol. 3043.
- Scheidegger, C., & Goward, T. (2002). Monitoring lichens for conservation: red lists and conservation action plans, in: *Monitoring with lichens—monitoring lichens*. Springer, Dordrecht, Netherlands. pp. 163-181.

- Schmidtlein, S., & Fassnacht, F. E. (2017). The spectral variability hypothesis does not hold across landscapes. *Remote Sensing of Environment*, 192, 114-125.
- Scott, J. M., Davis, F., Csuti, B., Noss, R., Butterfield, B., Groves, C., ... & Wright, R. G. (1993). Gap analysis: a geographic approach to protection of biological diversity. *Wildlife monographs*, 3-41.
- Seaward, M. R. D. (2004). The use of lichens for environmental impact assessment. *Symbiosis*, 37, 293-305.
- Senn-Irlet, B., Heilmann-Clausen, J., Genney, D., & Dahlberg, A. (2007). Guidance for conservation of macrofungi in Europe. ECCF, Strasbourg, France. 39 pp.
- Seto, K. C., Fleishman, E., Fay, J. P., & Betrus, C. J. (2004). Linking spatial patterns of bird and butterfly species richness with Landsat TM derived NDVI. *International Journal of Remote Sensing*, 25(20), 4309-4324.
- Sexton, J. O., Song, X. P., Feng, M., Noojipady, P., Anand, A., Huang, C., ... & Townshend, J. R. (2013). Global, 30-m resolution continuous fields of tree cover: Landsat-based rescaling of MODIS vegetation continuous fields with lidar-based estimates of error. *International Journal of Digital Earth*, 6(5), 427-448.
- Simard, M., Lecomte, N., Bergeron, Y., Bernier, P. Y., & Paré, D. (2007). Forest productivity decline caused by successional paludification of boreal soils. *Ecological Applications*, 17(6), 1619-1637.
- Simpson, M. G. (2010). *Plant systematics*. Academic press, San Diego, California, USA. 752 pp.
- Skowronek, S., Ewald, M., Isermann, M., Van De Kerchove, R., Lenoir, J., Aerts, R., ... & Feilhauer, H. (2017). Mapping an invasive bryophyte species using hyperspectral remote sensing data. *Biological Invasions*, 19(1), 239-254.
- Skowronek, S., Van De Kerchove, R., Rombouts, B., Aerts, R., Ewald, M., Warrie, J., ... & Feilhauer, H. (2018). Transferability of species distribution models for the detection of an invasive alien bryophyte using imaging spectroscopy data. *International journal of applied earth observation and geoinformation*, 68, 61-72.
- Skre, O., & Oechel, W. C. (1981). Moss functioning in different taiga ecosystems in interior Alaska. *Oecologia*, 48(1), 50-59.

- Socolar, J. B., Gilroy, J. J., Kunin, W. E., & Edwards, D. P. (2016). How should beta-diversity inform biodiversity conservation?. *Trends in ecology & evolution*, 31(1), 67-80.
- Söderström, L., & During, H. J. (2005). Bryophyte rarity viewed from the perspectives of life history strategy and metapopulation dynamics. *Journal of bryology*, 27(3), 261-268.
- Söderström, L., Hallingbäck, T., Gustaffson, L., Cronberg, N., & Hedenäs, L. (1992). Bryophyte conservation for the future. *Biological conservation*, 59(2-3), 265-270.
- Soliveres, S., Manning, P., Prati, D., Gossner, M. M., Alt, F., Arndt, H., ... & Allan, E. (2016). Locally rare species influence grassland ecosystem multifunctionality. *Philosophical Transactions of the Royal Society B: Biological Sciences*, 371(1694), 20150269.
- Song, L., Lu, H. Z., Xu, X. L., Li, S., Shi, X. M., Chen, X., ... & Liu, W. Y. (2016). Organic nitrogen uptake is a significant contributor to nitrogen economy of subtropical epiphytic bryophytes. *Scientific reports*, 6(1), 1-9.
- Sousa-Silva, R., Alves, P., Honrado, J., & Lomba, A. (2014). Improving the assessment and reporting on rare and endangered species through species distribution models. *Global Ecology and Conservation*, 2, 226-237.
- Spiers, J. A., Oatham, M. P., Rostant, L. V., & Farrell, A. D. (2018). Applying species distribution modelling to improving conservation based decisions: a gap analysis of Trinidad and Tobago's endemic vascular plants. *Biodiversity and Conservation*, 27(11), 2931-2949.
- Spribile, T., Tuovinen, V., Resl, P., Vanderpool, D., Wolinski, H., Aime, M. C., ... & McCutcheon, J. P. (2016). Basidiomycete yeasts in the cortex of ascomycete macrolichens. *Science*, 353(6298), 488-492.
- Su, D., Yang, L., Shi, X., Ma, X., Zhou, X., Hedges, S. B., & Zhong, B. (2021). Large-scale phylogenomic analyses reveal the monophyly of bryophytes and neoproterozoic origin of land plants. *Molecular biology and evolution*, 38(8), 3332-3344.
- Syfert, M. M., Joppa, L., Smith, M. J., Coomes, D. A., Bachman, S. P., & Brummitt, N. A. (2014). Using species distribution models to inform IUCN Red List assessments. *Biological Conservation*, 177, 174-184.

- Sykes, L., Santini, L., Etard, A., & Newbold, T. (2020). Effects of rarity form on species' responses to land use. *Conservation Biology*, 34(3), 688-696.
- Takezawa, D. (2018). Mechanisms underlying freezing and desiccation tolerance in bryophytes, in: Iwaya-Inoue, M., Sakurai, M., Uemura, M. (eds.). *Survival Strategies in Extreme Cold and Desiccation. Advances in Experimental Medicine and Biology*, vol 1081, Springer, Singapore. pp. 167-187.
- Thell, A., & Moberg, R. (2011). *Nordic Lichen Flora Volume 4–Parmeliaceae*. Nordic Lichen Society, Uddevalla, Sweden. 184 pp.
- Thomas, C. D., Cameron, A., Green, R. E., Bakkenes, M., Beaumont, L. J., Collingham, Y. C., ... & Williams, S. E. (2004). Extinction risk from climate change. *Nature*, 427(6970), 145-148.
- Thuiller, W., Georges, D., Engler, R., & Breiner, F. (2020). biomod2: Ensemble platform for species distribution modeling. R package version 3.4.6.
- Tibell, L. (1992). Crustose lichens as indicators of forest continuity in boreal coniferous forests. *Nordic Journal of Botany*, 12(4), 427-450.
- Tolkkinen, M. J., Mykrä, H., Virtanen, R., Tolkkinen, M., Kauppila, T., Paasivirta, L., & Muotka, T. (2016). Land use impacts on stream community composition and concordance along a natural stress gradient. *Ecological Indicators*, 62, 14-21.
- Townsend, J., & DiMiceli, D. (2015). University of Maryland and MODAPS SIPS - NASA. MOD44B MODIS/Terra Vegetation Continuous Fields Yearly L3 Global 500m SIN Grid. NASA LP DAAC. <http://doi.org/10.5067/MODIS/MOD44B.006>
- Trotta-Moreu, N., & Lobo, J. M. (2010). Deriving the species richness distribution of Geotrupinae (Coleoptera: Scarabaeoidea) in Mexico from the overlap of individual model predictions. *Environmental Entomology*, 39(1), 42-49.
- Turetsky, M. R. (2003). The role of bryophytes in carbon and nitrogen cycling. *The bryologist*, 106(3), 395-409.
- Turetsky, M. R., Bond-Lamberty, B., Euskirchen, E., Talbot, J., Frolking, S., McGuire, A. D., & Tuittila, E. S. (2012). The resilience and functional role of moss in boreal and arctic ecosystems. *New Phytologist*, 196(1), 49-67.

- Turetsky, M. R., Mack, M. C., Hollingsworth, T. N., & Harden, J. W. (2010). The role of mosses in ecosystem succession and function in Alaska's boreal forest. *Canadian Journal of Forest Research*, 40(7), 1237-1264.
- Turner, W., Spector, S., Gardiner, N., Fladeland, M., Sterling, E., & Steininger, M. (2003). Remote sensing for biodiversity science and conservation. *Trends in ecology & evolution*, 18(6), 306-314.
- Turtureanu, P. D., Palpurina, S., Becker, T., Dolnik, C., Ruprecht, E., Sutcliffe, L. M., ... & Dengler, J. (2014). Scale-and taxon-dependent biodiversity patterns of dry grassland vegetation in Transylvania. *Agriculture, Ecosystems & Environment*, 182, 15-24.
- Tuszynski, J. (2018). caTools: Tools: moving window statistics, GIF, Base64, ROC AUC, etc. R package version 1.17.1.1.
- Tweddale, S.A., & Melton, R.H. (2005). Remote Sensing for Threatened and Endangered Species Habitat Assessment on Military Lands: A Literature Review. ERDCCERL TR-05-11, ADA435908. U.S. Army Engineer Research and Development Center. U.S. Army Engineer Research and Development Center, Champaign, Illinois, USA. 46 pp.
- Tyler, T., Bengtsson, F., Dahlberg, C. J., Lönnell, N., Hallingbäck, T., & Reitalu, T. (2018). Determinants of bryophyte species composition and diversity on the Great Alvar of Öland, Sweden. *Journal of Bryology*, 40(1), 12-30.
- Umaña, M. N., Mi, X., Cao, M., Enquist, B. J., Hao, Z., Howe, R., ... & Swenson, N. G. (2017). The role of functional uniqueness and spatial aggregation in explaining rarity in trees. *Global Ecology and Biogeography*, 26(7), 777-786.
- Underwood, J. G., D'AGROSA, C. A. T. E. R. I. N. A., & Gerber, L. R. (2010). Identifying conservation areas on the basis of alternative distribution data sets. *Conservation biology*, 24(1), 162-170.
- Usher, M. B. (1986). Wildlife conservation evaluation: attributes, criteria and values, in: *Wildlife conservation evaluation*. Springer, Dordrecht, Netherlands. pp. 3-44.
- Valeria, O., Laamrani, A., & Beaudoin, A. (2012). Monitoring the state of a large boreal forest region in eastern Canada through the use of multitemporal classified satellite imagery. *Canadian Journal of Remote Sensing*, 38(1), 91-108.

- Vanderpoorten, A., & Hallingbäck, T. (2009). Conservation biology of bryophytes. *Bryophyte Biology*, 487-533.
- Vanderpoorten, A., Sotiaux, A., & Engels, P. (2005). A GIS-based survey for the conservation of bryophytes at the landscape scale. *Biological Conservation*, 121(2), 189-194.
- Vanderpoorten, A., Sotiaux, A., & Sotiaux, O. (2001). Integrating bryophytes into a forest management plan: lessons from grid-mapping in the forest of Soignes (Belgium). *Cryptogamie Bryologie*, 22(3), 217-230.
- Vanderpuyse, A. W., Elvebakk, A., & Nilsen, L. (2002). Plant communities along environmental gradients of high-arctic mires in Sassendalen, Svalbard. *Journal of Vegetation Science*, 13(6), 875-884.
- Vaughan, I. P., & Ormerod, S. J. (2005). The continuing challenges of testing species distribution models. *Journal of applied ecology*, 42(4), 720-730.
- Vellak, K., & Ingerpuu, N. (2005). Management effects on bryophytes in Estonian forests. *Biodiversity & Conservation*, 14(13), 3255-3263.
- Venier, L. A., Walton, R., Thompson, I. D., Arsenault, A., & Titus, B. D. (2018). A review of the intact forest landscape concept in the Canadian boreal forest: its history, value, and measurement. *Environmental Reviews*, 26(4), 369-377.
- Venier, L. A., Thompson, I. D., Fleming, R., Malcolm, J., Aubin, I., Trofymow, J. A., ... & Brandt, J. P. (2014). Effects of natural resource development on the terrestrial biodiversity of Canadian boreal forests. *Environmental reviews*, 22(4), 457-490.
- Vila-Viçosa, C., Arenas-Castro, S., Marcos, B., Honrado, J., García, C., Vázquez, F. M., ... & Gonçalves, J. (2020). Combining satellite remote sensing and climate data in species distribution models to improve the conservation of iberian white oaks (*Quercus* L.). *ISPRS International Journal of Geo-Information*, 9(12), 735.
- Vincent, J. S., & Hardy, L. (1977). L'évolution et l'extension des lacs glaciaires Barlow et Ojibway en territoire québécois. *Géographie physique et Quaternaire*, 31(3-4), 357-372.
- Virtanen, O., Constantinidou, E., & Tyystjärvi, E. (2020). Chlorophyll does not reflect green light—how to correct a misconception. *Journal of Biological Education*, 1-8.

- Vogelmann, J. E., & Moss, D. M. (1993). Spectral reflectance measurements in the genus *Sphagnum*. *Remote Sensing of Environment*, 45(3), 273-279.
- Walker, M. D., Wahren, C. H., Hollister, R. D., Henry, G. H., Ahlquist, L. E., Alatalo, J. M., ... & Wookey, P. A. (2006). Plant community responses to experimental warming across the tundra biome. *Proceedings of the National Academy of Sciences*, 103(5), 1342-1346.
- Walsh, S. J., Butler, D. R., & Malanson, G. P. (1998). An overview of scale, pattern, process relationships in geomorphology: a remote sensing and GIS perspective. *Geomorphology*, 21(3-4), 183-205.
- Walthall, C. L., Loechel, S. E., Huemrich, K. F., Brown de Colstoun, E., Chen, J., Markham, B. L., Miller, J., & Walter-Shea, E. A. (1997). Spectral Information Content of the Boreal Forest, in: *Proceedings of Physical Measurements and Signatures in Remote Sensing*. Courchevel, France. pp. 607-611.
- Waser, L. T., Kuechler, M., Schwarz, M., Ivits, E., Stofer, S., & Scheidegger, C. (2007). Prediction of lichen diversity in an UNESCO biosphere reserve—correlation of high resolution remote sensing data with field samples. *Environmental Modeling & Assessment*, 12(4), 315-328.
- Waser, L. T., Stofer, S., Schwartz, M., Kuechler, M., Ivits, E., & Scheidegger, C. (2004). Prediction of biodiversity—regression of lichen species richness on remote sensing data. *Community Ecology*, 5(1), 121-133.
- Weibull, H., & Rydin, H. (2005). Bryophyte species richness on boulders: relationship to area, habitat diversity and canopy tree species. *Biological Conservation*, 122(1), 71-79.
- Weisser, W. W., Roscher, C., Meyer, S. T., Ebeling, A., Luo, G., Allan, E., ... & Eisenhauer, N. (2017). Biodiversity effects on ecosystem functioning in a 15-year grassland experiment: Patterns, mechanisms, and open questions. *Basic and applied ecology*, 23, 1-73.
- Whitehead, S. C., & Baines, D. (2018). Moorland vegetation responses following prescribed burning on blanket peat. *International Journal of Wildland Fire*, 27(10), 658-664.
- Whittaker, R. H. (1960). Vegetation of the Siskiyou mountains, Oregon and California. *Ecological monographs*, 30(3), 279-338.

- Whittaker, R. H. (1972). Evolution and measurement of species diversity. *Taxon*, 21(2-3), 213-251.
- Whittaker, R. J., Araújo, M. B., Jepson, P., Ladle, R. J., Watson, J. E., & Willis, K. J. (2005). Conservation biogeography: assessment and prospect. *Diversity and distributions*, 11(1), 3-23.
- Williams, J. N., Seo, C., Thorne, J., Nelson, J. K., Erwin, S., O'Brien, J. M., & Schwartz, M. W. (2009). Using species distribution models to predict new occurrences for rare plants. *Diversity and Distributions*, 15(4), 565-576.
- Wisn, M. S., Hijmans, R. J., Li, J., Peterson, A. T., Graham, C. H., Guisan, A., & NCEAS Predicting Species Distributions Working Group. (2008). Effects of sample size on the performance of species distribution models. *Diversity and distributions*, 14(5), 763-773.
- Wood, A. J. (2007). The nature and distribution of vegetative desiccation-tolerance in hornworts, liverworts and mosses. *The Bryologist*, 110(2), 163-177.
- Xu, G., Zhang, Y., Zhang, S., & Ma, K. (2020). Biodiversity associations of soil fauna and plants depend on plant life form and are accounted for by rare taxa along an elevational gradient. *Soil Biology and Biochemistry*, 140, 107640.
- Xu, K., Guan, K., Peng, J., Luo, Y., & Wang, S. (2019). DeepMask: an algorithm for cloud and cloud shadow detection in optical satellite remote sensing images using deep residual network. arXiv preprint arXiv:1911.03607.
- Xu, Y., Dickson, B. G., Hampton, H. M., Sisk, T. D., Palumbo, J. A., & Prather, J. W. (2009). Effects of mismatches of scale and location between predictor and response variables on forest structure mapping. *Photogrammetric Engineering & Remote Sensing*, 75(3), 313-322.
- Yang, X., Skidmore, A. K., Melick, D. R., Zhou, Z., & Xu, J. (2006). Mapping non-wood forest product (matsutake mushrooms) using logistic regression and a GIS expert system. *ecological modelling*, 198(1-2), 208-218.
- Zavaleta, E. S., & Hulvey, K. B. (2004). Realistic species losses disproportionately reduce grassland resistance to biological invaders. *Science*, 306(5699), 1175-1177.
- Zavaleta, E. S., Pasari, J. R., Hulvey, K. B., & Tilman, G. D. (2010). Sustaining multiple ecosystem functions in grassland communities requires higher

- biodiversity. *Proceedings of the National Academy of Sciences*, 107(4), 1443-1446.
- Zechmeister, H. G., Tribsch, A., Moser, D., Peterseil, J., & Wrbka, T. (2003). Biodiversity 'hot spots' for bryophytes in landscapes dominated by agriculture in Austria. *Agriculture, ecosystems & environment*, 94(2), 159-167.
- Zellweger, F., Braunisch, V., Morsdorf, F., Baltensweiler, A., Abegg, M., Roth, T., ... & Bollmann, K. (2015). Disentangling the effects of climate, topography, soil and vegetation on stand-scale species richness in temperate forests. *Forest Ecology and Management*, 349, 36-44.
- Zhang, P. (2019). Effective predictors of herbaceous plant diversity responses to changes in nutrient availability and herbivory. Doctoral dissertation, Utrecht University, Utrecht, Netherlands.
- Zhang, Y., Peng, C., Li, W., Fang, X., Zhang, T., Zhu, Q., ... & Zhao, P. (2013). Monitoring and estimating drought-induced impacts on forest structure, growth, function, and ecosystem services using remote-sensing data: recent progress and future challenges. *Environmental Reviews*, 21(2), 103-115.
- Zheng, D., Rademacher, J., Chen, J., Crow, T., Bresee, M., Le Moine, J., & Ryu, S. R. (2004). Estimating aboveground biomass using Landsat 7 ETM+ data across a managed landscape in northern Wisconsin, USA. *Remote sensing of environment*, 93(3), 402-411.
- Zimmermann, N. E., Edwards Jr, T. C., Moisen, G. G., Frescino, T. S., & Blackard, J. A. (2007). Remote sensing-based predictors improve distribution models of rare, early successional and broadleaf tree species in Utah. *Journal of applied ecology*, 44(5), 1057-1067.